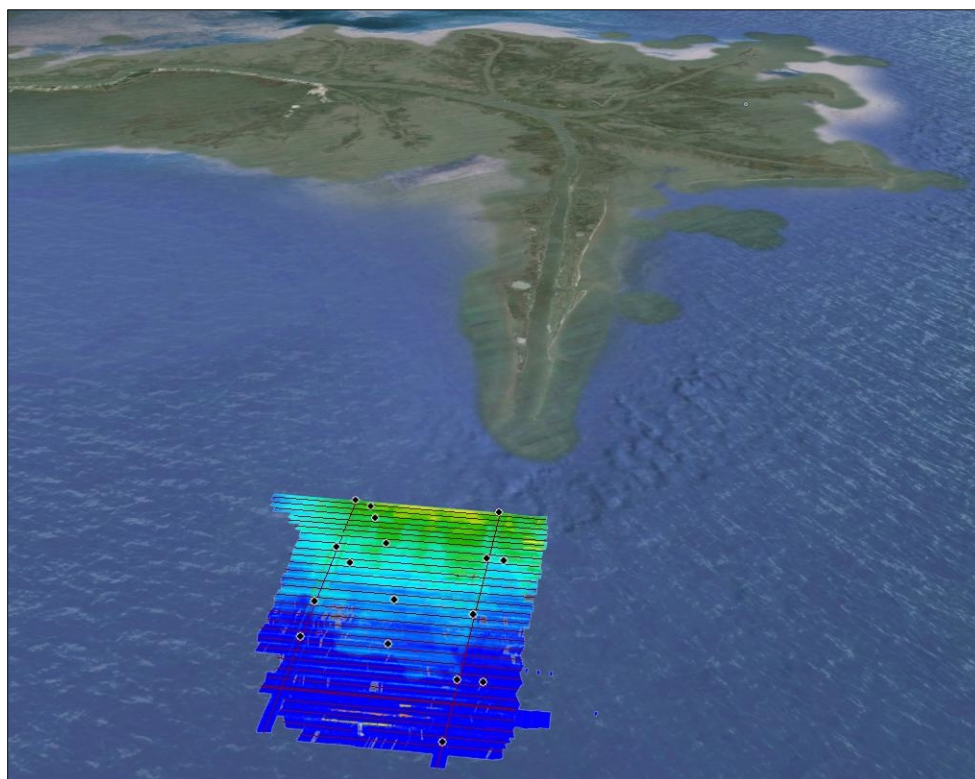# Mass Wasting Processes and Products of the Mississippi Delta Front: Data Synthesis and Observation

Mass Wasting Processes and Products of the Mississippi Delta Front: Data Synthesis and Observation

Authors

Samuel J. Bentley, Sr.
Kehui Xu
Ioannis Y. Georgiou
Jillian M. Maloney

DISCLAIMER

Study collaboration and funding were provided by the US Department of the Interior, Bureau of Ocean Energy Management, Environmental Studies Program, Washington, DC, under Agreement Number CA M13AC00013. This report has been technically reviewed by BOEM and it has been approved for publication. The views and conclusions contained in this document are those of the authors and should not be interpreted as representing the opinions or policies of the US Government, nor does mention of trade names or commercial products constitute endorsement or recommendation for use.

REPORT AVAILABLILTY

To download a PDF file of this Environmental Studies Program report, go to the US Department of the Interior, Bureau of Ocean Energy Management, Environmental Studies Program Information System website (http://www.boem.gov/Environmental-Studies-EnvData/) and search on OCS Study BOEM 2022-007.

CITATION

ABOUT THE COVER

Perspective view from southwest of the Mississippi River's bird foot delta, showing color-shaded bathymetry near Southwest Pass of the river. This was created using a regional elevation model, over which survey data from the 2014 Pilot Study was draped.

Contents

List of Figures

List of Tables

Abbreviations and Acronyms

Short Form	Long Form
ADCP	acoustic Doppler current profiler
BOEM	Bureau of Ocean Energy Management
BSEE	Bureau of Safety and Environmental Enforcement
CRDS	cavity ring-down spectroscopy
CSDMS	community sediment transport model
CTD	conductivity temperature depth sensor
DEM	digital elevation model
DoD	difference of depth
FEMA	Federal Emergency Management Agency
GOM	Gulf of Mexico
HYCOM	HYbrid Coordinate Ocean Model
LISST	laser in-situ scattering and tranmissometry
MARUM	Center for Marine Environmental Sciences, University of Bremen, Germany
MLLW	mean lower low water
MMS	Minerals Management Service
MR	Mississippi River
MRD	Mississippi River Delta
MRDF	Mississippi River Delta Front
NARR	North American Regional Reanalysis
NOAA	National Oceanic and Atmospheric Administration
NRL	Naval Research Laboratory
OCS	Outer Continental Shelf
OTRC	Offshore Technology Research Center
PAD	proximal accumulation dominated
PCATS	Pressure Core Analysis Transfer System
ROMS	Regional Ocean Modeling System
ROV	remotely operated vehicle
SAR	sediment accumulation rate
SDR	sediment deposition rate
SDSU	San Diego State University
SEASWAB	Shallow Experiment to Assess Storm Waves Affecting Bottom
SGF	sediment gravity flow
TS	tropical storm
UNO	University of New Orleans
US-ACE	US Army Corps of Engineers
USGS	United States Geological Survey
VENUS	Victorian Experimental Network under the Sea
WAVCIS	WAVes Current Surge Information System

List of Authors

Author	Affiliation
Samuel J. Bentley, Sr. Principal Investigator	Department of Geology and Geophysics, and the Coastal Studies Institute Louisiana State University
Kehui Xu	Department of Geology and Geophysics, and the Coastal Studies Institute Louisiana State University
Ioannis Y. Georgiou	Department of Earth and Environmental Sciences, and the Pontchartrain Institute for Environmental Sciences University of New Orleans
Jillian M. Maloney	Department of Geological Sciences San Diego State University

Summary

Over the last four decades and longer, the Minerals Management Service (MMS) and later the Bureau of Ocean Energy Management (BOEM) have invested considerable resources in improving our understanding of sediment deposition, stability, mass-wasting, and other sediment-transport processes on the Mississippi River Delta Front (MRDF), in order to better predict seabed phenomena (such as submarine landslides) that impact seabed hydrocarbon exploration and production activities. However, the last major comprehensive seabed mapping program, on which many hazard assessments are based, was conducted in the late 1970s. Seabed geological and geotechnical studies since then have been largely focused on localized seabed mudflows caused by a single event, such as a major hurricane. As a result, information needed to understand seabed hazards and risks is generally outdated and/or too sparsely distributed in time and space to allow hazard evaluation for the entire region, >2000 km^2, into the future.

These limitations were the motivation for a study to pursue the following four objectives:

1.   Integrate existing scientific understanding and data sets for the MRDF;

2.   Identify knowledge gaps in the behavior of seabed mudflows over a range of spatial and temporal scales, and triggered by a range of events;

3.   Conduct a pilot study to evaluate new analytical approaches that have never (or not recently) been applied to the MRDF;

4.   Outline a future research program that will help bridge these data gaps, and provide the basis for a hazard- and risk-management framework.

During the years 2013-2018, a team of scientists from Louisiana State University, University of New Orleans, San Diego State University, and the Bureau of Ocean Energy Management conducted research toward these objectives, with the following general results.

Data Review and Synthesis

An ArcGIS© geodatabase of selected existing datasets from the MRDF has been created that incorporates historical data from a wide range of sources, from 19th-century leadline surveys to 3D seabed elevation models using advanced technology ca. 2006–2017. Of these data sets, only the most recent multibeam sonar bathymetric data have great utility for advanced measurement of seabed properties, and these datasets are small in number, small in individual coverage, and cover only a small fraction of the study area. Two locations, one near SW Pass, and the other south of Garden Bay (Enterprise Pipeline) have multiple surveys at different times, and are useful for time-series study.

An Endnote® literature database has been created incorporating >450 articles and reports spanning 1955 to present. Analysis of this database by time and topic demonstrates that many studies were performed in response to seabed infrastructure damage from major hurricanes. Also, the most recent regionally and topically comprehensive study was conducted ca. 1977–1985, and the most recent detailed in situ geotechnical study was conducted ca. 1983.

Data gaps identified in our synthesis include the following:

1.   The most recent regionally comprehensive seabed mapping program occurred in 1977–1979.

2.   Localized studies have been conducted 1981–2017, but have generally focused on one individual storm event or slide.

3.   No long-term in situ study has ever been conducted to quantify mode and frequency of seabed failures.

4.	Since the mid 20th century, sediment delivery in the Mississippi Delta has declined precipitously, greatly changing the sedimentation regime that drives seabed failures. No study before our data synthesis takes this into account.

5.	Rates and spatial and temporal scales of failures are not well constrained and most estimates are based on repeated single-beam sonar surveys with high uncertainty.

6.	The presence of natural biogenic gas (primarily methane produced in the shallow seabed) has been widely documented and often attributed as a potential pre-conditioning factor that could facilitate seabed failures, but this phenomenon has never been fully investigated.

7.	Triggering mechanisms have been enumerated, but are not well understood. Only large-scale catastrophic failures have been documented based on impacts to infrastructure, but our work demonstrates that flows and failures also occur during periods of quiescence, with regard to major ($\geq$ category 3) hurricane strikes.

8.	Waves are widely recognized as important triggers for mudflows, but most work on this topic to date has been conducted using oversimplified linear wave models. These models, as our study here shows, under-predict the forces applied by real ocean waves to the seabed.

9.	Advanced geochronological and geological analytical methods exist that can help provide detailed information on the rates and distributions of mudflows in time and space, but these methods have mostly been applied outside of the most dynamic regions of the MRDF, one exception being our study by Keller et al. (2016).

Results from Pilot Studies

Analysis of cores collected near Southwest Pass in the 2014 Pilot Study demonstrate that most of the seabed in that study area to a depth of <3 m below the seabed is characterized by vertical sediment deposition from the Mississippi River Plume. Evidence for mudflow reworking of sediments was found in one core out of 20, at a depth of 1–2.5 meters below the seabed. Collectively these results suggest that most deformation produced by gravity-driven flows in this location occurs at depths >3 m below the seabed.

Spatiotemporal analysis of three collocated swath bathymetry sonar datasets from this same region (collected in 2005, 2009, and 2014) demonstrate that mudflows in gullies can continue to alter seabed depth and morphology even during periods when major hurricane strikes to not occur. Rates of deepening and shoaling are on the order of 1 m/y. However, overall plan view morphology of gullies did not change during this period.

A second pilot study in 2017 consisted of paired collaborative cruises for the US Geological Survey (USGS) and Louisiana State University (LSU) (May 2017) and LSU, the University of New Orleans (UNO), San Diego State University (SDSU), Naval Research Laboratory (NRL), and MARUM (Center for Marine Environmental Sciences, University of Bremen, Germany) (June 2017). Those cruises demonstrated that the suite of sonar tools deployed by the USGS can provide excellent information on seabed morphology and also subbottom stratigraphy where gas does not mask signal from subbottom sediments. Subsurface gas is widespread but not ubiquitous. USGS sonar data were used to target geological and geotechnical sampling on the June 2017 cruise, from which data are now revealing details about seabed geological and rheological properties that influence submarine landslide occurrence. Mapping and coring around the wreck of the SS *Virginia* (sunk 1942) are revealing new information about rates and forcing mechanisms for possible creep-like seabed motion of mud lobes at this site, which is likely to be characteristic of other locations on the MRDF.

Future Mississippi River Delta Front Research Plan

This report includes a proposal for the next phase of comprehensive MRDF study (see Appendix). This proposal includes technologies and methods for developing a modern baseline map of the MRDF seabed and subsurface, and addressing data gaps identified above. The first step of the proposed effort is to be a comprehensive mapping program (led by USGS), augmented with time-series measurements of waves, currents, and in situ seabed properties (conducted by the team of universities). Following initial mapping and field observations, a deep coring program will be undertaken to study sediment rheology and composition (especially gas) using special tools for keeping core samples at in situ pressures (to retain gas) for laboratory analysis. These field observations will be integrated with numerical modeling of seabed forcing and response, to better understand past seabed dynamics, and predict future hazards and risk.

Synthesis and Application to Resource and Infrastructure Management

The existing state of knowledge for seabed mudflows on the MRDF is presently inadequate to provide a hazard- and risk-management framework for the entire region, spanning > 2000 km^2. This is because existing seabed maps and measurements on which many hazards are assessed are far outdated, and because appropriate measurements and numerical models of the forces that drive mudflows, and the seabed response to these failures, do not exist. This study has identified basic seabed and oceanographic knowledge gaps that must be bridged to develop such a hazard- and risk-management framework. This study also identifies scientific and engineering approaches to bridging those gaps in a future comprehensive study of the MRDF.

1. Project Introduction, Background, and Methods

1.1 Motivation and BOEM Information Needs Addressed

Over the last four decades and longer, the Minerals Management Service (MMS) and later the Bureau of Ocean Energy Management (BOEM) have invested considerable resources in improving our understanding of sediment deposition, stability, mass-wasting, and other transport processes on the Mississippi River Delta Front (MRDF), to better predict seabed phenomena (such as submarine landslides, for example) that impact seabed hydrocarbon exploration and production activities. Important understanding has developed from this research. Highlighted by the seminal work of Coleman et al. (1980), we now know sediment gravity flows (SGFs) are widespread across the MRDF, and are influenced by rapid sedimentation, seabed oversteepening, and flow activation by hurricane-generated waves. We learned that these processes are capable of destroying platform and pipeline structures, which are numerous in the areas affected by SGFs. We also know that these dynamic processes are strongly influenced by, and in turn influence, bathymetry and seabed morphology, which vary in space and time. These insights are largely derived from a series of bathymetric surveys from 1872–1874, 1940, and 1977–1979. Since then no surveys of sufficient breadth and detail have been conducted to allow regional and updated hazard assessment. Up to 2013, the large number of smaller studies conducted since the last regional survey (1977–1979) remain largely uncoordinated. This lack of updated regional data, knowledge, and synthesis have hindered comprehensive and updated understanding of these seabed processes, products, and impacts, and have reduced the utility of some excellent hazard assessments and models that have been developed in the last few decades (examples including but not restricted to Hooper and Suhayda, 2005; Hitchcock et al., 2006; Guidroz, 2009). In parallel with these BOEM and/or MMS-funded studies, observational and theoretical developments in seabed sedimentary processes have advanced worldwide, particularly in the past decade (including but not limited to wave-enhanced sediment-gravity flows; Macquaker et al., 2010). However, seabed dynamics of the MRDF have not been evaluated with respect to many of these newly developed concepts.
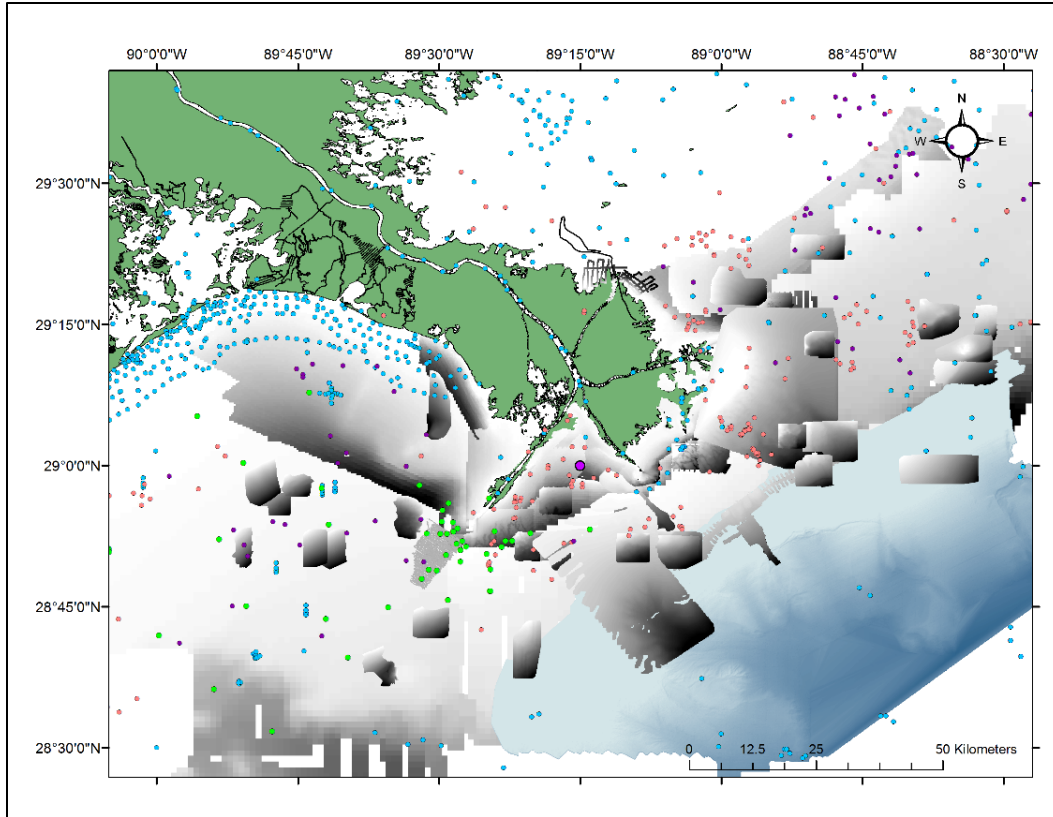
Figure 1. Study area

Map of study area, including data from various sources used in this study compiled in the ArcGIS© geodatabase of bathymetric datasets and sediment core locations visible across the offshore Mississippi River Delta. The geodatabase also includes infrastructure data and historical charts.

The MRDF study addressed by this report was conceived as a new study of data synthesis, integration of new concepts for sediment stability and dynamics, and pilot data collection to provide multiple benefits to BOEM for evaluating geotechnical stability of the evolving MRDF. The work has been conducted by an interdisciplinary team of three marine geologists (Bentley, Maloney, and Xu), combining expertise in delta front geology, muddy sediment behavior, sediment geochemistry, seabed coring, seismic, and hydrodynamic methods), and a physical oceanographer with expertise in fluvial and ocean hydrodynamics, and sediment dynamics (Georgiou). Data sources include published and unpublished data sets made available through collaboration with BOEM and other federal agencies, including surveys and studies conducted by various industry, academic, and government groups. We have identified knowledge gaps, and provide alternate perspectives for formative processes (e.g., forcing of seabed flows by annual winter storm waves, Obelcz et al., 2017), products, and impacts. We also developed and outlined here a clear path forward for a more extensive and in-depth study that could be initiated in the near future. If undertaken, such a new future research program will be of scale comparable to the surveys and synthesis of Coleman et al. 1980, but will seek to fill gaps in understanding identified in this report, and seek to provide a more extensive investigation of new aspects such as seabed rheology and dynamic response to forcing by waves and other phenomena. The present project, reported herein, is a logical first step toward design and execution of the larger research program. Deliverables for this present proposed work include reports to BOEM documenting progress and guidance for future work, published manuscripts, geodatabases and databases (ArcGIS© and Endnote©, respectively) that include interpreted datasets of seismic profiles and seabed morphology in time-series, seabed geological, geochronological, and geotechnical datasets, and a large collection of reports and articles from a range of sources.

The present study has been conducted in the context of recent research documenting shifting depositional patterns in the lower Mississippi River Delta (MRD), which is a fundamentally different perspective from studies in the era of Coleman et al. (1980), at which time the MRD was thought to be rapidly prograding as it had for centuries. Figure 2 demonstrates that two of the three historically important outlets of the Mississippi River (South Pass and Pass a Loutre) are now exceeded by three other outlets farther upstream, with respect to average annual sediment discharge (Fort St. Philip, Grand Pass, and Baptiste Collette). Sediment discharge from South Pass and Pass a Loutre is probably also impeded by use of these channels for dredge material disposal, by the US Army Corps of Engineers (US-ACE, 2004). Further, numerous studies (reviewed in Blum and Roberts, 2009, 2012; Bentley et al., 2016 [supported by this study]) demonstrate the important long-term declines (> 50% over the past century) of total sediment discharge from the Mississippi.
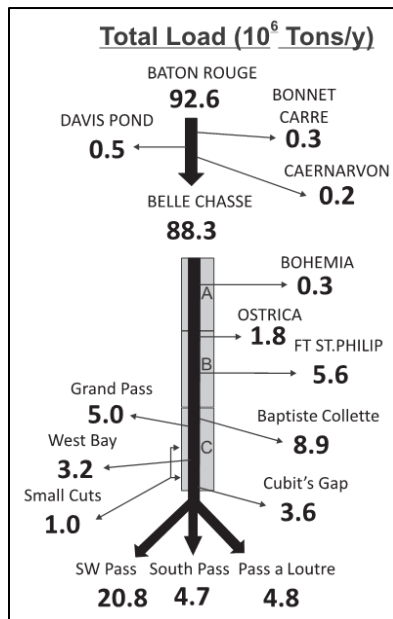
Figure 2. Mississippi River sediment load

Illustration of average annual suspended sediment discharge from all outlets of the lower Mississippi River during flood years 2008–2010, demonstrating that South Pass and Pass a Loutre are no longer major outlets of the Mississippi, in terms of sediment supply. Adapted from Allison et al. 2012.

Important early studies of seabed instabilities on the MRDF indicated that rapid sediment deposition at rates of up to several meters per month played an important role in developing weak, oversteepened regions that were prone to failure. All models and risk matrices published to date are predicated on an unchanged historic sediment discharge from the primary Mississippi River outlets. However, as a result of declining and shifting sediment discharges, we hypothesized in this study that extent and location of areas prone to seabed failure are changing. For example, based on the declining sediment supply to the MRD, and continued marine transport processes, at the start of this project we hypothesized that the delta front is entering or will soon enter a degradational phase, in which seabed erosion will dominate over deposition (and mudflow transport), particularly near areas with the greatest decline in sediment discharge, such as Pass a Loutre and South Pass. Though affirmation of this hypothesis is a major result of this study (project publication Maloney et al., 2018), our evaluations discussed here represent a small first step, and we do not know the potential impacts, or the response time of seabed changes to shifting sedimentation patterns. This condition would have the potential to destabilize seabed infrastructure, such as pipelines, as the delta front degrades.

In this report, we synthesize existing literature and unpublished data relevant to the subaqueous MRD. We critically evaluate the range of seabed morphologies evident in sonar data, and compare with morphological classifications and spatial scales described previously (discussed below). We critically evaluate the range of risk and hazard assessment tools developed to date, and explicitly incorporate seabed-wave effects on initiating SGFs, which have been documented, but not incorporated explicitly into the GIS-based risk assessment tools available (such as Hitchcock et al. 2006). We also critically evaluate the roles of newly developed sediment-transport theory for waves, currents, and fine sediments. This synthesis work has been complemented by pilot field mapping of hotspots identified in data synthesis. Data synthesis and results of our pilot study are then followed by guidance on a path forward for a more comprehensive, long-term study and/or monitoring program of the evolution, mechanics, and processes governing this failure-prone area.

1.2 Study Area, Hypotheses, and Project Objectives

1.2.1 Description of Study Area

A substantial portion of sediments delivered to the ocean by the mouths of the Mississippi River deposit rapidly near the subaerial portions of the delta, forming a subaqueous apron of fine sediments around the subaerial delta, in water depths of 0–200 m. Regions of the MRDF may be defined based on bathymetry as follows, after Coleman et al. (1998): 0-10 m, interdistributary bays; 10–70 m, upper delta front; 70–120 m, intermediate delta front; 120–200 m, lower delta front. Frequent mass-transport processes in this region are largely confined water depths shallower than 200 mbsl. These young sediments retain high water and gas content, and generally possess low strengths, making the deposits prone to failure and mass transport. The slope of this apron is on average very gentle, 1–30 m/km; nevertheless this low gradient is sufficient to allow down-slope flow of sediments under the force of gravity, when local disturbing forces exceed resisting forces. Seabeds that are shaped primarily by sediments transported by waves and currents are generally relatively smooth and undulatory. In contrast, settings like the MRDF that are shaped by sediment instabilities and gravity-driven processes (like slumps, slides, and flows) possess seabed features that are often irregular, with morphologies that can be related to formative processes as described in Fig. 3). In particular, key features of the MRDF created by sediment instabilities include the following, illustrated in Figure 3 (from Coleman et al. 1980, 1998):
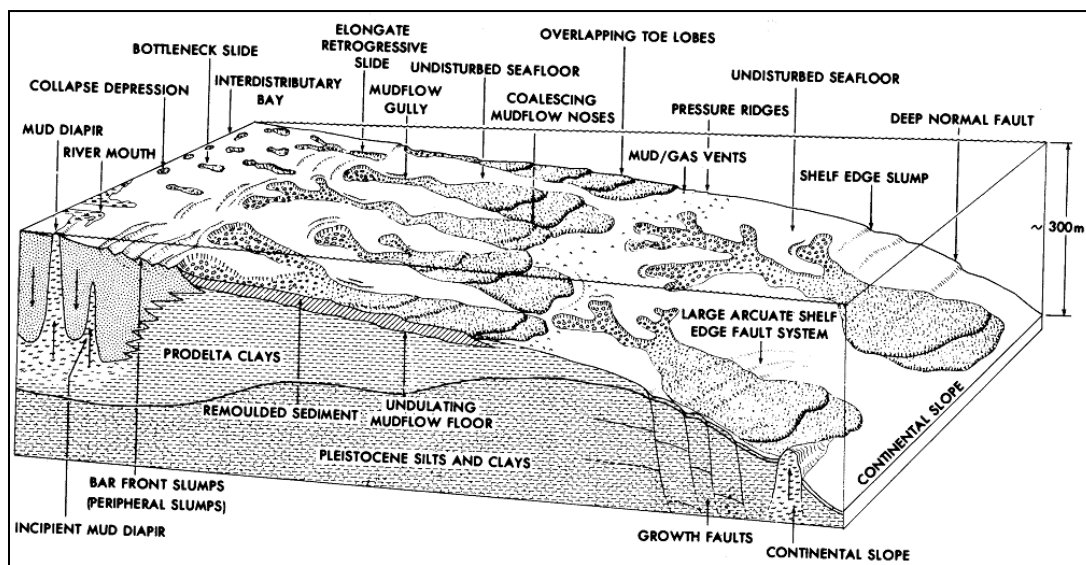
Figure 3. Mississippi River Delta Front geomorphology

Features of the MRDF produced by sediment instability, adapted from Coleman et al. 1980. Features most relevant to this project are described below.

<u>Collapse depressions and bottleneck slides</u>. Water depths to ~15 m, and slopes of <9 m/km (<0.5°). These relatively small features, with depths of < 3 m and lengths of < 600 m are most commonly located in interdistributary bays (bays between major river outlets), and the adjacent upper delta front.

<u>Peripheral rotational slides.</u> Water depths to ~30 m, on slopes of 3–18 m/km (0.17°–1°). These features are most commonly located on seaward slopes of distributary-mouth bars of major river outlets, where sediments deposited closest to river mouths create relatively steep gradients.

<u>Mudflow gullies</u>. Water depths of 7–100 m, on slopes of 3–9 m/km (0.17°–0.5°). These elongate features can consist of channels up to 20 m deeper than the adjacent undisturbed seabed, and contain both soft remolded fluidized sediment and large rigid blocks carried by the flow.

<u>Mudflow lobes.</u> Water depths to ~150 m, slopes <9 m/km (<0.5°). These features commonly form from the coalescence of sediments transported by mudflow gullies. Individual lobes are up to hundreds of meters wide, >1000 m long, and up to 20 m thick, but stacked lobes may form composite features up to 100 m thick. The seabed immediately downslope of mudflow lobes is often disturbed by compressive forces of mudflows, and may contain mud volcanoes and vents that expel fluids from overpressurized sediments below.

<u>Erosional furrows.</u> Coleman et al. (1980) documented the presence of erosional furrows in water >100 m deep in the southern and eastern portions of the study area. These features were shown to be 10–30 m wide, with vertical relief of 1–3 m.

Coleman et al. (1998, p. 880) summarized the major factors contributing to the formation of the above features in water depth of 5–200 m as follows:

1. Rapid sedimentation near river outlets results in widespread loading of the upper delta-front slopes.
2. Coarse-grained sands and silts of the distributary mouth bars have higher bulk density than underlying prodelta clay, differentially loading the underlying clays.
3. Fine-grained delta deposits retain high water content (i.e., are under-consolidated), contributing to large excess pore pressure and low strength.
4. Rapid microbial degradation of organic material in clays leads to the formation of abundant methane, which accumulates as bubbles and also contributes to excess pore pressures.
5. Ocean waves from hurricanes and other storms cause cyclic loading on the sea floor, imparting motion to the soft seabed, allowing dilation and compression of gas bubbles, and creating direct downslope shear stresses on the sea-floor sediments.

Other potential triggers exist, such as earthquakes and critical oversteepening by rapid deposition, and are discussed below.

Previous studies have clearly defined overall morphological characteristics of the seabed; determined that many mass transport phenomena are associated with impacts of hurricane waves; and have demonstrated that these sediment-transport phenomena are significant hazards to offshore infrastructure associated with petroleum exploration and production. The limitations to our knowledge, based on these previous studies, are as follows.

- Much of this understanding is based on three regional seabed bathymetric surveys conducted from 40 to 141 years ago, using methods not nearly as advanced as are possible with current theory and technology, in a geological setting known to be very dynamic over short time periods.
- These findings have demonstrated the occurrence of seabed movements associated with river discharge and storms. However, these previous observations do not provide detail on the rate of the relevant processes (steady compared to pulsed flows, gentle compared to catastrophic), or the

spatial distribution of interacting seabed and wave properties (i.e., cross-shelf changes in wave properties mapped against cross-delta variation in seabed rheology), in part due to the low temporal and spatial resolution of available regional data, and due to the lack of tools at that time for in-situ observation.

- This understanding was developed largely without consideration of annual to decadal changes in river sediment supply and routing, whereas we now know that both the overall supply as well as routing of sediment has changed considerably over recent decades.
- Detailed local studies of more recent seabed failures (i.e., since 1979) and associated infrastructure damage have not been integrated effectively, to provide a more regional perspective. This is important because many of these recent studies (i.e., Hooper 1996; Hooper and Suhayda 2005; Walsh et al. 2006) have been conducted using advanced technology, based on recent theory, and so integration could provide important new detail and insight.

Based on the above evaluation of present knowledge and data availability, we initially proposed three overarching hypotheses, and a series of specific objectives that we have pursued to evaluate our hypotheses.

Hypothesis 1. Based on the declining sediment supply to the MRD, and continued marine transport processes, we hypothesized that the delta front has entered, or will soon enter, a degradational phase, in which seabed erosion will dominate over deposition (and mudflow transport), particularly near areas with the greatest decline in sediment discharge, such as Pass a Loutre and South Pass. Further, based on new developments in our understanding of sediment transport under the combined effects of gravity, waves, and currents (such as coupled effects of storm waves and sediment-gravity flows), we suggest that important sedimentary processes and products identified by earlier studies may be better understood and thus better predicted and their effects mitigated, through our re-evaluation. This hypothesis has been validated to a significant extent in our recent publication Maloney et al. (2018), described in Chapter 2.3.

Hypothesis 2. Based on Henkel (1970) evaluation of wave mechanics and Guidroz (2009) evaluation of wave temporal and spatial variations, with respect to Coleman et al. (1980) morphological characterization of seabed failures on the MRDF, ***we hypothesized that the horizontal scale of the pressure gradient under waves, which is controlled by wave length and height, might be a strong control on the horizontal scale of seabed failures***. This is also supported by the occurrence of smaller failures (collapse depressions and bottleneck slides) near shore, where waves are smaller, and more extensive gullies and lobes in deeper water, where wave length and height are generally greater. This could be evaluated by GIS-based comparison of seabed failure properties with the cross-delta variation of wave length, height, and seabed pressure, as predicted by wave models from previous studies (e.g. Guidroz 2009; Georgiou and Schindler 2009). The results could improve our ability to assess spatial and temporal scales and distributions of seabed hazards. This hypothesis has been partially validated by the analysis in our recent publication, Obelcz et al. (2017), which identified seabed motions forced by annual storm waves that were previously thought too weak to drive seabed mass transport. Significant questions remain, however, which are addressed in Chapter 3.2.

Hypothesis 3. We hypothesized that, on the MRDF, two general classes of mass transport exist: rapid, deep, and extensive failure under large hurricane waves, mostly driven by pressure gradients under waves, and thinner, steadier, and more frequent flows created by interaction of fluidized deposits supported by wave turbulence in the near-bed water column. This hypothesis is based on recently developed theory and observations relating wave resuspension to the formation of wave-enhanced sediment-gravity flows on gradients as low as 0.5 m/km (Wright et al. 2001; Bentley and Nittrouer 2003; Friedrichs and Wright 2004; Rotondo and Bentley 2003; Macquaker et al. 2010; Denommee et al. 2016 and 2017). Although these thinner flows (thickness less than 2–3 m approximately) are not likely to be catastrophic in nature, they present an important mechanism for cross-shelf redistribution of sediments under the combined effects of waves and gravity, that might either increase or decrease local seabed stability, depending on local transport patterns. This theory has not been previously applied to study or

modeling of MRDF sediment dynamics, but this application will be one specific objective of our field and data synthesis activities. Evaluation of this hypothesis awaits collection of seabed hydrodynamic data.

To evaluate the above hypotheses, and further explore sediment dynamics on the MRDF, we pursued the following objectives:

Objective 1: Review of Existing Research. We have reviewed and synthesized relevant research including studies sponsored by BOEM and/or BSEE (MMS-USGS-BLM) since the 1970s and other relevant research conducted in the MRDF and analogous subaqueous delta mass-wasting research globally. Types of research include, but are not restricted to, geotechnical, geomorphic evolution, slide/flow mechanics, rheological, hydrodynamic forcings, and sediment instabilities. Alternative perspectives and new scientific advances (e.g., wave-enhanced sediment-gravity flows described above, and updated and more realistic models of wave-seabed interaction, discussed below) were also considered.

Objective 2: Collection and Review of Unpublished Datasets. We have incorporated existing and previously-unpublished data to better document and understand processes and products of delta front evolution, to advance knowledge beyond what has been captured in the published literature, and to truly assess the current status of data holdings. Data include recent industry subbottom profiler, bathymetry, and side-scan sonar surveys, sediment core or geotechnical data, physical oceanographic parameters, recent storm-associated wave modeling results, available through BOEM, industry repositories, and other agency reports and data sets (e.g., the Federal Emergency Management Agency [FEMA], USACE, and the National Oceanic and Atmospheric Administration [NOAA]).

Objective 3: Evaluation of Research, Data, and Identification of Data Gaps. We have identified major gaps in understanding that should be addressed by new research. As part of this, we have evaluated observed sediment dynamics in the context of recent research documenting shifting depocenters in the MRD as well as advanced concepts and models of mudflow dynamics, as influenced by waves and currents, rather than gravity alone. In addition to the previously discussed seabed properties and processes that contribute to MRDF seabed instabilities, we have undertaken initial evaluation of new questions and topics of seabed landslides, including but not restricted to the following:

- What are spatial and temporal distributions of mass wasting processes and rates (e.g., flows compared to slides, catastrophic compared to pulsed, or quasi-steady)?
- Does evidence exist for/against the triggering of slides and flows by earthquakes and motion along known faults in and near the study area?
- Can acoustic 'wipeout' produced by gas in seismic profiles (i.e., zones in subbottom seismic profiles where sediment layering is masked by the presence of gas) be used to map gas-charged zones, as a proxy measurement for instability?
- Can other advances in understanding muddy seafloor – storm wave interaction, not discussed in this proposal, be used for more effective risk assessment in our study area?
- What is the role of Mississippi River high-discharge events on initial shelf deposition and production of unstable deposits?
- How rapidly do mudflow gully geometry and mudflow lobes evolve? Are the interfluves stable or is there headward and gully wall erosion? What are the spatial timescales over which these rates vary? Can repeated hazard surveys of individual blocks, and newer NOAA (2009) coastal surveys provide relevant insights?

Objective 4: Pilot Field Study of Seabed Hotspots, based on outcomes from objectives 1-3. We conducted two pilot studies of hotspots of deposition and degradation identified in objectives 1 and 2, using advanced seabed imaging sonars and coring ground-truth, that can form the basis for long-term and more extensive future change-detection surveys of the MRDF. Some of the questions posed above involve mapping both the distribution and age of very recent deposits (i.e., Walsh et al. 2006). For these questions, application of radiometric dating methods including $^7Be/^{210}Pb$ were used to provide insight into the age and deposition rates of sediment layers over seasonal, annual, and decadal timescales (e.g.,

Bentley et al. 2002, Rotondo and Bentley 2003, and from this study, Keller et al. 2016) and Methods section below). This pilot field study allowed preliminary evaluation for some hypotheses above, and build on the historical data analysis of Hitchcock et al. (2006).

Objective 5:Plan development for future comprehensive regional observation, monitoring, and modeling study. From the review above, it is apparent that the MRDF is spatially and temporally dynamic over a wide range of temporal and spatial scales, but data and research do not exist that allow us to fully understand processes and products of sediment instability on the MRDF, and the resultant hazards to offshore infrastructure. Accordingly, design of a plan to achieve a better understanding of this complex geological setting was a central component of our study, from a preliminary plan in Y1, to a more fully developed plan incorporated into this final project report.

The preliminary work reported herein only provides a starting point to fully address our hypotheses above. However, during this initial stage of data synthesis and integration, these hypotheses will provide an important theoretical framework for our activities. This preliminary work suggests these hypotheses merit more extensive and detailed evaluation, and can be one element in a larger subsequent study, including field observations and modeling. Both this preliminary study and any related future work are likely to contribute to both basic understanding of these phenomena on other river-dominated deltas, as well as this important risk-related application to MRDF.

1.3 Methods

1.3.1 Data sources

We have worked closely with partners including BOEM (Dr. Michael Miner), BP (Dr. Walter Guidroz, now at USGS), and Louisiana State University (LSU) Coastal Studies Institute (Dr. James Coleman, Boyd Professor Emeritus) to compile data from multiple sources, including but not restricted to examples below:

- Bathymetry and seabed morphology of the MRDF from Coleman et al. (1980), digitized by William Lettis and Associates (Hitchcock et al., 2006), used with permission of BOEM (Fig. 1). This data set includes georeferenced Arc-GIS layers for: bathymetric surveys of 1874, 1940, and 1977–1979; isopachs of sediment accumulation between bathymetric surveys; and location of major instability features identified in 1977–1979 sidescan.
- Multibeam bathymetric grid from Walsh et al.(2006), survey of Southwest Pass region following Hurricane Katrina (Fig. 1), used with the author's permission.
- Previously unpublished mapped wave simulations and other model-generated results across the MRDF of Guidroz (2009) from major hurricanes impacting MRDF (Fig. 4).
- Data from 178 geotechnical borings across the MRDF archived at the LSU Coastal Studies Institute (Dr. James Coleman, personal communication and unpublished data) (data include shear strength, grain size, and other parameters; core locations in Appendix L of Guidroz, 2009).
- Key data sets were acquired through collaboration with BOEM, include digital sidescan, multibeam bathymetry, and subbottom profiles through areas impacted by major hurricanes since 1979 (especially Ivan and Katrina), such as small multibeam mosaics presented in Hitchcock et al. (2006), collected after Katrina, a post-Katrina pipeline survey of South Pass 53 and vicinity collected by Enterprise Associates (2005). The Enterprise (2005) data set is one of 46 site surveys used by Guidroz. Dr. Guidroz was a geophysics manager at BP at the time, and had excellent data access through company holdings.

These and other previously unpublished interpretations of data collected by OCS lease holders for compliance with BOEM's shallow hazards and archeological resources survey requirements were incorporated into the spatial database and analyzed as below. The reports and associated maps from these block surveys, intended to identify and map many of the seafloor and sub-seafloor features that are the

focus of this study, were provided to LSU by BOEM for areas available within the study area. After acquiring many bathymetric surveys, we decided to analyze only digital multi-beam surveys, with or without accompanying side-scan data.

1.3.2 Data integration

Data from sources identified above was incorporated into geodatabases of several types, to facilitate the most effective comparison and visualization, depending on the type of data (e.g., core-based geotechnical data and lithologic logs, geospatial data sets such as bathymetry [Fig. 1], or wave simulations [Fig. 4], as examples). ArcGIS® is a widely available geographic information system that served as the backbone for our data integration. Many types of georeferenced data can be incorporated into ArcGIS® projects, and the software allows for versatile mathematical comparisons and transformations of different data layers, such as analysis of bathymetric change from one survey to another.
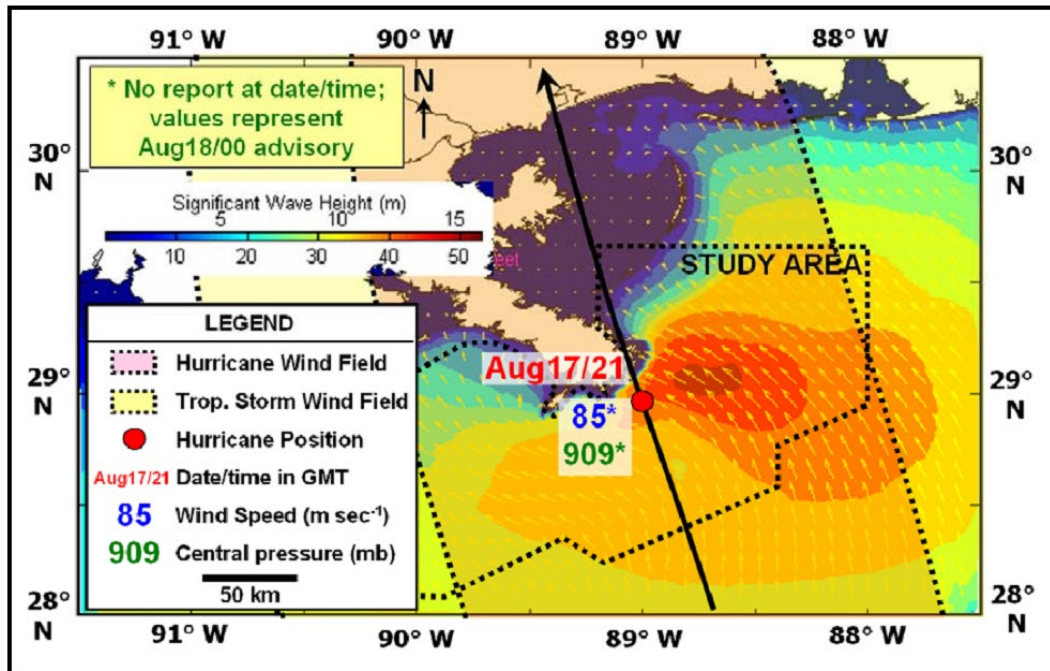
Figure 4. Waves produced by Hurricane Camille

Hurricane Camille, August 17, 1969 2100 Z, near time of landfall, significant wave height results from simulation conducted by Guidroz (2009).
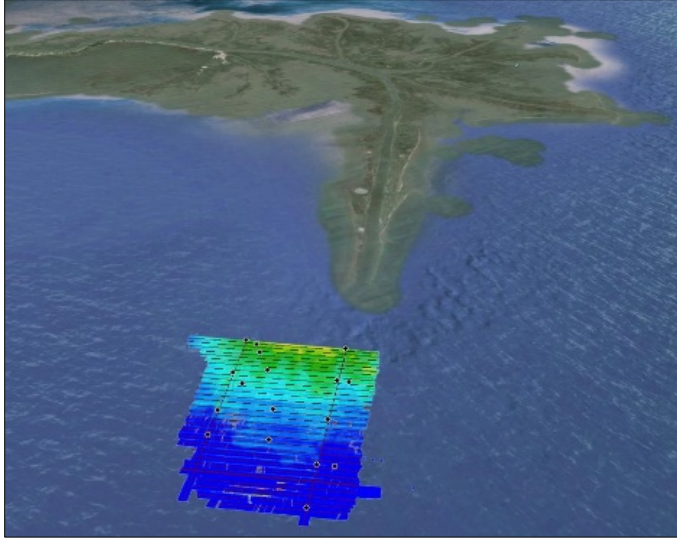
Figure 5. Perspective view of Southwest Pass in 3D visualization software

Perspective view of Southwest Pass generated in Fledermaus, showing land area, and the 2014 Pilot Study swath survey described in Obelcz et al. (2017) and Chapter 3.2.
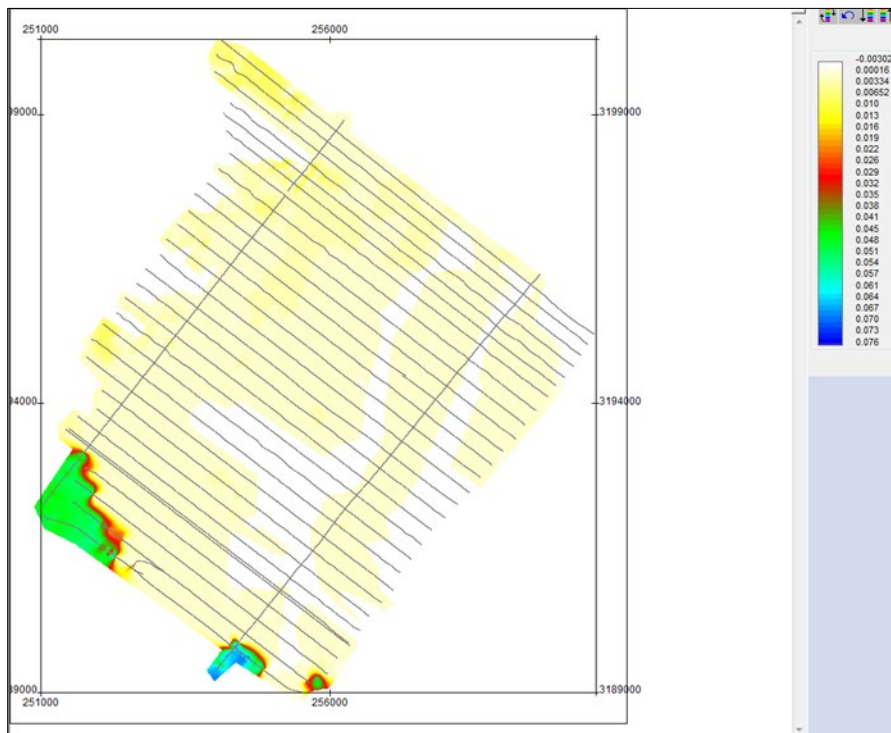
Figure 6. Example geoacoustic model using Kingdom software

Example of Kingdom Suite project map of the Southwest Pass study area, showing depth to gas-charged sediments (represented in two-way travel time of sound, in milliseconds) interpreted from CHIRP data. Black lines are traces of CHIRP seismic profiles, as shown in Figure 10 below. Horizontal and vertical axes are in meters, UTM projection.

A second software tool that the team has used for visualization and analysis is Fledermaus 4D, which is widely used for integration and study of bathymetric and seismic data, as shown in Figure 5. Fledermaus allows geospatial data to be rendered in 3D for "fly throughs", and also allows evaluation and animation of time-series datasets, for example to evaluate seabed morphology change through time. The third

software system that was used for this project is Kingdom Suite. Kingdom Suite is an industry-standard platform for integration and study of geological, geotechnical, and seismic data sets, including core data, seismic cross sections, or integrated geoacoustic data, as shown in Figure 6. Kingdom is more suited to the integration of seismic and bathymetric data than either ArcGIS® or Fledermaus, but is also more complex and expensive. LSU Geology and Geophysics maintains a site license for Kingdom, which was used for this study.

The ability to render, display, and evaluate these data sets in 3D plus time has greatly facilitated our ability to explore interrelations among forcing and destabilizing mechanisms (slope, waves, gassy sediments), and resultant bathymetry and morphology.

1.3.3 Data analysis and synthesis: initial theoretical framework

The following paragraphs present the initial theoretical framework for our analysis.

Sediment-gravity flows (SGFs) are initiated when disturbing forces exceed forces resisting motion. For the case of the MRDF, numerous studies have demonstrated that important seabed characteristics involved in disturbing motion include seabed slope (steeper slopes are more prone to SGFs), seabed strength (weak soils are more prone to failure), as well as seabed history (recently disturbed and/or deposited sediments may be, but are not always, more prone to failure than sediments long in place) (Henkel, 1970; Suhayda and Prior, 1978, and many others). These factors have been incorporated into geotechnical models (Hooper and Suhayda, 2005; Guidroz, 2009) and GIS-based risk-assessment matrices tools developed by Hitchcock et al. (2006) and Guidroz (2009) to evaluate potential seabed instability on the MRDF. The presence of gas in sediments (produced by microbial degradation of sediments) is also a factor, via the ability of gas bubbles to dilate and contract under pressure changes, thus weakening seabed strength. The impact of gas has been discussed extensively (Coleman et al. 1974; Whelan et al. 1975; Guidroz 2009, and many others), but has not been incorporated as an explicit term into risk assessment tools of which we are aware. (Specific studies of gas impacts on SGFs in our study area have not been conducted since the 1980s.) These factors combined (i.e., steep slopes and weak sediments) can create conditions conducive to generation of SGFs, but are not often sufficient alone to instigate flows. Generally, additional disturbing forces are thought to be necessary or at least important, for the generation of deep and extensive SGFs on the MRDF.

Ocean waves created by hurricanes are the most powerful, frequent, and widely accepted mechanism for providing additional disturbing force to instigate SGFs on the MRDF (Coleman et al. 1974; Hooper 1996; Hooper and Suhayda 2005, and many others). Ocean waves interact with the seabed in three ways to help induce seabed failures: (1) Change in pressure on the seabed created by a passing wave form (i.e., as first the trough then the crest passes a location) creates a change in pressure on the seabed under the wave, that is a function of water depth, wavelength, wave height, and wave period (Wright, 1995). The local change in pressure can cause excess pore-water pressures (including compression and dilation of gas bubbles, where present in the sediment), which can act to weaken seabed strength. (2) This same pressure difference beneath trough and crest also creates a lateral pressure gradient (Fig. 7) (Henkel 1970). The passing wave form, creating a laterally moving pressure field on the seabed, can also cause vertical and horizontal deformations of the seabed, thereby contributing to sediment softening. Key early studies include Forristall and Reese (1985), and Hooper (1996). Three studies resulting from this project include Obelcz et al. (2017) and Denommee et al. (2016 and 2017), which demonstrated that waves from routine annual storms (i.e., much smaller than hurricane waves) are also capable of inducing SGFs. (3) Direct current motion (peak bottom orbital velocity, or U_{bmax} [m/s]) at the seabed produced by waves also provides a force parallel to the seabed, quantified as a wave-generated bed-shear stress τ_w, that can both erode sediment, and impart motion to the seabed.

Δp	Magnitude of pressure change	
γ'z	Submerged weight of sediment	
L	Wavelength	
x	Half length	
2θ	Arc of sliding	
β	Slope angle	
z	Water depth	
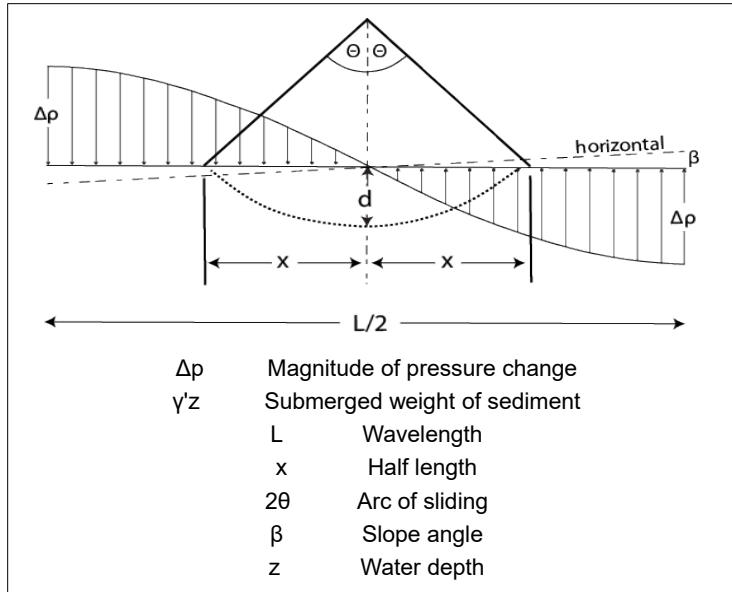
Figure 7. Henkel's (1970) model

Schematic diagram from Henkel (1970; redrafted by Denommee et al. 2017) illustrating the relationships among seabed pressure gradients (2Δp) created beneath an ocean wave of wavelength L, seabed slope angle β, and slide length 2x.

Guidroz (2009) conducted an extensive numerical study of seabed wave impacts on the MRDF from the most powerful hurricanes to strike the MRDF since the onset of petroleum exploration and production (Betsy [1965], Camille [1969], Andrew [1992], Ivan [2004], and Katrina [2005]). This work involved shelf-wide computer simulations of waves created by these storms, for the full history of each hurricane, followed by an examination of evidence for seabed failures associated with each hurricane. An example of wave modeling results is shown in Figure 4.

Guidroz (2009) demonstrated several important factors regarding the impact of hurricane waves on the MRDF. First, each hurricane created unique wave conditions controlled by the direction of approach, hurricane forward speed, hurricane size, and intensity. As a result, an infinite number of simulations would be required to simulate all possible outcomes for all hurricanes. Second, although seabed mapping observations were limited in some cases, sufficient seabed bathymetric data were available to study SGFs in association with each hurricane. Third, although each hurricane was unique, Guidroz observed that in general, extensive seabed failures only occurred where/when significant wave heights exceeded 15 m at a location with a time exposure of seven hours or more. Finally, simulations of seabed pressure, bed shear stress, and documented seabed failures suggested that both pressure variations and bed shear stress contributed to seabed failures. Evaluating the history of hurricanes impacting the MRDF since 1851 demonstrates that only three hurricanes in this period (Katrina, Ivan, and Camille) met these criteria of intensity and relatively long duration on the MRDF.

Guidroz's (2009) determination of approximate threshold wave criteria required to generate SGFs on the MRDF provides a tool for improving existing GIS-based risk assessment tools, by allowing inclusion of georeferenced wave data and simulations, for comparison with georeferenced seabed characteristics. We can simulate worst case scenario for threshold wave conditions, assuming that at each location, waves meeting threshold criteria arrive from directions perpendicular to the local bathymetric slope, experience no energy attenuation due to interaction with the soft seabed, and no change in wave characteristics due to shoaling and refraction. With these conservative simplifications, the change of wavelength and wave height from deep water conditions can be easily predicted based on linear wave theory. These results can then be used to compute seabed pressure fluctuations and bed shear stresses, as below, which are first-order controls on initiation of SGFs. Additionally, we compared these predictions using selected non-

linear theories, to better constrain the impact of differential pressures on the seabed, by a simple proof-of-concept application of a fully non-linear numerical model FLOW3D, which can better simulate the free surface of a wave form, to help establish variance and uncertainty in the predictions from linear wave theory. Comparisons of results from linear and non-linear wave theory and the generation of SGFs are given in Chapter 3.2, and demonstrate that linear theory under predicts forces applied by actual ocean waves (Obelcz et al. 2017).

Maximum and minimum pressures on the seafloor (P) during passing of a wave trough and crest can be calculated using linear wave theory from prescribed wave period (seconds), water depth, and wavelength (Wright 1995, p. 56), which can also be calculated from water depth and wave period (Wright 1995, p. 56). Wave height (H) can be calculated using linear wave theory from prescribed deep water wave height (H_d), shoaling coefficient K, and group velocity in intermediate and deep water depths (Cg and Cg_d, respectively):

$$H = H_d \frac{Cg_d}{Cg} K \qquad\qquad \text{Equation 1}$$

Maximum local wave height will occur where waves approach shore parallel to local bed slope, in which case K=1 (Kinsman 1984, p. 153–158). Henkel (1970) evaluation on the controls of ocean waves on seabed failures (Fig. 7) suggests that the spatial scale of seabed failure (such as the initial length of seabed that fails) is related to wavelength, which generally decreases as waves progress into shallower water. We evaluated this hypothesis in part (Obelcz et al. 2017), but more work remains (Chapter 5).

1.3.4 2014 pilot field study

Methods for the 2014 Pilot Study are described below, and results from the 2014 Pilot Study are described in Chapter 3. During the first year of the proposed project, we searched for "hot spots" of seabed change, through comparison of all collocated time-series data we have for seabed properties (for example, comparison of the Walsh et al. [2006] seabed morphology with Coleman et al.'s [1980] sidescan and bathymetry data) (Fig. 1). Based on this evaluation, we executed the first pilot-scale field program described below, during Summer 2014, near the end of Y1 and start of Y2. The objectives of this study were to field-test hypotheses and concepts developed during the first year of the study, and evaluate field and data processing approaches that can be pursued in future work that might be more extensive and in-depth.

The R/V *Coastal Profiler* from LSU's Coastal Studies Institute (LSU-CSI) was used to collect three types of geophysical data (swath bathymetry, Chirp sub-bottom profiler and sidescan sonar) at the selected study area offshore of the MRDF. An Edgetech 4600 swath bathymetry and sidescan sonar system was used to collect data up to four times water depth in width (shown in Figure 8). The 4600 system produces real-time high resolution three dimensional maps of the seafloor while providing co-registered simultaneous sidescan (example in Fig. 9 for collapse depressions in deltaic muds on the SW Louisiana coast) and bathymetric data. Seafloor features, such as mudslides and erosional furrow structures, can be captured. Edgetech 2000 DSS combined sidescan sonar & sub-bottom profiler system was used to collect CHIRP seismic profiles using a range of frequency of 2–16 kHz and sidescan data using simultaneous frequencies at both 100 and 400 kHz. The 2000 DSS system's working depth is up to 2,000 m, and its CHIRP seismic profiles can reveal erosional and depositional structure with a vertical resolution of 6–10 cm and a 60 m penetration depth on muddy sea floor. Another seismic profiler, Edgetech 0512i, was used simultaneously with Edgetech 2000 to collect seismic data using frequencies of 0.5 to 12 kHz, with a deeper penetration depth of 200m but lower vertical resolution of 8–20cm. The R/V *Coastal Profiler* was berthed at Venice, Louisiana and used to collect data on the MRDF. A total of 11 days of R/V *Coastal Profiler* were budgeted for the field work. During this time, we surveyed ~60 km^2, between water depths of 20 and 80 m. Swath bathymetry coverage varied between 80-400 m width per swath. This area is comparable to that of Walsh et al. (2006) post-Katrina survey (Chapter 3.2).
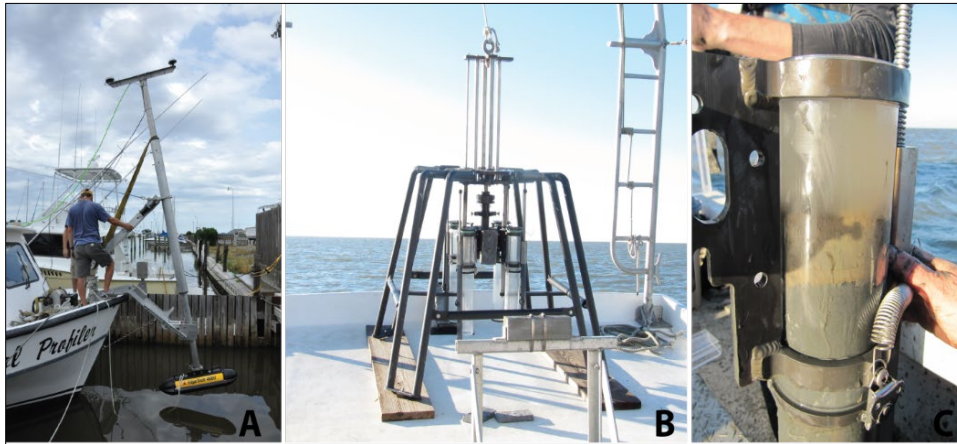
Figure 8. Instruments used for 2014 pilot study

Illustrations of the bow-mounted Edgetech 4600 swath system owned by LSU-CSI on the R/V *Coastal Profiler* (A), as well as the multicorer (B), with example core (C).
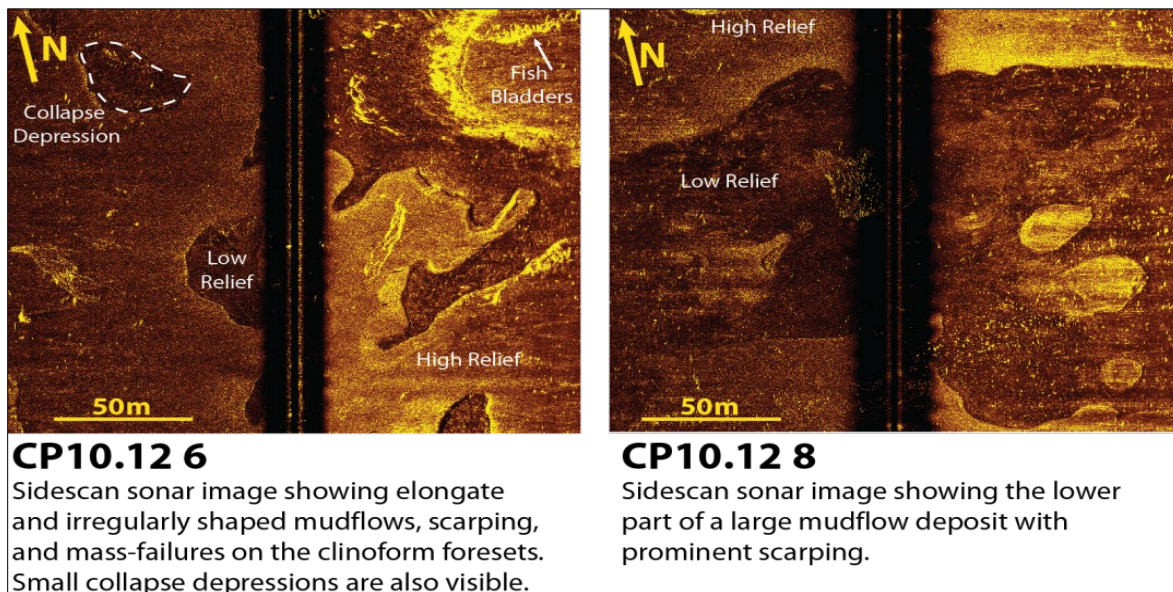
Figure 9. Example sonar maps of collapse depressions and bottleneck slides

Seabed sonar data collected with LSU-CSI Edgetech 4600 swath/sidescan, in an inner-shelf mudflow region south of Pecan Island, Louisiana (adapted from Dennomee et al. 2017). Example sidescan images of collapse depressions (labeled in upper left), mudflow channels (dark elongate regions in left and right images) with isolated harder sediment blocks. These morphologies and sediment types are very similar to those described by Coleman et al. (1980).

Based on real-time evaluation of geophysical data in the field (e.g., Figs. 9 and 10), core sediment samples were collected to target specific features of interest (e.g., slumps, mudslides). Two types of coring devices were used for sediment collection. An Ocean Instruments four-tube multi-corer was used to collect short cores (about 0.5m) which preserve the water-sediment interface very well (Fig. 8B and 8C). Another gravity corer was used to collect longer core with a maximum penetration of about 3 m in muddy sediment. The multicorer, gravity corer, and Edgetech 512i are presently owned by LSU-CSI. The

LSU-CSI Edgetech 4600 system is presently equipped with a 460 kHz transducer (Fig. 8A), but a 230 kHz transducer was rented for this project.
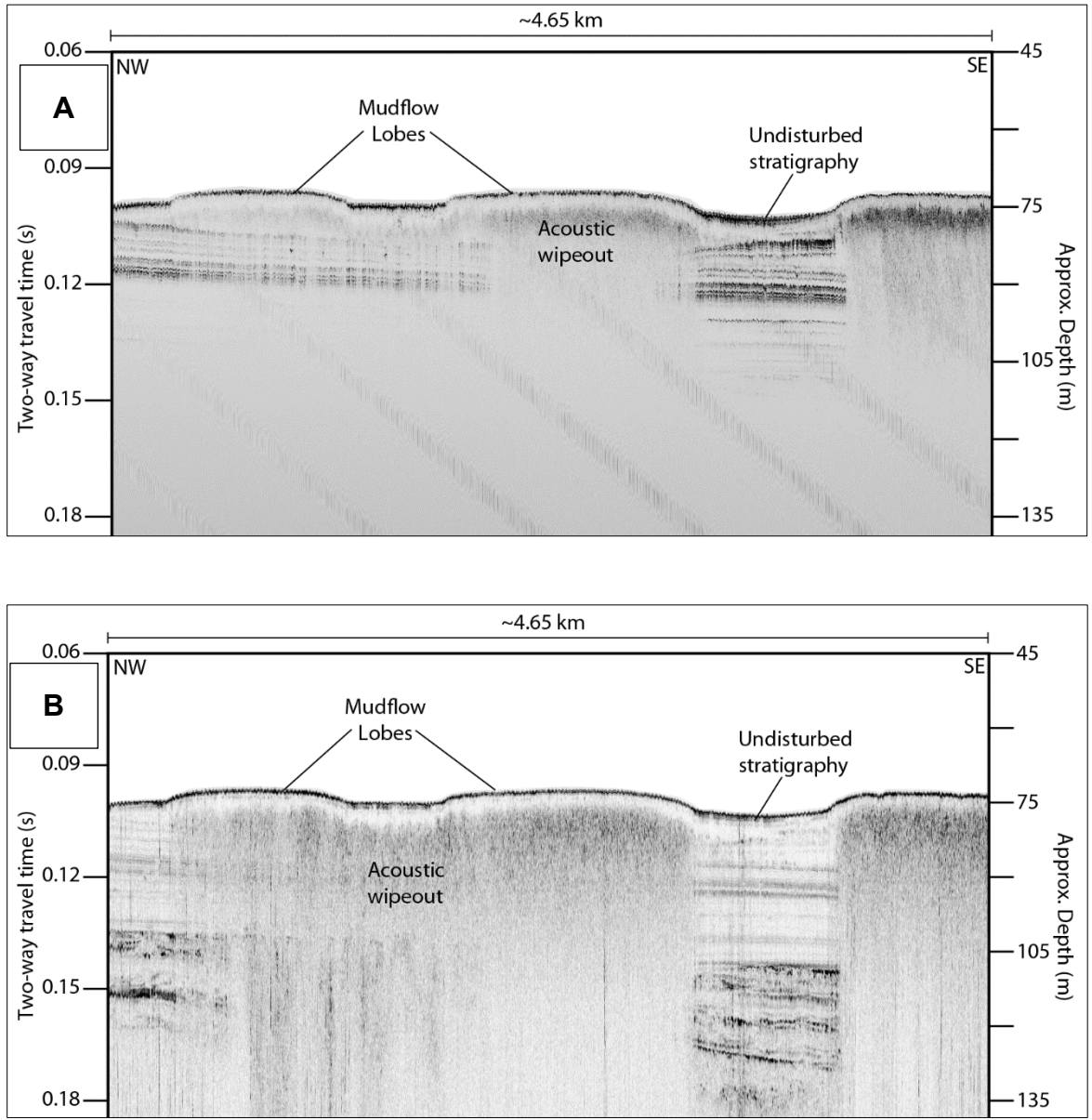
Figure 10. Subbottom data for two CHIRP SONAR systems

Example CHIRP subbottom data collected on the R/V *Coastal Profiler* simultaneously with the sidescan in Figure 9. Gas in the seabed masks sediment layering on the left side of the image, but sediment layering is readily visible on the right side of the image. A) Higher resolution (EdgeTech 2000 DSS) data image shallow structures at penetration depths up to ~35 m below seafloor with better vertical resolution. B) Lower resolution (EdgeTech 0512i) data image deeper, up to ~60 m below seafloor, but the fine scale stratigraphy observed in A is not evident. Area of acoustic wipeout indicates the presence of gas in the seabed, in both cases nearly reaching the sediment surface, as shown in Figure 6.

1.3.5 2017 pilot study

Methods for the 2017 pilot study are described below, and results from the 2017 field work are described in Chapter 3.3. Field observations for the 2017 pilot study were carried out in two cruises on board the R/V *Point Sur*, operating out of Gulfport, Mississippi. The first cruise was led by Dr. Jason Chaytor of the USGS during May 19–26, 2017, with LSU participants Bentley and Xu. The primary objective of the

cruise was to assess the suitability of seafloor mapping and shallow sub-surface imaging tools in the challenging environmental conditions found across delta fronts (e.g., variably-distributed water column stratification and wide-spread biogenic gas in the shallow subsurface). More than 600 km of multibeam bathymetry/backscatter/water column data (dual head Reson T20P), 425 km of towed CHIRP data (Edgetech 512i), and >500 km of multi-channel seismic data (boomer/mini-sparker sources, 32-channel Geoeel streamer) were collected. Varied mudflow (gully, lobe), pro-delta morphologies, and structural features, some of which have been surveyed more than once, were imaged in selected survey areas from Pass a Loutre to Southwest Pass.
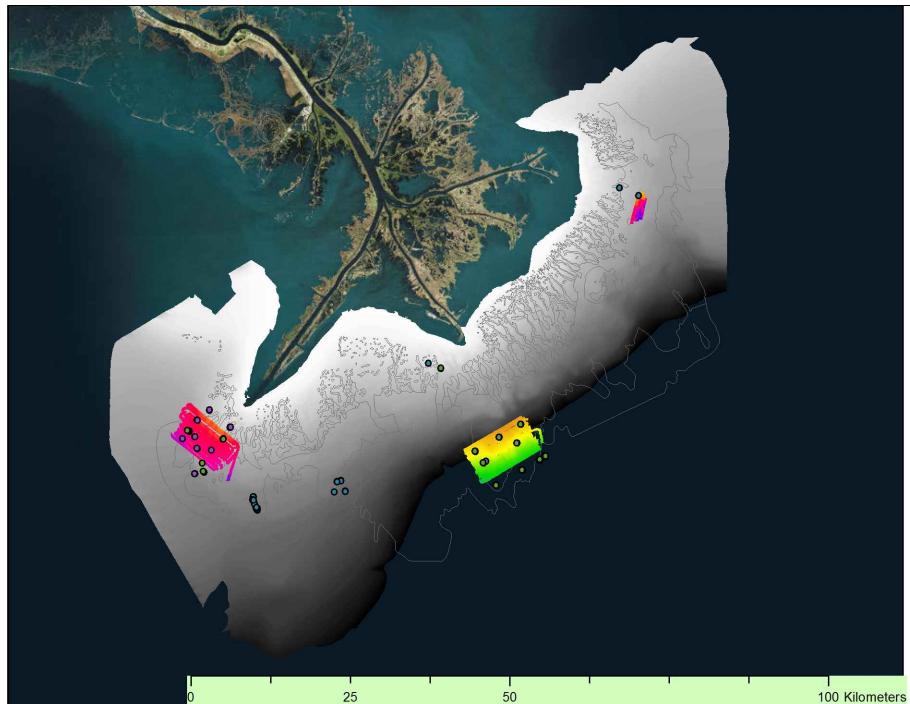
Figure 11. Map of 2017 pilot study surveys and core locations

Map of MRDF region (shaded gray) with multibeam grids surveyed by USGS shown in color, and with coring and cone penetrometer stations shown as colored dots.

The second cruise of the 2017 pilot study occurred June 2–9, 2017, and was focused on geological and geotechnical sampling of seabed locations mapped on the previous US Geological Survey (USGS) cruise. Cruise participants included personnel from LSU, the University of New Orleans (UNO), San Diego State University (SDSU), the US Naval Research Lab (NRL), and MARUM, University of Bremen. Sampling tools included an Ocean Instruments MC800 multicorer that belonged to the ship (10 x 60 cm cores), a Benthos piston corer (7.5 cm x 9 m cores) provided by LSU, and a free-fall cone penetrometer (penetration depth 2.5–8.5 m) provided by the University of Bremen.
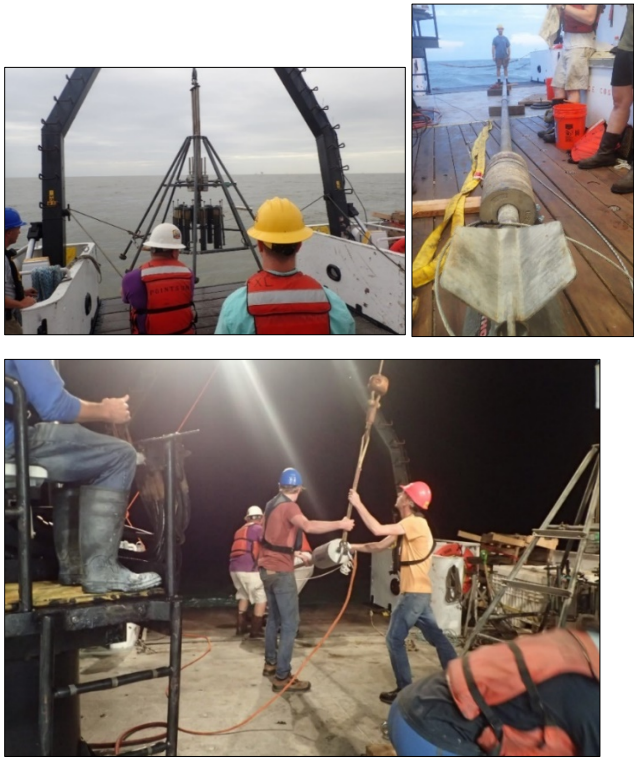
Figure 12. 2017 operation of multicorer, piston corer, and cone penetrometer

MC800 multicorer (above left) and Benthos piston corer (above right) used for core collection in 2017; (bottom) recovery of the MARUM free-fall cone penetrometer.
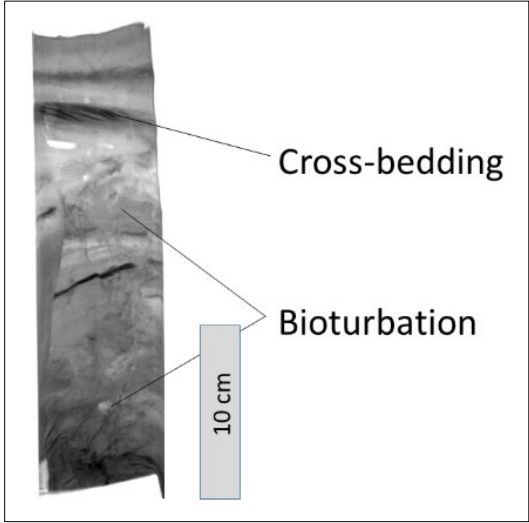
Figure 13. X-radiograph of gully core

1.3.6 Geological core analysis

2014 pilot study: Laboratory analyses included: laser-diffraction granulometry; radioisotope geochronological analyses, multi-sensor logging for P-wave speed and bulk density using a Geotek Multi Sensor Core Logger, and digital X-radiography of cores to study sediment layering (Fig. 13); as well as triaxial shear strength test (by lab on UNO Campus; Georgiou). Sediment geochronological analyses were conducted through gamma spectrometric analysis of the radioisotopes ^{234}Th, ^{7}Be, ^{210}Pb, and ^{137}Cs, which can be used to determine sedimentation rates and absolute ages of sediment layers over timescales of weeks to months (using ^{234}Th and ^{7}Be) to decades (with ^{210}Pb and ^{137}Cs). By learning the relationships among sediment layering, age of sediment deposits, and sediment density and strength, among other factors, we were able to begin to evaluate absolute rates of geological processes, such as mudflow transport and plume sedimentation rates (examples include the project publication of Keller et al. [2016] and project conference presentation of Courtois et al. [2017]). These geological data will are used to help identify characteristics of important processes, to aid in the interpretation of geophysical data, and to provide a baseline dataset for the comparison with future studies.

2017 pilot study: After initial collection at each station, separate cores were chosen for radiochemistry, X-radiography, and a third to be archived. Cores chosen for radiochemical analysis were subsampled at 2 cm intervals immediately following initial collection aboard the vessel. X-radiograph cores were also subsampled following initial collection and stored into acrylic trays (2 cm thickness). Acrylic trays used for X-radiography were comprised of two pieces; the first piece was inserted into the core tube following the second to seal the tray as to not disturb any sedimentary features. All samples were stored in a cold room (4°C) following the return of the cruise until analysis.

Radiochemical analysis on 11 multicores was performed immediately following the return from the cruise. Analysis was completed in the sedimentology lab at the Louisiana State University Geology Department. Samples were analyzed for Beryllium-7 (half-life of 53.2 days) to quantify short-term sediment accumulation rates. Before testing samples for ^{7}Be activity, the samples were weighed and dried for 24 hours to remove water content, then ground up using a mortar and pestle and then sealed into petri dishes. All samples run for ^{7}Be activity were analyzed within one half-life of ^{7}Be after initial collection. Samples were analyzed on Canberra detectors and each core was restricted to a single detector. Detection of ^{7}Be activity is associated with a 477 keV peak from radiochemical analysis.

The 31 piston cores (5–9m in length) collected in June 2017 were run on the Geotek MSCL core logger for bulk density, magnetic susceptibility, impedance, resistivity, P-wave amplitude, and P-wave velocity measurements down core. Plots of magnetic susceptibility, bulk density, and resistivity were created for each core. Distinct variations in down core measurements are recognizable in the plots and infer a heterogeneous substrate (Figure 9). Seismic facies have been assigned to coring locations based on the geophysical data collected in May 2017. The pairing of seismic facies in the study area with down core plots of data from the Geotek MSCL core logger allows for preliminary interpretations to be made on: variations in sedimentation, consolidation, biogenic gas production, and zones of weakness across the delta front.

2. Results of Data Review and Synthesis

2.1 Description of the Geodatabase (ARC Project)

We established an ArcGIS™ database to compile existing datasets across the Mississippi River Delta Front (MRDF) (Fig. 14). The database contains relevant background data including offshore infrastructure (pipelines, platforms), lease blocks, and regional National Oceniac and Atmospheric Administration (NOAA) bathymetry. Selected historical charts have been georeferenced to verify older data and interpret long-term delta morphology. Across the MRDF, the following geophysical datasets have also been added to the database:

- 29 gridded bathymetry files created from NOAA Hydrographic Survey data ranging from 1900-2009
- Maps 2–7 from Coleman et al. (1980), digitized for Hitchcock et al. (2006)
- 40 gridded bathymetry files from Guidroz (2009) (3 multibeam)
- Multibeam bathymetry from Walsh et al. (2006)
- Five multibeam bathymetry datasets from Fugro Geoservices, Inc.
- Data sets developed by the Principle Investigators of this project, for Keller et. al (2016), Obelcz et al. (2017) and Maloney et al. (2018).

It is important to understand the limitations of working with the bathymetric datasets contained in the geodatabase. Of all the digitized bathymetry datasets collected thus far, only nine are multibeam bathymetry data. The remaining were gridded from single-beam surveys or hydrographic charts with variable spacing between soundings. Multibeam bathymetry data provides much higher resolution data with almost 100% seafloor coverage, resulting in very little interpolation. Multibeam surveys are ideal for observing fine scale morphology and measuring seafloor change through time. Though the lower resolution, single-beam surveys are useful for observing large scale, long term trends, multibeam data can provide better constraints on mudslide patterns and rates of change.

Furthermore, in order to accurately compare multiple bathymetry datasets, they must be referenced to the same vertical datum. Some of the newer NOAA datasets and navigation charts reference a datum such as mean lower low water (MLLW), but older datasets often are simply referenced to the sea surface, without tidal corrections. In other cases, a vertical reference is not indicated at all. The sea surface height fluctuation due to tides around the MRDF is ~0.5 m. Although this change is relatively small, it does introduce uncertainty into any quantitative assessment of sea floor change through time. Additional vertical uncertainty may exist in several datasets where an assumed sound velocity was used to convert travel time to depth. In the case of the Coleman 1977–1979 data, a single beam echosounder was used and depths were calculated assuming a constant 1,524 m/s (5,000 ft/s) sound velocity in the water. Sound velocity varies with temperature and salinity, which both change dramatically across the MRDF and with depth. The sea surface temperature can range from 4.5–32°C over the course of a year and salinity varies between the fresh Mississippi River plume and the seawater of the northern Gulf of Mexico. These conditions can result in a range of potential sound velocities from 1424-1550 m/s. At ~100 m water depth, this range translates to ~8 m of uncertainty, with increasing uncertainty at greater depths. Although this is likely an overestimate of uncertainty, it illustrates the need for well constrained, modern survey techniques in order to track changes in bathymetry through time. A more detailed evaluation of uncertainty in comparing different types of data sets is provided as supplementary material for Maloney et al. (2018), which is a time-series study of bathymetric change on the MRDF.

We also worked with Fugro Geoservices, Inc. (Fugro) and C&C Technologies, Inc. (C&C) to identify and obtain multibeam surveys conducted in the last 10 years. Fugro provided a list of 15 projects with multibeam data. We were granted access to two surveys. These include a W&T Offshore survey covering West Delta 106-108 lease blocks and a Stone Energy survey covering South Pass 70-Mississippi Canyon

107 lease blocks. The W&T dataset was located over the same area as our pilot survey and a 2005 dataset, and provided us with an intermediate time step (2009) to assess changes to the seafloor morphology. Three additional datasets were also acquired from Fugro based on surveys for Chevron (Mississippi Canyon 63), Shell, (Main Pass 151–73), and Energy XXI (South Pass 34 & 39). C&C Technologies provided a list of 55 projects conducted on the MRDF since 2004. For surveys where permission was granted, we obtained the data from Fugro and C&C, and it has been added to the geodatabase.
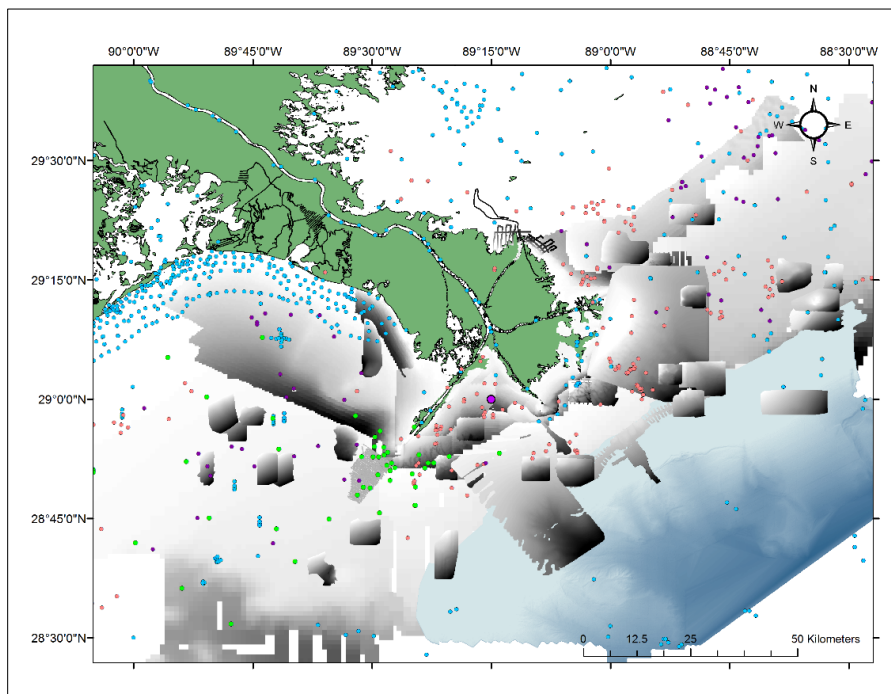
Figure 14. Study area map showing data sets in geodatabase

Image showing ArcGIS™ geodatabase with selection of bathymetric datasets and sediment core locations visible across the offshore Mississippi River Delta. The geodatabase also includes infrastructure data, historical charts, and data products from the data synthesis and pilot studies.

In addition to geophysical datasets, we also included four sets of geotechnical borehole data in the Arc GIS™ geodatabase. These include data from the US Geological Survey (USGS) usSEABED database (USGS and University of Colorado 2006), a Louisiana State University-Coastal Studies Institute (LSU-CSI) database (Guidroz 2009), an OTRC database (Dunlap et al. 2004), and a RAPID cruise from 2005 (Walsh et al. 2006). The attribute tables for each set of cores includes some information on geotechnical and geologic data. PDF files of core logs are also available for the LSU-CSI cores and the OTRC cores.

During analysis of the datasets, several new files were generated and are now also included in the geodatabase. These files include seafloor contours, difference of depth maps, and slope maps. Datasets acquired during the 2014 and 2017 pilot studies were also incorporated into the geodatabase. The compiled datasets have been studied to assess their utility, identify data gaps, and chart trends in MRDF sediment processes. See Chapter 2.3 for more details.

2.2 Endnote© Literature Database

We have collected and organized a database of over 370 publications related to the MRDF, MRDF landslides, and relevant global delta and submarine landslide studies, spanning the years 1939–2018. The database is available as an Endnote© citation-management software library with attached digital copies of each publication, where available (Fig. 15). Additionally, literature specific to the MRDF published from

31

1955–2014 was organized into a Microsoft® Excel® spreadsheet which identifies up to two major subjects per study (e.g., morphology, geotechnical properties, geochemistry), the primary methods used, and provides a concise summary of major contributions. The Excel® spreadsheet has been used to plot trends and identify gaps in research topics through time (Fig. 16).
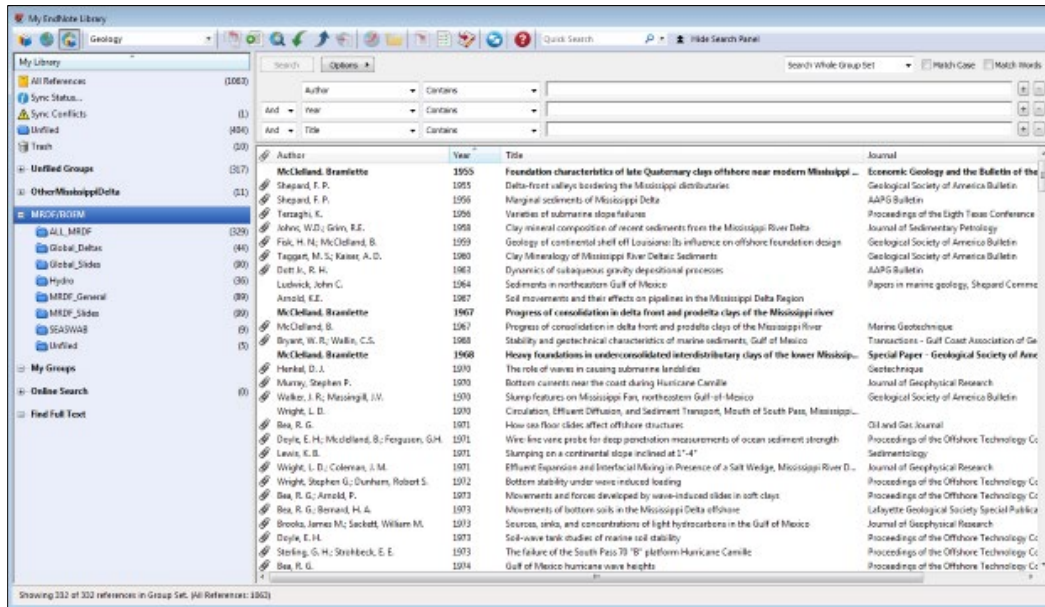
Figure 15. MRDF Endnote© database

Screenshot of MRDF Endnote© database containing >370 references related to submarine landslides, global deltas, and the Mississippi River Delta.

The synthesis of these articles and reports is presented in chapter 2.3, and is being adapted for an invited review journal article in Elsevier's *Earth Science Reviews*, for submission in late 2018. The literature database is an extensive gathering of research conducted on the MRDF that can easily be queried for future research and hazard assessment projects.
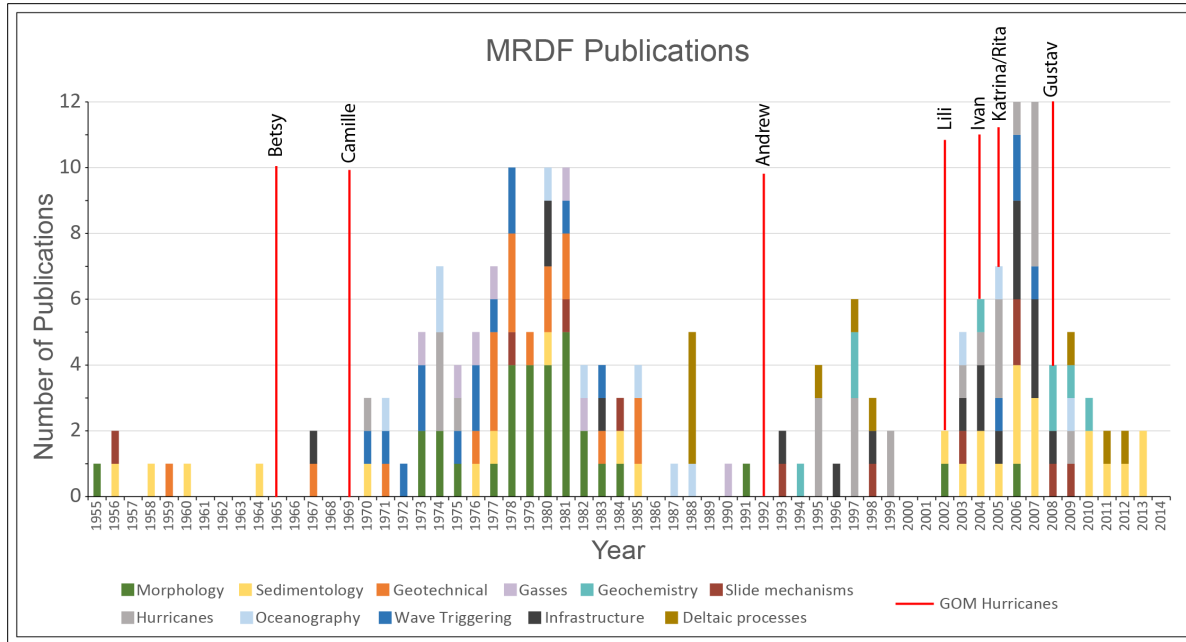
Figure 16. MRDF publications through time

Chart of publications on MRDF processes grouped by subject and plotted through time. Red lines mark several major hurricanes in the Gulf of Mexico and are labeled with the storm name. The largest outputs are associated with hurricanes (e.g., increase after Betsy and Camille, and again with Lili, Ivan, Katrina, and Rita). Research in the late 1970s–1980s focused on seafloor morphology and geotechnical properties; research in the 2000s was often related to sediment processes and oceanographic modeling.

2.3 Literature Review, Synthesis, and Determination of Data Gaps

2.3.1 Introduction

This section reviews and synthesizes geological and geotechnical research on the MRDF, particularly with respect to SGFs: their occurrence, geological and geotechnical controls, triggering mechanisms, and knowledge gaps related thereto. These insights will be used to guide recommendations for future research, presented in Chapter 5.

The Mississippi River Delta is one of the most well studied deltas in the world. The earliest research focused on subaerial portions of the delta (e.g., Russell and Russell, 1939), but in the 1950s, significant research efforts began offshore, prompted by the commencement of oil and gas exploration on the shelf. Since that time, a wealth of knowledge and data has been generated on subaqueous processes of the MRDF, defined here as the area of the delta between ~5–200 meters below sea level (mbsl) (Coleman et al., 1998) (Fig. 17). Much of that work focused on submarine landslides, which have been identified as a hazard to offshore infrastructure. Evidence for landslides on the MRDF was first identified by Shepherd (1955) in bathymetry data that showed a series of shallow valleys creasing the subaqueous delta. Shepherd attributed these features to sediment mass movements. In 1969, three offshore platforms were damaged during Hurricane Camille, and it was found that the damage was caused by submarine landslides (Bea, 1971). Since the early 1970s, numerous studies have demonstrated that submarine landslides are a common occurrence on the MRDF and research efforts have attempted to identify triggering mechanisms and assess associated risks to offshore infrastructure.
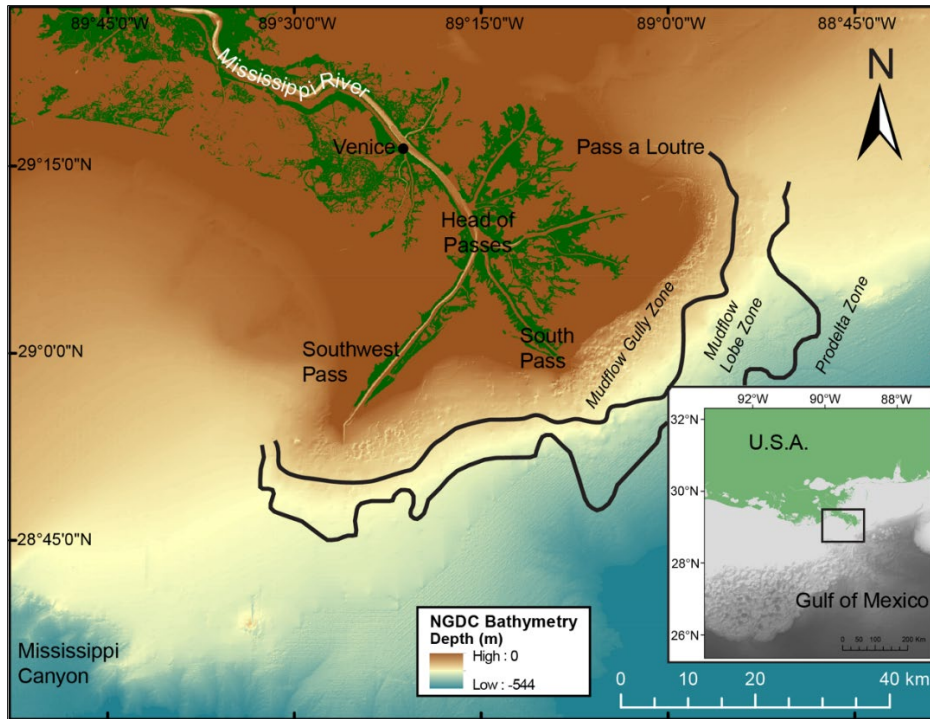
Figure 17. Overview map

Overview map of the Mississippi River delta showing subaerial birdfoot morphology formed by distributaries. Inset shows regional overview with black box defining area shown in large view image. Black lines delineate zones of MRDF instability features as defined by Coleman et al. 1980. Bathymetry data from NOAA database (Love et al. 2012).

Seafloor landslides are ubiquitous across continental margins worldwide, can pose a hazard to human populations and infrastructure, and are an important mechanism of sediment transport to the deep sea (Hampton et al. 1996). Nevertheless, we lack quantitative measures of the frequency and distribution of landslides in different geographic settings, and the pre-existing conditions and external triggers that lead to these landslides remain poorly understood. While most research on seafloor landslides relies on data collected from existing landslide deposits (i.e., only after the event), the MRDF provides a unique opportunity to observe landslide processes in action. Because of the wide distribution of landslides on the MRDF and the variety of triggering mechanisms, processes can be observed over relatively short time scales. Data from the MRDF can support research on global subaqueous landslides by quantifying seafloor characteristics that lead to instability and linking landslides to different external stresses that may be present on other margins. Research on MRDF landslides also provides a useful comparison with many other geologic settings that are susceptible to seafloor instability.

Additionally, deltas form the link between continental and marine environments and are an important feature of the source to sink pathway (Walsh et al. 2015). As such, they play vital roles in biogeochemical cycling, sediment transport and deposition, and they also host productive and impacted ecosystems (Leithold et al., 2015). Sediment dispersal processes on the delta front include multiple cycles of transport, deposition, and reactivation (Wright and Nittrouer 1995), for which submarine landslides are an important transport mechanism for moving large amounts of sediment into deeper water (Obelcz et al. 2017). The Mississippi River is 7th largest river in the world in terms of discharge and sediment load (Milliman and Meade 1983) and it is classified as proximal accumulation dominated (PAD) in terms of fine-grained sediment dispersal (Walsh and Nittrouer 2009). We expect that processes observed on the MRDF could be useful for evaluating sediment processes in other major river-delta systems, particularly those classified as PAD (i.e., Po, Nile, and Yellow Rivers; Walsh and Nittrouer, 2009).

Currently, the Mississippi River system and other river systems worldwide are undergoing unprecedented changes due to the effects of climate change and anthropogenic alterations to rivers and deltas (Blum and Roberts 2009; Blum and Roberts 2012; Bentley et al. 2016; Yang et al. 2017). Locally, land loss in the Mississippi River delta plain has accelerated and efforts to restore these regions are underway in order to preserve important habitats and human communities and resources (LaCPRA 2017). Because deltas commonly serve as economic and population centers (Vorosmarty et al. 2009), this scenario is being repeated on other major delta systems worldwide (Syvitski et al. 2009; Yang et al. 2017). In order to best respond to these changes, it is vital to understand the role of delta front processes and how they relate to processes in the subaerial delta (e.g., Maloney et al. 2018). This will in turn allow for better prediction of future changes that will impact delta communities.

We complete this synthesis of MRDF sediment instability research at a time of dramatic anthropogenically driven change in global delta sedimentary processes and of rapid advancement of seafloor research technology. Much of the important early research conducted on MRDF instabilities indicated that rapid sediment deposition played an important role in developing weak, oversteepened regions that were prone to failure (e.g., Coleman and Garrison 1977). All models and risk matrices published to date are predicated on an unchanged historic sediment discharge from the primary Mississippi River outlets (e.g., Hitchcock et al. 2006; Nodine et al. 2007; Guidroz 2009). However, as a result of declining and shifting sediment discharges (e.g., 50% reduction in Mississippi River suspended sediment load since the 1950s (Kesel,1988)), sediment accumulation patterns on the delta front have changed significantly, and the extent, timing, and location of areas prone to seabed failure may also be changing (Maloney et al. 2018). Additionally, observational and theoretical developments in seabed sedimentary processes have advanced worldwide, particularly in the past decade (including but not limited to wave-enhanced sediment-gravity flows; Macquaker et al. 2010; Denommee et al. 2016, 2017), but seabed dynamics of the MRDF have not been evaluated with respect to many of these newly developed concepts. Here, we synthesize existing research on MRDF landslides in the context of these developments and provide a framework from which to advance future research on the MRDF.

2.3.2 Overview

The MRDF is a highly heterogeneous morphologic feature set in a complex environment (Figs. 17–19). Multiple processes interact on the delta front to control morphology, sediment deposition and characteristics, and sediment instability. Mississippi River sediment is transported to the delta front through multiple pathways; the delta front undergoes seasonal cycles of storms, floods, and hurricanes; and biogenic gasses are known to be present across the delta front. All of these factors may influence spatial and temporal patterns of sediment instability, and play a role in preconditioning or triggering of subaqueous landslides. The following brief overview outlines some of the major properties and processes of the MRDF that are important for understanding subaqueous landslides. References are made to subsequent sections that provide more detail on each topic as it relates to sediment instability.

The Mississippi River drains the central continental US into the northern Gulf of Mexico (Gulf) and is the 7th largest river in the world in terms of discharge and sediment load (Milliman and Meade 1983). The estimated annual sediment load from the Mississippi River is ~2.1 x 10^{11} kg with ~80% of the total load represented by fine silt and clay in suspension (Milliman and Meade 1983). The Mississippi River has deposited sediment across multiple delta lobes in southern Louisiana during the Holocene, with lobe switching every 1,000–1,500 years (Blum and Roberts 2012). The current depositional lobe is known as the Plaquemines-Balize delta, which was initiated ~1,200 yrs BP (Tornqvist et al. 1996) and has accumulated Holocene sediment over 100 m thick (Coleman and Roberts 1988; Kulp et al. 2002).

Subaerially, the modern delta exhibits a "birdfoot" morphology, extending across the shelf to very near the shelf edge where it bifurcates into several distributaries. The major distributaries are, from west to east, Southwest Pass, South Pass, and Pass a Loutre (Fig. 17). Sand is deposited along the distributary channels creating bar-finger sands beneath and adjacent to each pass (Fig. 18; Fisk, 1961). The mouth

bars prograde into the GOM at variable rates that have exceeded 100 m/year (Prior and Coleman 1981; Maloney et al. 2018). These rapidly prograding sand bars produce mud diapirs, or "mudlumps", by loading sand on top of less dense clays (Fig. 19, Hanor 1981; Morgan 1961; Morgan et al. 1968). Mudlumps were some of the first recognized sediment instabilities in the Mississippi River delta (Section 2.3.3).

Beyond the subaerial delta, the subaqueous delta front extends beyond the outermost continental shelf to water depths of ~200 m and was built by Mississippi River deposits into the Gulf. The modern distribution of suspended sediment load transported through each pass is approximately 69% Southwest Pass, 15% South Pass, and 16% Pass a Loutre (Allison et al., 2012). Moving away from the distributary mouth bars, sediment becomes finer, both within the interdistributary bays and moving radially outward from the mouths (Fig. 18, Fisk et al., 1954). These subaqueous delta deposits overlay prodelta clay deposits of the continental shelf. The three dominant clay minerals in Mississippi River sediment are smectite, illite, and kaolinite, which are also the dominant minerals in delta front deposits with spatially variable abundances (Taggart and Kaiser 1960; Griffin and Parrott 1964; Roberts 1985). Sedimentation rates along the delta front are variable but are generally higher closer to the distributary mouths. Estimates of sedimentation rate range from less than a centimeter per year at distances beyond 17 km from Southwest Pass in >100 m water depth (Ruttenberg and Goni 1997) to >1 m/yr immediately adjacent to distributary mouths (Coleman et al. 1991). Since the 1950s, the sediment load in the Mississippi River has decreased by approximately 50% due to dam construction upstream (Kesel et al. 1992), which has recently begun to impact sedimentation rates in the subaqueous delta (Maloney et al. 2018). The high sedimentation rates and spatial patterns of deposition are important factors governing the strength and stability of delta front deposits (Section 2.3.3).
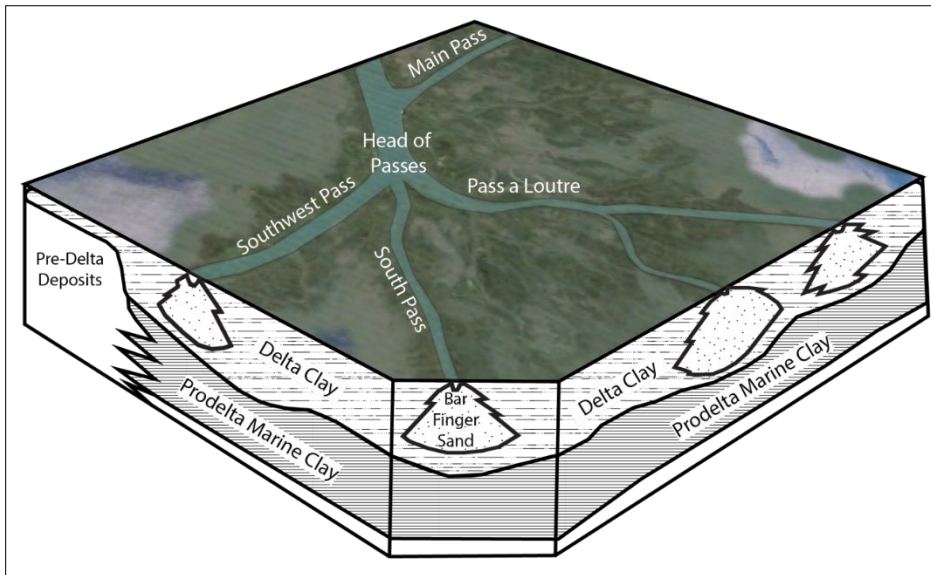
Figure 18. Block diagram of the Mississippi River Delta

Diagram depicting sub-seafloor geology of the MRD, modified from Fisk (1961). Bar finger sands are deposited along the distributary mouths and clays are deposited away from the mouth bars. The delta is building out over prodelta marine clays.
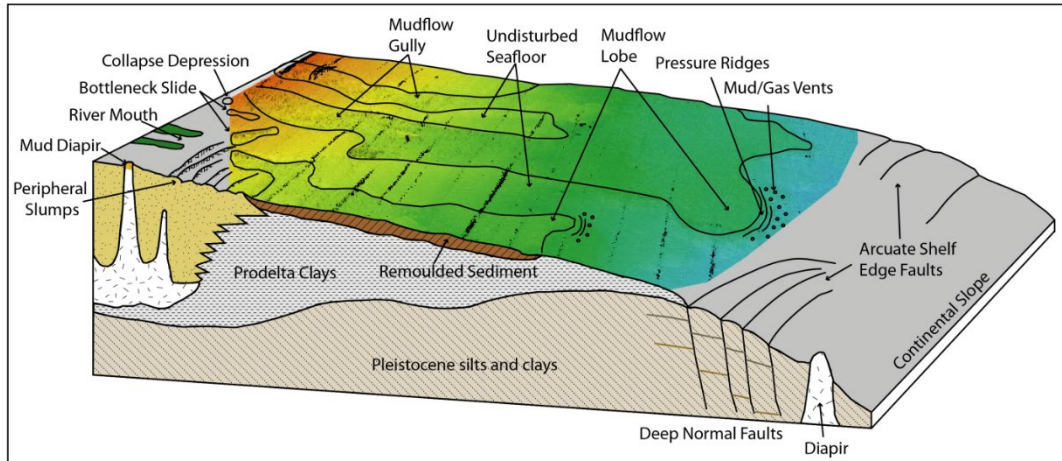
Figure 19. Block diagram of the Mississippi River Delta Front

Block diagram illustrating seabed morphology and structure/stratigraphy of the Balize lobe delta front, based on Coleman et al. (1980). Bathymetry from Walsh et al. (2006) illustrates mudflow gullies and lobes at intermediate depths (rainbow bathymetric grid).

Before the 1950s, the morphology of the delta front seafloor was assumed to be relatively smooth and homogenous until seafloor mapping revealed a series of shallow valleys creasing the subaqueous delta (Shepherd, 1955). Subsequent research has identified a highly complex morphology attributed before subaqueous mass movements. Prominent features were thoroughly mapped and described by Coleman et al. (1980) and include collapse depressions, bottleneck slides, mudflow gullies, and mudflow lobes (Fig. 19). Overall, the slope of the delta front is generally low, ranging from 0.1° to 2.2° (1.1-38 m/km), but is mostly <1.5° (<26 m/km) (Coleman et al. 1980). Despite the low slope, delta front morphology indicates that landslides are pervasive across the delta front and that several mechanisms of instability operate to create a wide array of morphologic features (Section 2.3.3).

Geotechnical properties of the delta are spatially variable due to heterogeneous sedimentation patterns and instability features. Profiles of undrained shear strength compared with depth vary both between and within instability features (Hooper and Suhayda 2005; Bea et al. 1983; Dunlap et al. 2004; Hooper 1980). Profiles typically range between underconsolidated (2 pounds per square foot/ft (psf/ft); 0.314 kPa/m) and normally consolidated (8 psf/ft; 1.26 kPa/m)) and commonly exhibit crustal type profiles where a higher shear strength zone in the upper sediments overlies a weak shear strength or failure zone (Fig. 20) (Quiros et al. 1983; Whelan et al. 1976). Sediment shear strength is an important factor governing instability on the delta front (Section 2.3.3.2). Additionally, gasses are commonly observed in sediments of the delta front (primarily methane; Anderson and Bryan, 1990; Coleman and Garrison 1977; Whelan et al. 1976; 1977), which can influence shear strength and act as a potential trigger for slope failure (Section 2.3.3.2.3). These gasses are formed from the biogenic decomposition of organic material within the sediments.

Hydrodynamic processes near the MRDF are diverse and include influences from river flow, tides, oceanographic currents, seasonal winds, large storms and hurricanes, and deeper Gulf currents. Oceanographic currents along the shelf near the modern birdfoot delta are predominantly shallow wind driven currents that are seasonably variable. During the summer (June–August), wind directs currents northward (onshore), and during the remainder of the year, wind directs currents towards the southwest (Cho et al. 1998; Johnson 2008). Deeper currents may be controlled by the Gulf Loop Current (Wiseman and Dinnel 1988). Both winter storms (Obelcz et al. 2017) and hurricanes (Wang et al. 2005; Guidroz 2009) can generate large waves near the delta front. Since 1852, twenty-five Category 3 or stronger hurricanes have tracked within 200 km of the Mississippi River delta (National Hurricane Center 2015), and hurricanes have been shown to cause failure on the MRDF (Bea 1971). Mississippi River floods,

hurricanes, and winter storms are all potential triggering mechanisms for submarine landslides with complex temporal patterns (Fig. 23, Section 2.3.3).

As can be seen from the above summary of MRDF processes and characteristics, the MRDF is a highly complex environment with several factors that can affect sediment stability. These delta front processes and their role in subaqueous landslides are detailed in the following sections.

2.3.3 Mississippi River Delta Front mass wasting

Much of the work on submarine landslides in the MRDF was spurred by the damage to three oil platforms during Hurricane Camille in 1969. Hurricane Camille made landfall near Waveland, Mississippi as a Category Five hurricane (Roberts 1969; Wright et al. 1970; Simpson et al. 1970; Thom and Marshall 1971). The storm passed just west of South Pass Block 70 where two recently constructed Shell Oil Company platforms were severely damaged (Bea, 1971). One platform was knocked completely over and fell to the ocean floor on its side, while the other remained standing, but was moved 0.9-1.2 m to the southeast (Bea 1971). A Gulf Oil Company platform in nearby South Pass Block 61 was also destroyed. A comparison of soil borings and geophysical surveys collected before and after Camille in South Pass Block 70, showed changes in bottom topography and soil strength profiles, which indicated that the platform damage was caused by submarine landslides (Bea 1971; Sterling and Strohbeck 1973). Much of the subsequent work on MRDF landslides has focused on understanding landslide characteristics, timing and extent of instability, and potential triggering mechanisms, in an effort to assess the hazard they pose to offshore infrastructure. The following sections provide a review of the state of knowledge of various aspects of MRDF seafloor instability.

2.3.3.1 Geomorphology

Much of our understanding of MRDF sediment instability has been derived from geophysical surveys (e.g., sidescan sonar, sub-bottom echosounders, multi-channel seismic, bathymetric echosounders), which image the morphology of the seafloor, as well as sub-seafloor structure. The first regional bathymetric surveys were conducted over the delta front by the US Coast and Geodetic Survey from 1872 to 1874 and again in 1940 (Coleman et al. 1980). The 1940 survey lines were retraced by Shell in 1967 (Bea and Bernard 1973) and another regional survey was conducted in 1974 (Garrison, 1974). The most recent regional survey was conducted between 1977 and 1979 for Bureau of Land Management Reports 80-01 and 80-02 (Coleman et al. 1980). In addition to the regional surveys, local surveys have been conducted since the 1950s associated with offshore infrastructure construction, and to assess seafloor change and damage to infrastructure after major storms. All of the regional bathymetric surveys, and the majority of the local surveys, use single-beam echosounders at various grid spacing to map the seafloor. Since the 1980s–1990s, multibeam echosounder technology has vastly improved and can map the seafloor with better resolution and accuracy than single beam methods. A few local multibeam surveys have been conducted on the MRDF in recent years (e.g., Thomson et al. 2005; Walsh, et al. 2006; additional industry surveys cited in Maloney et al. 2018) and multibeam and interferometric bathymetric surveys are becoming more common in industry hazard assessments.

Although seafloor features on the MRDF had been mapped prior to the 1977–1979 regional surveys, the 1980 BLM reports related to these surveys provide the most expansive overview of MRDF morphologySubsequent to the BLM reports, several papers were published that elaborate on, and provide additional detail on some of the instability features (e.g., Coleman et al. 1981; Coleman et al. 1983, Prior and Coleman 1980). Figure 19 was updated from these reports and illustrates the major instability features described therein. Table 1 summarizes important details about these features from the text of the reports.

Table 1. MRDF Morphometric Parameters

Morphometric parameter summary of main MRDF seafloor disturbances. All dimensions and descriptions are from Coleman et al. (1980) unless indicated by footnotes: [1]Obelcz et al. 2017; [2]Coleman et al. 1981.

	Length Scale (m)	Relief (m)	Seafloor gradient (degrees)	Wall gradient (degrees)	Characteristic depth (m)	Morphology	Subsurface Features
Rotational slumps	100–1000	3–8	0.2–0.6	1–4	2–10	Hummocky, irregular topography, displaced blocks of sediment	Concave shear planes that merge into single bed-parallel plane
Collapse depressions	50–150	>1–3	0.1–0.4	3–10	2–20	Irregular, hummocky	Large amounts of methane gas
Bottleneck slides	150–600	>1–3	0.2–0.4	3–15	2–30	Undulating, lobate shape, occasional rafted debris blocks	Concave shear planes, large amounts of methane gas
Mudflow gullies	8000–10000	3–20	1–5	1–19	10–100	Irregular, chaotic topography, large, irregular rafted blocks	Highly disrupted stratigraphy large amounts of methane gas
Mudflow lobes	2000–5000[1]	20–60	0.1–0.3	1–3	50–100	Mud vents, volcanos	Lack of internal structure
Erosional furrows[2]	1000–5000	1–2	0.85–>2	Not available	150–380	Coarser than surrounding extremely fine, saturated sediments	Unknown (no subbottom data available)
Growth faults[2]	<1000–10000	25–40	1–2.5	Not available	130–400	Mud volcanos on downthrown side	Alternating layers of pelagic and nearshore sediments, higher rates of sedimentation on downthrown side

These morphological features are not always discrete and frequently merge into each other, making quantification of their dimensions somewhat difficult. The diffuse nature of the morphological features is unsurprising considering their genetic relationship. For example, bottleneck landslides form when the downslope bounding scarp of a collapse depression fails, and several bottleneck landslides can coalesce to form a mudflow gully; gullies are negative relief features that converge to form lobes, which are features of positive relief (Figs. 19 and 20) (Keller et al. 2016; Obelcz et al. 2017). Rotational slumps can also become the arcuate headwalls of gullies (Prior and Coleman 1980). In general, the morphological features observed along the MRDF can be categorized as a depth-bounded succession increasing in both area and relief from shallow to deep: collapse depressions, bottleneck slides, mudflow gullies, and finally to mudflow lobes (Fig. 19, Table 1).

Erosional furrows and growth faults are discrete MRDF features separate from those described above due to both their large size and absence in shallow water. Erosional furrows are long, narrow incisions that trend perpendicular to isobaths. They begin near the shelf edge and have been traced into the heads of submarine canyons (~380 m water depth). Proposed origins of the furrows are highly varied; Coleman et al. (1981) believe the furrows are incised into soft bottom sediments by Taylor-Gortler secondary countercurrent loops, which trend across shelf and can produce currents from 25–50 cm/s. However, an origin related to mass failures similar to those observed in shallower depths cannot be ruled out.
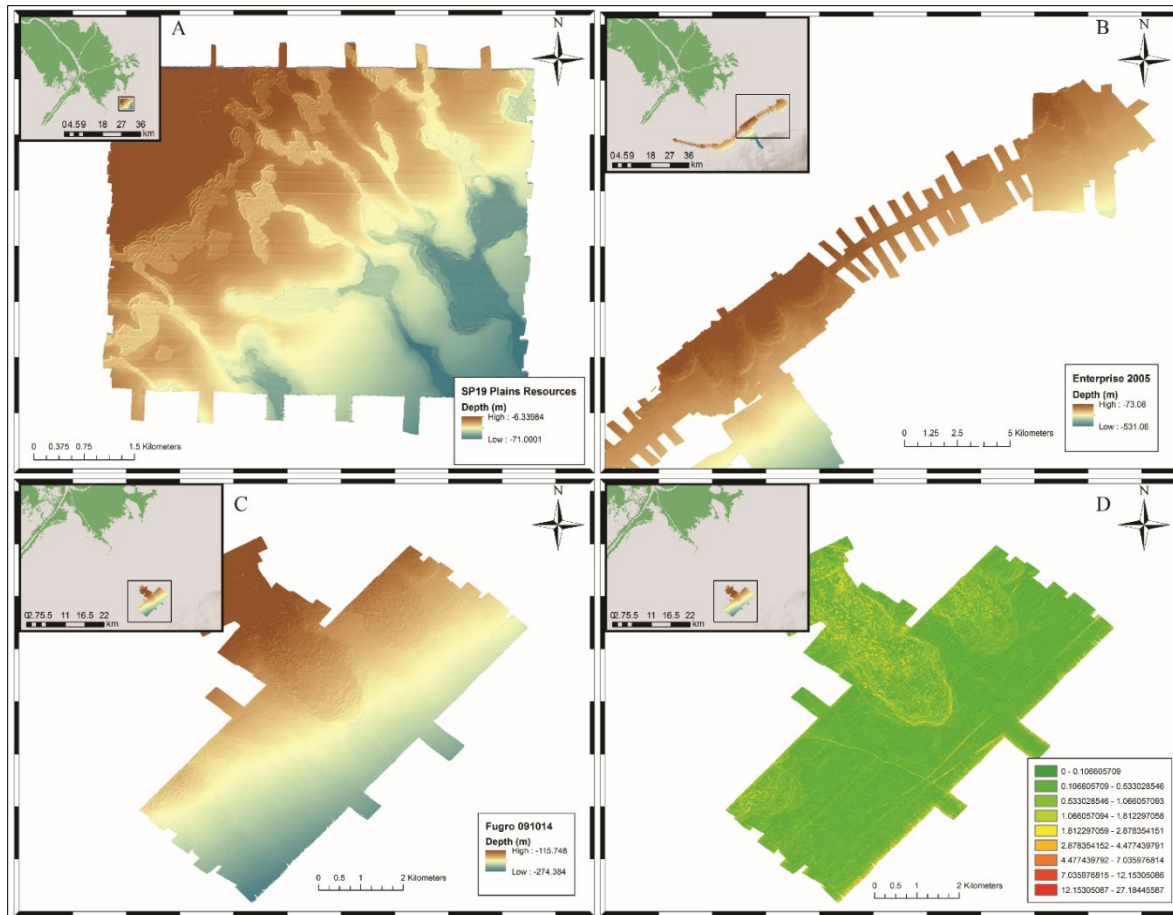
Figure 20. Industry survey maps

Multi-beam bathymetry data from the MRDF. Panel A shows the complex nature of mudflow gullies. Panel B shows multiple mudflow lobes terminating at similar depths on the delta front. Panel C shows mudflow lobes southeast of South Pass. Panel D shows seafloor slope in degrees, outlining the same mudflow lobes as panel C.

Growth faults in the MRDF region trend parallel to isobaths and evolve synchronously with sediment deposition (Watkins and Kraft 1978; Coleman et al. 1980). The internal stratigraphy of faulted areas consists of alternating layers of hemipelagic and fluvial sediments, with thicker deposits on the downthrown sides of the faults. The presence of fluvial sediments in water depths exceeding 200 m indicates mass transport deposits play an important role in the initiation and/or maintenance of the continually offsetting features.

Overall, seabed slopes on the MRDF are low compared to terrestrial settings (Table 1). Nevertheless, in many locations, these slopes are sufficient to sustain downslope motion of sediments under the force of gravity acting alone. Wright et al. (2001) evaluated force balances acting on submarine SGFs, and established that seabed gradients near 12 m/km, or ~0.7°, are sufficient to allow some flows to continue movement downslope, once motion is initiated. This gradient is near the middle value for MRDF seabed slopes in Table 1, further supporting observations that gravity driven flow is, and should be widespread in this setting.

2.3.3.2 Sedimentology

2.3.3.2.1 Sedimentation rates and patterns

Sediment output from the Mississippi River to the delta amounts to ~2.1 x 10^8 tons annually in the period of 1963-1979 (Milliman and Meade 1983; Meade 1996). For the water years 2008–2010, suspended sediment loads measured in the three major distributary passes were 20.8 x 10^6 tons/yr for Southwest Pass, 4.7 x 10^6 tons/yr for South Pass and 4.8 x 10^6 tons/yr for Pass a Loutre (Allison et al. 2012). The most rapid sediment accumulation occurs adjacent to the distributary mouth bars and rates decrease seaward and into the interdistributary bays. Average sedimentation rates just seaward of the mouth of the passes are ~1 m/yr, but floods may increase deposition to 3–5 m over a 4-month period. Interdistributary bay sedimentation rates are generally a few centimeters per year, and overall sedimentation rates decrease moving seaward from the delta towards the shelf edge (Prior and Coleman 1982). Ruttenberg and Goni (1997) calculated sedimentation rates along a transect moving offshore from Southwest Pass with results showing this seaward decrease: 0.8 cm/yr at 17 km from the mouth, 0.2 cm/yr at 34 km from the mouth, 0.005 cm/yr at 110 km from the mouth. Inshore from the head of Mississippi Canyon (~60 km west of Southwest Pass), sedimentation rates are estimated to be ~0.2-0.3 cm/yr (Swarzenski et al. 2008). Recent measurements of sediment accumulation off Southwest Pass give short-term rates (^{7}Be) of 0.25–1.5 mm/day (during flood season) and decadal-scale rates (^{210}Pb) of 1.3-2.9 cm/yr (Keller et al. 2016). The spatial pattern showed higher rates near the distributary mouth, decreasing seaward, with little variation in rates between instability features.

The rapid deposition at the distributary mouth bars has resulted in seaward progradation of the passes at variable rates up to >100 m/yr. (Coleman et al. 1991; Fisk 1961; Prior and Coleman 1982). Southwest Pass hydrographic profiles between 1838 and 1973 indicate progradation of the distributary mouth bar over 8 km at an average rate of 60 m/yr. Maximum thickness accumulated during this time was 42 m and an average sedimentation rate at a water depth of 30 m was 0.3-0.5 m/yr (Coleman and Garrison 1977). At South Pass, an accumulation rate over the distributary mouth bar was 37 cm/yr with mouth bar progradation of ~1.8 km between 1867 and 1953 based on bathymetric changes (Lindsay et al. 1984). Lindsay et al. (1984) also estimated that ~50% of sediment originally deposited at the bar is eventually moved into deeper water. Recent work has shown a decrease in progradation rates of all three major passes since the 1950s, with South Pass and Pass a Loutre retrograding from 1979–2009 (Maloney et al. 2018) (Figs. 21 and 22).
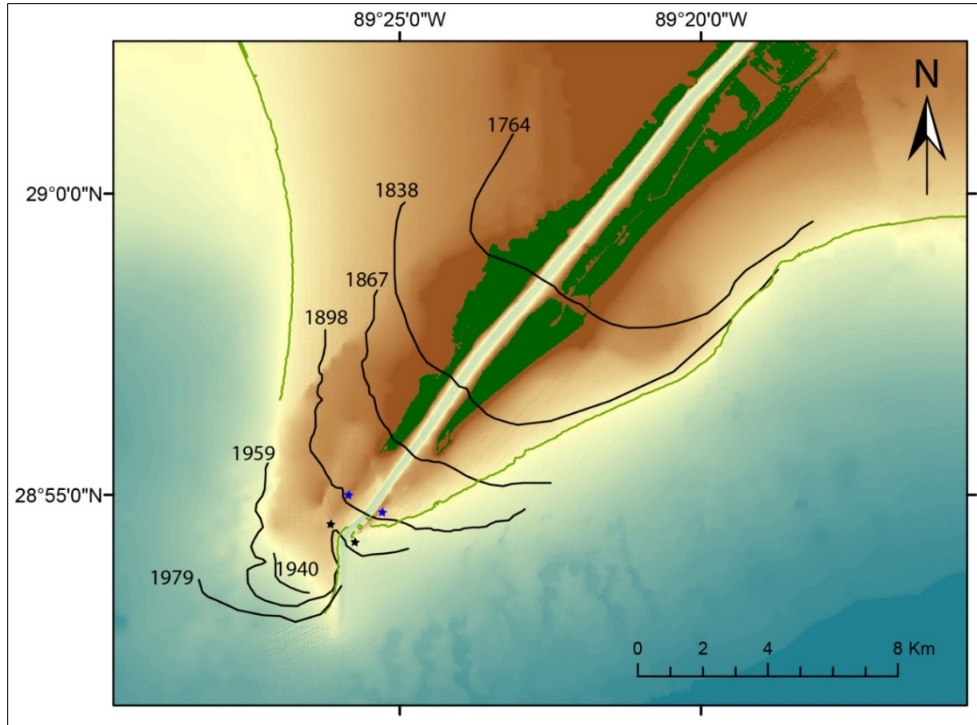
Figure 21. Progradation of Southwest Pass

Historic locations of the 10 m contour at Southwest Pass (Maloney et al. 2018)
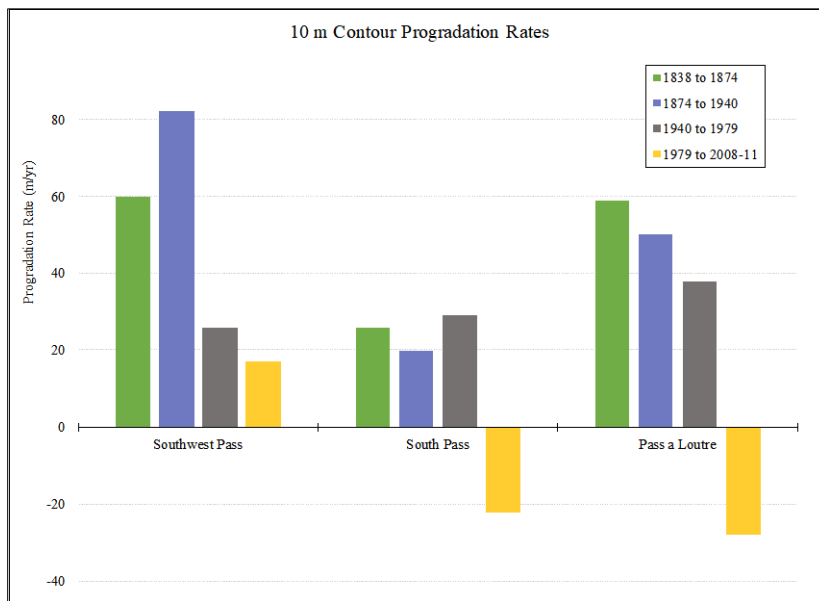
Figure 22. Graphs of delta progradation

Progradation rate of the 10 m contour measured at Southwest Pass, South Pass, and Pass a Loutre at four different time intervals, after Maloney et al. 2018.

Sediment concentration and water current characteristics have been measured offshore Southwest Pass in ~60 m water depth (Adams et al. 1987). Results indicated that current velocities were not significant to cause erosion along the seafloor during the winter-spring period of high river flow and strong surface

winds. Instead, high concentrations of suspended sediment near the seafloor were attributed to settling from the surface plume. A settling velocity of 0.05–0.67 cm/s was determined with deposition during short-period, high turbidity events, which may be related to the Mississippi River surface plume movements. Sediment deposition was a few millimeters during short term events, which is consistent with lamina observed in sediment cores. This study was conducted in relatively deep water depths (~60 m) and so the impact of waves on the seafloor was not considered. More recent work has shown the importance of wave-induced resuspension of sediment for sediment gravity flows over low gradient slopes similar to the MRDF and continental shelf.

In recent decades, a series of publications has discussed results of short time scale geochronology to study seasonal to decadal scale variability in sediment processes on the MRDF. In particular, these research efforts consider the relative importance of winter storms, river floods, and cyclones for sediment transport, deposition, and reworking (e.g., Corbett et al. 2004; Allison et al. 2000; Corbett et al. 2007; Corbett et al. 2006; Dail et al. 2007; Walsh et al. 2006; Keen et al. 2004; Rotondo and Bentley 2003; Bentley et al.,2002; Goni et al. 2007). In addition to being potential triggering mechanisms for seafloor failure, these seasonal variations in wind, waves, and river discharge are known to impact sediment deposition and resuspension (Fig. 23).
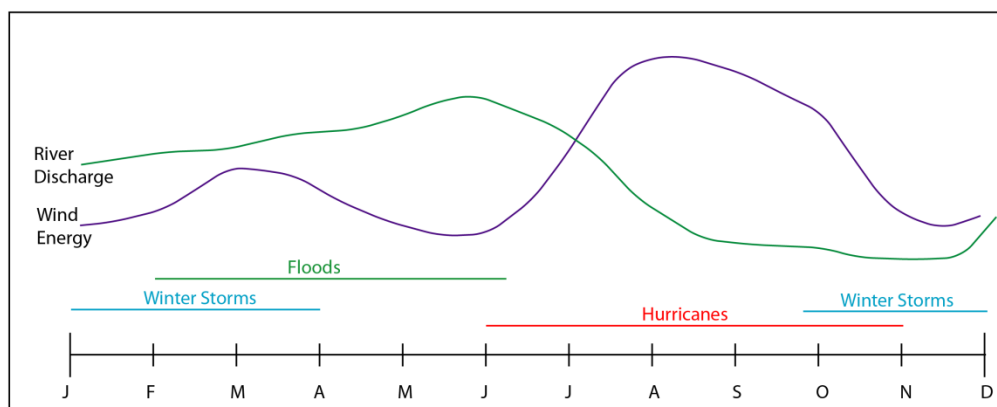
Figure 23. Landslide-triggering mechanisms

Generalized annual timeline showing temporal patterns in various mudflow triggering mechanisms. River discharge trends based on USGS gauge 07374000 at Baton Rouge, mean daily statistic (8 yrs). Wind energy based on average wind speed from 1984–2007 at Southwest Pass.

Corbett et al. (2004) observed that thickness of mobile mud layers (recently deposited sediments) is greatest near the mouth of Southwest Pass (up to 12 cm thick) and decreases away from the river mouth to the west (<3 cm). During the fall, mobile mud layers were thicker than during the spring. This could be attributed to increased sediment input through the spring, resuspension from seabed disturbance, or biological mixing. The observed seasonal variations in short lived radioisotopes show increased deposition during the summer and/or fall (October) and lower deposition in the spring (April) and indicate remobilization of sediment during the high energy winter months. Furthermore, longer term accumulation rates are lower than short term rates indicating off-shelf transport.

The impact of hurricanes on seafloor sedimentation patterns have also recently been examined. For example, Goni et al. (2007) observed up to 8 cm of erosion during a post Hurricanes Katrina and Rita rapid-response cruise. In the Mississippi Bight region, they observed net erosion without new storm deposition. Cores from the shelf offshore from the Atchafalaya River showed only one storm layer, attributed to Hurricane Rita, which traveled closer to this area. However, cores collected offshore from Southwest pass contained two storm layers attributed to both Katrina and Rita. The overall pattern observed on the MRDF was erosion in depths shallower than ~20 m with storm deposits at depths greater than ~30 m. The deep deposits were attributed to gravity flows triggered by the hurricanes. Sediment

analysis west of the MRDF has also demonstrated that hurricane-related event deposits on the middle and outer shelf are up to an order of magnitude thicker than deposits created by smaller scale winter storms (Dail et al. 2007). Patterns of distribution of these large event deposits, which thin away from the delta, indicate that hurricanes are the primary driver of sediment redistribution to deeper water through sediment gravity flows.

2.3.3.2.2 Geotechnical properties

In the northern Gulf of Mexico, typical undrained shear strength gradients for normally consolidated clay are ~8 psf/ft (1.26 kPa/m), whereas underconsolidated undrained shear strength gradients for fine-grained soils are closer to ~2 psf/ft (0.314 kPa/m) (Quiros et al. 1983). Shear strength profiles are highly variable across the delta between different instability features, and even within a single feature (Hooper and Suhayda 2005; Bea et al. 1983; Dunlap et al. 2004; Hooper 1980). For modeling wave-seafloor interactions on the MRDF between South Pass and Southeast Pass, Hooper and Suhayda (2005) defined an upper-bound and lower-bound shear strength profile based on borehole data from the area (Fig. 20). The lower-bound (weaker) profile is very close to the gradient for underconsolidated clay. The upper bound is stronger than the normally consolidated profile in shallower depths, but decreases to a gradient between underconsolidated and consolidated shear strength at depths below ~30 m. The upper bound profile has a distinct pattern that is commonly observed in MRDF shear strength profiles and has become known as a crustal profile (Bea and Arnold 1973). In these types of sediments, an upper zone (crust zone) of relatively high shear strength overlies a low shear strength zone (failure zone) (Figure 20b) (from Whelan et al. 1976). Below the failure zone, shear strength increases with depth through a transition zone into a high shear strength basement zone. The crusts represent zones of high shear strength that are unusual at their shallow depth (<15 m). The crust zones had not been previously observed because sample disturbance using earlier techniques resulted in underestimates of shear strength in the upper layers of sediment.A detailed study on the properties of crustal zones was conducted by Bohlke and Bennett (1980). In their study, crustal zones showed a marked increase in shear strength compared to sediments above and below (~5x larger), as well as a marked decrease in water content and void ratio, and a subtle increase in dry bulk density. While the high shear strength of crustal zones had previously been attributed to an increase in silt content (Roberts et al. 1976), Bohlke and Bennett (1980) observed little variation in percent silt through their sediment cores. However, they did observe an increase in the coarse silt fraction within the crust zone. This observation was also made by Shepard et al. (1978). Although the increase in coarse silt does not appear to directly increase shear strength, it may play a role in the fabric created through sediment remolding.

Bohlke and Bennett (1980) observed that the crust zones appear to have a different microfabric than surrounding shallow prodelta clay (using Transmission Electron Microscopy and Scanning Electron Microscopy). The non-crust microfabric is made up of domains with few individual particles, randomly oriented, with edge-to-face contacts forming large open voids. This fabric is similar to models for shallow, high porosity marine sediments. Conversely, the crust zone fabric has denser domains with a strong degree of preferential orientation, which occurs as relatively long chains of stepped face-to-face, edge-to-edge, and oblique arrangements. Preferential orientation changes from one direction to another, often times forming a swirling pattern, similar to artificially remolded sediments. Bohlke and Bennett (1980) attribute the crust zone fabric to shearing and remolding that redistributes and orients the clay particles. This, in turn, decreases water content and void space, which then leads to increased shear strength and other geotechnical properties associated with overconsolidated sediments. Crusts observed in sediment cores have been associated with mapped mudflows lobes (Bea and Arnold 1973; Bohlke and Bennett 1980; Hooper 1980), and therefore, anomalously high shear strength observed deeper in the cores was thought to represent older landslide events.
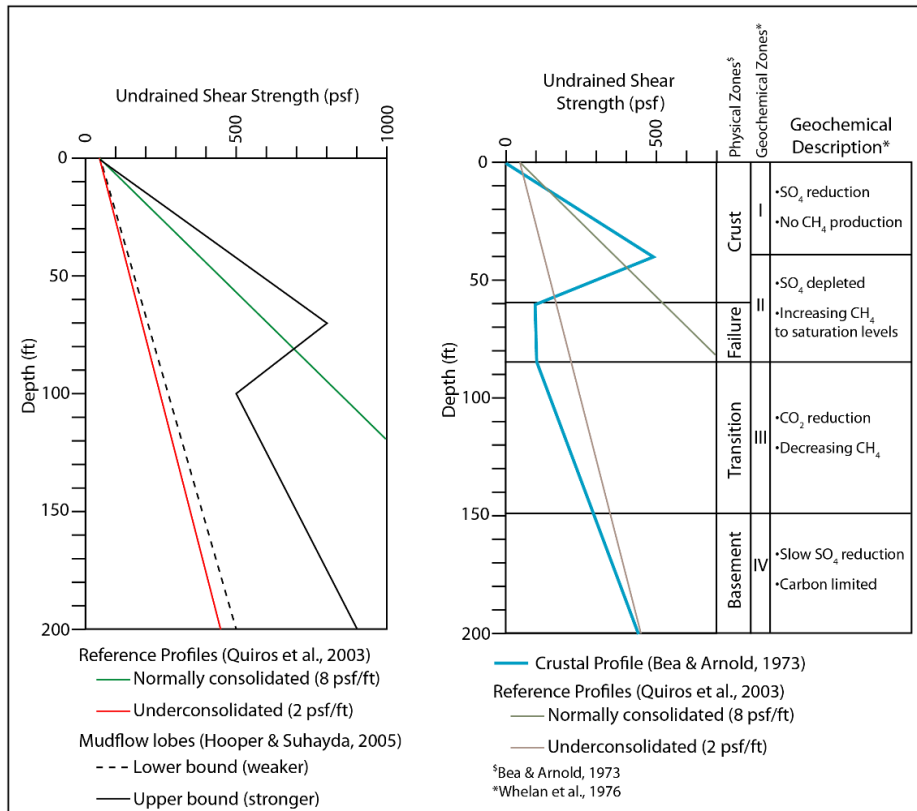
Figure 24. Mississippi River Delta Front geotechnical profiles

Typical range of shear strength profiles from MRDF mudflow lobes overlaid on profiles for normally consolidated and underconsolidated sediment. B. Typical crustal profile from MRDF with coinciding zones of geochemical processes. Citations provided within diagram.

In situ pore-pressure measurements have also been recorded on the delta front. One such effort was conducted in 1975–1976 as part of the SEASWAB (Shallow Experiment to Assess Storm Waves Affecting Bottom) project conducted by USGS (Bennett et al. 1976). During this experiment, a piezometer was installed in South Pass Block 28, at a water depth of 19 m, to record pore pressure and hydrostatic pressure beneath the seafloor over time. The piezometer was in place during passage of Hurricane Eloise in 1975.

Results from the SEASWAB experiment indicated excess pore pressures of ~32 kPa at depths of 6.4 and 8.4 meters below sea floor (mbsf) and ~72 kPa at 15 mbsf (Hirst and Richards 1977; Bennett, 1977). Significant wave heights during Hurricane Eloise were ~1.5 m near the piezometer, which recorded cyclic fluctuations in excess pore pressure of ± 4 kPa during the storm. Excess pore pressures at 6.4 mbsf returned to an average of 32 kPa after passage of Eloise, but some irregular, long period (240 s mean), low amplitude (±2 kPa) fluctuations in excess pore pressure persisted for 4 days. The fluctuations were characterized by a rapid increase in excess pore pressure, followed by a slow decline that terminated with an abrupt return to ambient conditions. As amplitude decreased with time after the storm, period tended to increase.

Additionally, measurements of pore-pressure variations during the storm were observed to be approximately half of the hydrostatic pressure variations, which may reflect dampening through the sediment column (Bennett 1977). Pore pressure variations associated with the storm were larger at ~15 mbsf compared with ~8 mbsf, which may be due to the influence of variable gas concentrations with

depth. Also observed was long term variability in excess pore pressures following the passage of the storm. Pore-water pressures continued to gradually change over a 25 day period.

Results from the SEASWAB experiment on pore water pressure were complicated by the presence of gas in the sediments at the experiment site (Hirst and Richard 1977; Bennett, 1977; Whelan et al. 1975; 1977). The measurements of excess pore pressure may reflect both pore-wate and pore-gas pressures, and calculations of effective stress based on these values may have been underestimated. However, the experiment did show that sediments at South Pass block 28 were significantly underconsolidated and that excess pore-water pressure was affected by the passage of storm waves.

A follow up experiment, SEASWAB II, placed similar instrumentation inside a collapse depression located in East Bay which is between Southwest Pass and South Pass and measured pore pressures at ~3 mbsf and ~12.5 mbsf (Dunlap 1981). The instruments recorded impacts on pore pressure from several winter storms and two hurricanes. Although instrumentation problems did not allow for thorough analysis of seafloor movement related to storm waves, it was concluded that the sediments at the experiment site had high excess pore pressure that increased during storms. Excess pore-water pressure increased rapidly during the storm and then slowly dissipated. Excess pore-gas pressure, however, continued to increase gradually for several days. There was also a lag in the increases in mean pore pressure after the storm started, indicating that some threshold was reached after many cycles of cyclic loading from waves. The results suggest that loss of strength under cyclic loading from storm waves is possible.

Abbott et al. (1985) compared hydraulic conductivity and thermal gradients in disturbed vs. undisturbed sediments on the delta front. Hydraulic conductivity and shear strength decreased with increasing degree of disturbance (ranges from 4–18 x 10^{-7} cm/s and 3.5–7.6 kPa, respectively). Thermal gradient averaged 0.12 ± 0.07° C/m in disturbed sediments and a gradient was not detected in undisturbed sediment. High thermal gradients may indicate high rates of upward fluid flow.

2.3.3.2.3 Geochemistry and gasses

Input of organic material and high sedimentation rates from the Mississippi River create conditions conducive to biogenic methane production in MRDF sediments. Many geophysical surveys in the MRDF have imaged broad areas of acoustic wipeout, which indicate the presence of gas beneath the seafloor. Whelan et al. (1976, 1977) determined that acoustic wipeout on the delta occurs where methane concentrations are > 30 ml/l. Coleman et al. (1980) regionally mapped the extent of acoustic wipeout in sub-bottom data and the updip limit of acoustic returns is variable between ~70–130 m water depth. This limit is deepest in the area between South Pass and Pass a Loutre. Gas charging in sediments can reduce shear strength by exerting pressure on surrounding pore-water and thereby increasing the pore-water pressure.

Whelan et al. (1975 and 1976) analyzed geochemistry and gas concentrations in cores offshore South Pass. Dissolved methane was detected in interstitial pore waters ranging from 2 x 10^{-3} to 1.7 ml/l, and total methane, including bubble phase, ranged from 5 x 10^{-3} to >300 ml/l. Dissolved concentrations are likely minimum values due to depressurizing during sample collection. High methane concentrations were correlated to low shear strength and low sulfate concentrations. Cores from undisturbed sediment were characterized by classical anaerobic geochemical gradients (high methane associated with low sulfate concentrations); cores from mudflow zones were characterized by zones where methane and sulfate coexisted. The geochemistry of the mudflow zones was explained by convective mixing of sediments with seawater. Under normal conditions, methane accumulates only after sulfate has been removed by sulfate reducing bacteria. Therefore, sulfate and methane do not generally coexist within sediments. In the case of the disturbed, mudflow sediments, convective mixing of sediment with seawater could have incorporated sulfate-rich seawater into sediment already producing methane, resulting in the erratic vertical distribution of sulfate and methane observed in these cores. A model of geochemical and geotechnical conditions in MRDF undisturbed sediment is shown in Figure 24.

In the cores analyzed by Whelan et al. (1975 and 1976), remolded sediment in X-ray radiography correlates with high methane concentrations and low sulphate levels, however, high methane concentrations were also correlated to relatively undisturbed sediment and the relationship appears highly variable (Roberts et al., 1976). Gas-related structures including expansion and migration features, from small voids to large separations, were imaged with X-ray radiography of cores from mudflow gullies, interlobe deposits, and prodelta sediments, and were most common in mudflow lobe deposits (Table 1) (Roberts 1980).

Coleman and Garrison (1977) describe a correlation between collapse depressions observed in sidescan sonar data and acoustic "windows" in subbottom data. The windows are areas where geophysical data is not wiped out by acoustic scattering due to the presence of gas in sediments. As such, the authors suggest that these depressions may be generated by localized degassing or dewatering of sediment, which would change acoustic character, decrease volume, and result in collapse.

One of the main difficulties in assessing gas concentrations and associated geotechnical properties is that samples are often observed to "degas" as they are brought up to atmospheric pressure. In the early 1980s, new sampling techniques were designed and used to avoid this degassing and measure soil properties at "in situ" conditions. One of these techniques was the pressurized core barrel (Denk et al., 1981), which was used to measure in situ pressures and gas concentrations on MRDF sediments and found numerous differences in texture, gas content, and geotechnical properties compared to degassed samples at the same location (Johns et al. 1982; 1985). However, this line of research did not continue long, and little work on methane genesis and distribution has been conducted since the 1980's.

2.3.3.2.4 Structures and mineralogy

Structural features within MRDF sediments were identified with X-ray radiography on sediment cores by Roberts et al. (1976) and Roberts (1980). Table 1 lists observed structures and illustrates that different environments of deposition on the delta are characterized by different sets of structures. For example, prodelta and interlobe deposits are less deformed and reworked than mudflow gullies and lobes, and also more commonly include bioturbation features and microfossils. An important distinction was identified in X-ray radiographs between mudflow deposits and undisturbed sediments of similar depths and environments. Sediment cores between mudflow events include bioturbation, microorganism tests and shell debris, and diagenetic products (pyrite, carbonate). They also lack gas related features that are commonly observed in mudflow sediments.

The fabric of clays from the MRDF can be described as domains which range in size from <0.1 µm to several micrometers and combine to form aggregates (Bennett 1976; Bohlke and Bennett 1980). Small grains of montmorillonite are found around the periphery of particles and domains and within void spaces and illite and kaolinite make up the denser, more crystalline minerals of the domains. Clay- and small silt-sized quartz and feldspar are also prevalent in prodelta muds (Bohlke and Bennett 1980).

Roberts (1985) showed that the relative abundance of clay minerals can be used to identify the base of mudflow deposits in sediment cores from the MRDF. Mudflow deposits were found to have higher smectite abundance compared to illite and kaolinite, while deeper, undisturbed delta sediments contained less smectite and more illite and kaolinite. Roberts (1985) also suggested that this was because shallower delta clays have been shown to contain more smectite, so as these clays flow out over the outer shelf, they create a sharp contact with deeper clays that contain less smectite. Fig. 25 shows the influence of composition of kaolinite (e= 0.95), sodium illite (e= 1.29), and calcium (e= 1.68) and sodium montmorillonite (e= 3.71). The shearing resistance of sodium montmorillonite at 300 kPa is 33 kPa, which equates to a drained friction angle of only 2°. In comparison, the drained friction angles of kaolinite and sodium illite are 28° and 19° for 300 kPa, respectively. The difference in shearing resistance is controlled by density, which is reflected in porosity, void ratio, and water content. The densities attainable under normal geologic conditions are related mainly to the size, shape, surface characteristics, and strength of the particles. The mineralogy of soil particles and the physiochemical environment

influence shearing resistance only indirectly through their control of these important particle characteristics. Therefore, the main reason the difference in shearing resistance between kaolinite and sodium montmorillonite is the difference in void ratios, where decreased void ratio implies an increase in interparticle contact area.
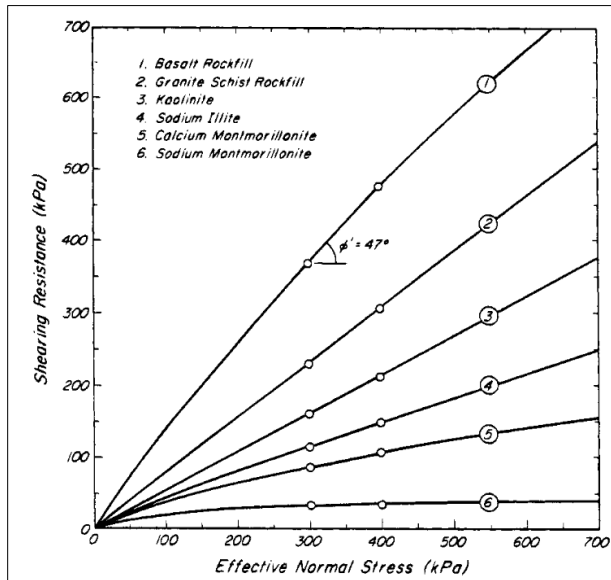
Figure 25. Sediment composition and strength

Influence of composition on shearing resistance of various soils (obtained from Terzaghi et al. 1996).

2.3.3.3 Timing and extent of mass wasting

Mudflows in the MRDF region can be grouped into two broad temporal categories: creeplike (plug) motion and catastrophic downslope failures. Creep motion can be characterized as a continuous, but slow downslope transportation of sediment that is generally confined to gullies that connect upslope retrogradational failures with downslope depositional lobes. Modeling work by Adams and Roberts (1993) indicates that if mudflows behave similar to kinematic waves, an inverse relationship would exist between mudflow height (vertical distance between basal shear plane and water bottom) and mudflow stability. This means thin mudflows may move downslope almost constantly and thick mudflows require either steep shear plane gradients and/or high rates of sedimentation to mobilize.

Creep and mudflow magnitude and velocity respond to a number of internal (mudflow shear plane slope, mudflow thickness, gully cross-sectional width) and external (sedimentation/erosion rate, bed shear stress) variables. In general, steeper shear planes, narrower gullies, and thinner mudflows are preconditioned for constant downslope movement. High rates of sedimentation further promote instability, hence the relationship observed between river floods and changing bathymetric profiles (Prior and Suhayda 1979). Repeat surveys indicate the rate of creep movement is on the order of 100 m/year (Coleman et al. 1978), although a lack of in situ data leads to ambiguity whether this is constant flow or simply smaller-scale episodic movements.

Though many efforts have been made to define the extent of mudflow-prone areas (Fig. 24 in Coleman 1988), several factors make mapping the spatial extent of creep like mudflows a difficult proposition. The aforementioned lack of in situ data makes defining flows as episodic or constant difficult, and the heterogeneous and dynamic geometry of mudflow gullies means two gullies adjacent to one another can have vastly different rates of movement.

48

Episodic, large magnitude downslope failures are relatively better studied than creep movement due to significant human concerns and easier observation. While creep movement generally occurs at velocities below 1 m/day and appears to be prevalent in thinner mudflows (resulting in smaller volumes of sediment moved), catastrophic mudslides can move sediments kilometers downslope in the span of days and disturb sediments to depths of >20 m below the seafloor (Bea et al. 1983). Catastrophic failures are almost always associated with triggering factors, which can be broken into two categories: meteorological (including hurricanes, tropical storms, and winter cold fronts) and fluvial (generally related to periods of high Mississippi River sediment and water flux). The current knowledge base regarding the timing and magnitude of MRDF mudflows is largely derived from repeat geophysical surveys of the same areas, often before and after likely triggering events (such as strong hurricanes).

Regions of rapid long-term sediment accumulation are more prone to mass failure, so the three areas immediately offshore the main distributaries of the Mississippi River (South Pass, Southwest Pass, and Pass a Loutre) have often been the targets of time series geophysical observations. Table 2 summarizes the studies that have centered on the distributaries, where mass movements seem largely tied to fluvial dynamics.

Table 2. Geophysical Survey Summary

Summary of findings of repeat geophysical surveys conducted offshore the major distributaries of the Mississippi River. Asterisks indicate surveys in which major river flood(s) occurred in between initial survey and reoccupation.

Survey	Distributary	Time between surveys (years)	Mudflow horizontal movement (km)	Max positive elevation change (m)	Max negative elevation change (m)
Prior and Suhayda (1979)*	Unspecified	1	1.9	7.5	2
Coleman and Garrison (1977)	South Pass	1	>1.5	8	4
Prior and Coleman (1981)*	South Pass/Pass a Loutre	0.42	N/A	N/A	N/A (new collapse depressions noted)
Son-Hindmarsh et al. (1984)*	South Pass	3 (1978–1981)	~1.3	>6	N/A
Obelcz et al. (2017)	Southwest Pass	5 (2005–2009)	N/A	4	4

Repeat surveys have also conducted in areas that while not immediately proximal to distributaries, still experienced large mudflows due to hurricane forcing. Bea (1971) conducted a repeat survey of South Pass Block 70 (approximately 100 m water depth) before and after Hurricane Camille (1969) and observed over 1 km of downslope movement and bathymetricchanges in excess of 10 m. Many surveys occur post-storm without a pre-storm baseline, but proxies such as pipeline displacement (575 m following Hurricane Ivan, Thomson et al. 2005) can yield a rough estimate of mudflow movement.

2.3.3.4 Triggering mechanisms

Slides occur when the forces acting on sediment exceed the shearing resistance (strength) of the sediment. Therefore, an increase in shear stress, a decrease in shear strength, or a combination of both, may result in sediment failure and mass movement (Fig. 26). In many cases, drivers of sediment failure work to both increase stress and decrease strength, resulting in a complex interplay of these factors (Figs. 26 and 27). For example, storm waves generate shear stresses on the seafloor between the crest and trough of passing waves (e.g., Henkel 1970), and also increase pore pressure through cyclic loading, which weakens the sediments.
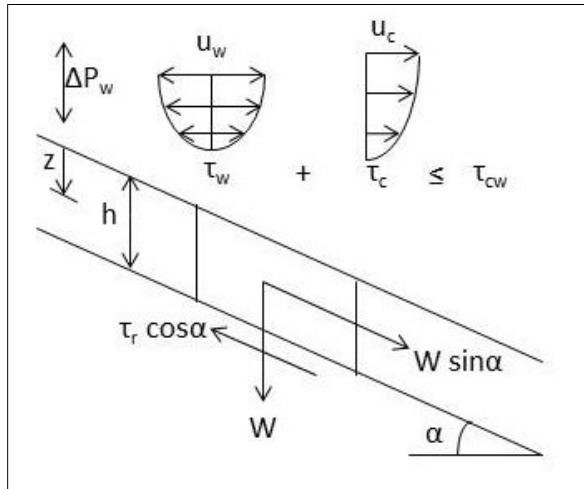
Figure 26. Forces acting on submarine landslides

Schematic of forces acting on a slab of sediment on an infinite submarine slope above wave base, adapted from Hampton et al. (1996) to include waves and currents. Parameters are U_c and τ_c, velocity and shear stress from unidirectional currents; u_w and τ_w, velocity and shear stress from waves, τ_{wc}, combined wave-current shear stress; Δp, pressure differential under waves from peak to crest; $\tau_r \cos \alpha$, shear resistance of sediment; W sin α, gravitational shear stress in the direction of potential movement; W, vertical component of body force (γ'h in the equation below); z, depth in sediment; h, height of slab; and α, slope angle. Note that velocity and shear stresses from waves may have any orientation with respect to slope direction, due to morphological complexity of the MRDF seabed.

For sloping surfaces, as is the case for the MRDF, gravity is a constant downslope driving stress. A simple equation illustrates the relationship between gravitational shear stress, sediment characteristics, and seafloor gradient (also Fig. 26):

$$\tau_s = \gamma' h \sin \alpha \qquad\qquad \text{Equation 2}$$

where τ_s is the gravitational shear stress, γ' is the average buoyant density of the sediment, h is the thickness of the sediment layer, and α is the seafloor slope. Failure will occur under the force of gravity alone if the shear strength of sediments is less than τ_s. Otherwise, the sediments will be stable unless additional forces contribute to the overall shear stress, or work to reduce sediment strength. The gravitational shear stress can increase though increased weight of sediments, or increased slope. Additional stresses can also combine with the gravitational shear stress to initiate failure. In the MRDF, studies have shown that the primary driving mechanisms for sediment failure are rapid sediment accumulation, gas charging, and storm waves (e.g., Coleman and Garrison 1977). These mechanisms can increase stress and decrease strength of sediments and are discussed in detail in subsequent sections.

Coleman and Garrison (1977) outlined some of the major factors contributing to sediment instability on the MRDF and suggest that failures are caused by the interplay of these factors over various temporal and spatial scales. The factors they discuss are:

1. Rates and location of sediment accumulation: Rates are variable across the delta (mm/yr–>1m/yr), but in areas with high accumulation, sediments are normally underconsolidated and prone to failure.

2. Size and composition of sediment: A range of grain sizes are deposited on the delta from the Mississippi River, each with different properties affecting stability.
3. Dynamics of marine and riverine processes: The delta is a diverse hydrodynamic region with influence from river mouth flow, oceanographic currents, and storm waves that can all impact seafloor stability.
4. Geochemical environment: Geochemical properties can influence sediment strength through diagenesis and cementation. Additionally, decaying organic material can produce gas within sediments, which also impacts sediment strength and can potentially trigger failures.
5. Tectonic and geologic history of the region: Deep seated faulting has been observed near the shelf edge and mud and salt diapirs are common near the delta and throughout the northern Gulf of Mexico.

In the following sections, some of the research on these factors will be described in more detail.

2.3.3.4.1 Rapid Sedimentation

On the very low gradient MRDF (0.1°–2.2°) (Table 1) gravitational shear stress is low, but rapid accumulation can lead to instability by decreasing shear strength through increased excess pore pressures from underconsolidation and gas charging, and by increasing shear stress through gravitational loading and slope steepening. Sedimentation rates on the MRDF vary locally, but approach 1 m/yr close to distributary mouth bars (Prior and Coleman 1982). Terzaghi (1956) concluded that high pore-water pressures from rapidly accumulated sediments would decrease shear strength enough that gravity forces alone could be responsible for landslides on the MRDF.

Prior and Suhayda (1981) used infinite slope analysis to calculate pore water pressures necessary to induce failure in MRDF sediments (using MRDF sediment characteristics and slope). They determined that pore water pressures would need to be in excess of hydrostatic pressure (ratio ~1.5) and approaching geostatic pressure (total vertical stress). These indicate conditions of almost zero effective stress. Pore pressures approaching geostatic pressure have been measured on the MRDF (Bennett et al. 1976) and other indirect evidence of high pore pressure has been documented in the form of gas vents and mudlumps (Prior and Coleman 1978). The authors concluded that pore pressures on the MRDF are high enough to result in failure under gravitational stresses alone.

2.3.3.4.2 Diapirism

Diapirs intrude vertically through overlying geologic layers and can create instability by increasing slope steepness. In the northern Gulf of Mexico, active salt diapirism has been linked to sediment instability on the continental slope (Martin and Bouma 1982; Tripsanas et al. 2003, 2004). Jurassic salt deposits underlie much of the northern Gulf of Mexico slope and outer shelf environments and are intruding through Cenozoic deposits creating complex seafloor morphology on the slope. Within the MRDF, a salt diapir has been mapped intruding to the near surface in South Pass blocks 60 and 67 (south of the mouth of Pass a Loutre), while other salt diapirs are buried beneath delta front deposits (Coleman et al. 1980). Several oil platforms and pipelines are located on or adjacent to the near surface diapir in South Pass blocks 60 and 67 and hazard mapping indicates a low hazard rating over the diapir (Hitchock et al. 2008). Given the recent sediment deposits draping the diapirs of the MRDF, they do not appear currently active or are active on longer time scales than sediment deposition. In either case, they have not been linked to sediment instability on the MRDF.

In the shallow areas of the MRDF, "mudlumps" are characteristic features, which have been described since early exploration of the delta in the 1500s (Morgan 1961; Morgan et al. 1968; Coleman et al. 1974; Coleman and Garrison 1977). Mudlumps are mounds of mud that form shoals or low relief islands near the distributary mouths (Coleman et al. 1998). They are diapiric mud intrusions that form as denser mouth bar sands prograde over less dense, plastic prodelta clay deposits, which are pushed vertically upwards towards the seafloor (Morgan 1961; Morgan et al. 1968). Chemical analyses of fluids from subaerial

springs on mudlumps indicate that fluid is sourced from deeply buried prodelta clays that have undergone early burial diagenesis (Hanor 1981). Some mudlumps exist for years, while others are more ephemeral, eroding under oceanographic conditions and reforming with increased mud diapirism. Growth of mudlumps generally coincides with river floods that bring increased sedimentation to the mouth bars (Morgan et al. 1968). Mudlump formation has also been observed to prograde seaward with distributary mouth bar progradation (Morgan et al. 1968). These mudlumps are often described as a sediment instability themselves, but they have not been investigated as triggers for more widespread failures on deeper parts of the shelf. The coincidence of mudlump growth with river floods may make discerning the triggering role of mudlumps difficult because river floods are also a potential trigger. It is possible that these two processes may work together to destabilize slopes during times of river floods.

2.3.3.4.3 Gas charging

Gas charging is known in MRDF sediments and can reduce shear strength by exerting pressure on surrounding pore-water and thereby increasing the pore-water pressure. Therefore, areas of the delta front with high gas concentrations may be more susceptible to failure than degassed areas. In order for failure to occur solely due to the presence of gas, the gas would have to weaken the sediment enough that the force of gravity alone would trigger failure.

Alternatively, gas concentrations could make slopes more susceptible to failure during other external triggering events. For example, gas charging may play a role in the failure of delta front sediments when combined with storm wave triggering. Coleman et al. (1974) suggested that gas within sediments would make failure more likely during storms because cyclic wave pressures would cause repeated contraction and expansion of gas between sediment grains. A large enough expansion could release gas and cause sediments to collapse and become fluid-like. In such a scenario, sediment characteristics after failure would be denser with lower porosity and gas content than prior to failure. However, laboratory experiments have shown that sandy sediments with high gas content are less susceptible to strength loss during cyclic loading, possibly because gas dissolves at higher pressures (Grozic et al. 2000). Model results also indicate that gassy, fine-grained soils strengthen under compressive loading, but weaken during unloading (Grozic et al. 2005). Nevertheless, the initial strength of gas charged sediments is reduced such that they would be more susceptible to external triggers including storm waves.

A sudden release of free gas caused by the dissociation of hydrates is also a potential trigger for seafloor failure. Hydrates are known on the continental slope of the northern Gulf of Mexico, and have been linked to landslides in the region (Cooper and Hart 2003). However, the stability zone for gas hydrate in the Gulf of Mexico is 300–500 m water depth, which is well below the water depths of the MRDF. It is therefore unlikely that hydrates are formed in MRDF sediments and hydrate dissociation is an unlikely trigger for subaqueous landslides on the MRDF.

After movement, convective mixing appears to increase sulfate concentrations in sediments and yield erratic methane and sulfate concentration profiles (Whelan III et al. 1976, 1975). With increased sulfate, methane production would decrease, rather than increase as suggested by Bea and Arnold (1973) (from Whelan III et al. 1976).

2.3.3.4.4 Floods

Previous research has shown a relationship between high-discharge events and mudflow activity on the MRDF. Coleman and Garrison (1977) reviewed more than 100 hydrographic charts from 1880–1961 that show the appearance of new mudflow gullies are strongly associated with high river floods and mudlump activity. They also proposed that observed stair-step seafloor profiles moving away from distributary mouth bars could be explained by repeated floods with increased deposition at the bar front that steepens the slope, which eventually becomes unstable and results in slumping. Finally, Coleman and Garrison (1977) hypothesized that mudflow gullies may be formed as tensional cracks or grabens caused by

increased stress from rapid deposition of coarse-grained sediment over prodelta clays. A modeling approach has also indicated that large river floods are sufficient to initiate failure in mudflow gullies with basal shear planes up to 30 m below the seafloor (Adams and Roberts, 1993). For a given sedimentation rate, mudflow stability increases in direct proportion to mudflow thickness.

Lindsay et al. (1984) observed the largest distributary mouth bar progradation during floods, followed by retreat of the bar 1–4 years later, due to failures on the bar front (at South Pass). These results were based on bathymetry charts of South Pass distributary mouth from 1867–1953. The 1927 flood was considered the most significant during this time period with the largest recorded discharge ($5.8x10^4$ m^3/s) and largest progradation. In areas along the bar front, the slope increased by as much as 2° during the flood. By 1931, failure of the accumulated sediments at the bar front had removed 50–90% of the sediment deposited during the flood, and returned slopes to pre-flood values. The oversteepening and rapid accumulation from flood events does lead to failures, however, the 1–4-year time delay between flood events and failures indicates that a secondary triggering mechanism is required for failure. Only two of the failures during this time period were associated with hurricanes, suggesting that winter-storms or gas charging may also play a role in triggering these failures.

2.3.3.4.5 Waves

Ocean waves can decrease slope stability by both increasing the shear strength acting on sediments and by decreasing the shear strength of the sediments through cyclic loading and associated pore-water pressure effects. Henkel (1970) was the first to assess the impact of waves on sediment instabilities in the MRDF. Henkel (1970) argued that, based on measurements of sediment shear strength (from recent boreholes) and seafloor slopes in the MRDF, gravity forces alone would not be sufficient to trigger slides. Using a linear wave model, he calculated pressure changes on the seafloor caused by a sinusoidal wave of varying heights and wavelengths (Fig. 26). Results showed that for waves moving on a shoaling shore, pressure differences develop on the seafloor, and these pressure differences may be large for storm waves where water depths are comparable to wave heights. These values were determined to be sufficient to cause failure in MRDF sediments up to ~120 m water depth based on sediment characteristics from boreholes. In water deeper than ~120 m, gravity landslides likely become the primary sediment transport mechanism, which agrees with an observed change in slope from 1:125 to 1:50 around the 120 m contour on the MRDF.

The geometry of the problem is illustrated in Figure 7 and it can be hypothesized that the seabed will be at the point of failure when disturbing moment (M_d) is equal to the moment of resistance (M_r), and failure will occur when $M_d > M_r$. The solution for the condition where $M_d = M_r$ can be written as:

$$\frac{\Delta p}{k\gamma'L} = 4\pi^2 \left(\frac{x}{L}\right)^3 \frac{1}{[A]}\left\{[B] - \frac{\beta}{3k}\right\} \qquad \text{Equation 3}$$

with:

$$[A] = \sin\alpha - \alpha\cos\alpha \qquad [B] = \frac{\sin\theta - \theta\cos\theta}{\sin^3\theta} \qquad k = \frac{c_u}{\gamma'z} \qquad \text{Equation 4}$$

where: Δp is the magnitude of the wave-induced sinusoidal pressure change, $\gamma'z$ is submerged weight of the overlying sediment (kg/m^2), L is wavelength (m), x is the half-length, α defines the portion of the wave-induced loading acting on the chosen length of the slide, 2θ is the arc of sliding, β is the slope angle, and c_u is the undrained shear strength of the shallow seabed, and z is depth (m) (Fig. 26; from Henkel, 1970).

Seed and Rahman (1978) improved upon the Henkel method and developed the following relation which shows that in addition to the characteristics of waves, induced shear stresses vary with water depth:

$$\tau_c = f_z f_d 2\pi \left(\frac{\gamma_w}{\gamma'}\right)\left(\frac{H}{L}\right)\sigma_v' \quad (3) \qquad\qquad \text{Equation 5}$$

with:

$$\sigma_v' = \sigma_v - u \qquad \sigma_v = hg\cos^2\theta\cos^2\theta\alpha\,(\gamma' - \gamma_w)\tan\phi \qquad \text{Equation 6}$$

where τ_c is the peak cyclic shear stress, σ'_v is vertical effective stress, $f_z = \exp(-2\pi z/L)$, $f_d = 0.5[1/\cosh(2\pi d/L)]$, γ_w is the unit weight of water, γ' is the buoyant unit weight of sediment, H is wave height, z is depth below seabed, L is wave length, d is water depth, u is the excess pore pressure, h is the landslide thickness, θ is the slope angle (term β from Henkel (1970)), and ϕ is the internal angle of friction. For sediment instability to occur, pore water pressures generated by rapid sedimentation, wave perturbation, and/or biogenic gas must exceed hydrostatic pressure such that $\tau_c/\sigma_v' > 1$ (Suhayda and Prior 1978). Although the Seed and Rahman (1978) model is generally considered to be an improvement on the Henkel (1970) model, because it incorporates an effective stress term it requires information on excess pore pressures generated in response to rapid sedimentation and gas charging. This is information that is not always readily available. Additional efforts including field and lab experiments, and theoretical modeling have also been made to assess the potential for waves to trigger submarine landslides on the MRDF, and build from Henkel's original model (e.g., Wright and Dunham 1972, Bea and Arnold 1973; Bea 1971, Doyle 1973; Esrig et al. 1975; Clukey et al. 1985; Suhayda et al. 1976; Suhayda 1977; Seed and Rahman 1978, Schapery and Dunlap 1978; Wright 1976; Kraft et al. 1990).

Denommee et al. (2017) applied the approach of Henkel (1970) and Seed and Rahman (1978) to the study of SGFs on the inner shelf of southwest Louisiana, where the seabed has muddy clinoformal morphology, and displays many features similar to the MRDF, including bottleneck slides and collapse depressions. Figure 9 in this report shows some of these features, and Figure 27 illustrates results of SGF modeling using the two models above, and linear wave theory from Denommee et al., 2017. Results indicate that waves typically produced by frequent winter storms (periods >6 s) are capable of initiating SGFs across the shelf to depths of at least 10 m. Similar processes are very likely active on the MRDF in deeper water, especially when forced by stronger waves from the strongest winter storms, and tropical cyclones.
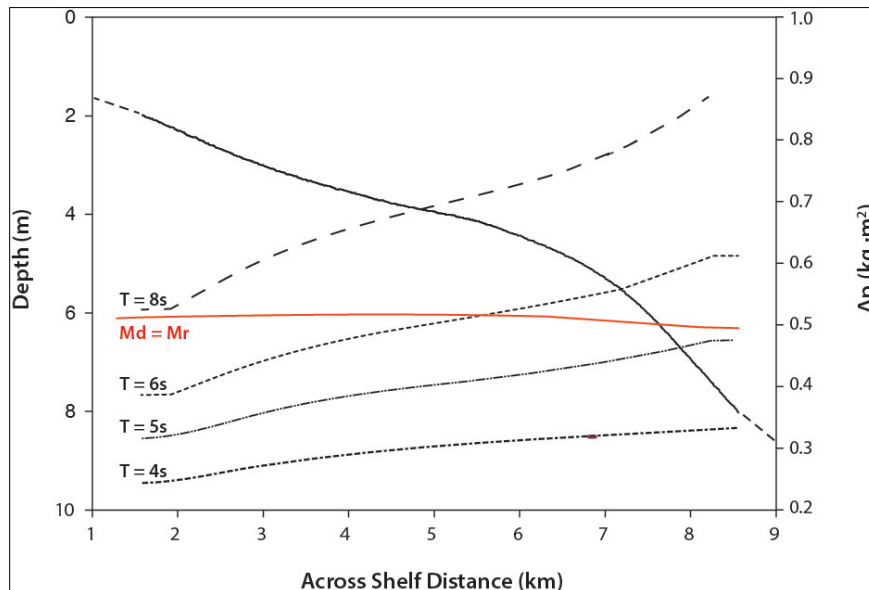
Figure 27. Waves and seabed stresses

Relationship between induced peak cyclic shear stress below the seabed and wave period across the southwestern Louisiana inner shelf from Denommee et al. (2017), as determined using the method proposed by Seed and Rahman (1978) compared to the value of τ_c as determined by Sahin et al. (2012). For values of wave period (greater than 6 s) and deep water wave height typical for the study area during winter storms, the shear stress generated by the cyclic loading of waves on the seabed exceeds the critical shear stress for sediments with 20% by volume solids of 2.74, roughly equitable to sediments 0.5m below the seabed.

As part of the SEASWAB experiment to observe in situ seafloor processes, Suhayda et al. (1976) and Suhayda (1977) measured wave action and seafloor response in South Pass block 28. They measured simultaneous wave pressure and bottom accelerations in conditions ranging from near calm (wave height < 0.1 m) to stormy (significant wave height ~1 m). Seafloor vertical displacements showed periodic, wave-like oscillations, ~180° out of phase with bottom pressures (seafloor pushed down under crest of wave). The relationship between magnitude of bottom displacement and bottom pressure appeared linear, but is likely more complex as demonstrated by a comparison of the spectra of each measurement (see Figure 10 from Suhayda et al. 1976). Horizontal motions were ~90° out of phase with vertical motions suggesting a Rayleigh-type wave motion. It was also observed that wave energy is dissipated as energy is lost to the muddy sediments.

More recent hurricanes have also spurred the analysis of wave triggered mass movement on the MRDF. Hooper and Suhayda (2005) modeled the effects of Hurricane Ivan waves on the mudflow lobe escarpment located at ~90-120 m water depth between South Pass and Southeast Pass. Their model was based on those by Schapery and Dunlap (1978) and Suhayda (1986) and used two end-member models for sediment shear strength due to significant variability in measurements from this area (Fig. 20). At the escarpment, the model showed that landslides were triggered by Hurricane Ivan-sized waves (maximum measured significant wave height = 16 m and peak period = 17 seconds), but not by smaller storm waves, and that the weaker end-member strength sediments were very likely to fail, while stronger sediments could sustain. Additionally, in shallower mudflow gullies linked to the lobes, both Hurricane Ivan-sized waves and small to moderate sized storm waves triggered mudflows that ran downslope towards the mudflow lobes. The authors suggest that over time, small and moderate storms trigger activity in shallower mudflow gullies that cause sediment to accumulate at the up-dip limit of mudflow lobes (near the top of the slope). Larger cyclones that occur more infrequently eventually trigger failures across all water depths, including the deeper mudflow lobe escarpment.

Hurricane Ivan did appear to cause extensive mass movement on the delta front with damage to offshore pipelines attributed to mudslides at eight locations, all but one located in the mudflow lobe zone (Nodine et al. 2006). Modeling of Hurricane Ivan waves by Nodine et al. (2006 and 2007), based on Henkel (1970), illustrates the importance of slope and wave period on whether or not failure occurs. Results showed that a longer wave period induces greater pressure on the seafloor to greater depths. For the same wave height, a longer period wave can trigger failures in deeper water (e.g., a 12.5 s period = failure to ~98 m compared to 16.1 s period = failure to ~165 m). Models were also extended to Hurricanes Katrina, Lili, Rita, and Andrew with similar results (Nodine et al. 2007). Results were further incorporated into a risk assessment for mudflows that found that mudflows are localized features (several hundred meter lateral extent, 15–45 m deep) and that the extent and depth are related to the size and length of the storms waves that trigger them. These wave studies were based on the Henkel (1970) model using linear wave theory. Obelcz et al. (2017) demonstrated that linear wave theory under predicts forces applied to the seabed by ocean waves; this is discussed further in Ch. 3.2.

2.3.3.4.6 Faults and earthquakes

Earthquakes are a well-established triggering mechanism for submarine mudslides, but studies of earthquakes as a potential trigger for MRDF landslides are lacking. This is likely because the region is not considered to be at high risk for seismic activity (USGS 2014a and 2014b). Nevertheless, faults have been mapped onshore southern Louisiana (LGS 2011) and across the shelf edge adjacent to the MRDF (e.g., Watkins and Kraft 1978; Coleman et al. 1980). Furthermore, geodetic measurements indicate motion of southern Louisiana towards the south at ~1.6–2.8 mm/yr relative to N. America (Dokka et al. 2006). The

delta region is also subsiding at ~10 mm/yr relative to sea-level (Tornqvist et al., 2008). Despite the observed motion and mapped faults, little is known about the paleoseismic record of the region or the characteristics of slip on mapped faults (aseismic compared with seismic). Shelf-edge faults are often described as growth, or contemporaneous faults with sedimentation keeping pace with slip, and represent large scale slump scarps. Many faults offset the seafloor with scarps up to 40 m high (Coleman et al. 1980).

Records of recent seismicity in the northern Gulf and onshore from Louisiana to Alabama show that earthquakes are not common, but have occurred with magnitudes up to M5.9 (Fig. 28; USGS 2014a). The epicenters of recent earthquakes in the Gulf are primarily located on the slope and in deeper waters. Since the start of the USGS database in 1974, there have not been any earthquakes recorded on the MRDF. In order to assess whether other Gulf earthquakes have triggered landslides on the MRDF, we must be able to correlate seismic events with dated mudslides. This would require a record of dated mudslides, which does not exist. The best temporal constraints on mudslides are recorded when they damage offshore infrastructure, as with several major hurricanes (e.g., Energo Engineering 2006; Teague et al. 2007). Incident reports of pipeline damage in the Gulf from 1974–2000 (BSEE, 2014) were examined to identify any temporal correlations between pipeline damage and earthquakes from the USGS database, but none were found. A more up to date and comprehensive database of infrastructure damage, however, would result in a more thorough examination of potential links. Additional research on the paleoseismic history and slip rates on shelf-edge faults would also improve hazard assessment.
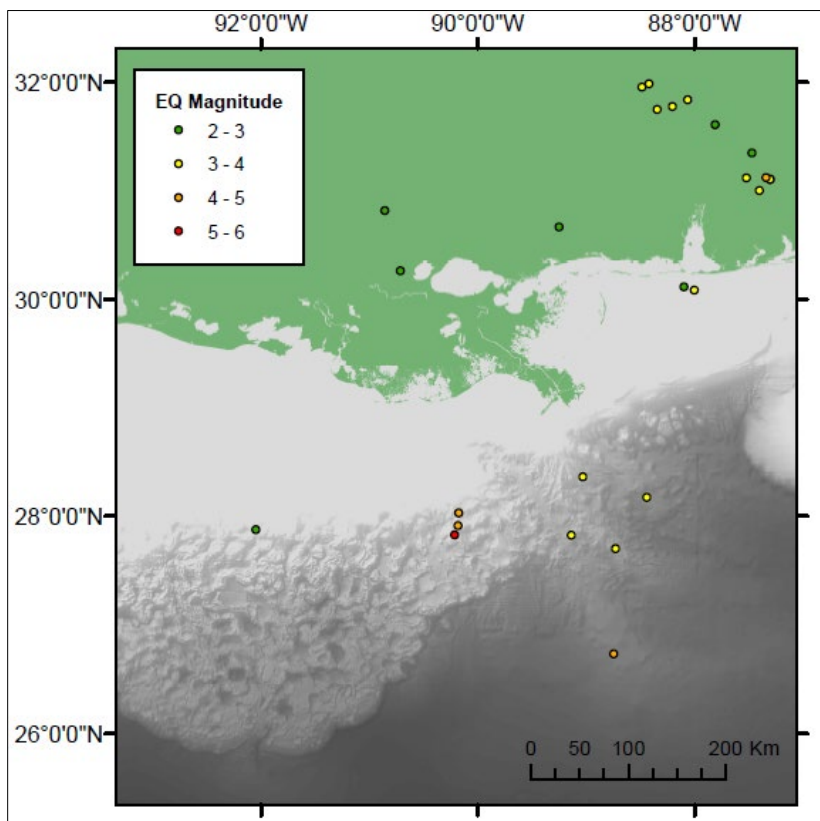
Figure 28. Earthquakes 1974–2014

Earthquakes ranging in magnitude M2-6 from 1974–2014 plotted over northern Gulf of Mexico bathymetry. Earthquake information from USGS (2014a).

2.3.4 Global subaqueous delta instability

Several other deltas worldwide have been studied to assess subaqueous sediment processes, and instability features have been documented in these depositional environments. During the 1980s, immediately following the research effort on MRDF instabilities, a similar effort was made to study processes of the Yellow River subaqueous delta (Keller and Prior 1986). As part of this work, seafloor instability features were identified including collapse depressions and wide, shallow gullies (Prior et al. 1986). Failures were attributed to pre-conditioning from high sedimentation rates, and triggering from storm waves and earthquakes (Prior et al. 1986). Furthermore, internal waves were measured using acoustic systems and it was proposed that these could induce bottom currents that re-suspended delta front sediments (Wright et al. 1986). The Yellow River delta is considered a proximal accumulation dominated delta, with similar hydrodynamic conditions to the MRDF, however it has ~3x the sediment load and ~70x the shelf width of the MRDF (Walsh and Nittrouer 2009). Nevertheless, the presence of very similar morphologic features suggests that similar mass movements are occurring in both deltas.

A deployment of in situ instrumentation on the Yellow River delta during storm conditions showed that areas of previously disturbed sediment (collapse depressions and gullies) were re-activated during storms, while undisturbed areas remained unaffected (Prior et al. 1989). This demonstrates that previous failures do not result in overall increased stability due to dewatering and consolidation as might be expected, or that sediments undergo cycles of strengthening and weakening (e.g., thixotropic sediments). Similar observations have been made on the MRDF with re-activation of existing features during storm-wave induced failure (e.g., SEASWAB experiments). Recent work on the MRDF has also demonstrated that during periods without cyclone activity, movement occurs within existing instability features while undisturbed areas remain unchanged (Obelcz et al. 2017). In both cases, movement of the sediments within the instability features was detected, but the overall morphology of the features did not change (i.e., gully width or headward erosion). On the Yellow river delta the movement was observed to be gradual, occurring over several hours, rather than abrupt and was hypothesized to occur as a type of liquefaction (Prior et al. 1989).

Recent modeling results indicate that an elasto-plastic model of the Yellow River delta's silty sediments best fits observations of wave-induced stresses in the seabed (Wang and Liu 2016). The model results also show that instabilities such as scour, seepage, and shear slides would occur mostly within 2–6 m of the seafloor. Alternatively, experimental results on Yellow River delta sediments have demonstrated that sediment liquefaction could be triggered by storm waves and result in the observed collapse depressions (Jia et al. 2014; Xu et al. 2016). These studies also considered the impact of underconsolidation and wave induced pore-pressure changes on re-suspension of silty sediments, where weakening of the sediment can lead to increased erosion and transport (Jia et al. 2014; Zhang et al. 2018). The re-suspension of sediment due to storms and tidal flows appears to explain observed sediment gravity flows (turbidity currents) on the Yellow River delta, which were originally hypothesized to be related to hyperpycnal flows during river floods (Wright et al. 1986; Wright et al. 1990).

The process of wave-induced, gravity-driven transport on deltas and across the continental shelf over low slopes is a relatively new development in continental margin sedimentology research. This new concept explains the transport of muddy sediment across low-gradient shelves through gravity flows caused by the re-suspension of seafloor sediment by ocean waves (e.g., Friedrichs and Wright 2004; Wright and Friedrichs 2006; Macquaker et al. 2010; Denommee et al. 2016, 2017). The discovery of these wave-enhanced sediment gravity flows (WESGFs) was in large part made possible by comprehensive multi-institutional field studies of the Amazon River delta (AMASEDS; Nittrouer and Kuehl 1995) and Eel River margin (STRATAFORM; Nittrouer 1999). Both of these efforts included deployment of seafloor tripods equipped with instrumentation to monitor hydrographic and seafloor conditions. Data from the instrumentation documented fluid mud layers moving downslope associated with times of increased wave activity. The WESGFs on the Eel margin were observed to occur when storm waves and river floods

occurred simultaneously, but also during times of high wave activity that did not correspond to river flood events (Ogston et al. 2000; Puig et al. 2003; 2004).

Evidence for WESGFs along the southern Louisiana coast has been documented in areas west of the MRDF and storm deposits are associated with both hurricane events and smaller winter storms (Wright et al. 2001; Corbett et al. 2004; Dail et al. 2007; Denommee et al. 2016, 2017). Nevertheless, observations of WESGF deposits on the MRDF have primarily been identified using sediment cores that capture the event layers after deposition. In situ monitoring of sediment transport and associated hydrodynamic conditions has not been conducted since the importance of WESGFs was recognized. Furthermore, additional work is needed on the relative importance of WESGFs during winter-storm and cyclone season and on the importance for potentially triggering more catastrophic slides that have been observed to damage infrastructure.

Other important findings on delta sediment instabilities have been documented in a well-studied fjord-head delta–the Squamish Delta in British Columbia (e.g., Hughes-Clark et al. 2012; 2014; Clare et al. 2014; 2016). Fjord-head deltas differ from the MRDF in morphology and sedimentological and hydrodynamic conditions but are also prone to failure (e.g., Lee et al. 2002). Recent work identified that different types of failure occur on the delta including both larger, infrequent, deep-seated failure of the shallow delta-lip and more frequent turbidity current flows that generate upslope migration of bedforms (Hughes-Clark et al. 2012; 2014). This may be similar to MRDF instability that appears to occur either as more frequent creep-like motion during quiet hydrodynamic conditions or as catastrophic failure during hurricane wave conditions (Obelcz et al. 2017). In the Squamish delta, in situ acoustic imaging sensors were deployed and suspended in the water column above a subaqueous delta channel (Hughes-Clark 2016). Over six days of monitoring, 14 turbidity currents were observed and their timing was linked to tidal conditions, clearly indicating that tides are a dominant control on sediment gravity flows in the Squamish delta. Several multibeam sensors were deployed in the instrument package and changes to the seafloor were also measured daily to link gravity flow processes to observed morphology.

The study on the Squamish delta also included collection of daily multibeam surveys over the course of ~93 days (Hughes-Clark et al. 2012; 2014; Clare et al. 2016). This unprecedented number of repeat surveys allowed for detailed monitoring of the recurrence of instability events and correlation to various potential triggering mechanisms. Because of the continuous nature of the dataset and observance of a large number of instability events, a statistical analysis was completed to assess the potential for various triggering mechanisms (Figure 29, Clare et al. 2016).
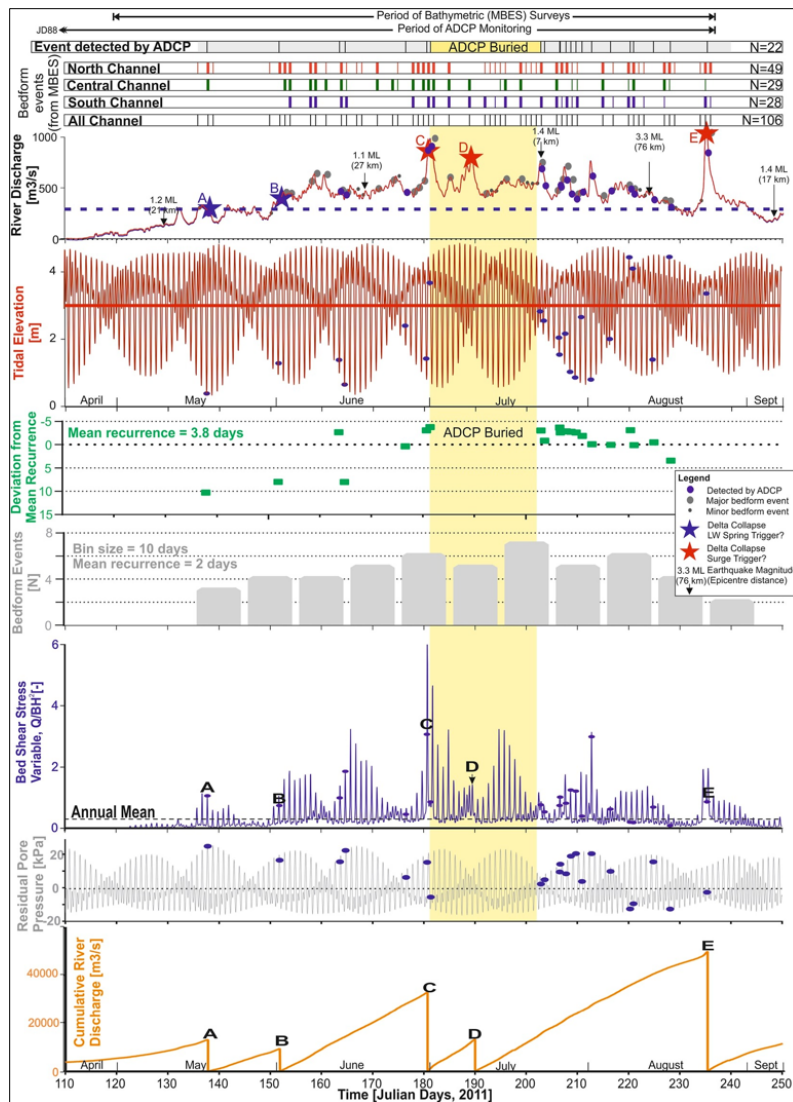
Figure 29. Squamish Delta monitoring

Figure from Clare et al. 2016, showing results of Squamish Delta monitoring.Top four staves show timing of turbidity currents recorded by acoustic current meters and bedform events detected from multibeam echosounders (thicker bars denote major [>0.5 m] change; thinner bars denote minor [<0.5 m] change), river discharge and earthquakes, tidal elevation, recurrence of turbidity currents detected at ADCP location, bedform event frequency per 10 day bins, delta-top bed shear stress variable, residual pore pressure at 10 m below seafloor, and cumulative river discharge leading up to delta-lip collapses A to E.

Results from the Squamish delta showed that high river discharge events do influence delta-lip collapse, but with an 8–11 hr delay between peak discharge and failure (Clare et al. 2016). This was attributed to preconditioning of the slope by rapid sediment accumulation and subsequent triggering by pore-pressure change due to tidal drawdown or rapid sedimentation. A similar delay between flood events and seafloor failure has been observed on the MRDF, but the delay was measured to be 1–4 years between flood and seafloor retreat (Lindsay et al. 1984). Nevertheless, the MRDF observations were based on much more infrequent seafloor datasets and smaller failures could have occurred more frequently during the 1–4 year period to result in the overall observed seafloor retreat. The seafloor slope of the two deltas also differs (MRDF is much lower gradient), which may influence the timing of failures related to flood events.

Other studies have used in situ measurements to study instabilities in the Fraser River delta offshore British Columbia and in Monterey Canyon offshore central California. An instrumented platform was installed in Canada's VENUS network to record delta processes. Instruments including an ADCP and turbidity sensor were used to document several sediment gravity flow events that result from the combination of high river discharge, high SSC, and strong tides (Ayranci et al. 2012). In Monterey Canyon instrumented moorings generated detailed profiles of flow velocity and sediment concentration (Xu et al. 2014). Tracking of flows in the canyon was also conducted with sensors embedded in moving near-bed layers that recorded acceleration, sense of rotation, and total displacement (Paull et al. 2010).

Decades of work on global subaqueous deltas and associated instabilities has been conducted since the last comprehensive study of the MRDF. This work includes very recent studies that employ advances in technology to monitor events and measure seafloor conditions. More work is needed to apply these concepts to MRDF instabilities and to employ new technologies for direct observations of the MRDF.

2.3.5 Knowledge gaps

Despite the many advances in our understanding of MRDF sediment instabilities, the frequency of mudslide activity is currently unknown beyond those triggered by major storms, and little is known about the importance of winter storms on mudslide initiation, or about mudslide activity during oceanographic quiescent periods. Recently, Hurricanes Ivan and Katrina in 2004 and 2005, respectively (Hooper and Suhayda 2005; Nodine et al. 2007; 2009) generated catastrophic mudslides that damaged offshore infrastructure, highlighting our poor understanding of these events and the need for updated information to support decision making.

The most recent regional study of MRDF sediment instabilities was conducted in the late 1970s and included the most recent regional seafloor mapping effort (1977–1979) (Coleman et al. 1980). Subsequent, more localized studies have attempted to document seafloor changes associated with hurricane events, collected and analyzed geotechnical and geochemical information from landslide deposits, and proposed methods for predicting or quantifying hazards risks. However, these studies have been limited to individual slides, were sampled using antiquated techniques, or developed predictive tools that are overly simplistic or have not been validated. Furthermore, significant changes to the Mississippi River sediment load have been documented since the 1950s (Kesel 2003), which appear to be reflected in offshore sedimentation patterns (Maloney et al. 2018). Coupled with historical changes in flow distribution among delta distributary channels (Morgan 1977; Clark et al. 2013), these changes are likely to affect mudslide processes and a new baseline dataset is vital to any hazard susceptibly assessments. Additionally, high resolution, regional bathymetry would provide an opportunity to use new approaches in GIS systems to understand slope stability and could be used in regional modeling for storm predictions.

Rates of failure for many instability features are not well constrained and estimates are generally based on repeat, single-beam surveys. The complex morphology and potential for both steady and episodic flow (e.g, Obelcz et al. 2017) make it difficult to measure rates of change on the MRDF. Infrastructure damage has historically been the method for constraining event timing, but even this results in significant variability and only records catastrophic events. Return periods for mudslides that damage structures varies with location between <10 years to >1,000 years with increased risk associated with shallower depths, greater slopes, and amount of infrastructure present (Nodine et al., 2007). Furthermore, no long-term in situ monitoring of mobile muds has occurred to characterize and quantify the frequency of this mode of failure. To better constrain rates of both the more steady and episodic events, new technology and methods could be employed to evaluate seafloor change over various spatial and temporal scales. For example, high-frequency repeat high resolution bathymetric surveys could be coupled with *in situ* monitoring of instability features. Repeat surveys could be used to estimate the magnitude of failures (e.g., downslope migration, sediment volume, headward erosion or gully widening), and to document seafloor changes before and after triggering events (e.g., river floods, hurricanes, winter storms) (e.g., Walsh et al. 2006; Paull et al. 2010; Hughes-Clark et al. 2012; 2014; Clare et al. 2016; Obelcz et al.

2017). Deployment of instrumentation to record movement within instability features would also greatly improve our understanding of event timing and help to differentiate between continuous and episodic movement while also providing data on characteristics of the flow, such as velocity, acceleration, and duration (Paull et al. 2010; Xu et al. 2014). Additionally, collection and analysis of long sediment cores could identify multiple sediment gravity flow deposits and establish a geochronology of events over longer time scales to determine event recurrence time (Droxler and Schlager 1985; Goldfinger 2011).

Triggering mechanisms and pre-conditioning factors are also poorly understood on the MRDF. Triggering mechanisms could include a multitude of forces (e.g., hurricanes, winter storms, floods, gas charging, mudlumps, earthquakes) that operate on different time scales, while pre-conditioning factors include underconsolidation of sediment and the presence of biogenic gas. Hurricanes are a known triggering mechanism for catastrophic slides based on impacts to offshore infrastructure (Nodine et al. 2007), but the relative importance of other triggers are not well known. High resolution geochronology and sedimentology (x-radiography and grain size) have recently been used to study hurricane event deposits in areas surrounding the MRDF (Allison et al. 2005, Keen et al. 2004), and most recently for seasonal deposition near Southwest Pass (Keller et al. 2016). This work holds promise for providing highly detailed timelines for processes active over ~monthly to ~decadal timescales.

Rapid-response bathymetric surveys following proposed catastrophic triggering events can be used to measure seafloor changes related to the event and more frequent surveys associated with in situ monitoring could also capture seafloor movement tied to more minor triggering events (Clare et al. 2016). Additionally, in situ measuring of hydrodynamic and seafloor conditions could also be used to measure how triggering events impact the seafloor (i.e., how do winter storm waves affect pore-water pressures, or how do river floods contribute to mobile mud layers?) (Paull et al. 2010; Xu et al. 2014; Hughes-Clark 2016). The data collected from these in situ surveys would also improve numerical and laboratory models of seafloor instability and triggering mechanisms by providing model constraints based on direct field observations. These models could elucidate the relative role of the different triggers on MRDF instabilities (Wang and Liu 2016; Denommee et al. 2017; Obelcz et al. 2017).

Although some information is known about preconditioning factors on the delta front including shear strength and geochemical profiles (Whelan et al. 1976; 1975; Bea et al. 1983; Bohlke and Bennett 1980) and some in situ measurements of pore-pressure have been collected (SEASWAB efforts), the existing data is limited in extent across the delta and influenced by the presence of sub-seafloor gas. More comprehensive measurements of in situ pore pressure across different instability features and during different hydrodynamic conditions would improve models of seafloor response to those conditions. Furthermore, no reliable data for in situ gas concentrations exist for any portion of the MRDF seabed, which presents a huge knowledge gap in our ability to assess submarine landslide hazard. New technologies for measuring gas in sediments could also be employed to map regions of gas beneath the seafloor and areas where gas escapes to the water column. Geotechnical analysis of sediment that has not de-gassed would also provide more realistic measurements of sediment properties of the MRDF (Denk et al. 1981).

Advancing knowledge on any one of these gaps would help to improve hazard assessments for the region, but recent studies have shown that a multi-faceted approach to study seafloor instabilities provides the data needed to fully assess failure timing, triggering, extent, and sediment characteristics (Talling et al. 2015).

2.3.6 Conclusions

Most research on seafloor landslides relies on data collected from existing landslide deposits (i.e., only after the event), but the MRDF provides a unique opportunity to observe landslide processes in action. Because of the wide distribution of landslides on the delta front and the high number of triggering factors, landslide events are more predictable in time and space and we are able to observe processes over

relatively short time scales. Additionally, the high frequency of events provides an opportunity to capture multiple landslides for an accurate estimate of recurrence time.

1. The most recent comprehensive seabed mapping program in the delta front region occurred in 1977–1979.

2. Localized studies have been conducted 1981–2014, but have generally focused on one individual storm event or slide.

3. No long-term in situ study has ever been conducted to quantify mode and frequency of seabed failures.

4. Since the mid-20th century, sediment delivery in the Mississippi Delta has declined precipitously, greatly changing the sedimentation regime that drives seabed failures. No study before our data synthesis takes this into account.

5. Rates and spatial and temporal scales of failures are not well constrained and most estimates are based on repeated single-beam sonar surveys with high uncertainty.

7. The role of gas is widely suspected to be important in preconditioning sediments for failure, but in situ gas concentrations have never been accurately determined, in situ rheologies influenced by gas are poorly documented, and the role of gas has never been incorporated into models of seabed failure.

6. Triggering mechanisms have been enumerated, but are not well understood. Only large-scale catastrophic failures have been widely documented, but recent work demonstrates that flows and failures also occur during periods of quiescence, with regard to hurricane strikes.

7. Waves are widely recognized as important triggers for mudflows, but most work on this topic to date has been conducted using oversimplified linear wave models. Predictive models used to date underpredict the forces applied by real ocean waves to the seabed.

8. Advanced geochronological and geological analytical methods exist that can help provide detailed information on the rates and distributions of mudflows in time and space, but these methods have mostly been applied outside of the most dynamic regions of the MRDF, one exception being Keller et al. 2016.

3. Results of Pilot Study

3.1 Geological Study

3.1.1 Abstract

To assess patterns of submarine mass-wasting events on the Mississippi River Delta Front, multicores and gravity cores (0.5 and <3 m length respectively) were collected seaward of the Mississippi River Southwest Pass in 25–75 m water depth. Cores were analyzed for radionuclide activity, grain size, bulk density, and fabric (x-radiography). Core sediments are faintly bedded and composed mostly of clay and fine silt. Short-term sedimentation rates (from ^{7}Be) are 0.05–0.42 cm/d during river flooding, while longer-term accumulation rates from ^{210}Pb are 1.3–7.9 cm/y. In most cores, ^{210}Pb activity displays undulatory profiles with steady overall declining activity versus depth. Undulations are not associated with grain-size variations and are interpreted to represent variations in oceanic ^{210}Pb scavenging by river-plume sediments. The ^{210}Pb profile of one gravity core from a mudflow gully displays ~uniform basal excess activity over a zone of low bulk density, interpreted to be a mass failure deposit that occurred 9–18 years before core collection. Spatial trends in sediment deposition (from ^{7}Be) and accumulation (^{210}Pb) indicate that proximity to the river mouth has stronger influence than local facies (mudflow gully, depositional lobe, prodelta), over the timeframe and seabed depth represented by our cores (<40 years, <3 m). This may be explained by rapid proximal sediment deposition from river plumes coupled with infrequent tropical cyclone activity near the delta in the last seven years (2006–2013), and by the location of most sediment-failure surfaces (from mass flows indicated by parallel geophysical studies) deeper than our core-sampling depth.

3.1.2 Introduction

Thick mud deposits on continental shelves form from supply of terrestrial sediment to the coastal ocean from rivers (Figure 30). The morphology of such deltaic deposits is further influenced by waves and tides to shape the final geometry of deposits (Wright and Coleman 1973; Galloway 1975; Walsh and Nittrouer 2009) (Figure 30). The Mississippi River Delta, including offshore submarine deposits (which are referred to as the Mississsippi River Delta Front, or MRDF) has long been considered a system dominated by riverine input, with lesser influence from waves and tides. This condition results in muddy river sediment depositing rapidly near the river mouth. These deposits are commonly weak with steep slopes, making them prone to failure and submarine landslides (Coleman et al. 1980).
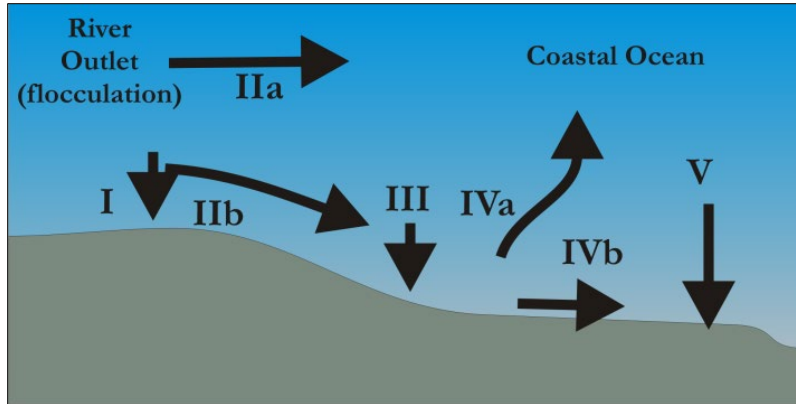
Figure 30. Sediment dispersal patterns

Patterns of fluvial sediment dispersal, deposition, and accumulation in the coastal ocean. After Wright and Nittrouer (1995) and Bentley (2002). Stage I: bedload deposition, bar formation; Stage IIa: seaward transport in buoyant plume; Stage IIb: seaward transport in hyperpycnal plume; Stage III: temporary deposition on shelf; Stage IVa: resuspension and transport in water column; Stage IVb: transport in gravity-driven flow from both mass wasting and hydrodynamic resuspension; Stage V: long-term accumulation.

Submarine landslides are associated with many river deltas worldwide that are considered "river dominated" (Prior and Coleman 1982; Walsh and Nittrouer 2009). Specific examples include the Niger (Sultan et al. 2007), Fraser (Hart et al. 1998), and Huanghe (Prior et al. 1989), among others. Because pipelines, communication lines, navigation aids and channels, and other infrastructure are commonly located in such areas, understanding specific forces that control seabed dynamics in such deltaic settings has wide significance.

The first major insights into submarine landslides of the MRDF were primarily derived from comparison of bathymetric surveys (Shepard 1955), and early applications of sidescan sonar that can provide a shaded acoustic image of the seabed (Coleman et al. 1980). Coleman et al. (1980) and Prior and Suhayda (1979) described the motion of sediments in mudflow lobes, gullies, and other similar landforms as either slow, steady creeps or rapid movements that pulse over time, with downslope movement rates from hundreds of meters to up to 2 km per year. More recent work has evaluated regional dispersal patterns by dating sediment layers using radioisotopes associated with marine sediments analogous to carbon-14 dating, but over timescales of seasons to decades, compared to the millennial timescales of carbon-14 (Corbett et al. 2006; Young 2014).
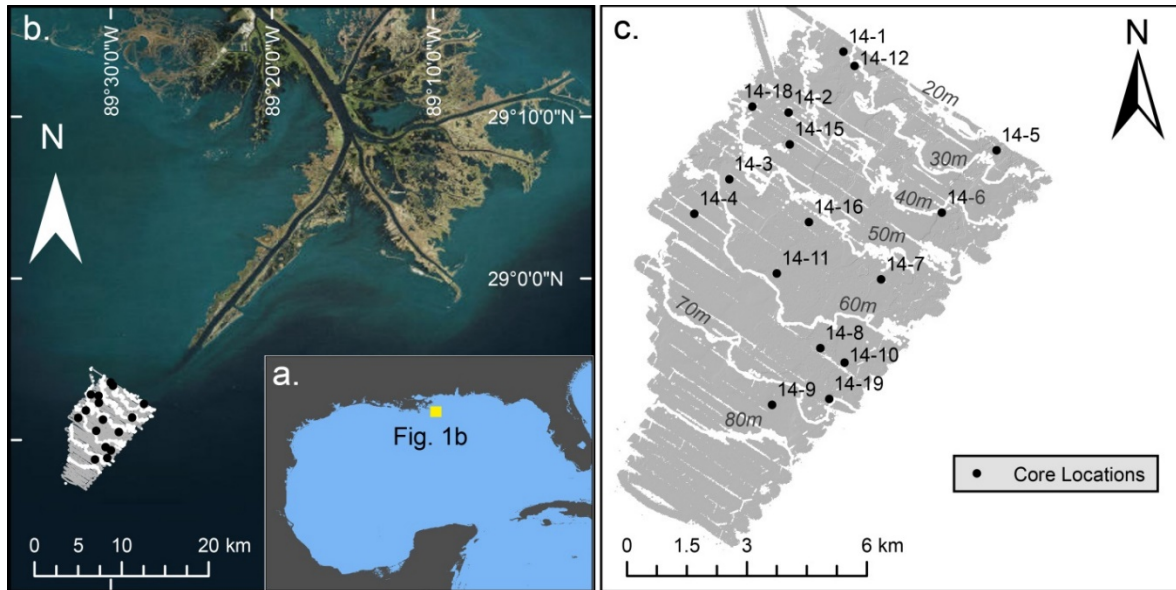
Figure 31. 2014 core locations

Map of study area. Coring locations are labeled with the core name. Some locations represent both a short core and a gravity core. In the text the gravity cores are identified by a "g" following the core location name. The yellow area in Panel a represents the region of mass wasting mapped by Coleman et al. (1980). Geophysical survey lines collected by Obelcz et al. 2014 are shown in Panel b. Background imagery is open source "World Imagery" from ESRI.

Concerns regarding seafloor stability of the MRDF, associated mass wasting, and risk to petroleum-production infrastructure have focused interest on MRDF mass failures (e.g., Bea, 1971), and have been renewed since hurricanes Ivan (2004) and Katrina (2005) (Guidroz 2009; Kaiser et al. 2009). Of particular interest are the range of temporal and spatial scales over which failures occur (Maloney et al. 2018; Obelcz et al. 2017), and the forcing mechanisms (Guidroz 2009). In this study, we apply radioisotope dating methods (^{210}Pb, ^{137}Cs, and ^{7}Be) and other geological core analyses to evaluate sedimentation processes across the MRDF, over timescales of seasons to decades, and sub-seabed depths up to 3 m, as governed by coring and analytical approaches.

3.1.3 Background

3.1.3.1 Study area

The study area is the continental shelf proximal to the Southwest (SW) Pass distributary of the Mississippi River (MR), spanning water depths from 25 to 75 m (Fig. 31). Southwest Pass is the largest of three major distributary outlets of the modern Balize or bird-foot delta of the Mississippi (Allison et al. 2012). The river delivers approximately $2\text{X}10^{8}$ metric tons of suspended sediment to the northern Gulf of Mexico (GOM) shelf each year (Meade 1996). For water years (October 1–September 30) 2008–2010, Southwest Pass discharged ~$2\text{X}10^{7}$ metric tons of sediment per year, with the remainder of sediment exiting the river from other outlets (Allison et al. 2012). Much of the sediment is initially retained near the distributaries (within ~30 km; Corbett et al. 2004; Xu et al. 2011), before being redistributed by tropical cyclones and other weather systems (Fig. 28)(Wright and Nittrouer 1995; Bentley 2002; Walsh et al. 2006). Submarine landslides and similar phenomena are dominant processes moving sediment after deposition (Coleman et al. 1980)(Fig. 32). These events pose a significant hazard to the vast array of oil and gas drilling platforms and pipelines in the area (Sterling and Strohbeck 1973; Guidroz 2009; Kaiser et al. 2009).

3.1.3.2 Types and causes of mass failures

3.1.3.2.1 Causes of mass failures

Mass failures develop where and when the downslope force of gravity acting on a mass of sediment exceeds resisting forces (Lee et al., 2009). Mass failures on the MRDF are facilitated by the low strength of sea-floor sediments. Coleman et al. (1980) proposed four conditions that promote submarine sediment flows and landslides: (1) rapid sedimentation that (2) prohibits compaction of sediments under their own weight followed by (3) production of biogenic gas, culminating in (4) failures triggered by storm waves.

Large waves (Coleman et al. 1980) produced by major hurricanes crossing the Mississippi River Delta are known to be major controls on development of large seabed failures (Guidroz 2009), but more recent work (Denommee and Bentley 2013) also demonstrates that much smaller waves from ~weekly winter cold fronts are also capable of initiating smaller flows closer to shore, in waters <10 m deep. Assessing the range of conditions over which such failures can occur, and their geological record, is one goal of this and the parent study (Maloney et al. 2018; Obelcz et al. 2017).
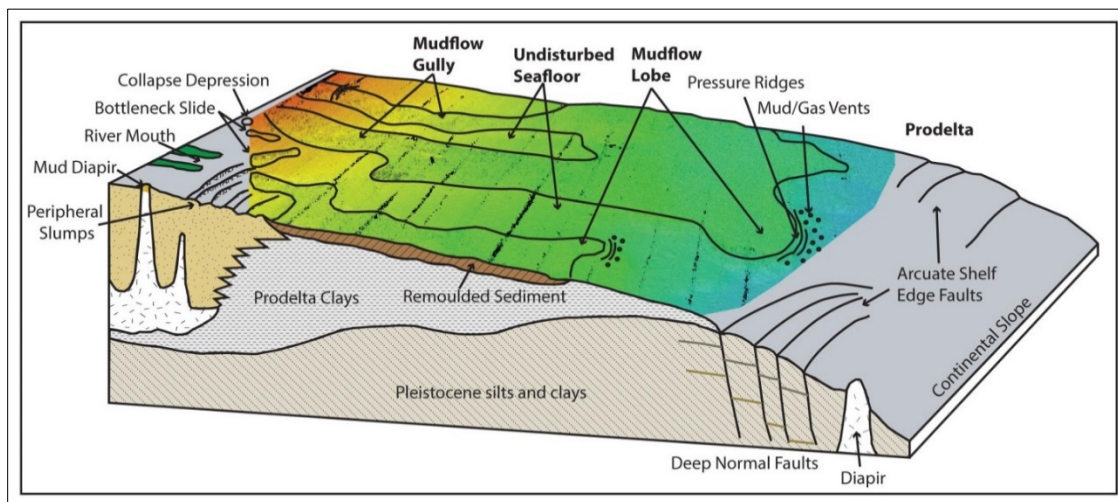
Figure 32. Mississippi River Delta Front block diagram

Seafloor diagram illustrating facies. Adapted from Coleman et al. (1980) by Maloney et al. (2014) using multi-beam bathymetry data from Walsh et al. (2006). Outlined mudflow gullies cut into undisturbed seafloor and convey sediment downslope to depositional lobes, which may stack and coalesce. The range of depth is 20–80m, with warmer colors corresponding to shallower depths, and cooler colors to deeper depths.

3.1.3.2.2 Sediment transport processes and seabed morphology

Figure 29 illustrates major elements of MRDF seabed morphology, using the terminology of Coleman et al. (1980), bathymetry from Walsh et al. (2006), and subsurface structure interpreted from Coleman et al. (1980) and Obelcz et al. (2014). Mudflow gullies are prevalent from coastal bays on the delta down through the intermediate submarine delta front (120 m). Gullies can incise up to 20m into the undisturbed seafloor, and extend laterally up to 10 km across the shelf, joining with other channels to form tributary networks (Bouma et al. 1991). Slope failures are common along the edges of some of the larger gullies, and deliver much of the material moving in gully mudflows (Coleman et al. 1980). Other modes of sediment transport range from transportation of intact blocks of seafloor (Coleman et al. 1980) to complete remolding during flows of nearly fluid mud (Roberts et al. 1980).

Mudflow lobes develop at downslope ends of gullies where sediment flowing through a feature with negative relief (gully) coalesces to form a depositional feature with positive relief (Fig. 29)(Coleman et al. 1980;). Lobes have an average thickness of 10 m (Coleman et al. 1980). No instantaneous rates of progradation have been measured, however lobes have been known to advance up to 900 m downslope in one year, and can extend for 4 km (Coleman et al. 1980). Failures in gullies have led to the transport and deposition of blocks up to 1 km wide in some lobes (Bouma et al. 1991).

3.1.3.2.3 Hurricane impact

Hurricanes are important triggers of mass movements offshore of the Mississippi River Delta. Wave motions produce bottom shear stresses capable of causing failure (Coleman et al. 1978). Guidroz (2009) studied historical hurricane impacts on the MRDF seabed in detail, and ascertained that only category 3+ hurricanes that slowly traverse the MRDF are likely to produce seabed mass failures of scales sufficient to induce catastrophic oil-platform collapse. Since the onset of Gulf of Mexico petroleum production, hurricanes in this category passing through or near MRDF include Betsy (1965), Camille (1969), Ivan (2004), and Katrina (2005). Mass movements associated with Hurricane Ivan destroyed seven platforms, and movements associated with Hurricane Katrina destroyed 46 platforms, with additional damage caused to infrastructure by both storms (Guidroz 2009).

Modeling efforts in the wake of Hurricane Ivan predicted maximum significant wave heights of 21 m (Wang et al. 2005; compared to 17.9 m observed), and associated bottom shear stresses high enough to cause sediment failures at water depths of up to 120 m (Hooper and Suhayda 2005). Xu et al. (2015) modeled extreme conditions on the MRDF during Hurricane Katrina, and reported 50 m/s wind speeds, 25 m waves, 3 m/s of nearbed wave orbital velocities that produced wave-current bed shear stresses of 50 Pa and up to 1.5 m of seabed scour. Although catastrophic movements only occur during major hurricanes, weaker hurricanes, tropical storms, and winter cold fronts are capable of producing smaller seabed disturbances in shallower waters. Allison et al. (2005) observed a 20 cm event deposit associated with the 2002 systems Tropical Storm Isidore and Hurricane Lili. In a similar inner-shelf depositional environment on the southwest Louisiana coast, Denommee et al. (2015) observed evidence of mud flows in side-scan sonar data from water as shallow as 4 m; their study suggests that waves associated with the passage of ~weekly winter cold fronts can generate failures in shallow coastal waters where such weak, muddy sediments exist.

3.1.3.3 Changes in the modern Mississippi River

The modern MRD is being strongly influenced by upstream anthropogenic alterations such as dams, diversions, and bank stabilization that have reduced sediment load in the river's mainstem. Additional factors influencing delta land area and morphodynamics include local subsidence and eustatic sea-level rise (driving decreased sediment-transport efficiency that accelerates in-channel sedimentation in the lower river), and upstream migration of major river discharge points (Kemp et al. 2014; Bentley et al. 2015). Allison et al. (2012) have shown that three outlets upstream of the Head of Passes (Fort St. Philip, Grand Pass, and Baptiste Collette) each currently discharge more suspended sediment than either South Pass or Pass a'Loutre (the other two main distributary outlets other than Southwest Pass). Collectively, these phenomena are likely to lead to landward retreat of the MRD (Bentley et al. 2015). Blum and Roberts (2009, 2012) present a long-term decrease in the sediment load reaching the Gulf of Mexico, with as much as a 50% decline in the last century. One possible outcome of these changing sediment delivery patterns may be an overall decrease and subsequent redistribution of sediment to different parts of the delta and continental shelf. This may increase the possibility of failures in historically stable areas fed by distributaries that are capturing more sediment, or reduce the driving forces for mass failures in areas where failures are presently driven in part by rapid sediment accumulation.

3.1.3.4 Methods

3.1.3.4.1 Field work and core processing

In June–July 2014, short (<50 cm depth, 10 cm diameter) cores and longer (up to 3 m depth, 10 cm diameter) gravity cores were collected across four different seabed types (undisturbed seafloor, mudflow gully, depositional lobe, and prodelta)(Fig. 31). Core locations are shown in Figure 31c. Throughout the text, gravity cores are indicated by a "g" following the core location name. Depositional environments and facies were identified by the study of seabed sonar data and maps collected from the R/V *Coastal Profiler* one week before coring (Obelcz et al., 2014).

Profiles of sediment density were collected from long cores using an automated core logging device. Long cores were subsequently split and sampled for grain size analysis, and other geological properties.

3.1.3.4.2 Grain Size analysis

Individual, disaggregated grain sizes were measure by way of laser diffraction for all cores at a 2 cm sample resolution.

3.1.3.4.3 Radionuclide analysis

Sediment layers were "dated" using the radionuclides ^{7}Be (natural cosmogenic, $t_{1/2}$=53.2 days) and ^{210}Pb (natural ^{238}U-series, $t_{1/2}$=22.2 years).

Inventories of ^{7}Be (disintegrations per minute per square cm, dpm/cm^2) were calculated for all short cores, to calculate the amount of ^{7}Be stored in the seabed, an indicator of rapid recent sedimentation. Sediment accumulation rates were determined for longer-term processes using the radioisotope ^{210}Pb, which can be used for this because of its half -life being much longer than that of ^{7}Be.

3.1.3.5 Results

3.1.3.5.1 Grain size

Frequency-contour plots of grain size are shown in Figure 33. Grain size does not vary greatly in analyzed samples. Silt is the most dominant grain size in the field area, making up 41–70% by volume. Clay content ranges from 16 to 42%. Sand content ranges from 0 to 39%. Most samples with >20% sand are isolated; however, there is an 8 cm interval (36–44 cm) in gravity core 14–3g with 32–38% sand.
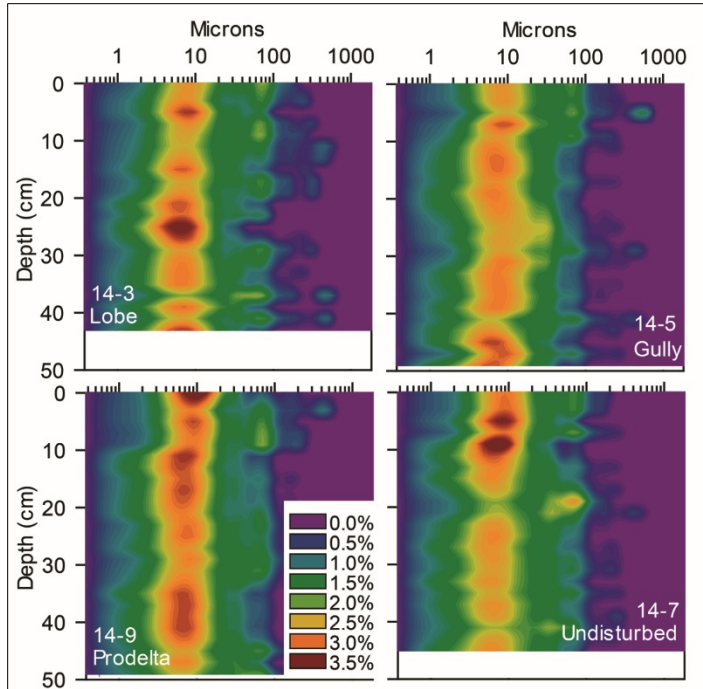
Figure 33. Grain size distributions

Selected grain size frequency plots representing depositional environments. All four cores have a modal grain size in the very fine/fine silt range as displayed by warm colors, as well as a few layers slightly enriched in very fine and/or fine sand. Colors in legend correspond to percent occurrence.
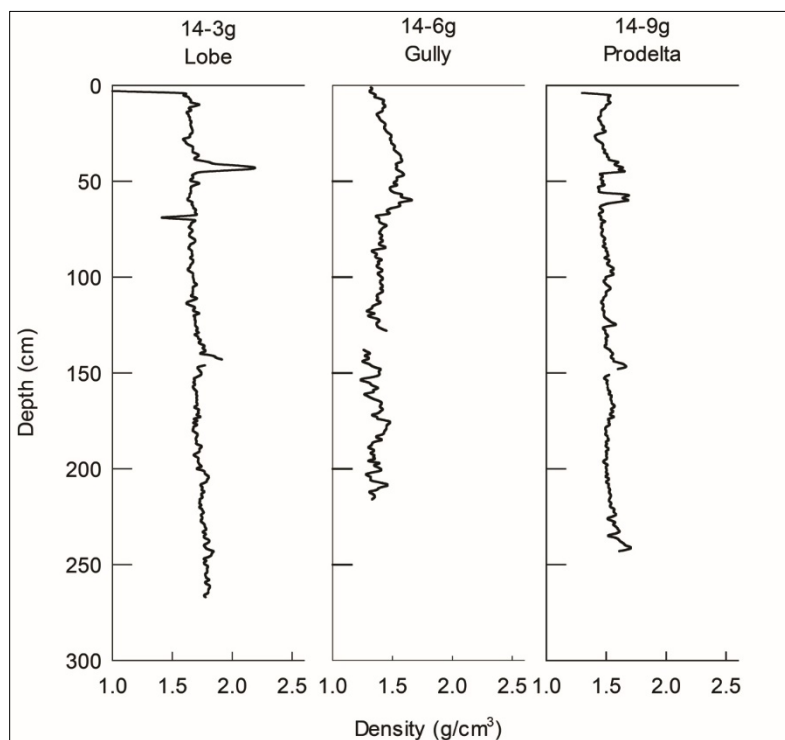
Figure 34. Gravity core density profiles

Downcore density profiles for the gravity cores. Core 14-6g has a low density layer beginning at 68 cm depth, corresponding with a layer of homogenized [210]Pb_{xs} activity. In all three cores, density variation decreases in the lower half of the cores.

3.1.3.5.2 Gamma density

Figure 34 displays gamma density profiles for cores 14–3g (depositional lobe), 14–6g (mudflow gully), and 14–9g (prodelta). Density profiles for the gravity cores show that sediments are generally low density, but variable, with high water content and low strength.
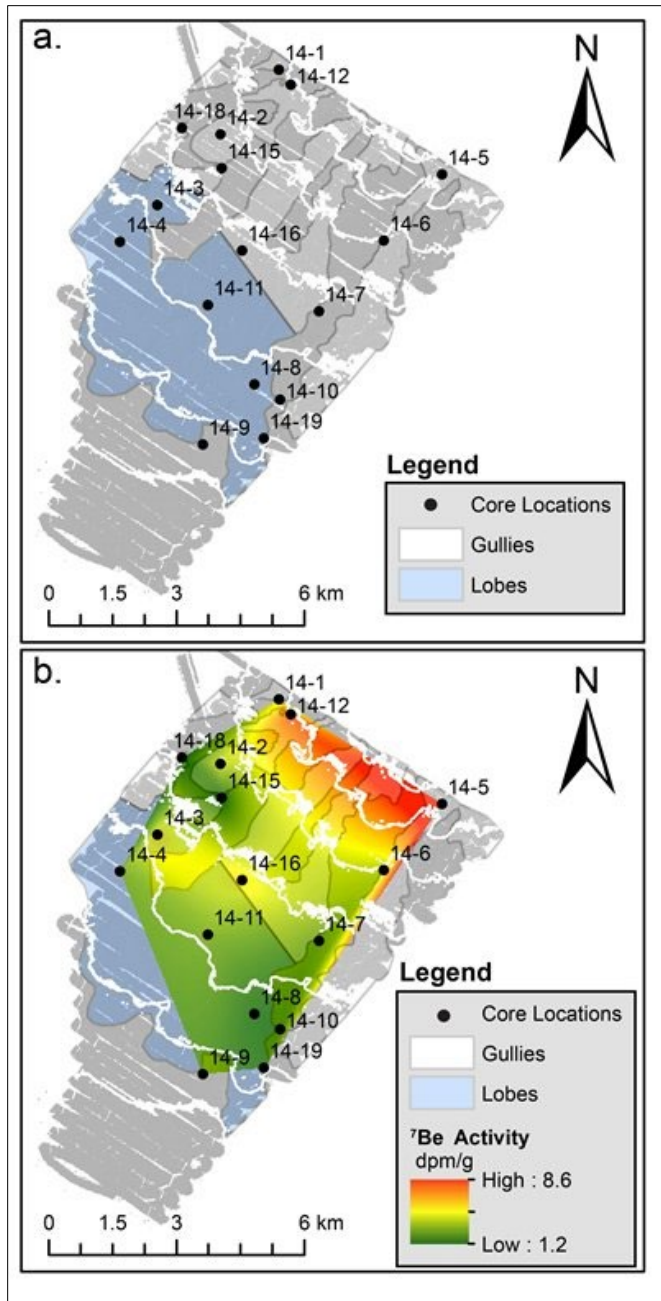
Figure 35. 2014 facies and [7]Be map

a. Facies distributions and core locations on contoured, hill-shaded bathymetry derived from Walsh et al. (2006), adapted from Fig. 31c. The yellow dashed line separating gully and lobe facies indicates a gradational boundary. Gray areas encompass undisturbed and prodelta facies, both of which are unaffected by mass movements.

b. Interpolated color-contoured map showing mass accumulation of sediment deposited in the 129±26 days calculated via 7Be activity. Results from each coring site were interpolated across the field area using the Natural Neighbor Interpolation method. The highest values occur in the northeast side of the field area, closest to Southwest Pass.
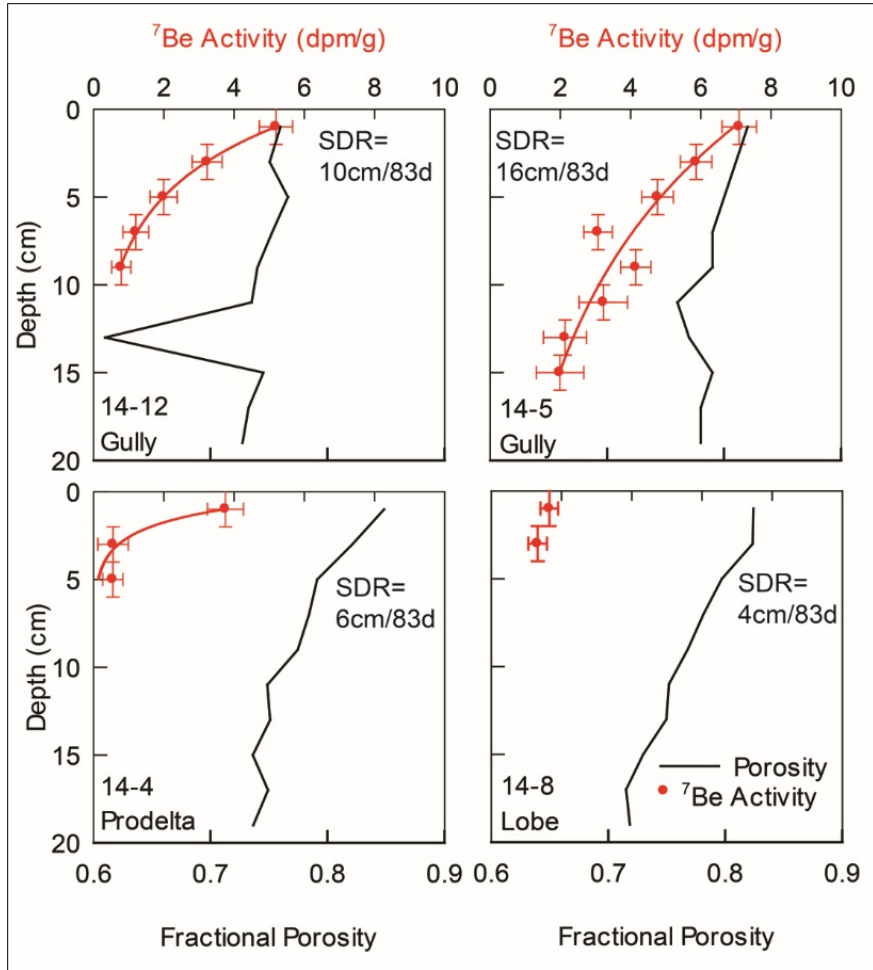
Figure 36. Example 2014 [7]Be profiles

Selected [7]Be activity profiles and modeled sediment deposition rates. 14-5 and 14-12 were taken from the northeastern-most part of the field area, closest to SW pass, and display the greatest depth of [7]Be penetration. Cores 14-4 and 14-8 were taken farther from Southwest Pass, and display less [7]Be penetration. Depositional facies of each core is indicated in the bottom left corner of each profile. See Figure 31 for core locations.

Table 3: Summary of Radionuclide Data of Multicore Samples

Station	Distance from SW (km)	Facies	^{7}Be Inventory (dpm/cm^2)	^{7}Be Penetration Depth (cm;+1)	^{210}Pb SAR (cm/y)	R^2
14-1	6.9	und	13.24	6	2.1	0.79
14-2	8.6	gul	10.76	6	2.8	0.21
14-3	10.4	lob	11.77	8	2.3	0.59
14-4	11.6	pro	4.08	6	2.9	0.79
14-5	5.27	gul	34.06	16	40.7	0.01
14-6	7.26	gul	6.57	6	2.8	0.61
14-7	9.38	und	2.85	4	1.5	0.86
14-8	11.54	lob	2.73	4	1.7	0.58
14-9	13.32	pro	6.26	6	2.4	0.62
14-10	11.6	und	4.51	4	2.4	0.79
14-11	10.9	lob	5.96	6	2.7	0.32
14-12	6.7	gul	15.73	10	1.3	0.68
14-15	8.8	gul	2.30	2	1.6	0.61
14-16	9.4	gul/lob	5.47	8	3.7	0.32
14-18	9.2	gul	3.88	2	2.5	0.35
14-19	12.4	lob	3.45	4	5.3	0.06
Average			8.35	6.13	2.3	0.58

210Pb SAR and R2 averages were calculated without the values from cores 14-5 and 14-19 due to the poor fit to the data.
Abbreviations : Und – undisturbed; gul – mudflow gully; lob – mudflow lobe; pro – prodelta.

Table 4: Comparison between Gravity Core and Multicore SAR

Core	Facies	^{210}Pb SAR (cm/y)	R^2
14-3	lob	2.3	0.59
14-3g	lob	6	0.56
14-6	gul	2.8	0.61
14-6g	gul	3.9	0.63
14-9	pro	2.4	0.62
14-9g	pro	7.9	0.75

Abbreviations : Und – undisturbed; gul – mudflow gully; lob – mudflow lobe; pro – prodelta.

3.1.3.5.3 Radionuclide analysis

Results from ^{7}Be analysis are shown in Figures 35–37. Generally, ^{7}Be inventories (2.73–35.1 dpm/cm^2), recent mass accumulation (1.2–8.7 g/cm^2), and penetration depths (2-16 cm) decrease away from the river mouth (Figs. 35–37).

Beryllium-7 activity is coincident with a high porosity muddy surface sediment layer detectable in all cores (Figure 36). There is no apparent relation between ^{7}Be mass accumulation, penetration depth, or inventory compared to facies (undisturbed, gully, mudflow lobe, and prodelta). Penetration depth, inventory, and mass accumulation from ^{7}Be data all appear to decrease away from Southwest Pass (Table 3, Figs. 35–37).
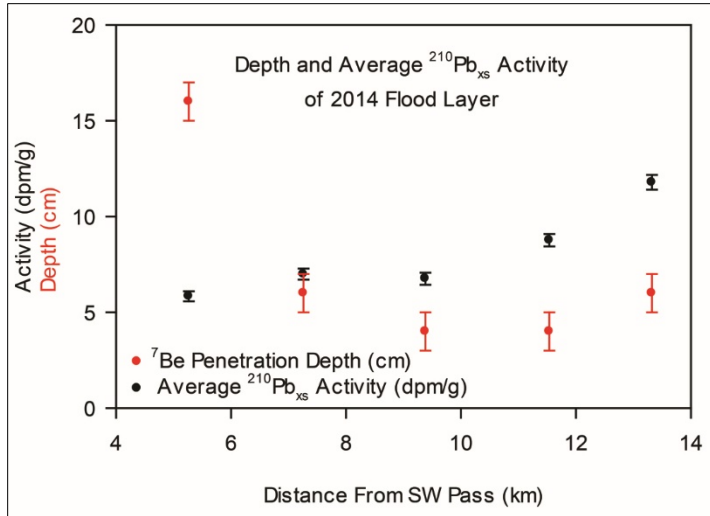
Figure 37. 2014 shelf transect of 7Be and 210Pb

Averaged $^{210}Pb_{xs}$ activity associated with 2014 flood layer. Red circles indicate depth of ^{7}Be penetration, which decreases in cores father from SW pass. Black circles indicate the average $^{210}Pb_{xs}$ activity of the samples for which ^{7}Be was present. Average activity increases with distance from SW Pass, indicating the increased signal of lead scavenging from seawater

Sediment accumulation rates (SARs) calculated from Equation 2 ranged from 1.5 to 3.7 cm/y measured using $^{210}Pb_{xs}$ activity in 14 multicores. On average, accepted SARs calculated using $^{210}Pb_{xs}$ activity from multicores are 2.6 times lower than rates calculated using ^{7}Be (Table 3).

SARs calculated with $^{210}Pb_{xs}$ activity from gravity cores are noticeably greater than rates from the multicores (Table 4) (Figs. 38–39).
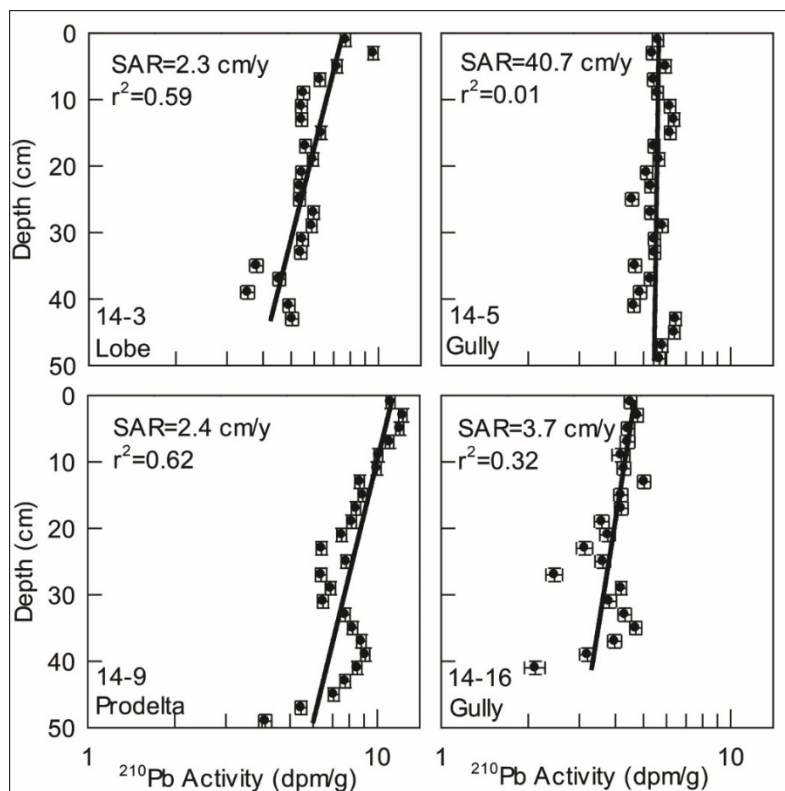
Figure 38. Selected 2014 210Pb profiles

Selected ^{210}Pb activity profiles. These four examples display the varied nature of surface activity as well as the presence and absence of mid-core minima.
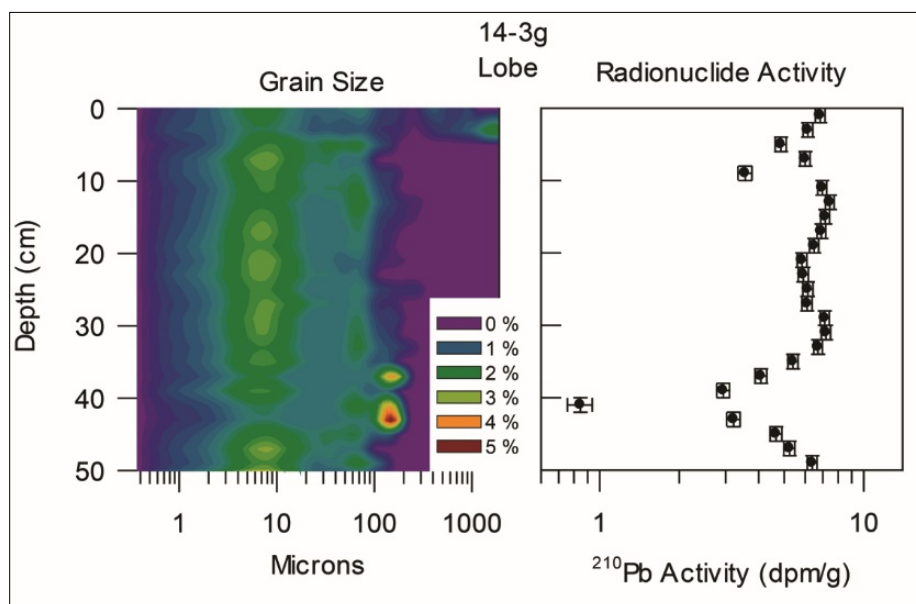
Figure 39. Grainsize and ^{210}Pb in core 14-3g

Summary of top 50 cm of 14-3g. Grain size is shown on the left and [210]Pb_{xs} activity on the right. There are two layers of decreased [210]Pb_{xs} activity, one between 8–10 cm, and between 36–44 cm. The 8–10 cm layer does not correlate with a change in grain size, however the lower horizon corresponds with the highest sand content measured in any sample from this study.
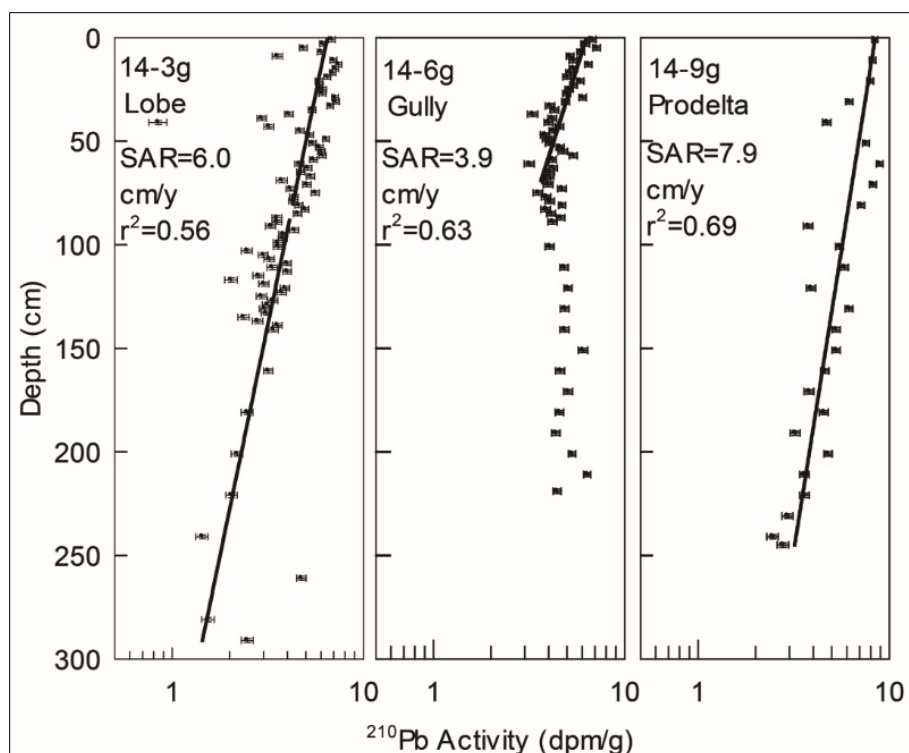
Figure 39. [210]Pb profiles for gravity cores

[210]Pb profiles for gravity cores: 14-3g (lobe), 14-6g (gully), 14-9g (prodelta). Activity steadily declines for the entirety of 14-3g and 14-9g. Activity decreases for the top 70 cm of 14-6g, before remaining constant for the remaining 150 cm of the core.

3.1.3.6 Discussion

Based on previous studies of shelf sedimentary processes on the Mississippi River Delta, dominant sediment delivery processes in our study area include suspension settling from surface river plumes (Moore and Scruton 1957; Coleman et al. 1980; Wright and Nittrouer 1995, and many others); storm wave/current induced resuspension (Keen et al. 2006; Walsh et al. 2006; Xu et al. 2015); sediment slides and seabed flows driven primarily by gravity acting on a slope (Coleman et al. 1980; Denommee and Bentley 2013; Obelcz et al. 2017, and many others); and sediment-gravity flows enhanced by waves and currents (Wright et al. 2001; Denommee et al. 2015).

Accumulation rates for ^{210}Pb are 1.5–7.9 cm/yr (highest values for gravity core results), but deposition rates for [7]Be are generally higher, 0.05–0.42 cm/d during peak-flow conditions. The results of Allison et al. (2012) show up to a 6-fold increase in daily sediment transport during the annual flood season (April to July). The highest measured water discharges during 2014 occurred during the three months prior to core collection (USACE 2015), indicating the greatest Sediment Deposition Rates (SDRs) should occur between April and June, and SDRs associated with low-flow seasons are likely much lower. This is supported by the age of 83 ± 45 days for the [7]Be-laden sediment layer in multicores. These results suggest that the potential age range for the base of a 50 cm multicore is 6.8–33 y, using all ^{210}Pb SARs, or <9 y, if gravity core SARs and [7]Be SDRs are considered. Using seasonal [7]Be SDRs from the 2014 flood deposit, the average age at the bottom of a 50 cm multicore is 8.7 years. Gravity cores encompass a longer period of time, 39–54 y, based on core length and ^{210}Pb SARs. Even given the young age of the collected sediment cores, it is still possible discern patterns of sediment deposition and retention.

Neither SARs nor SDRs appear to vary by facies. Instead, radioisotope depositional patterns appear to vary as functions of distance from Southwest Pass, with higher depositional rates and [7]Be inventories and activities closer to Southwest Pass, and higher ^{210}Pb activities, and lower SARs farther from Southwest

76

Pass (Tables, 3, 4; Figs. 35–37 and 39). Downcore variations of ^{210}Pb activities are mostly (but not always) independent of grain size (Fig. 37), suggesting that dissolved ^{210}Pb limitation, not grain size, controls sediment ^{210}Pb activities.

The gravity cores provide a much longer record of activity, yielding long term sediment accumulation rates. Sediment accumulation rates calculated from gravity cores are generally in agreement with average sedimentation rates from ^{7}Be in the multicores. This indicates that much of the deposited sediment is not removed through resuspension or other types of movement during the time frame captured in these cores. ^{210}Pb$_{xs}$ activity profiles from gravity cores indicate that sediment accumulation rates do not vary greatly over longer scales than were captured in the multicores, with one exception, detailed below.

A sediment accumulation rate of 6.0 cm/y was calculated (using ^{210}Pb$_{xs}$) using samples from 0-292 cm from mudflow lobe core 14-3g, which is in agreement with average sediment accumulation rates across the area using ^{7}Be, indicating no sediment within the 292 cm of sediment sampled by this core was reworked by mass failures in the last ~49 years (encompassing hurricanes Betsy [1965], Camille [1969], Ivan [2004], and Katrina [2005]). While this core does not appear to contain an obvious record of mud deposited by mass failure, the sediment record from the top of the mudflow lobe core is comprised of the mud settling out of the river plume.

In mudflow gully core 14-6g, the sediment accumulation from ^{210}Pb$_{xs}$ activity with the best fit is over the interval 0-70 cm (3.9 cm/year), which also falls in the range of river-plume sediment deposition rates. Scavenging effects (undulations of ^{210}Pb activity not associated with grain size variations) do appear in this upper section of the core, consistent with other cores in the area. From 70 cm depth to the bottom of the core at 246 cm the ^{210}Pb trend is nearly vertical with respect to depth, and the calculated sediment accumulation rate rises to 19 cm/yr. These factors suggest that the base of this core was deposited by a mudflow that deposited or reworked at least 176 cm of sediment (from 70 to 246 cm depth in core).

Time-series bathymetric data (Obelcz et al. 2014) from gully and lobe stations 14-6 and 14-3, respectively, suggest that gully locations have deepened and lobes have gotten shallower each by 3 ± 0.5 m, despite no obvious core evidence for sediment-gravity flows at these locations during this time frame. These contrasting results could be explained by the presence of a detachment surface below the depth sampled by gravity and multicores (0.5–3 m), above which sediments may be transported downgradient as a relatively cohesive and undisturbed block, consistent with previously observed "plug flow" phenomena (Coleman et al. 1978), and below which deep-seated motions likely occur. Overall, because our study is mainly focused on the top 0.5 or 3 m of cores on seabed, the possibility of subsurface mass failure activity deeper than 3 m cannot be totally excluded during the last seven years.

3.1.3.7 Conclusions

This study provides insight on the geochronology of the upper delta front of the Mississippi river, in particular the signals of recent deposition and mass failure. Analysis of sediment cores from four depositional facies provided a multi-faceted approach to the study of mass wasting events and accumulation patterns. Our major findings can be summarized as follows:

1. Beryllium-7 activity shows that 2–16 cm of sediment was delivered to the study area by the MR during the spring flood of 2014, before core collection. Sedimentation rates are highest near the Southwest Pass distributary and diminish with distance.
2. Data from longer cores indicate that in the absence of catastrophic sediment-mass-transport events in the top 3 m of seabed induced by major hurricanes, most of the annually deposited sediment is retained on the delta front.

3.2 Geophysical Study (non-technical summary of Obelcz et al. 2017)

Non-technical summary of:

3.2.1 Abstract

Many submarine landslides, including mudflows on the subaqueous Mississippi River Delta Front (MRDF), are thought to be triggered primarily by discrete energetic events such as earthquakes or large magnitude storm waves. Repeated bathymetric surveys (25 m^2 resolution) of the MRDF show that submarine landslides are active even in the absence of energetic events such as category three or above hurricanes and historic floods. Three surveys conducted in October 2005, February 2009, and June 2014 document >4 m depth change between surveys, primarily located in the mudflow gullies and lobes. The mudflow gullies at water depths of 15–50 m deepened up to 4 m between surveys, while the deeper mudflow lobes in water depths of 50–80 m shoaled by similar amounts. Outside the mudflow complexes, seafloor depths remained relatively stable, or showed slight (<1 m) accretion. Neither the gullies nor the lobes demonstrated prominent lateral migration between surveys; minor widening (<200 m) of gully walls and downslope progradation (<100 m) of the lobe noses were observed. These observations corroborate with nonlinear wave modeling efforts, which infer that even 1-year recurrence interval waves can generate differential seafloor pressures sufficient to trigger submarine landslides. These findings demonstrate that submarine landslides on the MRDF, and by extension perhaps on other proximal accumulation dominated-type deltas, are more frequent than previously conceptualized.

3.2.2 Introduction

Submarine landslides are active sediment transport processes from coastal zone to deep sea in which seafloor morphology can change dramatically. They have been the subject of numerous academic and industry studies because they happen in many sedimentary environments worldwide, and potentially can damage human infrastructure such as oil platforms and pipelines. The modern subaqueous Mississippi River Delta Front (MRDF) began formation approximately 1300 years before present (Frazier 1967). The MRDF accumulates approximately 70% of the Mississippi's total sediment load (~130–150 million tons per year, Mt/yr, [Corbett et al. 2006]) .

Water and sediment are discharged to the MRDF through three main distributaries, from west to east: Southwest Pass, South Pass, and Pass A Loutre (Fig. 40; [Coleman et al. 2002]). Southwest Pass currently receives the largest fraction of water and sediment input (163 km^3/year and 20.8 Mt/yr, respectively; [Allison et al. 2012]). All three distributaries have undergone rapid seaward progradation of >1 km/100 years since 1764 (Bentley et al. 2015), although recent evidence indicates that trend will slow and eventually reverse as the entire Mississippi River Delta is entering the declining phase of the deltaic cycle (Maloney et al. 2018; Roberts 1997).
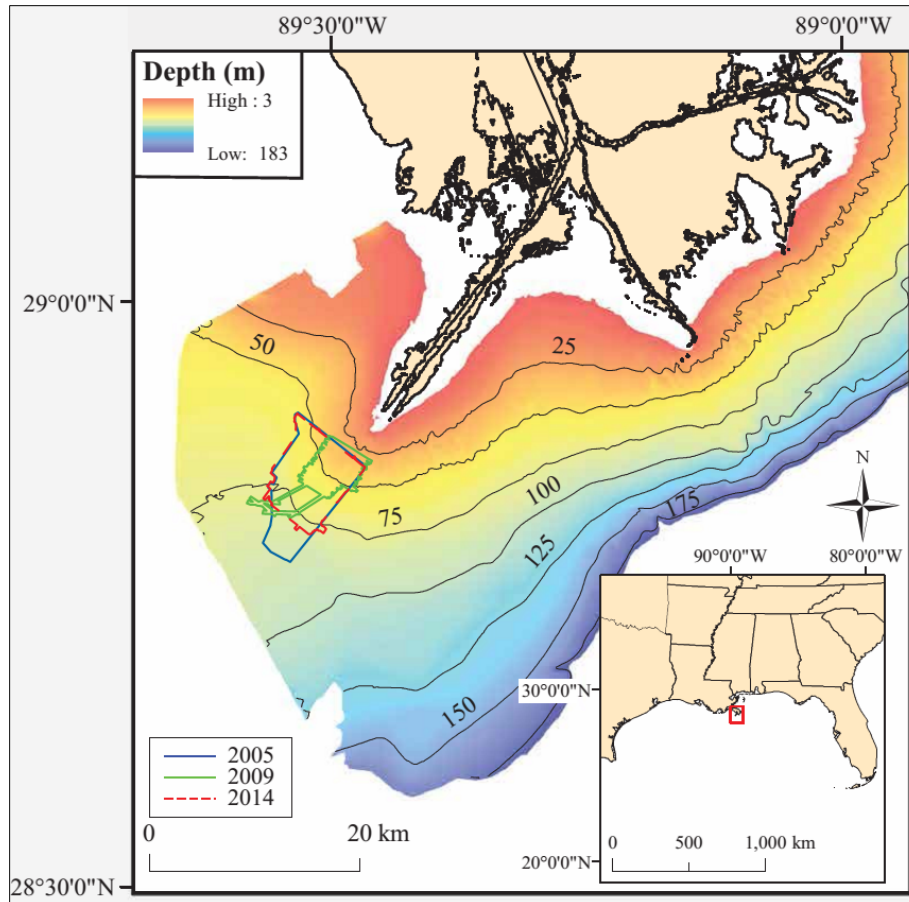
Figure 40. Study area of 2014 geophysical mapping

Base map showing survey area in reference to Mississippi River delta and Gulf Coast of the US (inset). Hill-shaded bathymetry is from Coleman (1979); isobaths are at 25 m intervals. Blue (2005), green (2009), and red (2014) polygons are spatial extents of bathymetric grids used in this study.

The MRDF is prone to submarine landslides despite its overall gentle gradient (rarely exceeding 1.5° of slope (Abbott et al. 1985)) due to multiple factors, including rapid deposition of muddy sediment with high water content (Keller et al. 2016), abundant organic material and subsequent methane production from decay of buried organic matter (Anderson and Bryant 1990; Goni et al. 1997). These factors promote local oversteepening, hinder normal sediment consolidation, both factors that make the seabed prone to failure in the form of submarine landslides (Bryant and Wallin 1968). The Northern Gulf of Mexico is subject to frequent tropical cyclones, and during the passage of large hurricanes wave heights can exceed 15 meters (Bea 1974; Cardone et al. 2007). These waves, and also waves from smaller storms that transit the region 15-30 times per year, create rapidly changing seabed pressures at the seabed. These pressure changes can destabilize the seabed, resulting in large-scale submarine landslides as well as less extensive flows of muddy sediment on the seabed (Prior and Coleman 1984). Due to the large amount of marine infrastructure (oil platforms and pipelines) in the Northern Gulf of Mexico, these submarine landslides have been the subject of numerous academic and industry studies. Most studies to date document seafloor movement caused by large (defined in this paper as greater than or equal to a category three on the Saffir-Simpson scale) tropical cyclones (Bea et al. 1983; Nodine et al. 2007; Wang et al. 2005), which has created the de facto assumption that such landslides are minimal or absent without a high-energy triggering event such as a category three or above hurricane or a major river flood (Coleman et al. 2002; Guidroz 2009). Analysis concerning effects of major events was introduced by (Henkel 1970) and supported further by (Bea and Aurora 1981), using the concept that waves produced pressure

variations that followed the form of a sinusoidal wave, also termed "linear wave theory." None of these or other studies accounted for the effects of more complex waveforms. In this study, we use three high-resolution MRDF bathymetric surveys conducted during a relatively quiescent period (October 2005–June 2014) in tandem with more sophisticated nonlinear wave modeling to test whether submarine landslides on the MRDF are intrinsically tied to energetic triggering events such as hurricanes or floods.

3.2.3 Geomorphic setting

Fluvial and coastal processes in the MRDF region form a suite of distinct geomorphological features, which are thoroughly documented in (Coleman et al. 1980). The most prominent of these features are mudflow gullies and mudflow lobes. Mudflow gullies are elongate seafloor depressions with typical lengths of tens of kilometers, widths of hundreds of meters, and relief of tens of meters (Prior and Coleman 1979). Mudflow lobes form at the downslope terminus of mudflow gullies and have similar dimensions, but they have positive relief (Prior and Coleman 1978). Mudflow gully side/headwalls and lobe "noses" can be sharply defined, often exceeding 10° slope (Roberts 1980). Mudflow gullies and lobes are typically concentrated in the delta front (0.5–1.5° slope, ~5–80 m water depth); the prodelta is downslope of the delta front and has a smaller gradient and greater distance from the distributary mouth that results in far less seafloor disturbance (Coleman et al. 1998).

3.2.4 Methods

The study site is an approximately 55 km^2 area ~30 km southwest of Southwest Pass (Fig. 40). The water depth spans 15 to 80 m, and covers both delta front and prodelta depositional environments. Data from three surveys were utilized for this study: a multibeam bathymetric survey collected in October 2005 by (Walsh et al. 2006), a multibeam bathymetric survey collected by Fugro Geoservices Inc. in February 2009, and an interferometric swath bathymetric survey collected by Louisiana State University, University of New Orleans, and the Bureau of Ocean Energy Management in June 2014. No hurricanes of category three or greater passed within 100 km of the MRDF during the nine years from 2006 to 2014 (NOAA, 2016) and only one major Mississippi River flood (peak discharge >20,000 m^3/s, (Falcini et al., 2012)) during this time frame. Three datasets collected during these three surveys have varying degrees of overlap, as shown in Fig. 40. The bathymetric datasets were gridded into a common 25 m^2 horizontal resolution and subtracted from one another, producing two Difference of Depth (DoD) grids (2014–2009, 2009–2005; only 2009–2005 is shown due to large data gaps in 2014–2009 DoD), accounting for uncertainty in elevation differences between surveys.

To evaluate waves as a driving force for mudflows, a non-linear wave model was used to propagate waves over the study area and calculate the local wave height, length, period, and resulting crest-to-trough pressure under the influence of the most energetic wave conditions that occur on average once per year (such as produced by winter storms and/or cold fronts). Results and observations from (Guidroz 2009) were used to generate Stokes waves at the marine boundary using the (Fenton 1999) approach, and simulated their propagation along the MRDF. The results of this modeling effort were then compared with an earlier linear wave model approach (Henkel 1970).

3.2.5 Results

The 2009–2005 DoD shows dramatic (±4 m) depth changes within the boundaries of the gullies and/or lobes (Figs. 39; 40a). In general mudflow gullies in 15–50 m water depths deepened, and deeper gullies and mudflow lobes in 50–80 m water depths became shallower. Outside the mudflow features the seafloor showed small positive elevation change, which was generally within the uncertainty range and rarely exceeded 1 meter. The trend of gullies deepening and lobes shoaling is not uniform spatially; there are small (<1 km^2) patches shoaling gullies, and an entire gully in the northwest corner of the survey area appears to have been infilled and the downslope lobe slightly deepened (Figs. 41 and 42). The most

drastic deepening (>+4 m) occurred in the shallow (15–40 m) reaches of the mudflow gullies, while the most extreme shoaling (>-4 m) was observed at the downslope end of a mudflow lobe.
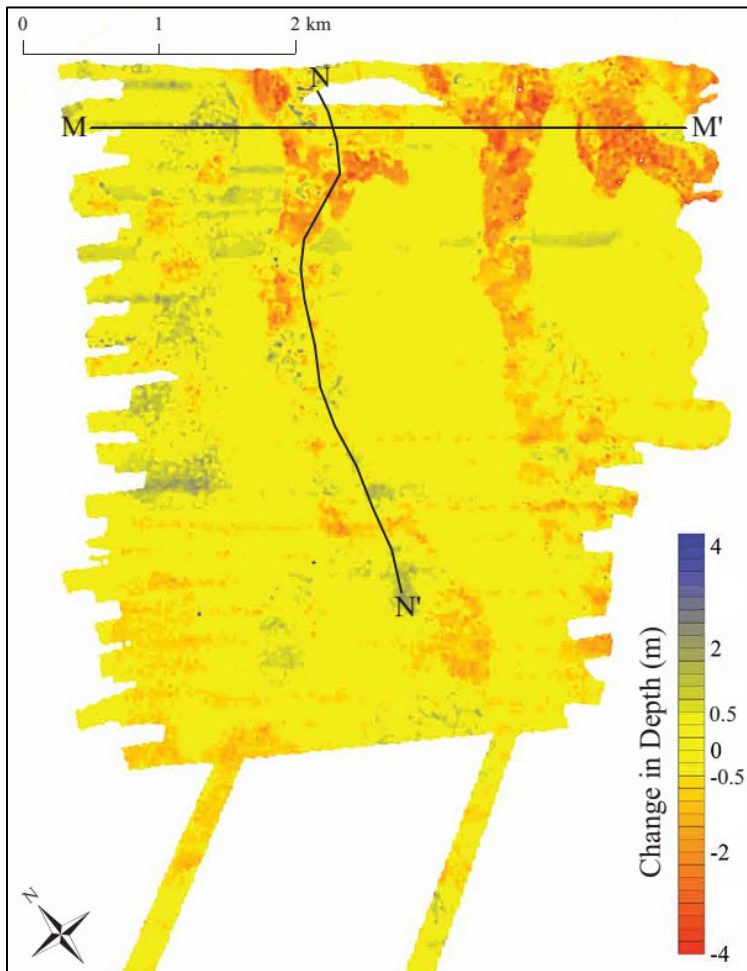
Figure 41. Difference of depth 2005 to 2009.

Difference of Depth (DoD) calculated by subtracting the 2005 Digital Elevation Model (DEM) from the 2009 DEM. Red values indicate depth increase and blue values indicate depth decrease. Yellow pixels are values within the uncertainty range (95% confidence interval, ±0.5 m). Lines M-M' and N-N' show extents of Figures 40A and 40B, respectively.
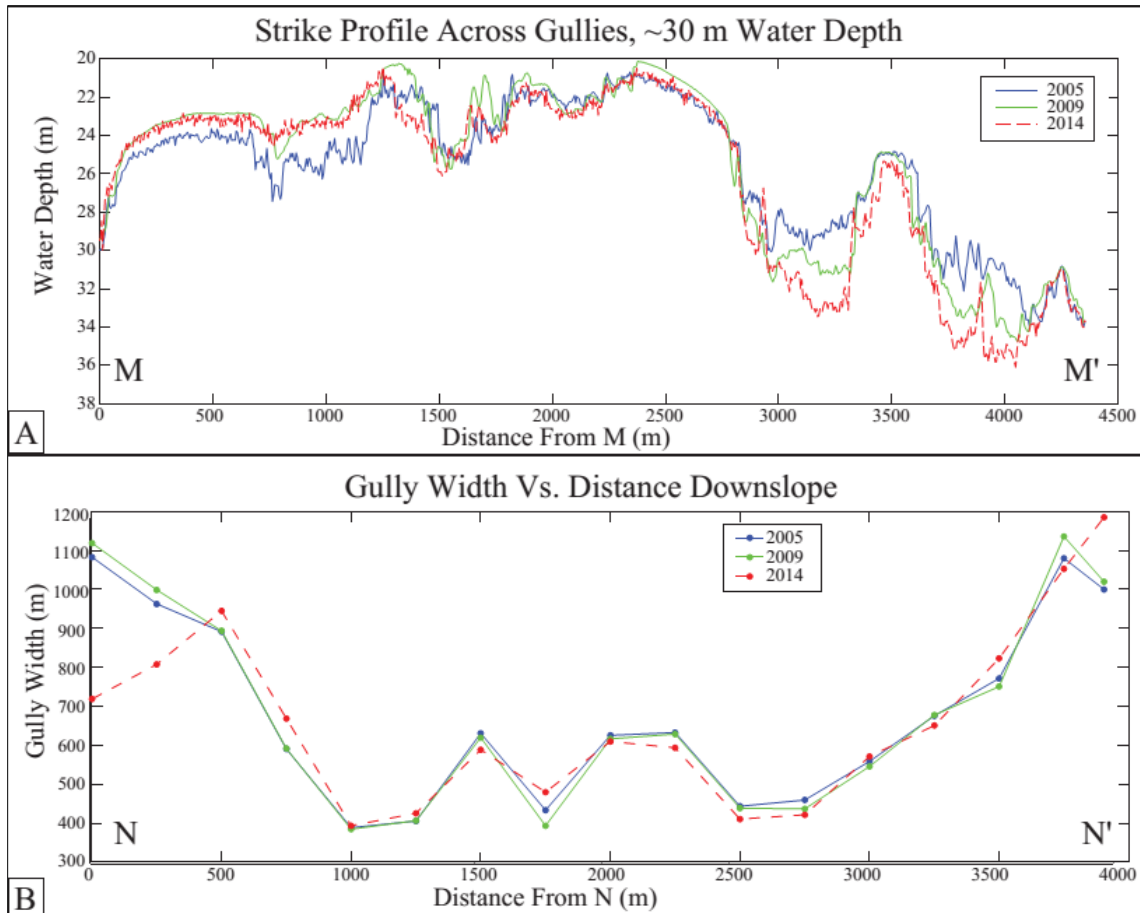
Figure 42. 2014 bathymetric profiles

A: Profile M-M' across survey area showing change in gully depth between surveys. Gully depth decreases in the westernmost gully, but increases in all other gullies. B: Width of MRDF gully plotted against distance from origin along profile N-N'. Note this origin is not the head of the gully, but the shallowest depth common to all three datasets. See Fig. 39 for locations of profiles M-M' and N-N'.
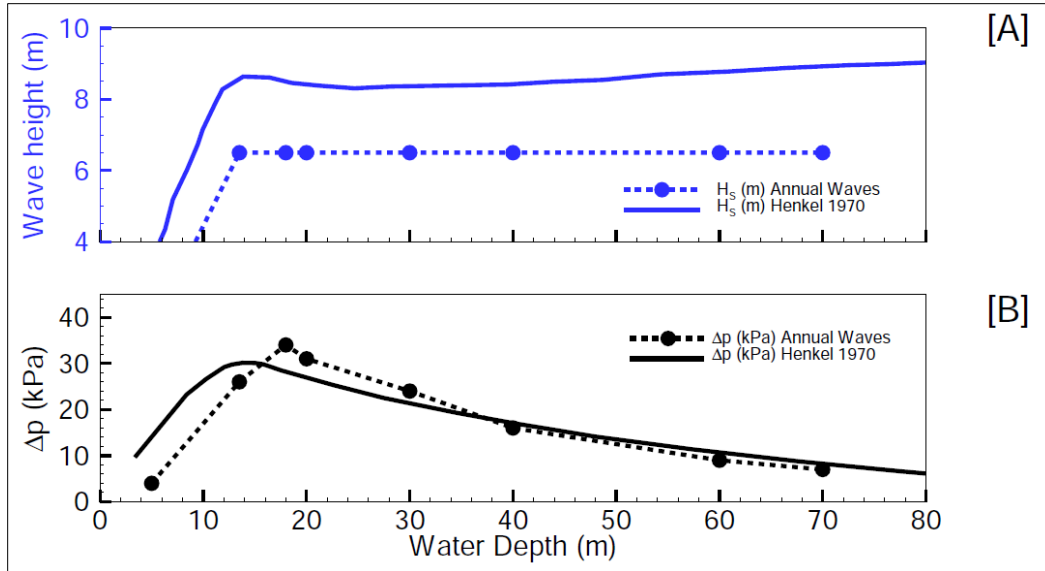
Figure 43. Wave forcing on seabed

Relationship between water depth, wave height (blue) and pressure change (black) on the sea bottom. (A) Modified from (Henkel 1970) where the author used a sinusoidal pressure change resulting from linear waves to establish the pressure fields across a wavelength, (B) this study, using fully non-linear waves propagated across the delta front on an assumed flat slope and across variable depth. The evolution of pressure change (black) from water depths between 5–70 m look similar between linear sinusoidal and fully non-linear waves, however, during our study these pressure changes can be achieved with wave heights (blue) that occur more frequently, i.e. ~1-year return period.
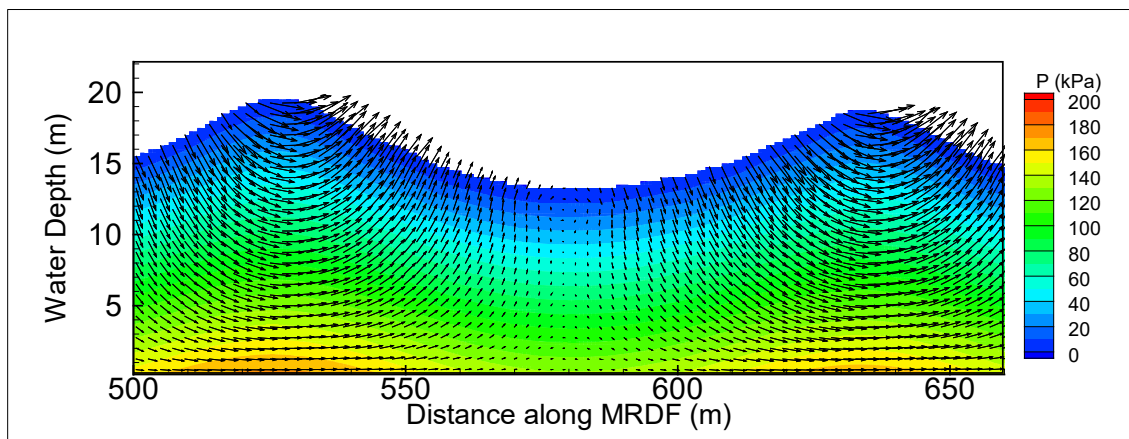
Figure 44. Nonlinear wave simulation

Example pressure distribution and velocity variation along a non-linear wave using FLOW3D; the approximate wave at the boundary (left – outside the frame) is Hs = 6.5 m, T = 9 seconds). At the right boundary, outflow boundary was selected, to radiate the entire wave outside the domain and avoid wave reflections back into the domain. Minimal lateral movement of the gully/lobe "footprint" was observed from 2005 to 2014. The gully walls did not dramatically shift between surveys; some degree of upslope narrowing (~400 m change, narrowing from 1100 to 700 m) and minor downslope widening (~200 m change, widening from 1000 to 1200 m, Fig. 40b) occurred, but along the majority of gullies, width changes did not exceed 100 m.

Similarly, the mudflow lobes did not prograde more than 100 m downslope between 2005 and 2014 (Fig. 42). Modeling results show that non-linear waves (Figures 43 and 45) produce higher pressure differentials (i.e., range between highest and lowest pressures) at the seabed across the entire study area compared to those produced by linear waves. This finding can be attributed to the preservation of the waveform shape in nonlinear modeling, where wave crests are steeper and produce higher pressures. Smaller non-linear waves (4.5–6.5 m) having a return period of one year create pressure differentials

comparable to larger hurricane waves (8.5–10.5 m) when linear conditions were assumed (Figures 41 and 42).

3.2.6 Discussion

This study confirms that seafloor movement occurred on the MRDF despite the relatively quiescent tropical cyclone seasons in between October 2005 and June 2014. Measurements of depth change between surveys show that although the lateral boundaries of the gully/lobe complexes did not change drastically between surveys, depths did change appreciably within the gullies and lobes. Despite the vertical movement within the reaches of mudflow gullies and lobes observed, the lateral extents of these geomorphic features did not change drastically between 2005 and 2014.

The lateral expansion of mudflow gullies (thought to occur via successive upslope failure, [Prior and Suhayda 1979]) and downslope progradation of mudflow lobes have been used in previous studies to quantify scope and scale of MRDF seafloor movement before and after large hurricanes (Hitchcock et al. 1996; Son-Hindmarsh et al. 1984). These studies documented kilometer-scale downslope mudflow lobe movement and the "draining" (drastic deepening) and widening of mudflow gullies attributed to the passage of large tropical cyclones. The lack of prominent lateral movement of specific features between 2005 and 2014 may indicate that seafloor shear stress (and subsequent sediment pore pressure) has to exceed a certain threshold before encroachment of mudflow complexes onto relatively undisturbed (inter-gully and prodelta) facies occurs. Because widespread lateral sediment movement attributed to large tropical cyclone passage has been associated with MRDF infrastructure damage (Guidroz 2009), quantifying this threshold will be essential to understanding mudflow periodicity, magnitude, and geohazard potential.

It is apparent that the MRDF was not a morphologically static system from October 2005 to June 2014, even without large tropical cyclones or multiple major floods. These results initially appear to contrast with those from a companion study that utilized ^{210}Pb/^{137}Cs/^{7}Be geochronology to determine that sedimentation in this area of the MRDF is dominated by vertical settling from river plumes, with little to no evidence of mudflows or submarine landslides within the top 2-3 m of seafloor (Keller et al. 2016, in review). Previous studies of MRDF mass failures have determined that the planes of failure (the layer in the seabed where sliding initiates) of mudflows are typically deeply seated, up to 30 m below the seafloor (Bea and Arnold 1973; Hooper 1980). The seafloor movement observed during this study may be more deeply seated than 2–3 m below the seabed, moving translationally downslope with little surface deformation; if so, these conditions would reconcile the present study with the apparent lack of movement in the uppermost 2–3 m of the seabed observed in (Keller et al. 2016, in review).

The modeling results largely corroborate the findings observed in the geophysical data. The absence of large hurricanes during the period studied (2005–2014; Hs << 10 m) suggests that the movement observed were facilitated by non-hurricane waves (Fig. 43b). Peak pressure differentials at the seabed (Δp~35 kPa) in the study area (Hs~6.5 m; Fig. 4cb) reached similar peak conditions to those produced by hurricane waves (Fig. 43A) having nearly twice the wave height (Hs~10m), suggesting that movement can occur by such events annually. At depths in excess of 50 m, one-year waves have magnitudes that are 30–50% lower compared to hurricane waves, yet they produce pressure differentials that are only 5–15% lower. In depths of 14–50 m one-year waves (~6.5 m) produce pressure differentials that exceed those of larger events, such as hurricanes, by more than 15% (Fig. 43).

Bea and Aurora (1981) reported that a soft seabed that deforms under changing wave pressures could attenuate waves (lowering wave energy and height) and hence produce lower pressure differentials, decreasing the likelihood of seabed failure. However, even without attenuation the results show that pressure differentials exceed those reported by (Henkel 1970) in shallow water and in deeper water, which suggests that one-year wave events can indeed cause submarine failures.

The snapshot nature of bathymetric surveys does not tell us whether observed movement was triggered by smaller-scale impulse events, such as extratropical cyclones, tropical storms, or river floods, or whether the gully/lobe complexes exhibit continuous creep-like motion under the influence of gravity, as has been suggested by some studies (Adams and Roberts 1993). Earlier studies have recorded soil movement under cyclic wave loading-unloading characteristic of storm passage in a shallow water collapse depression (Hottman 1978), but an in situ study of mudflow gully/lobe rheology has not yet been conducted. Repeat geophysical surveys can quantify seafloor movement, numerical models can provide a simplified idea of triggering mechanisms, but in situ observation is necessary to truly assess mudflow failure thresholds, and speeds of motion.

This study documents depth change within MRDF mudflow gully and lobe complexes during a relatively quiescent period. Though earlier studies have speculated that seafloor movement may be triggered by less energetic weather events such as cold front and tropical storm passage, the general assumption was the net movement caused by these events would be relatively localized or altogether absent. It is demonstrated here that substantial MRDF mass transport can also be triggered by more frequent, less intense storms such as extratropical cyclones or tropical storms. These findings have widespread implications not only for the MRDF, but also to proximal accumulation dominated deltas worldwide (Walsh and Nittrouer 2009). These results also underscore the need for a consistent monitoring program in order to truly elucidate the patterns of mudflow movement on a subaqueous delta front entering the declining phase of the deltaic cycle.

4. The 2017 Pilot Study

4.1 Overview of the 2017 Pilot Study

In 2016, the opportunity for a second pilot field program arose, bringing together the Principal Investigators (PIs) of this project and a seafloor mapping team led by Dr. Jason Chaytor of the US Geological Survey (USGS) Woods Hole Coastal and Marine Science Center. This collaborative team arose due to:

(1) shared interests of the Mississippi River Delta Front (MRDF) and USGS teams in studying submarine landslides off the Mississippi River Delta (MRD);

(2) more specific interests of Dr. Chaytor in leading a potential seabed mapping program as part of the Path Forward proposal described in Chapter 5 (below);

(3) because the teams agreed on the need to test new sonar and sampling tools for their effectiveness in the study area before proposing a major project expansion (in Chapter 5); and

(4) because funds were available from the Bureau of Ocean Energy Management (BOEM) and USGS to conduct the second field season.

Through Fall 2016 and Spring 2017, plans were developed for two cruises on the R/V *Point Sur* to study the MRDF area (Fig. 45). The first seven-day cruise was planned for geophysical mapping of small areas with high geological (and archeological) interest on the MRDF (led by Chaytor of USGS). The second seven-day cruise a week later (led by PI Bentley of Louisiana State University [LSU]) was planned to collect geological samples and test geotechnical instruments to ground-truth geophysical data collected on the USGS cruise. Additional cruise participants included Dr. Allen Reed of the Naval Research Laboratory (NRL), who brought several geotechnical and geoacoustic instruments for testing, and Dr. Gauvain Wiemer of Bremen University (Germany) who brought a free-fall cone penetrometer for seabed geotechnical measurements penetrating up to 6 m into the sediment.

The 2017 cruises were planned to accomplish two broad objectives: to test the effectiveness of sampling and mapping tools in the study area, and to collect geophysical, geological, and geotechnical data in locations that had been mapped previously at least once, so that we could study seabed change over time (Fig. 45), using approaches described above, and in Obelcz et al. (2017) and Maloney et al. (2018). The specific study areas included:

(1) the mudflow region southwest of Southwest Pass (Keller et al., 2016; Obelcz et al.,2017);

(2) the wreck site of the SS *Virginia*, south of Southwest Pass (preliminary findings reported in Science Magazine: Ahmad 2017);

(3) shallow to deep mudflow deposits south of South Pass, mapped previously by NOAA (shallow survey) and by Fugro LLC (deeper survey, see Maloney et al. 2018); and

(4) a shallow region of mudflows east of Pass a Loutre (Fig. 43; Courtois et al. 2017).

The wreck of the SS *Virginia* is of archeological, cultural, and geological interest: she was sunk in 1942 by a German U-boat, and the wreck has been shown to be moving slowly downslope on top of a mudflow lobe (Ahmad 2017; Chaytor et al. 2017).

Data processing and analysis from these cruises are ongoing through the final year of this project. Preliminary results are provided for each cruise, below.
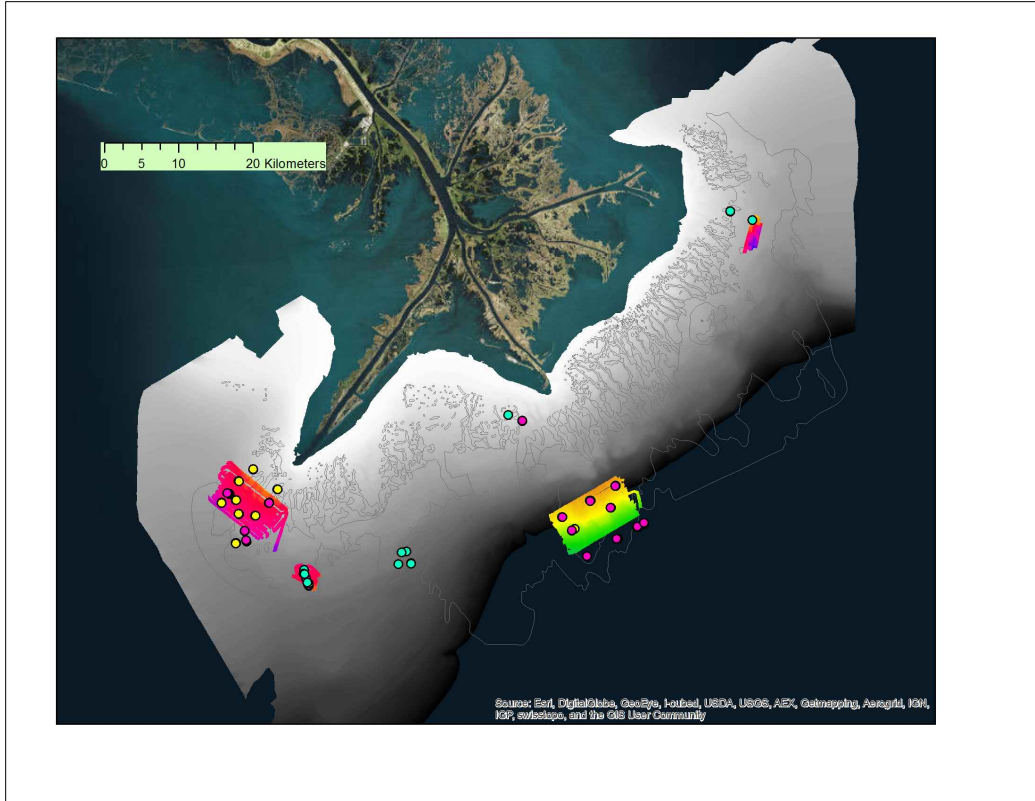
Figure 45. MRDF map and 2017 pilot study locations

Map of sampling locations from LSU-UNO-SDSU cruise (colored dots) and SONAR grids from USGS cruise (colored polygons). For most stations, the following samples were collected: multicore (yellow dot), piston core (6–9 m length, blue dot), and cone penetrometer (pink dot). At this scale, marks for individual deployments overlap. The shaded gray polygon and contours indicate the extent of mudflows and gullies from the Coleman 1980 study.

4.2 2017 Pilot Study: Geophysical Survey Summary

The objective of this cruise was to test high-resolution geophysical imaging techniques and investigate the morphology and shallow stratigraphy of the debris flows on the Mississippi River Delta as part of a cooperative effort among the USGS, BOEM, LSU, University of New Orleans (UNO), and the US Naval Research Lab (NRL) (Figure 45). The goal of the research is to assess the suitability of available imaging techniques for mapping in challenging water column and sub-bottom (e.g., widespread shallow biogenic gas) conditions present across the entire delta front.

Table 5. Personnel and Instruments on 2017 Cruises

	USGS Geophysical Cruise, 5/19/17–5/26/17	**LSU-UNO-SDSU-NRL-Bremen Cruise 6/2/17–6/7/2017**
Participants	Jason Chaytor (USGS)–Chief Scientist Seth Ackerman (USGS) Wayne Baldwin (USGS) Sam Bentley (LSU) Emile Bergeron (USGS) Bill Danforth (USGS) Eric Moore (USGS) Alex Nichols (USGS) Chuck Worley (USGS) Kevin Xu (LSU)	Sam Bentley (LSU)–Chief Scientist Jillian Maloney (SDSU) Ioannis Georgiou (UNO) Navid Jafari (LSU) Jeff Obelcz (LSU) Allen Reed (NRL) Gauvain Wiemer (Bremen University) Charlie Sibley (LSU) Andrew Courtois (LSU) Jack Cadigan (LSU) James Smith (LSU)

	USGS Geophysical Cruise, 5/19/17–5/26/17	LSU-UNO-SDSU-NRL-Bremen Cruise 6/2/17–6/7/2017
		Patrick Robichaux (LSU) Rosslyn King (SDSU) Ryan Clark (LSU) Tara Yocum (UNO) Suyapa Gonzales (LSU)
Instruments	All from USGS Reson T20P with dual-head transducer MVP30 moving velocity profiler SIG 300 J minisparker acoustic source towed at 1-m-depth. Applied Acoustics S-Boom System Applied Acoustics Single-plate Boomer system Edgetech 512i CHIRP GeoEel 32-channel hydrophone	Freefall Cone Penetrometer, 8m maximum seabed penetration (MARUM, University of Bremen) Benthos 3" x 30' Piston Corer (LSU) Ocean Instruments MC800 multicorer (LSU)

The last major investigation of failure processes spanning the entire MRDF was completed in the late 1970s/early 1980s (e.g., Coleman et al. 1980; Chapters 1 and 2 of this report), using single-beam echosounder records and analog-recorded airgun and/or boomer seismic reflection techniques. In subsequent years, focused mapping and geophysical imaging has occurred in support of infrastructure development and as part of renewed efforts to quantify mudflow hazards, with recent larger-scale bathymetry surveys completed as part of hazard to navigation updates. High-resolution geophysical imaging across the delta front, coupled with new and repeat bathymetric surveying can provide both critical information on the subsurface structure of the different morphological segments of the failures (channel, lobe, etc.) and help identify and fully characterize the spatial and temporal changes to the delta front. This cruise allowed us to identify imaging techniques and configurations that could provide the basis for possible more complete geophysical surveys of the region and to support sampling efforts described below.

Preliminary Results. Preliminary results of the geophysical cruise are adapted from Chaytor et al. (2017), Ahmad (2017), and Baldwin et al. (2018). More than 600 km of multibeam bathymetry/backscatter/water column data (dual head Reson T20P), 425 km of towed CHIRP data (Edgetech 512i), and >500 km of multi-channel seismic data (boomer and/or mini-sparker sources, 32-channel Geoeel streamer) were collected. Varied mudflow (gully, lobe), pro-delta morphologies, and structural features, some of which have been surveyed more than once, were imaged in selected survey areas from Pass a Loutre to Southwest Pass.
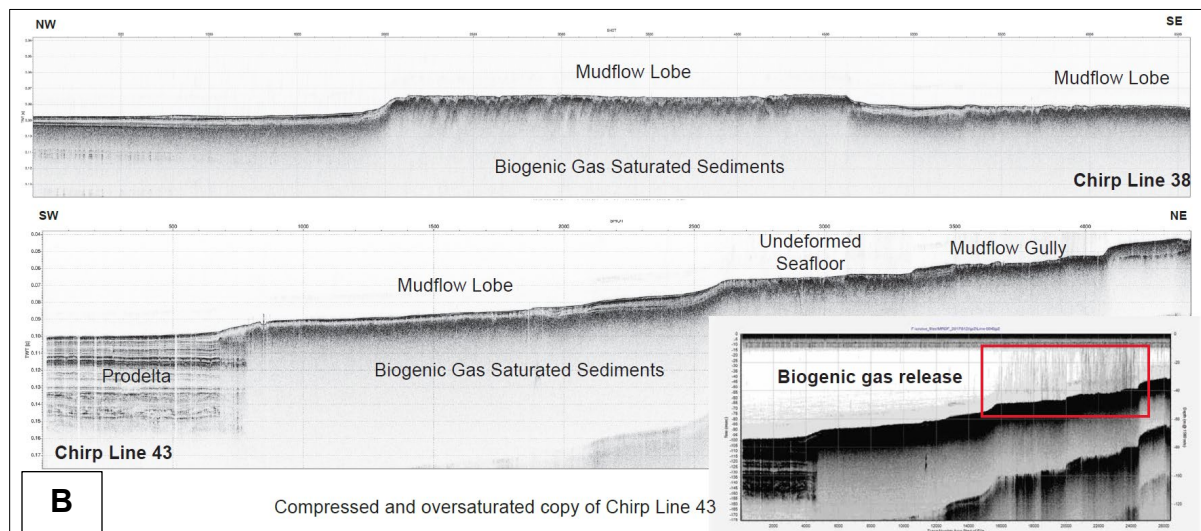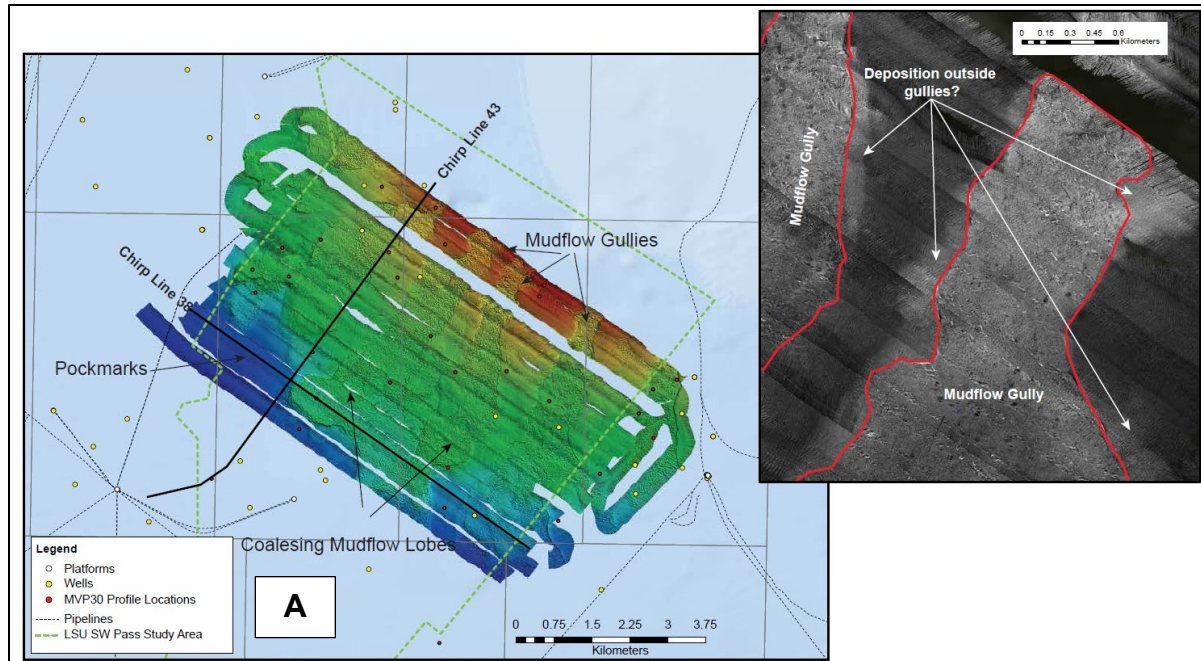
Figure 46. 2017 Southwest Pass survey

A: multibeam mosaic (left) and seabed reflectance (right) of the Southwest Pass survey; B: CHIRP lines 38 and 43, showing visible stratigraphy in prodelta sediments, signal masking by gas in mudflow lobes, and also likely gas emissions from the seabed (lower right panel).

The Southwest Pass survey area (Fig. 45) is the most proximal of the 2017 sites to the current primary outflow of the Mississippi River and the location of repeated surveying since 2005. Well developed retrogressive slide, mudflow gully, and coalescing lobe morphologies are present over a short spatial extent (<5 km). Biogenic gas is pervasive throughout the sediments at this site (see Fig. 46 above, Chirp Lines 38 and 43), with pockmarks and acoustic anomalies (see above) reflecting widespread release of the biogenic gas to the water column. A rapidly changing, variably stratified water column (right) resulting from input of fresh, sediment laden river water and the presence of gas in the water and subsurface created a challenging imaging environment.

Shipwrecks located in the MRDF provide invaluable markers of mudflow movement due to their known sinking histories (in most cases) and size. The SS *Virginia* (Fig. 47), a 503 ft long bulk oil tanker, was sunk by a U-boat in 1942 at the pilot buoy offshore Southwest Pass. The location of *Virginia* was identified in 2001 and then again during an oil and gas survey in 2003. In 2006 (following Hurricane Ivan), *Virginia* was again located - although it had moved 1200 ft downslope in the intervening period. During the 2017 survey (Fig. 45), *Virginia* was relocated and found to be a 200 ft south-south west of the 2006 position. During the 2006–2017 period, no major hurricanes transited the MRDF region. The ship is currently resting on its port side (part of which may have completely failed), with the bow oriented towards the northwest. Except for a shallow depression surrounding the bow, there is no evidence of movement of the ship within the mudflow lobe on which it sits. The absence of a noticeable path of movement in the sediment suggests that the ship and the lobe move as a single, large-scale mass. During 2006–2017, no major hurricanes transited the MRDF region, this suggests that major hurricanes are not required to force large-scale motion of mudflow lobes.
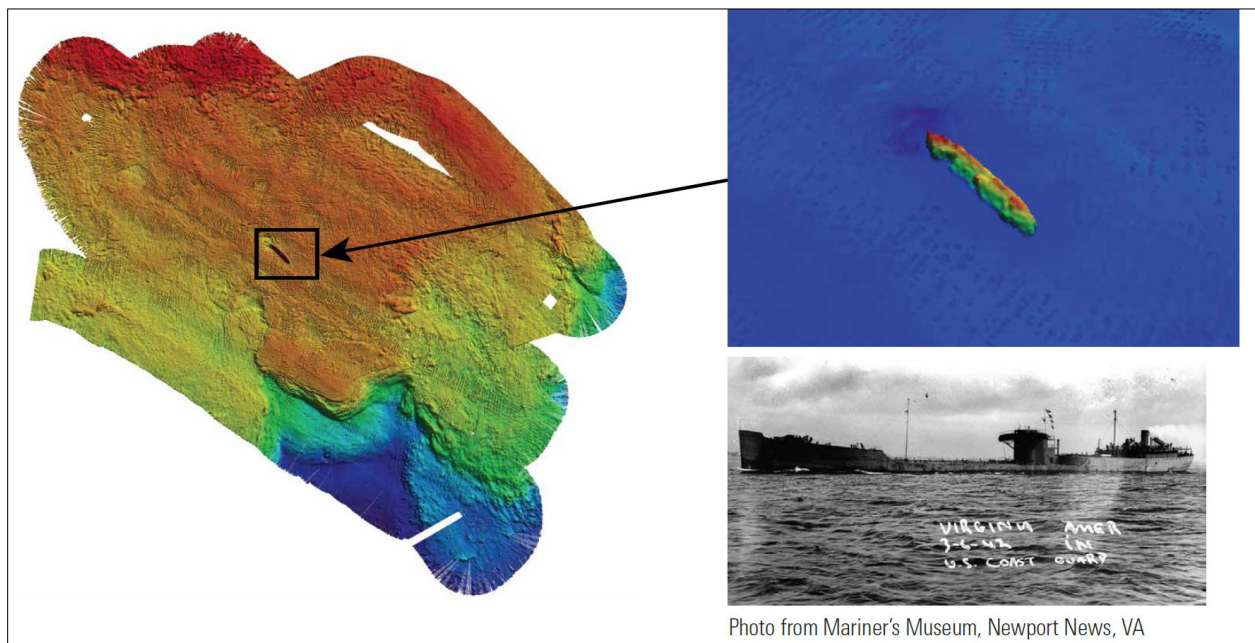
Figure 47. 2017 survey of the SS *Virginia*

(Left) Multibeam map overview of the mudflow lobe on which the SS *Virginia* rests, with warm shades indicating shallower water, and cool shades, deeper water; (upper right) closeup color bathymetric image of the wreck, using a different depth scale to highlight the ship's structure; (lower right) period photograph of the SS *Virginia*.

Patch testing of the dual-head Reson T20P sonar used for bathymetric data acquisition was performed over MC20A platform jacket displaced by a mudflow during Hurricane Ivan in 2004 (Fig. 48). Multibeam bathymetry data reveal a morphologically complex seafloor dominated by chaotic to parallel deformation ridges with sparker MCS profiles showing a thick (30–40 m) surficial chaotic MTD layer overlying well-stratified pro-delta and/or Pleistocene clays and silts, showing evidence of toe thrusts or the incorporation of coherent blocks of sediment into the flow.
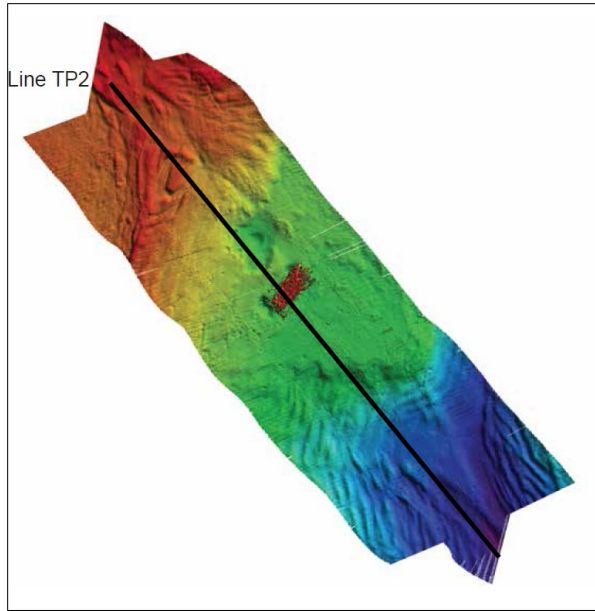
Figure 48.a. 2017 MC20 survey

Color-shaded bathymetric mosaic showing the MC20 platform jacked in the center of the image.
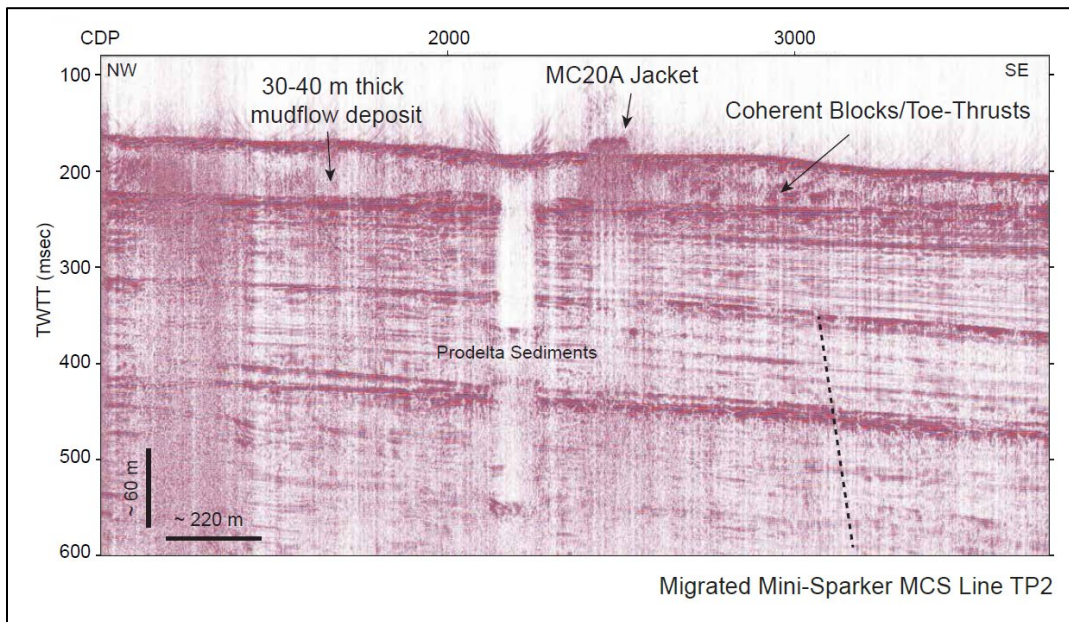
Figure 48.b. 2017 MC20 survey

Seismic image of the MC20 jacket and underlying seabed.

4.3 2017 Pilot Study: Geological and Geotechnical Cruise Summary

Target locations for core and cone penetrometer deployments were chosen from the data collected on the USGS Geophysical Survey. Southwest Pass, South Pass, Pass a Loutre, and the SS *Virginia* shipwreck were the main target areas. Deployments were also made in areas that previous sampling was done (2014 Pilot Study). Locations such as mudflow lobes, gullies, interfluves, prodelta, the surrounding undisturbed seafloor, and the SS *Virginia* shipwreck were sampled. In total, 31 multicores (Fig. 49), 31 piston cores (Fig. 50), and 36 cone penetrometer (CPT) samples were collected (Fig. 51), including piston cores up to 8.9 m in length. Five of the 36 CPT deployments were dissipation tests. The time period of the cruise was from June 3, 2017 to June 9, 2017. Figures 49, 50, and 51 show the pictures taken during field sediment collections
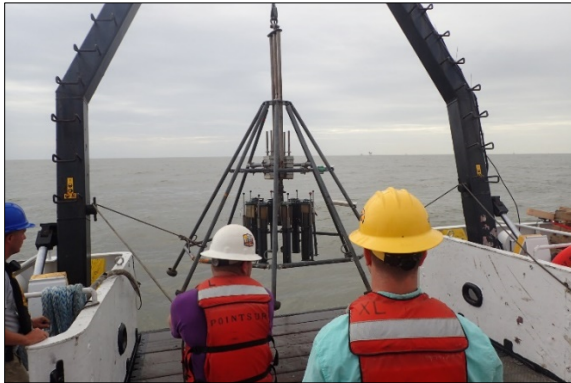
Figure 49. 2017 multicore operation.

Recovering the multicorer.

Figure 50A. 2017 piston core sampling

Scientists from LSU and San Diego State University with one of the two longest piston cores recovered (8.9 meters).

Figure 50B. 2017 piston core deployment

A 9.5 m piston core ready for deployment on the stern of the R/V *Point Sur*.

Figure 51. 2017 cone penetrometer deployment.

Nighttime deployment of the free-fall cone penetrometer.

Cores from the 2017 pilot study are currently being analyzed in various laboratories at LSU. Thirty one shallow Multicores (50–70cm depth) have been processed and analyzed by Andrew Courtois for X-radiography and are in the process for analysis of radiometric activity and grain size analysis. Duplicate and archive multicores have been logged on the Geotek MSCL logger for density, magnetic susceptibility, and resistivity measurements. The 31 piston cores (5–9m depth) have been logged on the Geotek MSCL logger as well, and are in the process of being sampled down core for radiometric analysis, grain size, and organic content by James Smith. The piston cores will be subjected to a wide variety of test and analysis described in greater detail below. Geotechnical testing will be administered by Navid Jafari on both piston and multi-cores collected. The primary engineering tests conducted on the cores will be triaxial compression, ring shear, and 1-D consolidation tests. These engineering properties will be complemented with index testing, including x-ray diffraction (XRD), x-ray fluorescence (XRF), geochemical constituents (salinity, cations, anions), water content, specific gravity, liquid limit, and plastic limit. The equipment for testing is currently being set up in the new Geotechnical Laboratory in the recently renovated lab of Dr. Jafari in Patrick F. Taylor Hall at LSU.

4.3.1 Multi-core analysis

Many studies of the Mississippi River Delta (MRD) have shown historic declines in sediment load reaching the main river distributaries over the last few decades. Recent studies also reported that ~50% of the suspended load during floods is sequestered within the delta. Though the impact of declining sediment load on wetland loss is well documented, submarine sedimentary processes on the delta front during this recent period of declining sediment load are understudied. To better understand modern sediment dispersal and deposition across the Mississippi River Delta Front, 31 multicores were collected in June 2017 from locations extending offshore from Southwest Pass, South Pass, and Pass a Loutre (the main river outlets) in water depths of 25–280 m (Smith et al. 2017). Core locations were selected based on multibeam bathymetry and morphology collected by the USGS in May 2017 (Chaytor et al. 2017; Baldwin et al. 2018); the timing of collection coincided with the end of annual peak discharge on the Mississippi River. This multi-agency survey is the first to study delta-front sedimentary processes regionally with such a wide suite of tools. Target locations for coring included the dominant depositional environments: mudflow lobes, gullies, and undisturbed prodelta. Cores were subsampled at 2 cm intervals and analyzed for Beryllium-7 activity via gamma spectrometry; in such settings, Be-7 can be used as a tracer of sediment recently delivered from fluvial origin. Example profiles of Be-7 activity versus sediment depth are shown in Figures 52 and 53. In each case, the penetration depth of Be-7 indicates the thickness of sediment deposited by the spring-summer river flood, also suggested by the prominent layering evident in x-radiographs of sediment cores (Fig. 54).

Results indicate a general trend of declining Be-7 activity with increasing distance from source, and in deeper water. Inshore samples near Southwest Pass show the deepest penetration depth of Be-7 into the sediment (24–26 cm), which is a preliminary indicator of rapid seasonal sedimentation. Nearshore samples from South Pass exhibited similar Be-7 penetration depths (Fig. 53), with results near Pass a Loutre to 14–16 cm depth (Fig. 52). Be-7 remains detectable to 2 cm in water 206 m deep, approximately 20 km from South Pass. Sediment dispersal remains detectable offshore from all three major river outlets, despite overall decline of sediment load in recent decades, and pronounced declines for South Pass and Pass a Loutre. Future research will focus on relationships among changing sediment loads, dispersal patterns, and sediment transport by mudflows, which are an important process for dispersal after initial deposition.
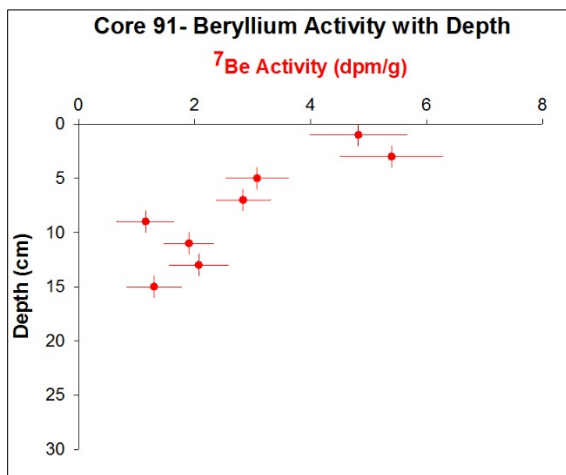
Figure 52. 2017 [7]Be data, multicore 91.

Beryllium Activity (disintegrations per minute/gram) with Depth (cm) for Core 91 (Pass a Loutre gully).
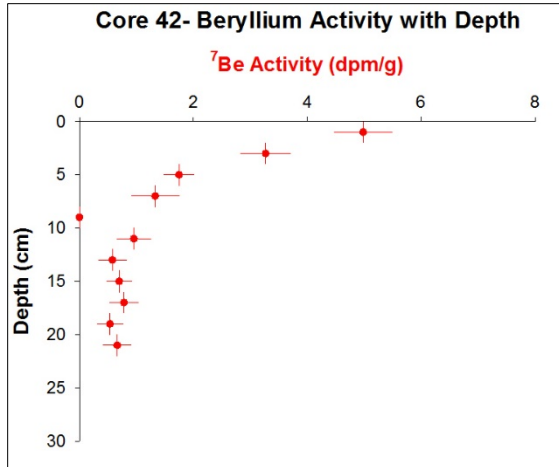
Figure 53. 2017 [7]Be core data, multicore 42.

Beryllium Activity (disintegrations per minute/gram) with Depth (cm) for Core 42 (South Pass gully).

X-radiography of 31 multicores was performed using a portable MinXray HF8015+dlp and Samsung Model SP501 detector panel at LSU to evaluate bioturbation and bedding features. Images were adjusted for brightness, contrast, saturation, etc. using ImageJ software (Figure 54).

Figure 54. 2017 X-radiograph, multicore 5

X-radiograph of Core 5 (Southwest Pass gully). Dimensions 8.2 X 47.6 cm. Bedding features and faint bioturbation present.

Grain-size analysis for multi-cores is in progress. All grain-size analysis will be performed on a Beckham Coulter LS13320 laser-diffraction particle analyzer within LSU's Geology Department.

4.3.2 Piston core analysis

Recent studies on the MRD have documented sub-aerial land loss, driven in part by declining sediment load over the past century. Impacts of changing sediment load on the subaqueous delta are less well known. The subaqueous MRDF is known to be shaped by extensive submarine mudflows operating at a range of temporal and spatial scales, however impacts of changing sediment delivery on mudflow deposits have not been investigated. To better understand seabed morphology and stratigraphy as impacted by plume sedimentation and mudflows, an integrated geological and/or geophysical study was undertaken in delta front regions offshore the three main MRD passes.

This study (Smith et al. 2017) focuses on stratigraphy and physical properties of 31 piston cores (5–9 m length) collected in June 2017 (Fig. 55). Coring locations were selected in gully, lobe and prodelta settings based on multibeam bathymetry and seismic profiles collected in mid-May 2017. Cores were analyzed for density, magnetic susceptibility, P-wave speed, and resistivity using a Geotek multi sensor core logger.

Core density profiles generally vary systematically across facies. Density profiles of gully cores are nearly invariant with some downward stepwise increases delineating units meters thick, and abundant gaps likely caused by gas expansion (Fig. 56). Lobe cores generally have subtle downward increases in density, some stepwise density increases, and fewer gaps. Prodelta cores show more pronounced downward density increases to >1.5 g/cm^3, decimeter-scale peaks and valleys in density profiles, but stepwise increases are less evident. We hypothesize that density profiles in gully and lobe settings (uniform profiles except for stepwise increases) reflect remolding by mudflows, whereas density variations in prodelta settings instead reflect grain size variations (decimeter-scale) and more advanced consolidation (overall downward density increase) consistent with slower sediment deposition. These hypotheses will be evaluated by a more detailed study of seismic stratigraphy and core properties, including geochronology, grain size distribution and x-radiographic imaging, to further relate important sedimentary processes with resulting deposits.
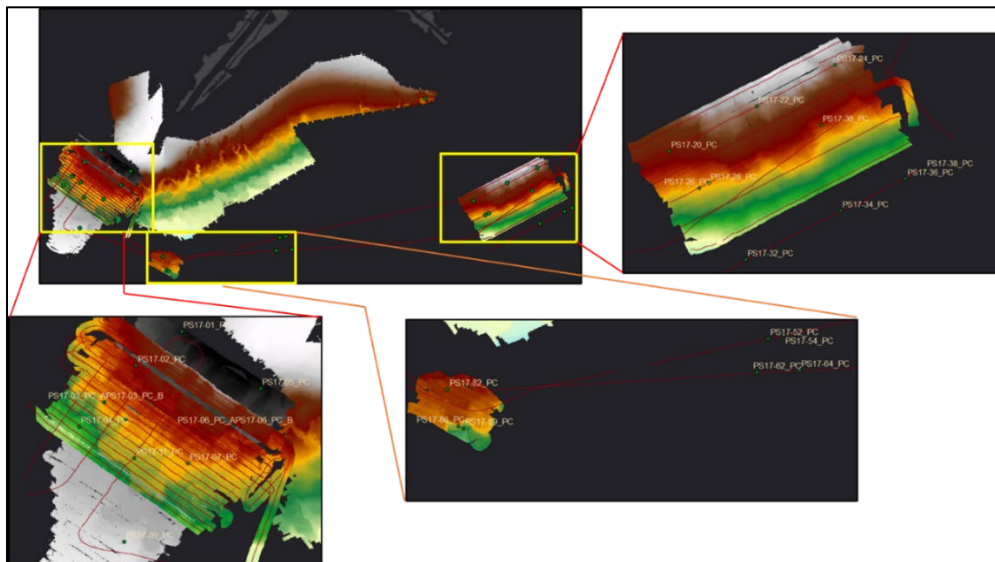
Figure 55. 2017 survey and piston core locations

Locations of 31 piston cores collected across the Mississippi River Delta Front in June 2017, on bathymetric data collected by Chaytor et al. (2017) and Baldwin et al. (2018). Coring locations where selected in gully, lobe, and prodelta settings based on multibeam bathymetry and seismic profiles collected in mid-May 2017.

Figure 56. Piston core logs

Example logs of density (blue) and magnetic susceptibility (red) for two piston cores. Pink bars identify the location of beds, as suggested by interpretation of density and magnetic data. Left: Core PS17-06PC is from a gully proximal to Southwest Pass, and abundant gas expansion gaps, and stepwise increase in density downcore. Right: Core PS17-09PC is from a prodelta location, and is characterized by few gas expansion intervals, subtle downcore increase in density, comblike density profile, and distinct spikes in magnetic susceptibility (Smith et al. 2017).

4.3.3 Geophysical and geotechnical data analysis

Drs. Weimer (Bremen), Jafari (LSU) and Georgiou (UNO) are seeking to integrate results from geotechnical and geological testing. Geophysical data are anticipated to be released to our team by the USGS in the second quarter of the next project year (y5).

Table 6. Core/CPT locations during the second R/V *Point Sur* cruise

Station ID	Instrument	Latitude	Longitude	Date Collected
PS17-01_MC	Multicore	28.890727 N	89.495982 W	6/3/2017
PS17-02_MC	Multicore	28.878187 N	89.513063 W	6/3/2017
PS17-03_MC	Multicore	28.864418 N	89.524778 W	6/3/2017
PS17-04_MC	Multicore	28.855433 N	89.534305 W	6/3/2017
PS17-11_MC	Multicore	28.843492 N	89.513782 W	6/3/2017
PS17-09_MC	Multicore	28.812377 N	89.517045 W	6/3/2017
PS17-07_ MC	Multicore	28.841587 N	89.493427 W	6/3/2017
PS17-07_CPT_A	Cone penetrometer	28.841558 N	89.49394 W	6/4/2017
PS17-07_CPT_B	Cone penetrometer	28.841483 N	89.49379 W	6/4/2017
PS17-07_CPT_C	Cone penetrometer	28.841523 N	89.493923 W	6/4/2017
PS17-07_CPT_D	Cone penetrometer	28.84149 N	89.493772 W	6/4/2017
PS17-06_CPT_A	Cone penetrometer	28.855215 N	89.477053 W	6/4/2017
PS17-06_CPT_B	Cone penetrometer	28.855278 N	89.476723 W	6/4/2017
PS17-05_CPT_A	Cone penetrometer	28.86949 N	89.467043 W	6/4/2017
PS17-05_CPT_B	Cone penetrometer	28.869617 N	89.467065 W	6/4/2017
PS17-01_CPT_A	Cone penetrometer	28.890637 N	89.496162 W	6/4/2017
PS17-01_CPT_B	Cone penetrometer	28.890927 N	89.496345 W	6/4/2017
PS17-02_CPT_A	Cone penetrometer	28.878678 N	89.513778 W	6/4/2017
PS17-02_CPT_B	Cone penetrometer	28.87866 N	89.513747 W	6/4/2017
PS17-03_CPT_A	Cone penetrometer	28.864682 N	89.524958 W	6/4/2017
PS17-03_CPT_B	Cone penetrometer	28.86456 N	89.525012 W	6/4/2017
PS17-04_CPT_A	Cone penetrometer	28.85548 N	89.534278 W	6/4/2017
PS17-04_CPT_B	Cone penetrometer	28.855458 N	89.534147 W	6/4/2017
PS17-11_CPT_A	Cone penetrometer	28.843353 N	89.513477 W	6/4/2017
PS17-11_CPT_B	Cone penetrometer	28.843413 N	89.513488 W	6/4/2017
PS17-08_CPT_A	Cone penetrometer	28.825215 N	89.506153 W	6/4/2017
PS17-08_CPT_B	Cone penetrometer	28.82538 N	89.506183 W	6/4/2017
PS17-09_CPT_A	Cone penetrometer	28.812487 N	89.516988 W	6/4/2017
PS17-09_CPT_B	Cone penetrometer	28.812618 N	89.516802 W	6/4/2017
PS17-19_CPT_A	Cone penetrometer	28.814177 N	89.50408 W	6/4/2017
PS17-19_CPT_B	Cone penetrometer	28.815563 N	89.504845 W	6/4/2017
PS17-16DT_CPT_A	Cone penetrometer	28.858165 N	89.517195 W	6/4/2017
PS17-16DT_CPT_B	Cone penetrometer	28.858175 N	89.517072 W	6/4/2017
PS17-16DT_MC	Multicore	28.858182 N	89.516783 W	6/4/2017
PS17-05_MC	Multicore	28.869578 N	89.46656 W	6/4/2017
PS17-09_PC	Piston core	28.812322 N	89.517422 W	6/4/2017
PS17-07_PC	Piston core	28.841668 N	89.493575 W	6/4/2017
PS17-06_PC_A	Piston core	28.855353 N	89.47677 W	6/4/2017
PS17-06_PC_B	Piston core	28.855387 N	89.47675 W	6/5/2017

Station ID	Instrument	Latitude	Longitude	Date Collected
PS17-03_PC_A	Piston core	28.864527 N	89.524813 W	6/5/2017
PS17-03_PC_B	Piston core	28.864442 N	89.52503 W	6/5/2017
PS17-04_PC	Piston core	28.855323 N	89.534197 W	6/5/2017
PS17-11_PC	Piston core	28.84355 N	89.513657 W	6/5/2017
PS17-16DT_PC	Piston core	28.858272 N	89.516793 W	6/5/2017
PS17-02_PC	Piston core	28.878143 N	89.512987 W	6/5/2017
PS17-01_PC	Piston core	28.890982 N	89.495985 W	6/5/2017
PS17-05_PC	Piston core	28.86955 N	89.466485 W	6/5/2017
PS17-03_CPT_C	Cone penetrometer	28.864755 N	89.525002 W	6/5/2017
PS17-03_CPT_D	Cone penetrometer	28.864927 N	89.524983 W	6/5/2017
PS17-03_CPT_E	Cone penetrometer	28.865317 N	89.526013 W	6/5/2017
PS17-03_CPT_F	Cone penetrometer	28.865675 N	89.527287 W	6/5/2017
PS17-06_CPT_C	Cone penetrometer	28.855045 N	89.477042 W	6/5/2017
PS17-06_CPT_D	Cone penetrometer	28.85503 N	89.47701 W	6/5/2017
PS17-20_MC	Multicore	28.840193 N	89.121957 W	6/5/2017
PS17-22_MC	Multicore	28.857443 N	89.087932 W	6/6/2017
PS17-24_MC	Multicore	28.873552 N	89.057427 W	6/6/2017
PS17-30_MC	Multicore	28.850027 N	89.063077 W	6/6/2017
PS17-28_MC	Multicore	28.827647 N	89.1069 W	6/6/2017
PS17-26_MC	Multicore	28.825695 N	89.11044 W	6/6/2017
PS17-32_MC	Multicore	28.798447 N	89.092272 W	6/6/2017
PS17-34_MC	Multicore	28.816922 N	89.054857 W	6/6/2017
PS17-36_MC	Multicore	28.829823 N	89.031632 W	6/6/2017
PS17-38_MC	Multicore	28.834267 N	89.023283 W	6/6/2017
PS17-38_PC	Piston core	28.832825 N	89.022997 W	6/6/2017
PS17-36_PC	Piston core	28.829227 N	89.030653 W	6/6/2017
PS17-34_PC	Piston core	28.816975 N	89.055812 W	6/6/2017
PS17-26_PC	Piston core	28.825727 N	89.110432 W	6/6/2017
PS17-28_PC	Piston core	28.827553 N	89.106845 W	6/6/2017
PS17-30_PC	Piston core	28.850038 N	89.06334 W	6/6/2017
PS17-24_PC	Piston core	28.873262 N	89.057945 W	6/6/2017
PS17-22_PC	Piston core	28.857342 N	89.088235 W	6/7/2017
PS17-20_PC	Piston core	28.83991 N	89.121975 W	6/7/2017
PS17-32_PC	Piston core	28.798162 N	89.092445 W	6/7/2017
PS17-32_CPT_A	Cone penetrometer	28.798362 N	89.092427 W	6/7/2017
PS17-32_CPT_B	Cone penetrometer	28.798382 N	89.092408 W	6/7/2017
PS17-34_CPT_A	Cone penetrometer	28.816987 N	89.056348 W	6/7/2017
PS17-34_CPT_B	Cone penetrometer	28.817112 N	89.056372 W	6/7/2017
PS17-36_CPT_A	Cone penetrometer	28.8301 N	89.030593 W	6/7/2017
PS17-36_CPT_B	Cone penetrometer	28.829945 N	89.030905 W	6/7/2017

Station ID	Instrument	Latitude	Longitude	Date Collected
PS17-38_CPT_A	Cone penetrometer	28.834195 N	89.023113 W	6/7/2017
PS17-38_CPT_B	Cone penetrometer	28.834253 N	89.023108 W	6/7/2017
PS17-26_CPT_A	Cone penetrometer	28.826017 N	89.110688 W	6/7/2017
PS17-26_CPT_B	Cone penetrometer	28.826112 N	89.110717 W	6/7/2017
PS17-30_CPT_A	Cone penetrometer	28.850055 N	89.063648 W	6/7/2017
PS17-30_CPT_B	Cone penetrometer	28.85003 N	89.063513 W	6/7/2017
PS17-24DT_CPT_A	Cone penetrometer	28.873145 N	89.05768 W	6/7/2017
PS17-24DT_CPT_B	Cone penetrometer	28.873335 N	89.057915 W	6/7/2017
PS17-22_CPT_A	Cone penetrometer	28.857465 N	89.088628 W	6/7/2017
PS17-22_CPT_B	Cone penetrometer	28.857283 N	89.08851 W	6/7/2017
PS17-20_CPT_A	Cone penetrometer	28.840022 N	89.122265 W	6/7/2017
PS17-20_CPT_B	Cone penetrometer	28.840052 N	89.122097 W	6/7/2017
PS17-54_PC	Piston core	28.803842 N	89.310713 W	6/7/2017
PS17-52_PC	Piston core	28.802625 N	89.31636 W	6/7/2017
PS17-62_PC	Piston core	28.7901 N	89.320437 W	6/7/2017
PS17-64_PC	Piston core	28.790983 N	89.30478 W	6/7/2017
PS17-64_MC	Multicore	28.790598 N	89.305085 W	6/8/2017
PS17-54_MC	Multicore	28.803608 N	89.310715 W	6/8/2017
PS17-52_MC	Multicore	28.802485 N	89.316307 W	6/8/2017
PS17-62_MC	Multicore	28.78989 N	89.320503 W	6/8/2017
PS17-86_PC	Piston core	28.770457 N	89.430407 W	6/8/2017
PS17-82_PC	Piston core	28.783877 N	89.434322 W	6/8/2017
PS17-82_CPT_A	Cone penetrometer	28.783988 N	89.434387 W	6/8/2017
PS17-82_CPT_B	Cone penetrometer	28.784033 N	89.434258 W	6/8/2017
PS17-80_CPT_A	Cone penetrometer	28.780013 N	89.435247 W	6/8/2017
PS17-80_CPT_B	Cone penetrometer	28.780115 N	89.435237 W	6/8/2017
PS17-84_CPT_A	Cone penetrometer	28.779653 N	89.433928 W	6/8/2017
PS17-84_CPT_B	Cone penetrometer	28.779865 N	89.433888 W	6/8/2017
PS17-87_CPT_A	Cone penetrometer	28.76915 N	89.429858 W	6/8/2017
PS17-87_CPT_B	Cone penetrometer	28.769377 N	89.429885 W	6/8/2017
PS17-89_CPT_A	Cone penetrometer	28.767328 N	89.428872 W	6/8/2017
PS17-89_CPT_B	Cone penetrometer	28.767437 N	89.428882 W	6/8/2017
PS17-85_CPT_A	Cone penetrometer	28.775507 N	89.432463 W	6/8/2017
PS17-85_CPT_B	Cone penetrometer	28.775308 N	89.432478 W	6/8/2017
PS17-86DT_CPT_A	Cone penetrometer	28.770443 N	89.430443 W	6/8/2017
PS17-86DT_CPT_B	Cone penetrometer	28.7705 N	89.430608 W	6/8/2017
PS17-89DT_CPT_A	Cone penetrometer	28.76769 N	89.429027 W	6/8/2017
PS17-89DT_CPT_B	Cone penetrometer	28.767702 N	89.429053 W	6/8/2017
PS17-89_PC	Piston core	28.7697 N	89.428642 W	6/8/2017
PS17-86_MC	Multicore	28.77066 N	89.43028 W	6/8/2017

Station ID	Instrument	Latitude	Longitude	Date Collected
PS17-82_MC	Multicore	28.784007 N	89.434443 W	6/8/2017
PS17-80_MC	Multicore	28.780103 N	89.435187 W	6/8/2017
PS17-84_MC	Multicore	28.779672 N	89.434052 W	6/8/2017
PS17-40_MC	Multicore	28.948393 N	89.18759 W	6/8/2017
PS17-42_MC	Multicore	28.942365 N	89.170382 W	6/9/2017
PS17-42_PC	Piston core	28.942307 N	89.170147 W	6/9/2017
PS17-42_CPT_A	Cone penetrometer	28.94219 N	89.170335 W	6/9/2017
PS17-42_CPT_B	Cone penetrometer	28.942295 N	89.170422 W	6/9/2017
PS17-42_CPT_C	Cone penetrometer	28.942342 N	89.170528 W	6/9/2017
PS17-42_CPT_D	Cone penetrometer	28.942388 N	89.170533 W	6/9/2017
PS17-91DT_CPT_A	Cone penetrometer	29.164153 N	88.918945 W	6/9/2017
PS17-91DT_CPT_B	Cone penetrometer	29.16424 N	88.91892 W	6/9/2017
PS17-91_PC	Piston core	29.164265 N	88.919032 W	6/9/2017
PS17-91_MC	Multicore	29.164242 N	88.919075 W	6/9/2017
PS17-90_MC	Multicore	29.155088 N	88.89187 W	6/9/2017

5. Conclusions

The major conclusions of this study are presented in this section.

5.1 Data Review and Synthesis

An ArcGIS™ geodatabase of selected existing datasets from the Mississippi River Delta Front (MRDF) has been created that incorporates historical data from a wide range of sources, from 19th century leadline surveys to 3D seabed elevation models using advanced technology ca. 2006–2013. Of these data sets, only the most recent multibeam sonar bathymetric data have great utility for advanced measurement of seabed properties, and these datasets are small in number, small in individual coverage, and cover only a small fraction of the study area. Two locations, one near Southwest Pass, and the other south of Garden Bay (Enterprise Pipeline) have multiple surveys at different times, and are useful for time-series study.

An Endnote© literature database has been created incorporating more than 450 articles and reports spanning 1955 to present. Analysis of this database by time and topic demonstrates that many studies were performed in response to seabed infrastructure damage from major hurricanes. Also, the most recent regionally and topically comprehensive study was conducted ca. 1977–1985, and the most recent detailed in situ geotechnical study was conducted ca. 1983.

Data gaps identified in the synthesis include the following:

1. The most recent regionally comprehensive seabed mapping program occurred in 1977–1979.
2. Localized studies have been conducted 1981-2014, but have generally focused on one individual storm event or slide.
3. No long-term in situ study has ever been conducted to quantify mode and frequency of seabed failures.
4. Since the mid 20th century, sediment delivery in the Mississippi Delta has declined precipitously, greatly changing the sedimentation regime that drives seabed failures. No study before our data synthesis takes this into account.
5. Rates and spatial and temporal scales of failures are not well constrained and most estimates are based on repeated single-beam sonar surveys with high uncertainty.
6. The role of gas is widely suspected to be important in preconditioning sediments for failure, but in situ gas concentrations have never been accurately determined, in situ rheologies influenced by gas are poorly documented, and the role of gas has never been incorporated into models of seabed failure.
7. Triggering mechanisms have been enumerated, but are not well understood. Only large-scale catastrophic failures have been widely documented, but our work demonstrates that flows and failures also occur during periods of quiescence, with regard to hurricane strikes.
8. Waves are widely recognized as important triggers for mudflows, but most work on this topic to date has been conducted using oversimplified linear wave models. Predictive models used to date, as our study here shows, underpredict the forces applied by real ocean waves to the seabed.
9. Advanced geochronological and geological analytical methods exist that can help provide detailed information on the rates and distributions of mudflows in time and space, but these methods have mostly been applied outside of the most dynamic regions of the MRDF, one exception being our study by Keller et al.

5.1.1 Pilot study results

2014 Geological Study. Analysis of cores collected near Southwest Pass demonstrate that most of the seabed in that study area to a depth of less than 3 m below the seabed is characterized by vertical sediment deposition from the Mississippi River Plume. Evidence for mudflow reworking of sediments was found in one core out 20, at a depth of 1–2.5 meters below the seabed. Collectively these results suggest that most deformation produced by gravity-driven flows occurs at depths greater than 3 m below the seabed.

2014 Geophysical study. Spatiotemporal analysis of three collocated multibeam sonar datasets from this same region (collected in 2006, 2009, and 2014) demonstrate that mudflows in gullies can continue to alter seabed depth and morphology even during periods when major hurricane strikes to not occur. Rates of deepening and shoaling are on the order of 1 m/y. However, overall plan view morphology of gullies did not change during this period.

2017 Geophysical study. Regional seabed creep for an entire mudflow lobe was found to have occurred in water depths of ~80 m, in the absence of major hurricanes. This type of seabed motion with modest forcing has never been documented previously, and could represent a hazard for seabed infrastructure, even without the forcing of hurricanes. Gas is widespread but not ubiquitous and can be detected as water column plumes. Geophyiscal tools used to map the seabed and subseabed sediments worked well and are suitable for a regional study.

2017 Geological study. Despite reduced sediment loads to South Pass and Pass a Loutre, widespread rapid deposition of seasonal flood layers is occurring offshore of these secondary river outlets. Piston cores and multicores, along with radiochemical measurements and x-radiographic imaging, can be used to detect plume sedimentation and also shallow seabed textures indicative of mudflows. A regional geological survey should be conducted to link observed seabed retreat described in Chapter 2 of this report to present sediment dispersal patterns.

5.2 Future Mississippi River Delta Front Research Plan

A proposal for the next phase of comprehensive MRDF study has been developed, including technologies and methods for developing a modern baseline map of the MRDF seabed and subsurface, and addressing data gaps identified above (see Appendix A). The effort is proposed to begin with a comprehensive mapping program, augmented with time-series measurements of waves, currents, and in situ seabed properties, extending to subseabed depths that encompass the maximum thickness of submarine landslides, and stacked flows (ca. 100 m sediment depth). These field observations will be integrated by numerical modeling of seabed forcing and response, to better understand past seabed dynamics, and predict future hazards and risk.

5.3 Synthesis and Application to Resource and Infrastructure Management

The existing state of knowledge for seabed mudflows on the MRDF is presently inadequate to provide a hazard+risk management framework for the entire region, spanning > 2000 km^2. This is because existing seabed maps and measurements on which many hazards are assessed are far outdated, and because appropriate measurements and numerical models of the forces that drive mudflows, and the seabed response to these failures, do not exist. This study has identified basic seabed and oceanographic knowledge gaps that must be bridged to develop such a hazard+risk management framework. This study also identifies scientific and engineering approaches to bridging those gaps in a future comprehensive study of the MRDF.

Works Cited

Abbott DH, Embley RW, Hobart MA. 1985. Correlation of shear-strength, hydraulic conductivity, and thermal gradients with desiment disturbace–South Pass region, Mississippi Delta. Geo Mar Lett. 5(2): 113-119.

Adams CE, Roberts HH. 1993. A model of the effects of sedementation rate on the stability of the Mississippi delta sediments. Geo Mar Lett. 13(1): 17–23.

Adams CE, Swift DJP, Coleman JM. 1987. Bottom currents and fluviomarine sedimentation on the Mississippi prodelta shelf. J Geophys Res: Oceans. 92(C13): 14595-14609.

Ahmad Z. 2017. The Germans torpedoed a ship during World War II. The wreck is now revealing secrets about underwater mudslides. Science Magazine. August 21, 2017. 362(6416) doi:10.1126/science.aap7308.8.

Allison MA et al. 2012. A water and sediment budget for the lower Mississippi–Atchafalaya River in flood years 2008–2010: Implications for sediment discharge to the oceans and coastal restoration in Louisiana. J Hydrol. (432-433):84-97. doi:10.1016/j.jhydrol.2012.02.020

Allison MA, Kineke GC, Gordon ES, Goni MA. 2000. Development and reworking of a seasonal flood deposit on the inner continental shelf off the Atchafalaya River. Cont Shelf Res. 20(16): 2267-2294.

Allison MA, Sheremet A, Goni MA, Stone GW. 2005. Storm layer deposition on the Mississippi-Atchafalaya subaqueous delta generated by Hurricane Lili in 2002. Cont Shelf Res. 25(18): 2213-2232.

Anderson AL, Bryant WR. 1990. Gassy sediment occurrence and properties: Northern Gulf of Mexico. Geo-Mar Lett. 10(4): 209-220.

Ayranci K, Lintern DG, Hill PR, Dastgard SE. 2012. Tide-supported gravity flows on the upper delta front, Fraser River delta, Canada. Mar Geol (326–328): 166–170.

Baldwin WE, Ackerman SD, Worley CR, Danforth WW, Chaytor JD. 2018. High-resolution geophysical data collected along the Mississippi River Delta front offshore of southeastern Louisiana. U.S. Geological Survey Field Activity 2017-003-FA: US Geological Survey data release. https://doi.org/10.5066/F7X929K6

Bea, R. G., 1974, Gulf of Mexico hurricane wave heights. Houston (TX): Proc Offshore Technol Conf. Ms. no. 2110. https://doi.org/10.4043/2110-MS

Bea RG. 1971. How sea floor slides affect offshore structures. Oil Gas J. 69(48): 88-92.

Bea RG, Arnold P. 1973. Movements and forces developed by wave-induced slides in soft clays. Offshore Technology Conference, 29 April–2 May, 1973, Houston, Texas. Proc Offshore Technol Conf. Ms. no. 1899.

Bea RG, Aurora RP. 1981. A simplified evaluation of seafloor stability. Offshore Technology Conference, 4–7 May, Houston, Texas. Ms. No. 3975.

Bea RG, Bernard HA. 1973. Movements of bottom soils in the Mississippi Delta offshore. In: Offshore oil and gas fields. Lafayette (LA): Lafayette Geological Society Special Publication. p. 13-28.

Bea RG, Bernard HA, Arnold P, Doyle EH. 1975. Soil movements and forces developed by wave-induced slides in the Mississippi Delta. J Petro Technol. 27(April):500–514.

Bea RG, Wright SG, Sircar P, Niedoroda AW. 1983. Wave-induced slides in South Pass Block 70, Mississippi Delta. J Geotech Eng. 109(4): 619-644.

Bennett RH, Bryant WR, Dunlap WA, Keller GH. 1976. Initial results and progress of the Mississippi Delta sediment pore water pressure experiment. Mar Georesour Geotechnol. 1(4): 327-335.

Bennett RH. 1977. Pore-water pressure measurements: Mississippi delta submarine sediments. Mar Geotechnol. 2(1–4): 177-189.

Bennett RH, Bryant WR, Dunlap WA, Keller GH. 1976. Initial results and progress of the Mississippi Delta sediment pore water pressure experiment. Mar Geotechnol. 1(4): 327-335.

Bentley SJ, Blum MD, Maloney JM, Pond L, Paulsell R. 2016. The Mississippi River source to sink system: Perspectives on tectonic, climatic, and anthropogenic influences, Miocene to Anthropocene. Earth Sci Rev. 153: 139-174. doi:10.1016/j.earscirev.2015.11.001

Bentley Sr SJ. 2002. Dispersal of fine sediments from river to shelf: Process and product. Gulf Coast Assoc Geolo Soc Trans. 52(2002):1055–1067.

Bentley SJ, Blum MD, Maloney J, Pond L, Paulsell R. 2016. The Mississippi River source-to-sink system: perspectives on tectonic, climatic, and anthropogenic influences, Miocene to Anthropocene. Earth-Sci Rev. 153(February): 139–174. [accessed 12 July 2021]; https://doi.org/10.1016/j.earscirev.2015.11.001

Bentley SJ, Furukawa Y, Vaughan WC. 2000. Record of event sedimentation in Mississippi Sound. Gulf Coast Assoc Geolo Soc Trans. 50(2000):715–723.

Bentley SJ, Keen TR, Blain CA, Vaughan WC. 2002. The origin and preservation of a major hurricane event bed in the northern Gulf of Mexico: Hurricane Camille, 1969. Mar Geol. 186:423–446.

Bentley SJ, Nittrouer CA. 2003. Emplacement, modification, and preservation of event strata on a flood-dominated continental shelf: Eel shelf. North Calif Cont Shelf Res. 23:1465-1493. doi:10.1016/j.csr.2003.08.005

Blum MD, Roberts HH. 2009. Drowning of the Mississippi Delta due to insufficient sediment supply and global sea-level rise. Nature Geosci. 2:488-491 doi:http://www.nature.com/ngeo/journal/v2/n7/suppinfo/ngeo553_S1.html

Blum MD, Roberts HH. 2012. The Mississippi Delta region: Past, present, and future. Annu Rev Earth Planet Sci. 40: 655-683.

Bohlke BM, Bennett RH. 1980. Mississippi prodelta crusts: Aclay fabric and geotechnical analysis. Mar Georesour Geotechnol. 4(1):55-82.

Bouma AH, Roberts HH, Coleman JM, Prior DB. 1991. Delta-front gullies as part of mass-movement phenomena. In: Osborne, RH (ed). From shoreline to abyss: Contribution to marine geology in honor of Francis Parker Shepard. Broken Arrow (OK): Society for Sedimentary Geology. Special Publication No. 46. p. 99-105.

Bryant WR, Wallin CS. 1968. Stability and geotechnical characteristics of marine sediments, Gulf of Mexico. Trans Gulf Coast Assoc Geol Soc. 18: 334-356.

Bureau of Safety and Environmental Enforcement (USDOI BSEE). 2014. Offshore incident statistics. Incident statistics and summaries, published reports, outer continental shelf, calendar years 1956–1990, 1991–1992, 1995–1996, 1997, 1998, 1999, and 2000. New Orleans (LA): US Department of the Interior, Bureau of Safety and Environmental Enforcement. http://www.bsee.gov/Inspection-and-Enforcement/Accidents-and-Incidents/Listing-and-Status-of-Accident-Investigations/

Cardone VJ, Cox AT, Forristall GZ. 2007. Hindcast of winds, waves and currents in Northern Gulf of Mexico in Hurricanes Katrina (2005) and Rita (2005). Offshore Technology Conference, 30 April–3 May, Houston, Texas. Houston (TX): Proc Offshore Technol Conf. Ms. no. 18652. https://doi.org/10.4043/18652-MS

Chadwell CD. 2017. Update on GPS-acoustics measurements on the continental slope of the Cascadia subduction zone. American Geophysical Union Fall Meeting, 11–15 December 2017, New Orleans, Louisiana.

Chaytor JD, Baldwin WE, Danforth, WW, Bentley SJ, Miner MD, et al. 2017. New high-resolution multibeam mapping and seismic reflection imaging of mudflows on the Mississippi River Delta Front. American Geophysical Union Fall Meeting, 11–15 December 2017, New Orleans, Louisiana.

Chen W, Pourghasemi HR, Panahi M, Panahi M, Kornejady A, Wang J, Xie X, Cao S. 2017. Spatial prediction of landslide susceptibility using an adaptive neuro-fuzzy inference system combined with frequency ratio, generalized additive model, and support vector machine techniques. Geomorphol. 297:69-85.

Cho KW, Reid RO, Nowlin WD. 1998. Objectively mapped stream function fields on the Texas-Louisiana shelf based on 32 months of moored current meter data. J Geophys Res: Oceans. 103(C5):10377-10390.

Clare MA, Talling PJ, Challenor P, Malgesini G, Hunt J. 2014. Distal turbidites reveal a common distribution for large (>0.1km3) submarine landslide recurrence. Geology.42(3):263–266.

Clare MA, Hughes Clarke JE, Talling PJ, Cartigny MJB, Pratomo DG. 2016. Preconditioning and triggering of offshore slope failures and turbidity currents revealed by most detailed monitoring yet at a fjord-head delta. Earth Planet Sci Lett. 450: 208-220.

Clark R, Georgiou I, Fitzgerald D. 2013. An evolutionary model of a retrograding subdeltaic distributary of a river-dominated system. The Gulf Coast Association of Geological Societies Meeting, October 6-8, New Orleans, LA.

Clukey EC, Kulhawy FH, Liu PLF, Tate GB. 1985. The impact of wave loads and pore-water pressure generation on initiation of sediment transport. Geo-Mar Lett. 5(3): 177-183.

Cochran JK, Masqué P. 2003. Short-lived U/Th Series radionuclides in the ocean: tracers for scavenging rates, export fluxes and particle dynamics. Rev Mineral Geochem. 52:461-492. doi:10.2113/0520461

Coleman JM. 1988. Dynamic changes and processes in the Mississippi River delta. Geol Soc Am Bull. 100(7): 999-1015.

Coleman JM, Garrison LE. 1977. Geological aspects of marine slope stability, northwestern Gulf of Mexico. Mar Geotechnol. 2: 9-44.

Coleman JM, Prior DB, Adams Jr CE. 1981. Erosional furrows on continental shelf edge, Mississippi delta region. Geo-Mar Lett. 1: 11-15.

Coleman JM, Prior DB, Garriso LE (Louisiana State University, Baton Rouge, LA). 1980. Subaqueous sediment instabilities in the offshore Mississippi River delta. New Orleans (LA): US Department of Interior, Bureau of Land Management. Contract No.: AA551-MU9-10. BLM Open-File Report 80-01.

Coleman JM, Prior DB, Garrison LE. 1978. Submarine landslides in the Mississippi River Delta. Annual Offshore Technology Conference, Houston, Texas 8–11 May 1978. Houston (TX): Proc Offshore Technol Conf. Ms. no. 3170.

Coleman JM, Prior DB, Lindsay JF. 1983. Deltaic influences on shelf edge instability processes. In: Stanley DJ, Moore GT (editors). The shelfbreak: Critical interface on continental margins SEPM Special Publication, vol. 33. p. 121-137.

Coleman JM, Roberts HH. 1988. Late Quaternary depositional framework of the Louisiana continental shelf and upper continental slope. Trans Gulf Coast Assoc Geol Soc. 38:407-419.

Coleman JM, Roberts HH, Bryant WR. 1991. Late Quaternary sedimentation. In:Salvador A. (ed). 1989. The Geology of North America, volume J, the Gulf of Mexico Basin. Boulder (CO): The Geological Society of America. 325-352.

Coleman JM, Roberts HH Stone GW. 1998. Mississippi River Delta: An overview. J Coast Res. 14(3): 698-716.

Coleman JM, Suhayda JN, Whelan T, Wright LD.. 1974. Mass movement of Mississippi River delta sediments. Trans Gulf Coast Assoc Geol Soc. 24:49-68.

Coleman JM, Walker HJ, Grabau WE. 1998. Sediment instability in the Mississippi River delta. J Coast Res. 14(3):872–881.

Cooper AK, Hart PE. 2003. High-resolution seismic-reflection investigation of the northern Gulf of Mexico gas-hydrate-stability zone. Mar Petrol Geol19(10): 1275-1293.

Corbett DR, Dail M, McKee B. 2007. High-frequency time-series of the dynamic sedimentation processes on the western shelf of the Mississippi River delta, Cont Shelf Res. 27(10-11):1600-1615.

Corbett DR, McKee B, Allison MA. 2006. Nature of decadal-scale sediment accumulation on the western shelf of the Mississippi River delta. Cont Shelf Res.26:2125-2140. doi:10.1016/j.csr.2006.07.012

Corbett DR, McKee B, Duncan D. 2004. An evaluation of mobile mud dynamics in the Mississippi River deltaic region. Mar Geol. 209:91-11. doi:10.1016/j.margeo.2004.05.028

Courtois AJ, Bentley SJ, Xu K, Georgiou IY, Maloney JM, et al. 2017. A regional survey of river-plume sedimentation on the Mississippi River Delta front. American Geophysical Union Fall Meeting, 11–15 December 2017, New Orleans, Louisiana.

Dail MB, Corbett DR, Walsh JP. 2007. Assessing the importance of tropical cyclones on continental margin sedimentation in the Mississippi delta region. Cont Shelf Res. 27(14):1857–1874.

Denk EW, Dunlap WA, Bryant WR, Milberger LJ, Whelan III TJ. 1981. A pressurized core barrel for sampling gas-charged marine sediments. Annual Offshore Technology Conference, 4–7 May, 1981, Houston, Texas. Houston (TX): Proc Offshore Technol Conf. Ms. no. 4120. https://www.onepetro.org/conference-paper/OTC-4120-MS

Denommee K, Bentley S. 2013. Influence of mass-transport processes on clinoform mechanics on the southwest Louisiana Shelf. Trans Gulf Coast Assoc Geol Soc. (2013):205–212.

Denommee KC, Bentley SJ, Harazim D. 2017. Mechanisms of muddy clinothem progradation on the Southwest Louisiana Chenier Plain inner shelf. Geo-Mar Lett. 38(3): 1-13.

Denommee KC, Bentley SJ, Jarazim D, Macquaker JH. 2016. Hydrodynamic controls on muddy sedimentary-fabric development on the Southwest Louisiana subaqueous delta. Mar Geol. 382:162-175.

Dokka RK, Sella GF, Dixon TH. 2006. Tectonic control of subsidence and southward displacement of southeast Louisiana with respect to stable North America. Geophys Res Lett. 33(23): L23308.

Doyle EH. 1973. Soil-wave tank studies of marine soil stability. Annual Offshore Technology Conference, 29 April–2 May, 1973, Houston, Texas. Houston (TX): Proc Offshore Technol Conf. Ms. no. 1901.

Droser ML, Bottjer DJ. 1986. A semiquantitative field classification of ichnofabric: Research method paper. J Sediment Res. 56(4):558–559.

Droxler AW, Schlager W. 1985. Glacial versus interglacial sedimentation rates and turbidite frequency in the Bahamas. Geology. 13 (11): 799–802.

Dunlap W, Holcombe L, Holcombe T (Texas A&M University, College Station, Texas). 2004. Shear strength maps of shallow sediments in the Gulf of Mexico. New Orleans (LA): US Department of the Interior Mineral Management Service. MMS/OTRC Cooperative Research Agreement 1435-01-99CA-31003, Task Order 17007, Project 367.

Dunlap WA. 1981. Geotechnical applications in soft sediments. In: BoumaA, Sangrey D, Coleman J, Prior D, Trippet A, Dunlap W, Hooper J. (editors). CN18: Offshore geologic hazards. Tulsa (OK): American Association of Petroleum Geologists. p. 2.3–2.41.

Spong RE, Puskar F (Energo Engineering, Houston, Texas). 2006. Assessment of fixed offshore platform performance in Hurricanes Andrew, Lili, and Ivan: Final Report. Herndon (VA): US Department of t he Interior Minerals Management Service. MMS Project No. 549.

Enterprise Products Partners, LLC. 2005. Multi-beam bathymetry data, South Pass 53 to Viosca, Knoll 985 Pipeline Route. Digital data only provided to Louisiana State University.

Esrig MI, Ladd RS, Bea RG. 1975. Material properties of submarine Mississippi Delta sediments under simulated wave loadings. Annual Offshore Technology Conference, 5–8 May, 1975, Houston, Texas. Houston (TX): Proc Offshore Technol Conf. Ms. no. 218.

Falcini F, Khan NS, Macelloni L, Horton BP, Lutken CB, et al. 2012. Linking the historic 2011 Mississippi River flood to coastal wetland sedimentation. Nat Geosci. 5(11): 803-807.

FEMA. 2012. Operating guidance No. 8-12, joint probability-optimal sampling method for tropical storm surge frequency analysis. https://www.fema.gov/coastal-flood-hazard-analysis-and-mapping, accessed 04/10/2018.

Fenton, JD. 1999. Numerical methods for nonlinear waves. In: Liu P L-F (editor). Advances in coastal and ocean engineering. Vol 5. Singapore: World Scientific. p. 241–324.

Fisk HN. 1961. Bar-finger sands of the Mississippi Delta. In: Peterson JA, Osmond JC (editors). Geometry of sandstone bodies: AAPG Symposium, SP22New Jersey, American Association of Petroleum Geologists. p. 29–52.

Fisk HN, McFarlan E, Kolb CR, Wilbert LJ. 1954. Sedimentary framework of the modern Mississippi Delta. J Sediment Petrol. 24(2): 76-99.

Flemings PB, Long H, Dugan B, Germaine J, John CM, et al. 2008. Pore pressure penetrometers document high overpressure near the seafloor where multiple submarine landslides have occurred on the continental slope, offshore Louisiana, Gulf of Mexico. Earth Planet Sci Lett. 269(3):309-325.

Flow-3D, 2010, FLOW-3D Excellence in flow modeling software: Sante Fe, New Mexico 87505. User Manual 9.4 volumes 1 and 2.

Forristall GZ, Reece AM. 1985. Measurements of wave attenuation due to a soft bottom: The swamp experiment. J Geophys Res. 90: 3367-3380.

Friedrichs CT, Wright LD. 2004. Gravity-driven sediment transport on the continental shelf implications for equilibrium profiles near river mouths. Coastal Eng. 51(8–9): 795-811.

Frazier DE. 1967. Recent deltaic deposits of the Mississippi River; their development and chronologyTrans Gulf Coast Geol Soc. 17(287–315).

Frenkel MC, Wright SG, Gilbert RB, Ward EG. 2006. Mudflows and mudslides during Hurricane Ivan. Paper presented at: Offshore Technology Conference, Houston, Texas, May 2006. Paper No.: OTC-18328-MS.

Galloway WE. 1975. Process framework for describing the morphologic and stratigraphic evolution of deltaic depositional systems. Society of Economic Paleontologists and Mineralogist (SEPM), Special Publication No. 31. 127-156.

Garrison LE. 1974. The instability of surface sediments on parts of the Mississippi Delta Front. USGS Open File Report 18, Corpus Christi, Texas. Reston (VA): US Department of the Interior, US Geologic Survey.

Georgiou IY, Schindler J. 2009. Numerical simulation of waves and sediment transport along a transgressive barrier island, Chapter H. In: Lavoie D (editor). Sand resources, regional geology, and coastal processes of the Chandeleur Islands coastal system—An evaluation of the Breton National Wildlife Refuge. Reston (VA): US Department of the Interior US Geological Survey. U.S. Geological Survey Scientific Investigations Report 2009–5252. p. 143–168.

Goldfinger C. 2011. Submarine paleoseismology based on turbidite records. Annu Rev Mar Sci. 3: 35–66.

Goni MA, Alleau Y, Corbett R, Walsh JP, Mallinson D, et al. 2007. The effects of Hurricanes Katrina and Rita on the seabed of the Louisiana shelf. Sediment Rec. 5(1):4–9.

Goni MA, Ruttenberg KC, Eglinton TI. 1997. Source and contribution of terrigenous organic carbon to surface sediments in the Gulf of Mexico: Nature. 389(6648): 275-278.

Gonzalez S, Bentley SJ, DeLong K, Kehui X, Obelcz J, et al. 2017. Facies reconstruction of a late Pleistocene cypress forest discovered on the northern Gulf of Mexico Continental Shelf. Trans Gulf Coast Assoc Geol Soc. (67): 133-146.

Griffin Gm, Parrott BS. 1964. Development of clay mineral zones during deltaic migration. Am Assoc Petrol Geol Bull . 48(1): 57-69.

Grozic J, Nadim F, Kvalstad T. 2005. On the undrained shear strength of gassy clays. Comput Geotech. 32(7): 483-490.

Grozic JL, Robertson P, Morgenstern N. 2000. Cyclic liquefaction of loose gassy sand. Can Geotech J. 37(4): 843-856.

Guidroz WS. 2009. Subaqueous, hurricane-initiated shelf failure morphodynamics along the Mississippi River Delta Front, North-Central Gulf of Mexico[dissertation]. Baton Rouge (LA): Louisiana State University.

Gwiazda R, Paull CK, Kieft B, Bird L, Klimov D, et al. 2017. Seabed motion during sediment density flows as recorded by displaced man-made [sic] motion-recording boulders and a heavy instrument platform. American Geophysical Union Fall Meeting, New Orleans, December 2017.

Hampton MA, Lee HJ, Locat J. 1996. Submarine landslides. Rev Geophys. 34(1):33-59.

Hanor JS. 1981. Composition of fluids expelled during compaction of Mississippi Delta sediments. Geo-Mar Lett. 1(3–4): 169-172.

Hart BS, Hamilton TS, Barrie JV. 1998. Sedimentation rates and patterns on a deep-water delta (Fraser Delta, Canada): Integration of high-resolution seismic stratigraphy, core lithofacies, and 137Cs fallout stratigraphy. J Sediment Res. 68(4) 556–568.

Henkel DJ. 1970. The role of waves in causing submarine landslides. Geotech. 20(1): 75-80.

Hirschberg DJ, Schubel JR. 1979. Recent geochemical history of flood deposits in the northern Chesapeake Bay. Estuar Coast Shelf Sci. 9:771-IN777. doi:http://dx.doi.org/10.1016/S0302-3524(79)80010-9

Hirst TJ, Richards AF. 1977. In situ pore-pressure measurement in Mississippi delta front sediments. Mar Geotechnol. 2(1–4):191–204.

Hitchcock C, Angell M, Givler R, Hooper J. 2008. Transport and depositional features associated with submarine mudflows, Mississippi Delta, Gulf of Mexico. Trans Gulf Coast Assoc Geol Soc. 58:755–758.

Hitchcock, C, Angell, Givler R, Hooper J (William Lettis & Associates, Walnut Creek, California). 2006. A pilot study for regionally-consistent hazard susceptibility mapping of submarine mudslides, offshore Gulf of Mexico. Reston (VA): US Department of the Interior Minerals Management Service. TAP Project No. 550.

Hooper JR. 1980. Crustal layers in Mississippi delta mudflows. Annual Offshore Technology Conference, 5–8 May, Houston, Texas. Houston (TX): Proc Offshore Tech Conf. Ms no. 3770.

Hooper JR. 1996. Foundation soil motion in South Pass 47. Annual Offshore Technology Conference, 6–9 May, Houston, Texas. Houston (TX): Proc Offshore Tech Conf. Ms no 7953.

Hooper JR, Suhayda JN. 2005. Hurricane Ivan as a geologic force: Mississippi delta front seafloor failures. Annual Offshore Technology Conference, 2–5 May, Houston, Texas. Houston (TX): Proc Offshore Tech Conf. Ms no. 17737.

Hottman WE, Suhayda JN, Garrison LE. 1978. SEASWAB II (shallow experiment to access storm wave affects on the bottom). Annual Offshore Technology Conference, 8–11 May, Houston, Texas. Houston (TX): Proc Offshore Tech Conf. Ms no. 3169.

Houssais M, Jerolmack DJ. 2017. Toward a unifying constitutive relation for sediment transport across environments. Geomorph. (277): 251-264. doi: 10.1016/j.geomorph.2016.03.026.

Houssais M, Ortiz C, Durian DJ, Jerolmack DJ. 2015. Onset of sediment transport is a continuous transition driven by fluid shear and granular creep. Nat Commun. 6(article no. 6527). doi:10.1038/ncomms7527

Hughes CJ, Brucker S, Muggah J, Hamilton T, Cartwright D, et al. 2012. Temporal progression and spatial extent of mass wasting events on the Squamish prodelta slope. In: Eberhardt E, Froese C, Turner K, Leroueil (editors). Landslides and engineered slopes: Protecting society through improved understanding. 2 vols. London (GB): Taylor & Francis Group. p. 1091–1096.

Hughes CJ, Clarke JE, Marques CRV, Pratomo D. 2014. Imaging active mass-wasting and sediment flows on a fjord delta, Squamish, British Columbia. In: Krastel S, Behrmann J-H, Völker D, Stipp M, Berndt C, et al. (editors). Submarine mass movements and their consequences, 6th International symposium. Advances in natural and technological hazards research, vol. 37. Cham (CH): Springer International Publishing. p. 249–260.

Hughes Clarke JE. 2016. First wide-angle view of channelized turbidity currents linking migrating cyclic steps to flow characteristics. Nat. Commun.7: 118960. http://dx.doi.org/10.1038/ncomms11896.

Hülse P, Bentley Sr SJ. 2012. A 210Pb sediment budget and granulometric record of sediment fluxes in a subarctic deltaic system: The Great Whale River, Canada Estuarine, Coastal and Shelf Science. 109:41-52. doi:http://dx.doi.org/10.1016/j.ecss.2012.05.019

Jia Y, Zhang L, Zheng J, Liu X, Jeng D-S, et al. 2014. Effects of wave-induced seabed liquefaction on sediment re-suspension in the Yellow River Delta. Ocean Eng. 89: 146-156.

Johns MW, Bryant WR, Dunlap WA. (Texas A&M University, College Station, Texas) 1985. Geotechnical properties of Mississippi River delta sediments utilizing in situ pressure sampling techniques. New Orleans (LA): US Department of the Interior Minerals Management Service. Contract No. 14-12-00001-G-709. Report No.: MMS 85-0047.

Johns MW, Taylor E, Bryant WR. 1982. Geotechnical sampling and testing of gas-charged marine sediments at in situ pressures. Geo-Mar Lett. 2(3–4): 231–236.

Johnson DR. 2008. Ocean surface current climatology in the Northern Gulf of Mexico. Ocean Springs, Mississippi: Gulf Coast Research Laboratory.

Kaiser MJ, Yu Y, Jablonowski CJ. 2009. Modeling lost production from destroyed platforms in the 2004–2005 Gulf of Mexico hurricane seasons. Energy 34:1156-1171.

Keen TR, Bentley SJ, Vaughan WC, Blain CA. 2004. The generation and preservation of multiple hurricane beds in the northern Gulf of Mexico. Mar Geol. 210: 79-105.

Keen T, Furukawa Y, Bentley S, Slingerland R, Teague W, Dykes J, Rowley C. 2006. Geological and oceanographic perspectives on event bed formation during Hurricane Katrina. Geophys Res Lett. 33(23): L23614. doi:10.1029/2006GL027981

Keen TR, Slingerland RL, Bentley Sr SJ, Furukawa Y, Teague WJ, et al. 2012. Sediment transport on continental shelves: storm bed formation and preservation in heterogeneous sediments. Int Assoc Sedimentol Spec Publ. 44:295-310.

Keller G, Bentley SJ, Xu K, Maloney J, Miner M, et al. 2016. River-plume sedimentation and 210Pb/7Be seabed delivery on the Mississippi River delta front. Geo-Mar Lett. 37(3):259–272. doi:10.1007/s00367-016-0476-0.

Keller GH, Prior DB. 1986. Sediment dynamics of the Huanghe (Yellow-River) Delta and neighboring Gulf of Bohai, Peoples-Republic-of-China:Project Overview. Geo-Mar Lett. 6(2): 63-66.

Keller G, Bentley SJ, Gorgiou IY, Maloney J, Miner M, Xu, K. 2017. River-plume sedimentation and 210 Pb/7Be seabed delivery on the Mississippi River delta front. Geo-Mar Let. 37:259–272. [accessed 12 July 2021]; doi.org/10.1007/s00367-016-0476-0

Kemp GP, Willson CS, Rogers JD, Westphal KA, Binselam SA. 2014. Adapting to change in the lowermost Mississippi River: Implications for navigation, flood control and restoration of the delta ecosystem. In: Day JW, Kemp GP, Freeman A, Muth DP (eds). Perspectives on the restoration of the Mississippi Delta: The once and future delta. Dordrecht (NL): Springer Nature. p. 51–84.

Kesel RH. 1988. The decline in the suspended load of the lower Mississippi River and its influence on adjacent wetlands. Environ Geol Water Sci. 11(3): 271-281.

Kesel RH. 2003. Human modifications to the sediment regime of the Lower Mississippi River flood plain. Geomorphology. 56(3–4): 325-334.

Kesel RH, Yodis EG, McCraw DJ. 1992. An approximation of the sediment budget of the lower Mississippi River prior to major human modification. Earth Surf Processes Landforms. 17(7): 711-722.

Kinsman B. 1984. Wind waves: their generation and propagation on the ocean surface. Mineola (NY): Dover Press.

Kraft Jr LM, Suhayda JN, Helfrich SC, Marin JE. 1990. Ocean wave attenuation due to soft seafloor sediments. Mar Geotechnol. 9(3): 227-242.

Kulp M, Howell P, Adiau S, Penland S, Kindinger J, et al. 2002. Latest Quaternary stratigraphic framework of the Mississippi River delta region. Gulf Coast Assoc Geol Soc Trans. 52(2002): 573–582.

Lee HJ, Greene HG, Edwards BD, Fisher MA, Normark WR. 2009. Submarine landslides of the Southern California Borderland. In: Lee HJ, Normark WR (eds). Earth science in the urban ocean: The Southern California continental borderland. Boulder (CO): Geological Society of America. p. 251–269. https://doi.org/10.1130/2009.2454(4.3)

Lee HJ, Schwab WC, Booth JS. 2002. Submarine landslides: An introduction. In: Schwab WC, Lee HJ, Twichell DC (editors). Submarine landslides: Selected studies in the U.S. Exclusive Economic Zone. US Geological Survey Bulletin 2002. Washington (DC): US Government Printing Office. p. 1-13.

Leithold EL, Blair NE, Wegmann KW. 2015. Source-to-sink sedimentary systems and global carbon burial: A river runs through it. In: Walsh JP, Wiberg P, Aalto R (editors). Source-to-sink systems: Sediment and Solute Transfer on the Earth surface. Earth-Sci Rev. 153(February 2006):30–42.

Lindsay JF, Prior DB, Coleman JM. 1984. Distributary-mouth bar development and role of submarine landslides in delta-growth, South Pass, Mississippi-Delta. Am Assoc Petrol Geol Bull. 68(11) 1732-1743.

Louisiana Coastal Protection and Restoration Authority (LaCPRA). 2017. Louisiana's comprehensive master plan for a sustainable coast, Effective June 2, 2017. Baton Rouge (LA): Coastal Protection and Restoration Authority of Louisiana.

Louisiana Geological Survey (LGS). 2011. 30x60 minute geologic quadrangle series, Terrebonne Bay map and New Orleans map. Baton Rouge (LA): Louisiana Geological Survey, Louisiana State University.

Love MR, Amante CJ, Eakins BW, Taylor LA. 2012. Digital elevation models of the Northern Gulf Coast: Procedures, data sources and analysis. Boulder (CO): National Oceanic and Atmospheric Administration, National Geophysical Data Center. NOAA Technical Memorandum NESDIS NGDC-59.

Macquaker JHS, Bentley SJ, Bohacs KM. 2010. Wave-enhanced sediment-gravity flows and mud dispersal across continental shelves: Reappraising sediment transport processes operating in ancient mudstone successions. Geology. 38(10): 947-950.

Maloney J, Bentley SJ, Obelcz J, Xu K, Miner M, et al. 2014. Assessing subaqueous mudflow hazard on the Mississippi River Delta Front, part 1: a historical perspective on Mississippi River Delta Front sedimentation. Paper presented at: American Geophysical Union Fall Meeting: San Francisco, CA.

Maloney JM, Bentley SJ, Xu K, Obelcz J, Miner M. 2018. Mississippi River subaqueous delta is entering a stage of retrogradation. Mar Geol . 400(2018)12–23. doi: 10.1016/j.margeo.2018.03.001

Martin KM, Wood WT, Becker JJ. 2015. A global prediction of seafloor sediment porosity using machine learning. Geophys Res Lett. 42(10640-10646).

Martin RG, Bouma AH. 1982. Active diapirism and slope steepening, northern Gulf of Mexico continental slope. Mar Georesour Geotechno. 5(1): 63–91.

Meade RH. 1996. River-sediment inputs to major deltas. In: Milliman JD, Haq BU (editors). Sea-level rise and coastal subsidence. Coastal systems and continental margins, vol. 2. Dordrecht (NE): Springer. p. 63-85.

Milliman JD, Meade RH. 1983. World-wide delivery of river sediment to the oceans. J Geol. 91(1): 1-21.

Moore DG, Scruton PC. 1957. Minor internal structures of some recent unconsolidated sediments Am Assoc Petrol Geol Bull. 41:2723-2751.

Morgan DJ. 1977. The Mississippi River Delta: Legal-geomorphologic evaluation of historic shoreline changes. Baton Rouge (LA): Louisiana State University, School of Geoscience.

Morgan J. 1961. Genesis and paleontology of Mississippi mud lumps, Part 1. Louisiana Geol. Survey Bull. 35:116.

Morgan JP, Coleman JM, Gagliano SM. 1968. Mudlumps: diapiric structures in Mississippi delta sediments. In: Braunstein J, O'Brien GD (editors). Diapirism and diapirs: A symposium. Am Assoc Petrol Geol Bull. (8):145–161.

Muhammad Z, Bentley SJ, Febo LA, Droxler AW, Dickens GR, et al. 2008. Excess 210Pb inventories and fluxes along the continental slope and basins of the Gulf of Papua. J Geophys Res Earth Surf. (2003–2012): 113.

Mullenbach B, Nittrouer C. 2006. Decadal record of sediment export to the deep sea via Eel Canyon. Cont Shelf Res. 26:2157-2177.

Nageswaran S. 1983. Effect of gas bubbles on the sea bed behavior [dissertation]. Oxford (GB): St. Catherine's College, Oxford University.

National Hurricane Center. 2015. Archive available at website of National Hurricane Center http://coast.noaa.gov/hurricanes/?redirect=301ocm, accessed on July 6, 2015.

Nittrouer CA. 1999. STRATAFORM: Overview of its design and synthesis of its results. Mar Geol. 154(1):3–12.

Nittrouer CA, DeMaster DJ, McKee BA, Cutshall NH, Larsen IL. 1984. The effect of sediment mixing on Pb-210 accumulation rates for the Washington continental shelf. Mar Geol. 54(3–4):201–222.

Nittrouer CA, Kuehl SA. 1995. Geological significance of sediment transport and accumulation on the Amazon continental shelf. Mar Geol. 125(3):175–176.

Nittrouer C, Sternberg R. 1981. The formation of sedimentary strata in an allochthonous shelf environment: The Washington continental shelf. Mar Geol. 42(1–4):201-232.

NOAA. 2016. Hurricane data. National Oceanic & Atmospheric Administration, Atlantic Oceanographic & Meterological Laboratory.

Nodine MC, Cheon JY, Wright SG, Gilbert RB (Texas Engineering Experiment Station, College Station, Texas). 2007. Mudslides during Hurricane Ivan and an assessment of the potential for future mudslides in the Gulf of Mexico: phase II project report. New Orleans (LA): US Department of the Interior, Minerals Management Service. Cooperative Agreement No.:1435-01-04-CA-35515. MMS TAR Project No.: 552.

Nodine MC, Cheon JY, Wright SG, Gilbert RB (Texas Engineering Experiment Station, College Station, Texas). 2009. Addendum to mudslides during Hurricane Ivan and an assessment of the potential for future mudslides in the Gulf of Mexico. College Station and Austin (TX): Offshore Technology Research Center. MMS/OTRC Cooperative Research Agreement No: 1435-01-04-CA-35515. Task Order: 39239. MMS TAR Project Number 552.

Nodine MC, Gilbert RB, Kiureghian SGW, Cheon JY, Wrzyszczynski M, et al. 2007. Impact of hurricane-induced mudslides on pipelines. Paper presented at: Offshore Technology Conference, Houston, Texas, April 2007. Paper No.: OTC-18983-MS.

Nodine MC, Wright SG. Gilbert RB. 2006. Mudflows and mudslides during Hurricane Ivan. Paper presented: Offshore Technology Conference, American Association of Peroleum Geologists; Houston, Texas, 1–4 May.

Obelcz J, Xu K, Bentley Sr SJ, Georgiou IY, Maloney J, et al. 2014. Assessing subaqueous mudslide hazard on the Mississippi River Delta Front, Part 2: Insights revealed by new high-resolution geophysical surveying. Paper presented at: American Geophysical Union, Fall Meeting, San Francisco, California, 15–19 December.

Obelcz J, Xu K, Georgiou IY, Maloney J, Bentley SJ, et al. 2017. Sub-decadal submarine landslides are important drivers of deltaic sediment flux: insights from the Mississippi River Delta Front. Geology. 45(8): G38688. [accessed 12 July 2021]; DOI:10.1130/G38688.1

Ogston AS, Cacchione DA, Sternberg RW, Kineke GC. 2000. Observations of storm and river flood-driven sediment transport on the northern California continental shelf. Cont Shelf Res. 20(16):2141–2162.

Paull CK, Ussler W, Caress DW, Lundsten E, Covault JA, et al. 2010. Origins of large crescent-shaped bedforms within the axial channel of Monterey Canyon, offshore California. Geosphere. 6(6):755–774.

Pohlman J, Ruppel C, Maue C. 2012. Real-time mapping of seawater and atmospheric methane concentrations offshore of Alaska's north slope. USGS Soundwaves Monthly Newsletter. (May–June 2012): 4-5.

Prior DB, Coleman JM. 1982. Active slides and flows in underconsolidated marine sediments on the slopes of the Mississippi Delta. In: Saxov S, Nieuwenhuis JK (eds). Marine slides and other mass movements. NATO Conference series IV, marine sciences vol. 6. New York (NY): Plenum Press. p. 21-49.

Prior DB, Coleman JM. 1982. Side-scan sonar mosaics chart mudslide areas. Petrol Eng Internat. v. June. p. 76–86.

Prior DB, Coleman JM. 1980. Sonograph mosaics of submarine slope instabilities, Mississippi River Delta. Mar Geol. 36(3–4): 227-239.

Prior DB, Coleman JM. 1978. Submarine landslides on the Mississippi River delta-front slope. Geosci Man. 19: 41-53.

Prior DB, Coleman JM. 1978. Disintegrating retrogressive landslides on very-low-angle subaqueous slopes, Mississippi Delta. Mar Geotechnol. 3(1): 37-60.

Prior DB, Coleman JM. 1979. Submarine landslides; geometry and nomenclature. Zeitschrift Geomorphol. 23(4): 415-426.

Prior DB, Coleman JM. 1984. Submarine slope instability. In: Brunsden D, Prior DB (eds). Slope Instability: United Kingdom. Chichester (GB): John Wiley and Sons. p. 419-455.

Prior DB, Suhayda JN. 1981. Application of infinite slope analysis to subaqueous sediment instability, Mississippi Delta. In: Bouma A, Sangrey D, Coleman J, Prior D, Trippet A, et al. (editors). CN18: Offshore geologic hazards. Tulsa (OK): American Association of Petroleum Geologists. p. 5.76–75.92.

Prior DB, Suhaayda JN. 1979. Submarine mudslide morphology and development mechanisms, Mississippi Delta. Paper presented at: Offshore Technology Conference, Houston, Texas, April 1979. Paper No.: OTC-3482-MS.

Prior DB, Suhayda JN, Lu N-Z, Bornhold BD, Keller GH, et al. 1989. Storm wave reactivation of a submarine landslide. Nature. 341:47-50.

Prior DB, Yang ZS, Bornhold BD, Keller GH, Lin ZH, Wiseman WJ, Wright LD, Lin TC. 1986. The subaqueous delta of the modern Huanghe (Yellow-River). GeoMar Lett. 6(2): 67-75.

Puig P, Ogston AS, Mullenbach BL, Nittrouer CA, Parsons JD, Sternberg RW. 2004. Storm-induced sediment gravity flows at the head of the Eel submarine canyon, northern California margin. J Geophys Res Oceans. 109(3):C03019. doi:10.1029/2003JC001918.

Puig P, Ogston AS, Mullenbach BL, Nittouer CA, Sternberg RW. 2003. Shelf-to-canyon sediment-transport processes on the Eel continental margin (northern California). Mar Geol. 193(1): 129–149.

Quiros GW, Young AH, Pelletier JH, Chan JHC. 1983. Shear strength interpretation for Gulf of Mexico clays: United States, In: Wright SG (ed). Proceedings of Conference on Geotechnical Practice in Offshore Engineering, Austin, Texas, April 27-29, 1983. New York (NY): Am Soc Civ Eng. p. 144-165.

Robbins JA, Edgington DN. 1975. Determination of recent sedimentation rates in Lake Michigan using Pb-210 and Cs-137. Geochim Cosmochim Ac. 39:285-304.

Roberts HH. 1997. Dynamic changes of the Holocene Mississippi River delta plain: The delta cycle. J Coast Res. (13)3: 605–627.

Roberts HH. 1985. Clay mineralogy of contrasting mudflow and distal shelf deposits on the Mississippi River delta front. Geo-Mar Lett. 5(3): 185–191.

Roberts HH, 1980. Sediment characteristics of Mississippi River Delta-front mudflow deposits. Trans Gulf Coast Assoc Geol Soc 30(1980): 485–496.

Roberts HH, Cratsley DW, Whelan III T. 1976. Stability of Mississippi Delta sediments as evaluated by analysis of structural features in sediment borings. Paper presented at: 8th Offshore Technology Conference, Houston, Texas, May 3–6. Paper No.: OTC-2425-MS.

Roberts H, Suhayda J, Coleman J. 1980. Sediment deformation and transport on low-angle slopes (stability): Mississippi River delta. In: Coates DR, Vitek JD (eds). Thresholds in geomorphology: Issue 9 of geomorphology symposia series. Stroudsburg (PA): Dowden and Culver Inc. p. 131–167.

Roberts NC. 1969. The story of extreme Hurricane Camille. New Orleans (LA): Privately published.

Rotondo K. 2004. Transport and deposition of fluid mud event layers along the Western Louisiana Inner Shelf [thesis]. Geneseo (NY): University of New York at Geneseo.

Rotondo KA, Bentley SJ. 2003. Deposition and resuspension of fluid mud on the western Louisiana inner shelf. Gulf Coast Assoc Geol Soc Trans. 53(2203):722–731.

Russell RJ, Russell RD. 1939. Mississippi River Delta sedimentation. Recent marine sediments, Vol 10. Tulsa (OK): Am Assoc Pet Geol.p. 153–177.

Ruttenberg KC, Goni MA. 1997 Phosphorus distribution, C:N:P ratios, and delta C-13(oc) in arctic, temperate, and tropical coastal sediments: Tools for characterizing bulk sedimentary organic matter. Mar Geol. 139(1–4):123–145.

Sahin C, Safak I, Sheremet A, Mehta AJ. 2012. Observations on cohesive bed reworking by waves: Atchafalaya shelf, Louisiana. J Geophys Res Oceans. 117(C9):C09025. https://doi.org/10.1029/2011JC007821

Schapery RA, Dunlap WA. 1978. Prediction of storm-induced sea bottom movement and platform forces. Paper presented at: 10th Annual Offshore Technology Conference, 8–11 May, Houston, Texas. Paper No.: OTC-3259-MS.

Schultheiss P, Holland M, Roberts J, Huggett Q, Druce M, et al. 2014. PCATS: Pressure core analysis & transfer system. Poster. Accessed through http://www.geotek.co.uk/services/pressure_core_analysis on December 5, 2014.

Seed HB, Rahman MS. 1978. Wave-induced pore pressure in relation to ocean-floor stability of cohesionless soils. Mar Geotechnol. 3(2): 123–150.

Shepard FP. 1955. Delta-front valleys bordering the Mississippi distributaries. Geol Soc Am Bull. 66(12): 1489–1498.

Shephard LE, Bryant WR, Dunlap WA. 1978. Consolidation characteristics and excess pore water pressures of Mississippi Delta sediments. 10th Annual Offshore Technology Conference, 8–11 May, Houston, Texas. OTC-3167-MS. Houston (TX): Proc Offshore Technol Conf.

Simpson RH, Sugg AL, Clark GB, Frank NL, Hope JR, et al. 1970. The Atlantic hurricane season of 1969. Mon Weather Rev. 98(4):293–306.

Slingerland R, Driscoll NW, Milliman JD, Miller SR, Johnstone EA. 2008. Anatomy and growth of a Holocene clinothem in the Gulf of Papua. J Geophys. Res. Earth Surf. (2003–2012):113.

Smith JE, Bentley SJ, Courtois AJ, Obelcz J, Chaytor JD, et al. 2017. Facies-dependent variations in sediment physical properties on the Mississippi River Delta front, USA: evidence for depositional and post-depositional processes. Paper presented at: American Geophysical Union Fall Meeting, 11–15 December 2017, New Orleans, Louisiana.

Sommerfield CK, Nittrouer CA. 1999. Modern accumulation rates and a sediment budget for the Eel shelf: a flood-dominated depositional environment. Mar Geol. 154:227–241.

Sommerfield CK, Nittrouer CA, Alexander CR. 1999. 7Be as a tracer of flood sedimentation on the northern California continental margin. Cont Shelf Res. 19:335–361.

Son-Hindmarsh, R., Ploessel, M. R., and Hughson, A. A. 1984. Time-lapse high-resolution seismic surveys in the Mississippi Delta mudflow area, offshore Louisiana. Annual Offshore Technology Conference, 7–9 May, Houston, Texas. OTC-4754-MS.

Stark TD, Eid HT. 1997. Slope stability analyses in stiff fissured clays. J Geotech Geoenviron Eng. 123(4):335–343.

Stegmann S, Sultan N, Kopf A, Apprioual R, Pelleau P. 2011. Hydrogeology and its effect on slope stability along the coastal aquifer of Nice, France. Mar Geol. 280(1–4):168–181.

Stegmann S, Sultan N, Pellau P, Apprioual R, Carziglia S, et al. 2012. A long-term monitoring array for landslide precursors: a case study at the Ligurian Slope (Western Mediterranean Sea). 48th Annual Offshore Technology Conference, 30 April–3 May, Houston, Texas. Houston (TX): Proc Offshore Technol Conf. p. 1-10.

Sterling GH, Strohbeck EE. 1973. The failure of the South Pass 70 "B" platform Hurricane Camille. 5th Annual Offshore Technology Conference, Vol. 2.29 April–2 May, Houston, Texas. Houston (TX): Proc Offshore Technol Conf. p. 719–730.

Suhayda JN. 1986. Interaction between surface waves and muddy bottom sediments. In: Mehta AJ, ed. Estuarine Cohesive Sediment Dynamics: Proceedings of a Workshop on Cohesive Sediment Dynamics with Special Reerence to Physical Processes in Estuaries, Tampa, Florida, November 12–14, 1984. Berlin (DE): Springer/Verlag. p. 401–428.

Suhayda JN. 1977. Surface-waves and bottom sediment response. Mar Geotechnol. (2):135–146.

Suhayda JN, Prior DB. 1978. Explanation of submarine landslide morphology by stability analysis and rheological models. 10th Offshore Technology Conference. 8–11 May, Houston, Texas. Proc Offshore Technol Conf. Vol 2. Ms. 3171.

Suhayda JN, Whelan III T, Coleman JM, Booth JS, Garrison LE. 1976. Marine sediment instability: Interaction of hydrodynamic forces and bottom sediments. Paper presented at: Offshore Technology Conference, Houston, Texas, May 3–6, 1976. Paper No.: OTC-2426-MS.

Sultan N, Voisset M, Marsset B, Marsett T, Cauquil E, et al. 2007. Potential role of compressional structures in generating submarine slope failures in the Niger delta. Mar Geol. 237 (2007): 169–190.

Swarzenski PW, Campbell PL, Osterman LE, Poore RZ. 2008. A 1000-year sediment record of recurring hypoxia off the Mississippi River; the potential role of terrestrially-derived organic matter inputs. Mar Chem. 109(1–2): 130–142.

Syvitski JPM, Kettner AJ, Overeem I, Hutton EWH, Hannon MT, et al. 2009. Sinking deltas due to human activities. Nat Geosci. 2(10): 681–686.

Talling PJ, Allin J, Armitage DA, Arnott RW, Cartigny MJ, et al. 2015. Key future directions for research on turbidity currents and their deposits. J. Sediment. Res. 85(2), 153–169.

Taggart MS, Kaiser AD. 1960. Clay mineralogy of Mississippi River deltaic sediments. Geol Soc Am Bull. 71(5): 521–530.

Teague WJ, Jarosz E, Wang DW, Mitchell DA. 2007. Observed oceanic response over the upper continental slope and outer shelf during Hurricane Ivan. J Phys Oceanog. 37(9):21812206.

Terzaghi K. 1956. Varieties of submarine slope failures. Proceedings of the Eighth Texas Conference on Soil mechanics and foundation engineering. Austin, Texas, 14–15 September 1956. Austin (TX): University of Texas.

Terzaghi K, Peck RB, Mesri G. 1996. Soil mechanics in engineering practice. 3rd ed. New York (NY): John Wiley.

Thomson J, Garrett M, Taylor M, George T, Melancon M, Behrens K. 2005 Sonar surveys for pipeline inspection show extent of pipeline displacement and seafloor instability following Hurricane Ivan. Paper presented at: Offshore Technology Conference, Houston, Texas, May 2005. Paper No.: OTC-17738-MS.

Tornqvist TE, Kidder TR, Autin WJ, van der Borg K. 1996. A revised chronology for Mississippi River subdeltas. Science. 273(5282): 1693.

Tornqvist TE, Wallace DJ, Storms JEA, Wallinga J, van Dam RL, Blaauw M, Derksen MS, Klerks CJW, Meijneken C, Snijders EMA. 2008. Mississippi Delta subsidence primarily caused by compaction of Holocene strata. Nature Geosci. 1(3): 173–176.

Tripsanas EK, Bryant WR, Phaneuf BA. 2004. Slope-instability processes caused by salt movements in a complex deep-water environment, Bryant Canyon area, northwest Gulf of Mexico. Am Assoc Petrol Geol Bull. 88(6): 801–823.

Tripsanas EK, Bryant WR, Prior DB, Phaneuf BA. 2003. Interplay between salt activities and slope instabilities, Bryant Canyon area, Northwest Gulf of Mexico. In: Locat J, Mienert J, Boisvert L (editors). Submarine mass movements and their consequences: 1st international symposium. Volume 19. The Netherlands: Springer Science. p. 307–315.

United States Army Corp of Engineers (USACE). 2004. Louisiana Coastal Area (LCA), Louisiana—Ecosystem restoration study, final report. New Orleans (LA): US Army Corps of Engineers.

US Geological Survey and University of Colorado. 2006. GMX_EXT: usSEABED EXTracted data for the entire U.S. Gulf of Mexico and Caribbean (Puerto Rico and U.S. Virgin Islands). http://pubs.usgs.gov/ds/2006/146/data/gmx_ext.zip , http://pubs.usgs.gov/ds/2006/146/htmldocs/data_cata.htm

US Geological Survey (USGS). 2014a. USGS Earthquakes Hazard Program, ANSS comprehensive earthquake catalog (ComCat). accessed August 15, 2014: http://earthquake.usgs.gov/earthquakes/search/

US Geological Survey (USGS). 2014b. National seismic hazards map, conterminous US (PGA, 2% in 50 yrs). accessed August 15, 2014: http://earthquake.usgs.gov/hazards/products/conterminous/

Vörösmarty CJ, Syvitski J, Day J, de Sherbinin A, Giosan L, Paola C. 2009. Battling to save the world's river deltas. Bull At Sci. 65(2): 31–43.

Walsh JP, Nittrouer CA. 2009. Understanding fine-grained river-sediment dispersal on continental margins. Mar Geol. 263(1–4)34–45.

Walsh JP, Wiberg PL, Aalto R, Nittrouer CA, Keuhl SA. 2015. Source-to-sink research: Economy of the Earth's surface and its strata. Earth-Sci Rev. 153 (February 2016):1–6.

Walsh JP, Corbet D, Mallison D, Goni M, Dail M, et al. 2006. Mississippi Delta mudflow activity and 2005 Gulf hurricanes. Eos. 87(44):477–478.

Wang D, Mitchell DA, Teague WJ, Jarosz E, Hulbert MS. 2005. Extreme waves under Hurricane Ivan. Science. 309(5736): 896–896.

Wang Z, Jia Y, Liu X, Wang D, Shan H, et al. 2017. In situ observation of storm-wave-induced seabed deformation with a submarine landslide monitoring system. Bull Eng Geol Environ. 77(3): 1091–1102. DOI 10.1007/s10064-017-1130-4.

Wang DW, Mitchell, DA, Teague WJ, Jarosz E, Hulbert MS. 2005. Extreme waves under Hurrican Ivan. Science. 309(5736):896.

Wang H, Liu HJ. 2016. Evaluation of storm wave-induced silty seabed instability and geo-hazards: A case study in the Yellow River delta. Appl Ocean Res. (58):135–145.

Warner JC, Armstrong B, He R, Zambon JB. 2010. Development of a coupled ocean-atmosphere-wave-sediment transport (COAWST) modeling system. Ocean Modell. 35(3): 230–244.

Watkins DJ, Kraft LM. 1978. Stability of continental shelf and slope off Louisiana and Texas: Geotechnical aspects. In: Bouma AH, Moore GT, Coleman JM (eds). Beyond the shelf break. New Orleans (LA): Am Assoc Petrol Geol short course. p. B1–B34.

Whelan III T, Coleman JM, Suhayda JN, Garrison LE. 1975. The geochemistry of recent Mississippi River Delta sediments: gas concentration and sediment instability. Paper presented at: Offshore Technology Conference, Houston, Texas, May 1975. Paper No.: OTC-2342-MS.

Whelan III T, Coleman JM, Robert HH, Suhayda JN. 1976. The occurrence of methane in recent deltaic sediments and its effect on soil stability. Bull Int Assoc Eng Geol. (14): 55–64.

Whelan III T, Coleman JM, Suhayda JN, Robert HH. 1977. Acoustical penetration and shear strength in gas-charged sediment. Mar Geotechnol. 2(1–4): 147–159.

Wiseman WJ, Dinnel SP. 1988. Shelf currents near the mouth of the Mississippi River. J Phys Oceanogr. 18(9): 1287–1291.

Wright L, Coleman JM. 1973. Variations in morphology of major river deltas as functions of ocean wave and river discharge regimes. AAPG Bulletin. 57:370–398.

Wright LD, Coleman JM. 1974. Mississippi River mouth processes - Effluent dynamics and morphologic development. J Geol. 82:751–778.

Wright L, Friedrichs C, Kim S, Scully M. 2001. Effects of ambient currents and waves on gravity-driven sediment transport on continental shelves. Mar Geol. 175:25-45.

Wright LD, Friedrichs CT. 2006. Gravity-driven sediment transport on continental shelves: A status report. Cont Shelf Res. 26(17–18): 2092–2107.

Wright LD, Nittrouer CA. 1995. Dispersal of river sediments in coastal seas - 6 contrasting cases. Estuaries. 18(3): 494–508.

Wright LD, Swaye FJ, Coleman JM. 1970. Effects of Hurricane Camille on the landscape of the Breton-Chandeleur Island Chain and the eastern portion of the Lower Mississippi Delta. Baton Rouge (LA): Louisiana State University. Technical Report 76. Reprinted from Coastal Studies Bulletin No. 4.

Wright LD, Wiseman WJ, Yang ZS, Bornhold BD, Keller GH, et al. 1990. Processes of marine dispersal and deposition of suspended silts off the modern mouth of the Huanghe (Yellow River). Cont Shelf Res. 10(1):1–40.

Wright LD, Yang ZS, Bornhold BD, Keller GH, Prior DB, et al. 1986. Hyperpycnal plumes and plume fronts over the Huanghe (Yellow-River) Delta Front. Geo-Mar Lett. 6(2):97–105.

Wright SG. 1976. Analyses for wave induced sea-floor movements. Paper presented at: Offshore Technology Conference, Houston, Texas, May 1976. Paper No.: OTC-2427-MS.

Wright SG, Dunham RS. 1972. Bottom stability under wave induced loading. Paper presented at: Offshore Technology Conference, Houston, Texas, April 1972. Paper No.: OTC-1603-MS.

Wu L, Ortiz CP, Jerolmack DJ. 2017. Aggregation of elongated colloids in water. Langmuir. 33(2): 622–629. doi: 10.1021/acs.langmuir.6b03962.

Xu K, Harris CK, Hetland RD, Kaihatu JM. 2011. Dispersal of Mississippi and Atchafalaya sediment on the Texas-Louisiana shelf: Model estimates for the year 1993. Cont Shelf Res. (31):1558–1575. doi:10.1016/j.csr.2011.05.008

Xu K, Mickey RC, Chen Q, Harris CK, Hetland RD, et al. 2015. Shelf sediment transport during hurricanes Katrina and Rita. Comp Geosci. 90(B)24–39.

Xu JP, Sequieros OE, Noble MA. 2014. Sediment concentrations, flow conditions, and downstream evolution of two turbidity currents, Monterey Canyon, USA. Deep-Sea Res I. (89): 11–34.

Xu GH, Liu ZQ, Sun YF, Wan X, Lin L, Ren YP. 2016. Experimental characterization of storm liquefaction deposits sequences. Mar Geol. (382):191–199.

Yang HF, Yang SL, Xu KH, Wu H, Shi B, et al. 2017. Erosion potential of the Yangtze Delta under sediment starvation and climate change. Sci Rep. (7) article no.10535. doi: 10.1038/s41598-017-10958-y.

Young DR. 2014. Examination of the 2011 Mississippi River flood deposit on the Louisiana Continental Shelf (thesis). Greenville (NC): East Carolina University.

Zhang S, Jia Y, Zhang Y, Shan H. 2018. Influence of seepage flows on the erodibility of fluidized silty sediments: parameterization and mechanisms. J Geophys Res Oceans. 123(5):3307–3321. doi: 10.1002/2018JC01380

Additional References

Ai, F, Strasser M, Preu B, Hanebuth TJJ, Krastel S, et al. 2014. New constraints on oceanographic vs. seismic control on submarine landslide initiation: a geotechnical approach off Uruguay and northern Argentina. Geo-Mar Let. 34: 300–427.

Arnold KE. 1967. Soil movements and their effects on pipelines in the Mississippi Delta Region [thesis]. New Orleans (LA): Tulane University.

Arpe K, Leroy SAG. 2009. Atlantic hurricanes–testing impacts of local SSTs, ENSO, stratospheric QBO-implications for global warming. Quat Int. 195:4–14.

Atigh E, Byrne PM. 2004. Liquefaction flow of submarine slopes under partially undrained conditions; an effective stress approach. Can Geotech J. 41(1):154–165.

Austin D, Carriker B, McGuire T, Pratt J, Priest T, et al. (Louisiana State University, Baton Rouge, LA). 2008. History of the offshore oil and gas industry in southern Louisiana: volume I: papers on the evolving offshore industry. 272 p. New Orleans (LA): US Department of the Interior, Minerals Management Service. Contract No.: 1435-01-02-CA-85169 . Report No.: OCS Study MMS 2008-042.

Badalini G, Redfern J, Samuel A, Heath R, Burley S, et al. 2004. Slope channel evolution; near-surface depositional processes inferred from 3D seismic data, offshore Nile Delta, Egypt. AAPG Abstracts. [accessed 27 July 2021]; https://www.searchanddiscovery.com/abstracts/html/2004/annual/abstracts/Badalini.htm

Bea, RG. 1998. Reliability characteristics of a platform in the Mississippi River Delta. J Geotech Geoenviron Eng. 124(8):729–738.

Bea RG. 2006. Reliability and human factors in geotechnical engineering. J Geotech Geoenviron Eng. 132(5):631–643.

Bea RG, Audibert JME, Lai NW, Schafer D. 1980. An assessment of facilities siting–South Pass blocks 42/43. In: Folger DW, Hathaway JC, eds. Conference on Continental Margin Mass Wasting and Pleistocene Sea-Level Changes, August 13–15, Woods Hole, Massachesetts. Reston (VA): U.S. Geological Survey. Circular 961. p. 9.

Bea RG, Aurora RP. 1983. Design of pipelines in mudslide areas, J Petro Technol. 35(11): 1985–1995. [accessed 12 July 2021]; https://doi.org/10.2118/12343-PA

Bennett RH, Bryant WR, Keller GH. 1978. Clay fabric and geotechnical properties of selected submarine sediment cores from the Mississippi Delta. 95 p. Rockville (MD): National Oceanic and Atmospheric Administration.

Bennett RH, Faris JR. 1979. Ambient and dynamic pore pressures in fine-grained submarine sediments: Mississippi Delta:. Appl Ocean Res. 1(3):115–123.

Best AI, Clayton CRI, Longva O, Szuman M. 2003. The role of free gas in the activation of submarine slides in Finneidfjord. In: Locat J, Mienert J, Boidvert L, eds. Submarine mass movements and their consequences, 1st International Symposium. Dordrecht (NL): Springer. p. 491–498. [accessed 21 July 2021]; https://doi.org/10.1007/978-94-010-0093-2

Blumberg R. 1974. Hurricane winds, waves and currents test marine pipeline design. Pipeline Industry. June-November. n.p.

Booth JS. 1979. Recent history of mass-wasting on the upper continental slope, northern Gulf of Mexico, as interpreted from the consolidation states of the sediment. In: Geology of continental slopes. SEPM Society for Sedimentary Geology, vol. 27. Tulsa (OK): Society of Economic Paleontologists and Mineralogists. p. 153–164. [accessed 1 July 021]; doi.org/10.2110/pec.79.27.0153

Bornhold BD, Yang ZS, Keller GH, Prior DB, Wiseman WJ, et al. 1986. Sedimentary framework of the modern Huanghe (Yellow-River) Delta. Geo-Mar Let. 6(2): 77–83.

Brooks JM, Sackett WM. 1973. Sources, sinks, and concentrations of light hydrocarbons in the Gulf of Mexico. J Geophys Res. 78(24):5248–5258.

Brothers DS, Luttrell KM, Chaytor JD. 2013, Sea-level-induced seismicity and submarine landslide occurrence. Geology. 41(9):979–982.

Brown LA, Bracci JM, Huste MB, Murff JD (Texas A&M University, College Station, TX). 2003. Assessment of seismic risk for subsea production systems in the Gulf of Mexico, Final Report. 165 p. New Orleans (LA): US Department of the Interior, Minerals Management Service. Cooperative Agreement No.: 1435-01-00-CA-31003.

Bryn P, Solheim A, Berg K, Lien R, Forsberg C, et al. 2003. The Storegga Slide Complex; repeated large scale sliding in response to climatic cyclicity. In: Locat J, Mienert J, Boidvert L, eds. Submarine mass movements and their consequences, 1st International Symposium. Dordrecht (NL):Springer. p. 215–222.

Buczkowski BJ, Reid JA, Jenkins CJ, Reid JM, Williams SJ, et al. 2006. usSEABED: Gulf of Mexico and Caribbean (Puerto Rico and U.S. Virgin Islands) offshore surficial sediment data release. US Geological Survey Data Series 146. 50 p. Reston (VA): US Department of the Interior, US Geological Survey.

Butterworth PJ, Moursy A, Ramadan I, Austin BJ, Cook P, et al. 2006. Pliocene and Holocene mass transport deposits of the west Nile Delta, Egypt [abstract]. In: Annual Convention of the American Association of Petroleum Geologists, "Perfecting the Search, Delivering on Promises." Houston, Texas, 9–12 August, 2006. Vol. 2. Red Hook (NY): Curran. p. 601–602.

Cardone VJ, Cox AT (Ocewanweather, Inc., Stamford, CT). 2003. MMS Hindcast Study of Hurricane Lili (2002) Offshore Northern Gulf of Mexico, final report. 67 p. New Orleans (LA): US Department of the Interior, Minerals Management Service. Technology Assessment Program Project 467. [accessed 28 July 2021]; https://www.bsee.gov/research-record/tap-467-hindcast-study-winds-waves-and-currents-n-gom-hurricane-lili-2002

Cardone VJ, Cox AT, Lisaeter KA, Szabo D. 2004. Hindcast of winds, waves and currents in Northern Gulf of Mexico in Hurricane Lili (2002). In: Proceedings of the Offshore Technology Conference, Held in Houston, Texas, 30 April–3 May 2007.OTC 18652. Houston (TX): Offshore Technology Conference. [accessed 28 July 2021]; DOI:10.4043/18652-MS

Chouinard LE, Liu C. 1997. Model for recurrence rate of hurricanes in Gulf of Mexico. J Waterw Coastal Ocean Eng. 123(3):113–119.

Chouinard LE, Liu C, Cooper CK. 1997. Model for severity of hurricanes in Gulf of Mexico. J Waterw Coastal Ocean Eng. 123(3):120–129.

Christian HA, Woeller DJ, Robertson OK, Courtney RC. 1997. Site investigations to evaluate flow liquefaction slides at Sand Heads, Fraser River delta. Can Geotech J. 34(3):384–397.

Coleman JM, Prior DB. 1988. Mass wasting on continental margins. Annu Rev Earth Planet Sci. 16:101–121.

Coleman JM, Prior DB, Adams Jr CE. 1981. Erosional furrows on continental shelf edge, Mississippi delta region. Geo-Mar Lett. 1:11–15.

Coleman JM, Roberts HH. 1988. Sedimentary development of the Louisiana continental shelf related to sea level cycles: Part I, sedimentary sequences. Geo-Mar Lett. 8(2):63–108.

Coleman JM, Roberts HH. 1988. Sedimentary development of the Louisiana continental shelf related to sea level cycles; Part II, seismic response. Geo-Mar Lett. 8(2):109–119.

Cox AT, Cardone VJ, Counillon F, Szabo D. 2005. Hindcast study of winds, waves, and currents in Northern Gulf of Mexico in Hurricane Ivan (2004). Paper presented at: Offshore Technology Conference, Houston, Texas, May 2005. Paper No.: OTC-17736-MS.

Dagg MJ, Bianchi T, McKee B, Powell R. 2008. Fates of dissolved and particulate materials from the Mississippi river immediately after discharge into the northern Gulf of Mexico, USA, during a period of low wind stress. Cont Shelf Res. 28(12):1443–1450.

Dalrymple RA, Liu PLF. 1978. Waves over soft muds: A two-layer fluid model. J Phys Oceanogr. 8(6):1121–1131.

De Blasio FV, Elverhøi A, Issler D, Harbitz CB, Bryn P, et al. 2005. On the dynamics of subaqueous clay rich gravity mass flows—the giant Storegga slide, Norway. Mar Pet Geol. 22(1–2):179–186.

De Blasio R, Elverhøi A, Issler D, Harbitz CB, Bryn P, et al. 2004. Flow models of natural debris flows originating from overconsolidated clay materials. Mar Geol. 213(1–4):439–455.

Dengler AT, Wilde P, Noda EK, Normark WR. 1984. Turbidity currents generated by Hurricane Iwa. Geo-Mar Lett. 4(1):5–11.

DiMarco SF, Kelly FJ, Zhang J, Guinasso Jr NL. 1995. Directional wave spectra on the Louisiana-Texas shelf during Hurricane Andrew. J Coast Res. (Spring): 217–233.

Dingle RV. 1977 The anatomy of a large submarine slump on a sheared continental margin (SE Africa). J Geol Soc (London, UK). 134 (3): 293–310.

Dixon JF, Steel RJ, Olariu C. 2013. A model for cutting and healing of deltaic mouth bars at the shelf edge; mechanism for basin-margin accretion. J Sediment Res. 83(3):284–299.

Dott Jr RH. 1963. Dynamics of subaqueous gravity depositional processes. Am Assoc Petrol Geol Bull. 47(1): 104–128.

Doyle EH, McClelland B, Ferguson GH. 1971. Wire-line vane probe for deep penetration measurements of ocean sediment strength. Paper presented at: Offshore Technology Conference, April 1971, Houston, TX. Paper No.: OTC-1327-MS.

Driscoll NW, Karner GD. 1999. Three-dimensional quantitative modeling of clinoform development. Mar Geol. 154(1–4);383–398.

Driscoll NW, Weissel JK, Goff JA. 2000. Potential for large-scale submarine slope failure and tsunami generation along the U.S. Mid-Atlantic coast. Geology. 28(5)407–410.

Dubois KD, Lee D, Veizer J. 2010. Isotopic constraints on alkalinity, dissolved organic carbon, and atmospheric carbon dioxide fluxes in the Mississippi River. J Geophys Res Biogeosci. 115(G2). [accessed 14 July 2021]; DOI:10.1029/2009JG001102.

Dunlap W, Holcombe L, Holcombe T (Texas A&M University). 2004. Shear strength maps of shallow sediments in the Gulf of Mexico. New Orleans (LA): US Department of the Interior, Minerals Management Service. MMS/OTRC Cooperative Research Agreement 1435-01-99CA-31003, Task Order 17007, Project 367.

Dunlap WA. 1981. Geotechnical applications in soft sediments. In: Bouma A, Sangrey D, Coleman J, Prior D, Trippet A, et al., eds. Offshore geologic hazards: a short course presented at Rice University, May 2–3, 1981 for the Offshore Technology Conference. Vol. 18. Tulsa (OK: American Association of Petroleum Geosciences. p. 2.3–2.41.

Earle MD. 1975. Extreme wave conditions during Hurricane Camille. J Geophys Res. 80(3):377–379.

Ebbesmeyer CC, Williams GN, Hamilton RC, Abbott CE, Collhpp, et al. 1982. Strong persistent currents observed at depth off the Mississippi River Delta. Paper presented at: Offshore Technology Conference, May 1982, Houston, Texas. Paper No.: OTC-4322-MS.

Edmonds DA, Slingerland RL. 2009. Significant effect of sediment cohesion on delta morphology. Nature Geosci. 3:105–109.

Ellwood BB, Balsam EL, Roberts HH. 2006. Gulf of Mexico sediment sources and sediment transport trends from magnetic susceptibility measurements of surface samples. Mar Geol. 230(3–4):237–248.

Energo Engineering, Inc. (Houston, Texas). 2006, Assessment of fixed offshore platform performance in Hurricanes Andrew, Lili, and Ivan: final report. 121 p. Herndon (VA): US Department of the Interior, Minerals Management Service. MMS Project No.: 549.

Energo Engineering, Inc. (Houston, Texas). 2007. Assessment of fixed offshore platform performance in Hurricanes Katrina and Rita: final report. 186 p. Herndon (VA): US Department of the Interior, Minerals Management Service. MMS Project No.: 578.

Esposito CR, Georgiou IY, Kolker AS. 2013. Hydrodynamic and geomorphic controls on mouth bar evolution. Geophys Res Lett. 40(8):1540–1545.

Fine, IV, Rabinovich AB, Bornhold BD, Thomson RE, Kilikov EA. 2005. The Grand Banks landslide-generated tsunami of November 18, 1929: preliminary analysis and numerical modeling. Mar Geol. 215(1–2): 45–47.

Fisk HN, McClelland B. 1959. Geology of continental shelf off Louisiana: its influence on offshore foundation design. Geol Soc Am Bull. 70(10):1369–1394.

Forristall GZ. 2007. Comparing hindcasts with wave measurements from Hurricanes Lili, Ivan, Katrina and Rita. 10th International Workshop on Wave Hindcasting and Forecasting and Coastal Hazard Symposium, Oahu, HI, November 11–16. [accessed 28 July 2021]; https://www.researchgate.net/publication/254137124_COMPARING_HINDCASTS_WITH_WAVE_MEASUREMENTS_FROM_HURRICANES_LILI_IVAN_KATRINA_AND_RITA

Forristall GZ. 2007. Wave crest heights and deck Ddmage in Hurricanes Ivan, Katrina, and Rita. Paper presented at: Offshore Technology Conference, Houston, Texas, April 2007. Paper No.: OTC-18620-MS.

Galloway WE. 2002. Cenozoic deepwater reservoir systems of the northern Gulf of Mexico basin. Trans Gulf Coast Assoc Geol Soc. 86(1):192–193.

Galloway WE, Ganey-Curry PE, Li X, Buffler R. 2000. Cenozoic depositional history of the Gulf of Mexico basin. AAPG Bull. 84(11):1743–1774.

Gauer P, Elverhoi A, Issler D, DeBlasio FV. 2006. On numerical simulations of subaqueous slides: Back-calculations of laboratory experiments of clay-rich slides. Norw J Geol. 86(3):295–300.

Gauer P, Kvalstad TJ, Forsberg CF, Bryn P, Berg K. 2005 The last phase of the Storegga Slide: simulation of retrogressive slide dynamics and comparison with slide-scar morphology. Mar Pet Geol. 22(1–2):171–178.

Goni MA, Ruttenberg KC, Eglinton TI. 1997. Source and contribution of terrigenous organic carbon to surface sediments in the Gulf of Mexico. Nature. 389(6648):272–278.

Gould HR. 1970. The Mississippi Delta Complex. Soc Econ Paleontol Mineral. In: Morgan JP, Shaver RH, eds. Delatic sedimentation, modern and ancient. SEPM Society for Sedimentary Geology, vol. 15. Tulsa (OK): Society of Economic Paleontologists and Mineralogists. p. 3–30.

Grymes III JM, Stone GW. 1995. A review of key meteorological and hydrological aspects of Hurricane Andrew. J Coast Res. (Spring): 6–23.

Hance JJ. 2003. Development of a database and assessment of seafloor slope stability based on published literature [thesis]. Austin (TX): University of Texas at Austin.

Helwick SJ, Bryant WR. 1978. Geotechnical characteristics of Mississippi Delta sediments, southeast Louisiana. Mar Geotechnol. 3(2):183–198.

Hemphill T, Campos W, Pilehvari A. 1993. Yield-power law model more accurately predicts mud rheology. Oil Gas J. 91(34):45–50.

Hilbe MJ, Anselmetti FS, Eilertsen R, Hansen L. 2008. Subaquatic morphology in a perialpine fjord-type lake; shaped by glaciers, mass movements, delta sedimentation and human impact. Proceedings of the 33rd International Geological Congress, Oslo, Norway, 6–14 August 2008. 8 vols. Red Hook (NY): Curran Associates. p. 2532.

Hitchcock C, Givier R, Angell M, Hooper J. 2006. A pilot study for regionally consistent hazard susceptibility mapping of submarine mudslides. Paper presented at: Offshore Technology Conference, May 2006, Houston, Texas. Paper No.: OTC-18323-MS.

Hooper JR. 1981. Soil properties and case histories of structure siting in delta mudflows: section 6. In: Bouma A, Sangrey D, Coleman J, Prior D, Trippet A, et al., eds. Offshore geologic hazards: a short course presented at Rice University, May 2–3, 1981, for the Offshore Technology Conference. Vol. 18. Tulsa (OK): American Association of Petroleum Geosciences. p.6.3.

Howes NC, FitzGerald DM, Hughes ZJ, Georgiou IY, Kulp MS, et al. 2010. Hurricane-induced failure of low salinity wetlands. Proc Natl Acad Sci USA. 107(32):14014–14019.

Hsiao SV, Shemdin OH. 1980. Interaction of ocean waves with a soft bottom. J Phys Oceanogr. 10(4): 605–610.

Il-Ju M, Ginis I, Tetus H, Tolman HL, Wright CW, et al. 2003. Numerical simulation of sea surface directional wave spectra under hurricane wind forcing. J Phys Oceanogr. 33(8):1680.

Ilstad T, De Blasio FV, Elverhøi A, Harbitz CB, Engvik L, et al. 2004. On the frontal dynamics and morphology of submarine debris flows. Mar Geol. 213(1–4):481–497.

Imran J, Harff P, Parker G. 2001. A numerical model of submarine debris flows with graphical user interface. Comput Geosci. 27(6):717–729.

Imran J, Parker G, Locat J, Lee H. 2001. 1D numerical model of muddy subaqueous and subaerial debris flows. J Hydraul Eng. 127(11):99–968.

Jibrin BW, Reston TJ, Westbrook GK. 2013. Seismic-derived seabed topography; insights from the outer fold and thrust belt in the deep-water Niger Delta. Leading Edge. 32(4):420–423.

Johns MW, Bryant WR, Dunlap WA (Texas A&M University, College Station, TX). 1985. Geotechnical properties of Mississippi River delta sediments utilizing in situ pressure sampling techniques. 113 p. New Orleans (LA): US Department of the Interior, Minerals Management Service. Contract No.: 14-12-0001-G-709. Report No.: MMS 85-0047.

Johns WD, Grim RE. 1958. Clay mineral composition of recent sediments from the Mississippi River Delta. J Sediment Petrol. 28(2):186–199.

Jordi A, Wang DP. 2008. Near-inertial motions in and around the Palamos submarine canyon (NW Mediterranean) generated by a severe storm. Cont Shelf Res. 28:25233–2534.

Kaiser MJ. 2008. The impact of extreme weather on offshore production in the Gulf of Mexico. Appl Math Modell. 32(10):1996–2018.

Keen TR, Glenn SM. 1999. Shallow water currents during Hurricane Andrew. J Geophys Res C: Oceans. 104(C10):23443–23458.

Keim BD, Muller RA, Stone GW. 2007. Spatiotemporal patterns and return periods of tropical storm and hurricane strikes from Texas to Maine. J Clim. 20(14):3498–3509.

Khalil SM, Finkl CW, Roberts HH, Raynie RC. 2010. New approaches to sediment management on the inner Continental Shelf offshore coastal Louisiana. J Coast Res. 26(4):591–604.

Khan NS, Horton BP, McKee KL, Jerolmack D, Falcini F, et al. 2013. Tracking sedimentation from the historic A.D. 2011 Mississippi River flood in the deltaic wetlands of Louisiana, USA. Geology. 41(4):391–394.

Kindinger JL. 1988. Seismic stratigraphy of the Mississippi-Alabama shelf and upper continental slope. Mar Geol. 83(1–4):79–94.

Kindinger JL. 1989. Depositional history of the Lagniappe Delta, northern Gulf of Mexico. Geo-Mar Lett. 9(2):59–66.

Kindinger JL, Bouma AH, 1981. Single-channel, high-resolution seismic data from six areas of the northern Gulf of Mexico continental slope. 2 p. Reston (VA): US Geological Survey. Open-file Report 81-400. [accessed 15 July 2012]; https://doi.org/10.3133/ofr81400

Kindinger JL, Miller RJ, Stelting CE, Bouma AH. 1982. Depositional history of Louisiana-Mississippi outer continental shelf. Reston (VA): US Geological Survey. Open-file Report 82-1077. [accessed 15 July 2012]; https://doi.org/10.3133/ofr821077

KindingerJL, Penland S, Williams SJ, Suter JR. 1989. Inner shelf deposits of the Louisiana-Mississippi-Alabama region, Gulf of Mexico. Trans Gulf Coast Assoc Geol Soc. 39:41–420.

Kindinger JL, Stelting CE, Miller RJ. 1982. High-resolution seismic data and bathymetric, gravimetric, and magnetic data from the northern Gulf of Mexico collected during R/V *Gyre* cruise G-81-6. 10 p. Reston (VA): US Geological Survey. Open File Report 82-842. [accessed 19 July 2021]; https://doi.org/10.3133/ofr82842

King S, Cartwright JA. 2010. Mass transport deposits and their role in thin skinned tectonics; an example from the NW Niger Delta. AAPG Datapages. [accessed 28 July 2021]; https://www.searchanddiscovery.com/pdfz/abstracts/pdf/2010/annual/abstracts/ndx_king2.pdf.html

Kostaschuk RA, McCann SB. 1989. Submarine slope stability of a fjord delta; Bella Coola, British Columbia. Géogr Phys Quat. 43(1):87–95.

Kraft Jr LM, Suhayda JN, Helfrich SC, Marin JE. 1990. Ocean wave attenuation due to soft seafloor sediments. Mar Geotechnol. 9(3):227–242.

Kuehl SA, Levy BM, Moore WA, Allison MA. 1997. Subaqueous delta of the Ganges-Brahmaputra river system. Mar Geol. 144(1–3): 81–96.

Kujau A, Nürnberg D, Zielhofer C, Bahr A, Röhl U. 2010. Mississippi River discharge over the last ~560,000 years—Indications from X-ray fluorescence core-scanning. Paleogeog Palaeoclimatol Palaeoecol. 298(3–4): 311–318.

Kvalstad TJ, Andresen L, Forsberg CF, Berg K, Bryn, et al. 2005. The Storegga slide: evaluation of triggering sources and slide mechanics. Mar Pet Geol. 22(1–2):245–256.

Lee H, Locat J, Dartnell P, Israael K Wong F. 1999. Regional variability of slope stability: application to the Eel margin, California. Mar Geol. 154(1–4):305–321.

Lee HJ. 2009. Timing of occurrence of large submarine landslides on the Atlantic Ocean margin. Mar Geol. 264(1–2):53–64.

Lee HJ, Edwards BD. 1986. Regional method to assess offshore slope stability. J Geotech Eng. 112:489–509.

Lee HJ, Schwab WC, Edwards BD, Kayen RE. 1991. Quantitative controls on submarine slope failure morphology. Mar Geotechnol. 10(1–2):143–157.

Leroueil S, Locat J, Levesque C, Lee HJ. 2003. Towards an approach for the assessment of risk associated with submarine mass movements. In: Locat J, Mienert J, Boisvert L, eds. Submarine mass movements and their consequences. Dordrecht (NL): Springer. p. 59–67.

Leroueil S, Vaunat J, Picarelli L, Locat J, Lee HJ, et al. 1996. Geotechnical characterization of slope movements. Paper presented at Landslides International Symposium, Trondheim, Norway.

Lewis KB. 1971. Slumping on a continental slope inclined at 1°–4°. Sedimentol. 16(1/2): 97–110.

Lin Z, Yang Z, Bornhold BD. 1995. Instability of the subaqueous delta slope of the modern Huang He. Mar Geol Quat Geol. 15(3):11–23.

Liu JP, Milliman JD, Gao S, Cheng P. 2004. Holocene development of the Yellow River's subaqueous delta, North Yellow Sea. Mar Geol. 209(1–4):45–67.

Locat J, Lee H, ten Brink U, Twichell D, Geist E, Sansoucy M. 2009. Geomorphology, stability and mobility of the Currituck slide. Mar Geol. 264(1–2):28–40.

Locat J, Lee HJ. 2002. Submarine landslides: advances and challenges. Can Geotech J. 39:193–212.

Loncke L, Gaullier V, Droz L, Ducassou E, Migeon S, et al. 2009. Multi-scale slope instabilities along the Nile deep-sea fan, Egyptian margin; a general overview. Mar Pet Geol. 26(5):633–646.

Lowe DR. 1979. Sediment gravity flows; their classification and some problems of application to natural flows and deposits. Soc Econ Paleon Mineralog. 27:75–82.

Ludwick JC. 1964. Sediments in northeastern Gulf of Mexico. In: Miller RL, ed. Papers in marine geology, Shepard commemorative volume. New York (NY): Macmillan. p. 204–238.

Lykousis V, Chronis G. 1989. Mass movements, geotechnical properties, and slope stability in the outer shelf-upper slope, northwestern Aegean Sea. Mar Geotechnol. 8(3):231–247.

Masson DG, Harbitz CB, Wynn RB, Pedersen G, Lovholt F. 2006. Submarine landslides; processes, triggers and hazard prediction. Philos Trans Royal Soc London, Ser A. 364(1845):2009–2039.

Mazzullo JM, Bates C. 1985. 1985, Sources of Pleistocene and Holocene sand for the Northeast Gulf of Mexico shelf and the Mississippi Fan. Trans Gulf Coast Assoc Geol Soc. 35:457–465.

McAdoo BG, Pratson LF, Orange DL. 2000. Submarine landslide geomorphology, US continental slope. Mar Geol. 169(1–2):103–136.

McBride RA. 1995. Surficial sediments and morphology of the southwestern Alabama/western Florida Panhandle coast and shelf. Trans Gulf Coast Assoc Geol Soc. 45:393–404.

McClelland B. 1955. Foundation characteristics of late Quaternary clays offshore near modern Mississippi delta (Louisiana). Econ Geol Bull Soc Econ Geol. 50(7):787–787.

McClelland B. 1967. Progress of consolidation in delta front and prodelta clays of the Mississippi River. In: Richards, AF, ed. Proceedings of International Resesarch Conference on Marine Geotechnique. Urbana (IL): U Illinois P. p. 22–33.

McGregor BA. 1981. Smooth seaward-dipping horizons–an important factor in sea-floor stability? Mar Geol. 39(3–4): M89–M98.

Mikos M, Cetina M, Brilly M. 2004. Hydrologic conditions responsible for triggering the Stoze landslide, Slovenia. Eng Geol. 73(3–4):193–213.

Milliman JD, Syvitski JPM. 1992. Geomorphic tectonic control of sediment discharge to the ocean - the importance of small mountainous rivers. J Geol. 100(5):525–544.

Miner MD, Kulp MA, FitzGerald DM, Flocks JG, Weathers HD. 2009. Delta lobe degradation and hurricane impacts governing large-scale coastal behavior, south-central Louisiana, USA. Geo-Mar Lett. 29(6):441–453.

Miner MD, Kulp MA, FitzGerald DM, Georgious IY. 2009. Hurricane-associated ebb-tidal delta sediment dynamics. Geology. 37(9):851–854.

Mohrig D, Elverhoi A, Parker G. 1999. Experiments on the relative mobility of muddy subaqueous and subaerial debris flows, and their capacity to remobilize antecedent deposits. Mar Geol. 154(1–4):117–129.

Mohrig D, Whipple KX, Hondzo M, Elis C, Parker G. 1998. Hydroplaning of subaqueous debris flows. Geol Soc Am Bull. 110(3):387–394.

Morton RA. 1993. Attributes and origins of ancient submarine slides and filled embayments; examples from the Gulf Coast Basin. AAPG Bull. 77(6):1064–1081.

Mostafa YE, El Naggar MH. 2006. Effect of seabed instability on fixed offshore platforms. Soil Dyn Earthquake Eng. 26(12):1127–1142.

Mulder T, Cochonat P. 1996. Classification of offshore mass movements. J Sediment Res. 66(1):43–57.

Muller RA, Stone GW. 2001. A climatology of tropical storm and hurricane strikes to enhance vulnerability prediction for the Southeast U.S. coast. J Coast Res. 17(4):949–956.

Murray SP. 1970. Bottom currents near the coast during Hurricane Camille. J Geophys Res. 75(24):4579–4582.

Nemec W, Steel RJ, Gjelberg J, Collinson JD, Prestholm E, et al. 1988. Exhumed rotational slides and scar infill features in a Cretaceous delta front, eastern Spitsbergen. Polar Res. 6(1):105–112.

Neurauter TW, Bryant WR. 1989. Gas hydrates and their association with mud diapir/mud volcanoes on the Louisiana Continental Slope. Paper presented at: Offshore Technology Conference, Houston, Texas, May 1989. Paper No.: OTC-5941-MS. [accessed 28 July 2021]; https://doi.org/10.4043/5941-MS

Niper E, Williams G. 1977. Project SEASWAB: Real-time acquisition/reduction of submarine sediment data. Paper presented at: Offshore Technology Conference, Houston, TX, May 1977. Paper No.: OTC-2867-MS. [accessed 28 July 2021]; https://doi.org/10.4043/2867-MS

Nodine MC, Wright SG, Gilbert RB. (Texas Engineering Experiment Station, College Station, TX). 2006. Mudslides during Hurricane Ivan and an assessment of the potential for future mudslides in the Gulf of Mexico. New Orleans (LA): US Department of the Interior, Minerals Management Service. TAP Project No. 552. [accessed 28 July 2021]; https://www.bsee.gov/research-record/tap-552-mudslides-during-hurricane-ivan-and-assessment-potential-future-mudslides

Normark WR, Wilde P, Campbell JF, Chase TE, Tsutsui B. 2002. Submarine slope failures initiated by Hurricane Iwa, Kahe Point, Oahu, Hawaii. In: Schwab WC, Lee HJ, Twichell DC, eds. Submarine landslides: selected studies in the U.S. Exclusive Economic Zone. Bulletin 2002. Washington (DC): US Geological Survey. p. 197–204.

Odonne F, Callot P Debroas E-J, Sempere T, Hoareau G, et al. 2011. Soft-sediment deformation from submarine sliding; favourable conditions and triggering mechanisms in examples from the Eocene Sobrarbe Delta (Ainsa, Spanish Pyrenees) and the Mid-Cretaceous Ayabacas Formation (Andes of Peru). Sediment Geol. 235(3–4);234–248.

Oliveira CMM, Hodgson DM, Flint SS. 2011. Distribution of soft-sediment deformation structures in clinoform successions of the Permian Ecca Group, Karoo Basin, South Africa. Sediment Geol. 235(3–4):314–330.

Panchang VG, Dongcheng L. 2006. Large waves in the Gulf of Mexico caused by Hurricane Ivan. Bull Am Meteorol Soc. 87(4):481–489.

Patterson MM. 1974. Oceanographic data from Hurricane Camille. Paper presented at: Offshore Technology Conference, Houston, TX, May 1974. Paper No.: OTC-2109-MS. [accessed 28 July 2021]; https://doi.org/10.4043/2109-MS

Pickrill RA, Irwin J. 1983. Sedimentation in a deep glacier-fed lake; Lake Tekapo, New Zealand. Sedimentol. 30(1):63–75.

Piper DJW, Mormark WR. 2009. Processes that initiate turbidity currents and their influence on turbidites: a marine geology perspective. J Sediment Res. 79(5–6):347–362.

Pisarska-Jamrozy M, Weckworth P. 2013. Soft-sediment deformation structures in a Pleistocene glaciolacustrine delta and their implications for the recognition of subenvironments in delta deposits. Sedimentol. 60(3):637–665.

PMB Engineering, Inc. (San Francisco, CA), 1993. Hurricane Andrew effects on offshore platforms. 151 p. New Orleans (LA): US Department of the Interior, Minerals Management Service. TAP Project No.: 210. [accessed 29 July 2021]; https://www.bsee.gov/research-record/tap-210-hurricane-andrew-effects-offshore-platforms

Porebski SJ, Steel RJ. 2003. Shelf-margin deltas; their stratigraphic significance and relation to deepwater sands. Earth-Sci Rev. 62(3–4):283–326.

Postma G. 1984. Slumps and their deposits in fan delta front and slope. Geology. 12(1):27–30.

Postma G. 1986. Classification for sediment gravity-flow deposits based on flow conditions during sedimentation. Geology. 14(4):291–294.

Pratson LF, Nittrouer CA, Wiberg PL, Steckler MS, Swenson JB, et al. 2007. Seascape evolution on clastic continental shelves and slopes. In: Nittrouer CA, Austin JA, Field ME, Kravitz, Syvitski JPM, et al, eds. Continental margin sedimentation: fromsediment transport to sequence stratigraphy. Special publication no. 37. Malden (MA): Blackwell [for International Assoc Sedimentologists]. p. 339–380.

Prior DB, Bornhold BD, Johns MW. 1984. Depositional characteristics of a submarine debris flow. J Geol. 92(6):707–727.

Prior DB, Coleman JM. 1978. Disintegrating retrogressive landslides on very-low-angle subaqueous slopes, Mississippi Delta. Mar Geotechnol. 3(1):37–60.

Prior DB. 1978. Submarine landslides on the Mississippi River delta-front slope. Geosci Man [sic]. 19:41–53.

Prior DB. 1980. Sonograph mosaics of submarine slope instabilities, Mississippi River Delta. Mar Geol. 36(3–4):227–239.

Prior DB, Coleman JM. 1982. Active slides and flows in underconsolidated marine sediments on the slopes of the Mississippi Delta. In: Saxov S, Nieuwenhuis JK, eds. Marine slides and other mass movements. NATO Conference Series, vol 6. Boston (MA): Springer. p. 21–49.

Prior DB, Coleman JM, Bornhold BD. 1982. Results of a known seafloor instability event. Geo-Mar Lett. 2(3–4):117–122.

Prior DB, Coleman JM, Garrison LE. 1979. Digitally acquired undistorted side-scan sonar images of submarine landslides, Mississippi River delta. Geology. 7(9):423–425.

Prior DB, Coleman JM, Garrison LE. 1981. Geologic mapping for offshore engineering, Mississippi Delta. Paper presented at: Offshore Technology Conference, Houston, TX, May 1981. Paper No.: OTC-4119-MS. [accessed 28 July 2021]; https://doi.org/10.4043/4119-MS

Prior DB, Coleman JM, Suhayda JN, Garrison LE. 1981. Subaqueous landslides as they affect bottom structures. In: Bouma A, Sangrey D, Coleman J, Prior D, Trippet A, et al., eds. Offshore geologic hazards: a short course presented at Rice University, May 2–3, 1981 for the Offshore Technology Conference. Vol. 18. Tulsa (OK): American Associastion of Petroleum Geologists. p. 5.112–115.

Prior DB, Wiseman WJ, Gilbert R. 1981. Submarine slope processes on a fan delta, Howe Sound, British Columbia. Geo-Mar Lett. 1(2):85–90.

Prior DB, Yang ZS, Bornhold BD, Keller GH, Lu NZ, et al. 1986. Active slope failure, sediment collapse, and silt flows on the modern subaqueous Huanghe (Yellow-River) Delta. Geo-Mar Lett. 6(2):85–95.

Puskar FJ, Ku AP, Sheppard RE. 2004. 2004, Hurricane Lili's impact on fixed platforms and calibration of platform performance to API RP 2A. Paper presented at: Offshore Technology Conference, Houston, TX, May 2004. Paper No.: OTC-16802-MS.

Puskar FJ, Spong RE, Ku AP, Gilbert RB, Choi YJ. 2006 Assessment of fixed offshore platform performance in Hurricane Ivan. Paper presented at: Offshore Technology Conference, Houston, TX, May 2006. Paper No.: OTC-18325-MS.

Roberts HH. 1984. Sedimentology of mudflow deposits in Mississippi River delta-front environment. AAPG Bull. 68(4):521–522.

Rodriguez AB, Hamilton MD, Anderson JB. 2000. Facies and evolution of the modern Brazos Delta, Texas: wave versus flood influence. J Sediment Res. 70(2):283–295.

Roesink JG, Weimer P, Bouroullec R. 2004. Sequence stratigraphy of Miocene to Pleistocene sediments of east-central Mississippi Canyon, northern Gulf of Mexico. Trans Gulf Coast Assoc Geol Soc. 54:587–601.

Rogers KG, Goodbred Jr SL. 2010. Mass failures associated with the passage of a large tropical cyclone over the Swatch of No Ground submarine canyon (Bay of Bengal). Geology. 38(11):1051–1054.

Rosenbauer RJ, Swarzenski PW, Kendall C, Orem WH, Hostettler FD, et al. 2009. A carbon, nitrogen, and sulfur elemental and isotopic study in dated sediment cores from the Louisiana Shelf. Geo-Mar Lett. 29(6):415–429.

Rosenthal W. 1978. Energy exchange between surface waves and motion of sediment. J Geophys Res. 83(C4):1980–1982.

Rossi A, Massei N, Laignel B, Sebag D, Copard Y. 2009. The response of the Mississippi River to climate fluctuations and reservoir construction as indicated by wavelet analysis of streamflow and suspended sediment load, 1950-1975. J Hydrol. 377(3–4):237–244.

Sager WW, Schroeder WW, Davis KS, Rezak R. 1999. A tale of two deltas; seismic mapping of near surface sediments on the Mississippi-Alabama outer shelf and implications for recent sea level fluctuations. Mar Geol. 160(1–2):119–136.

Sampere TP, Bianchi TS, Allison MA. 2011. Historical changes in terrestrially derived organic carbon inputs to Louisiana continental margin sediments over the past 150 years. J Geophys Res. 116(G1): np. [accessed 19 July 2021]; https://doi.org/10.1029/2010JG001420.

Samuel A, Kneller B, Raslan S, Sharp A, Parsons C. 2003. Prolific deep-marine slope channels of the Nile Delta, Egypt. AAPG Bull. 87(4):541–560.

Shepard FP. 1956. Marginal sediments of Mississippi Delta. AAPG Bull. 40(11):2537–2623.

Sheremet A, Mehta AJ, Liu B, Stone GW. 2005. Wave-sediment interaction on a muddy inner shelf during Hurricane Claudette. Estuarine Coast Shelf Sci. 63(1–2):225–233.

Sheremet A, Stone GW. 2003. Observations of nearshore wave dissipation over muddy sea beds. J Geophys Res. 108(C11):np. [accessed 19 July 2021]; https://doi.org/10.1029/2003JC001885

Stone GW, Grymes JM, Dingler JR, Pepper DA. 1997. Overview and significance of hurricanes on the Louisiana coast, USA. J Coastal Res. 13(3):656–669.

Stone GW, Stapor Jr FW. 1996. A nearshore sediment transport model for the northeast Gulf of Mexico coast, U.S.A. J Coastal Res. 12(3):786–793.

Stone, GW, Walker ND, Hsu SA, Babin A, Liu B, et al. 2005. Hurricane Ivan's impact along the northern Gulf of Mexico. Eos. 86(48):497–501.

Stone GW, Wang P, Pepper DA, Grymes III JM, Roberts HH, et al. 1999. Studying the importance of hurricanes to the northern Gulf of Mexico Coast. Eos. 80(27):301–308.

Stone GW, Xu JP, Zhang X. 1995. Estimation of the wave field during Hurricane Andrew and morphological change along the Louisiana coast. J Coastal Res. Special Issue No. 21. (Spring): 234–253.

Sultan N, Cochonat P, Canals M, Cattaneo A, Dennielou B, et al. 2004. Triggering mechanisms of slope instability processes and sediment failures on continental margins: a geotechnical approach. Mar Geol. 213(1–4):291–321.

Suter JR, Berryhill HL. 1985. Late Quaternary shelf-margin deltas, northwest Gulf-of-Mexico. AAPG Bull. 69(1):77–91.

Sydow J, Roberts HH. 1994. Stratigraphic framework of a Late Pleistocene shelf-edge delta, northeast Gulf-of-Mexico. APPG Bull. 78(8):1276–1312.

Talling PJ. 2014. On the triggers, resulting flow types and frequencies of subaqueous sediment density flows in different settings. Mar Geol. 352(1 June):155–182.

Teague WJ, Jarosz E, Carnes MR, Mitchell DA, Hogan PJ. 2006. Low-frequency current variability observed at the shelfbreak in the northeastern Gulf of Mexico: May-October, 2004. Cont Shelf Res. 26(20):2559–2582.

Trabant P, Bryant WR, Dunlap W. 1979. Shallow-submarine seismic stratigraphy, Mississippi River delta front [abstract]. AAPG Bull. 63(3):542.

Trabant PK. 1979. Submarine geomorphology and geology of the Mississippi River delta front. Paper presented at the Offshore Technology Conference, Houston, TX. April 1979. Paper No.: OTC-3572-MS.

Trefry JH, Metz S, Nelsen TA, Trocine RP, Eadie BJ. 1994. Transport of particulate organic-carbon by the Mississippi River and its fate in the Gulf of Mexico. Estuaries. 17(4):839–849.

Tripsanas EK, Bryant WR, Phaneuf BA. 2004. Slope-instability processes caused by salt movements in a complex deep-water environment, Bryant Canyon area, northwest Gulf of Mexico. AAPG Bull. 88(6):801–823.

Tripsanas EK, Bryant WR, Prior DB, Phaneuf BA. 2003. Interplay between salt activities and slope instabilities, Bryant Canyon Area, northwest Gulf of Mexico. In: Locat J, Mienert J, Boisvert L, eds. Submarine mass movements and their consequences. Dordrecht (NL): Springer. p. 307–315.

Turner RE, Milan CS, Rabalais NN. 2004. A retrospective analysis of trace metals, C, N and diatom remnants in sediments from the Mississippi River delta shelf. Mar Pollut Bull. 49(7–8):548–556.

Twichell D, Pendleton E, Baldwin W, Flocks J. 2009. Subsurface control on seafloor erosional processes offshore the Chandeleur Islands, Louisiana. Geo-Mar Lett. 29:349–358.

Urgeles R, Camerlenghi A. 2013. Submarine landslides of the Mediterranean Sea: trigger mechanisms, dynamics, and frequency-magnitude distribution. J Geophys Res F: Earth Surf. 118(4):2600–2618.

Urlaub M, Talling PJ, Masson DG. 2013. Timing and frequency of large submarine landslides: implications for understanding triggers and future geohazard. Quat Sci Rev. 72:63–82.

van Kessel T, Kranenburg C. 1998. Wave-induced liquefaction and flow of subaqueous mud layers. Coastal Eng. 34(1–2):109–127.

Vaunat J, Leroueil S. 2002. Analysis of post-failure slope movements within the framework of hazard and risk analysis. Nat Hazards. 26(1):83–109.

Det Norske Veritas. 2007. Pipeline damage assessment from Hurricanes Katrina and Rita in the Gulf of Mexico. 106 p. New Orleans (LA): US Department of the Interior, Minerals Management Service. TAP Project No.: 581. Report No. 44814183. [accessed 29 July 2021]; https://www.bsee.gov/research-record/tap-581-pipeline-damage-assessment-hurricane-katrinarita

Walker JR, Massingill JV. 1970. Slump features on Mississippi Fan, northeastern Gulf-of-Mexico. Geol Soc Am Bull. 81(10):3101–3108.

Ward EG. 1974. Ocean data gathering program –n overview. Paper presented at the Offshore Technology Conference, Houston, TX, May 1974. Paper No.: OTC-2108-B-MS.

Weight RWR, Anderson JB, Fernandez R. 2011. Rapid mud accumulation on the central Texas shelf linked to climate change and sea-level rise. J Sediment Res. 81(10):743–764.

Wells JT, Prior DB, Coleman JM. 1980. Flowslides in muds on extremely low-angle tidal flats, northeastern South-America. Geology. 8(6):272–275.

Williams SJ, Flocks J, Jenkins C, Khalil S, Moya J. 2012. Offshore sediment character and sand resource assessment of the Northern Gulf of Mexico, Florida to Texas. J Coast Res. 60(sp1):30–44.

Winn Jr RD, Roberts HH, Kohl B, Fillon RH, Bouma AH, et al. 1995. Latest Quaternary deposition on the outer shelf, northern Gulf of Mexico; facies and sequence stratigraphy from Main Pass Block 303 shallow core. GSA Bull. 107(7):851–866.

Wright LD. 1970. Circulation, effluent diffusion, and sediment transport, mouth of South Pass, Mississippi River Delta. Baton Rouge (LA): Louisiana State University.

Wright LD, Coleman JM. 1971. Effluent expansion and interfacial mixing in presence of a salt wedge, Mississippi River Delta. J Geophys Res. 76(36):8649–8661.

Wright LD, Yang ZS, Bornhold BD, Keller GH, Prior DB, et al. 1986. Short-period internal waves over the Huanghe (Yellow-River) Delta Front. Geo-Mar Lett. 6(2):115–120.

Wright SG (University of Texas at Austin, Austin, TX). 2003. Forum on risk assessment for submarine slope stability: report of a forum held in Houston, Texas,May 10–11, 2002. 40 p. New Orleans (LA): US Department of the Interior, Minerals Management Service. Cooperative Research Agreement 1435-01-99-CA-31003. [accessed 29 July 2021]; https://www.bsee.gov/sites/bsee.gov/files/tap-technical-assessment-program//445aa.pdf

Xu G, Sun Y, Wang X, Hu G, Song Y. 2009. Wave-induced shallow slides and their features on the subaqueous Yellow River delta. Can Geotech J. 46(12):1406–1417.

Xu K, Li A, Liu JP, Milliman JD, Yang Z, et al. 2012. Provenance, structure, and formation of the mud wedge along inner continental shelf o the East China Sea: a synthesis of the Yangtze dispersal system. Mar Geol. 291–294:176–191.

Yeager KM, Santschi PH, Rowe GT. 2004. Sediment accumulation and radionuclide inventories ((super 239,240) Pu, (super 210) Pb and (super 234) Th) in the northern Gulf of Mexico, as influenced by organic matter and macrofaunal density. Mar Chem. 91(1–4):1–14.

Zabel M, Schulz HD. 2001. Importance of submarine landslides for non-steady state conditions in pore water systems; lower Zaire (Congo) deep-sea fan. Mar Geol. 176(1–4):87–99.

Zhang Q, Suhayda JN. 1994. Behavior of marine sediment under storm wave-loading. Mar Georesour Geotechnol. 12(3):259–269.

Appendix A: Future Mississippi River Delta Front Research Plan, A Proposal for Future Research: Submarine Landslides on the Mississippi River Delta Front and the Critical Need for Next Generation Hazard Assessment

References can be found in the Works Cited list following the report Chapter 5.

A.1. Abstract

For decades, evaluation of the hazards presented by submarine landslides on the Mississippi River Delta Front (MRDF) has remained an ongoing objective of the Bureau of Ocean Energy Management (BOEM), the Bureau of Safety and Environmental Enforcement (BSEE), (formerly the Minerals Management Service [MMS]) (Fig. 57), and large knowledge gaps remain. We present a proposal for comprehensive regional observation, monitoring, and modeling of submarine mass wasting processes on the MRDF to develop the next-generation geohazard assessment for the region. Results from the five years of data synthesis (Bentley et al, 2018 [this report]; Maloney et al. 2018) and pilot field study (Keller et al. 2016; Obelcz et al. 2017; Chaytor et al. 2017) (under CA M13AC00013) have informed the details and scope of this plan.

A.1.1 Objectives

- The overarching objective is to develop the next-generation geohazard assessment methodology and map that addresses significant limitations and weaknesses of previous hazard assessments for the region. Our analysis will use results from the following science objectives:
- We will quantify the timing, extent and runout distance, and triggering of mudslide activity by monitoring the seafloor with repeat and rapid-response geophysical surveys and in-situ monitoring.
- We will collect new, regional, high-resolution oceanographic, geophysical, and sediment-core data to characterize oceanographic processes and geomorphic, geologic, and geotechnical heterogeneity across the delta front; this will allow us to update hazard assessments and provide a baseline from which to measure future seafloor change.
- We will develop and test predictive models using cutting-edge theory and approaches, and newly acquired geophysical, geologic, geotechnical, and hydrodynamic data to quantify mudslide hazard susceptibility to support leasing, Outer Continental Shelf (OCS) infrastructure, resource evaluation, and environmental assessments.

A.1.2 Approach and Methods

1. Regional seafloor bathymetric and sub-bottom geophysical mapping using latest sonar technologies to image the seabed and underlying geological features.
2. Repeat and rapid response geophysical mapping to document rates and processes of sediment mass transport processes and rates from extreme events (e.g., hurricanes) to seasonal to decadal timescales.
3. Sediment core collection and analysis using specialized tools for deep penetration, pressurized recovery, and non-destructive testing at seabed pressures to better reveal in-situ physical, rheological, and geochemical properties of sediments, particularly those containing abundant biogenic gas.
4. In-situ monitoring and field measurement using instrument packages deployed on and in the seabed and in the water column to measure temporal patterns in MRDF mudflows and related oceanographic processes governing mudflow activity.

5. Development of a process-based numerical model for prediction of submarine landslides in the MRDF region based on predicted wave forcings and known (and anticipated) geological and geotechnical conditions within the seabed. This model will be based on the first regional geophysical surveys in over 40 years and will include theory to describe important processes that drive landslide generation, but were never incorporated in previous risk assessments. These phenomena include new understanding of non-linear ocean waves, the interactions of gassy sediments with wave forcing, strain softening behavior of soils, and direct simulation of landslide development under a wide range of hurricane conditions, using an approach termed the "Joint Probability Method" that is widely used to predict the analogous problem of maximum hurricane surge on land.

6. Development of a data-driven machine learning model to predict submarine landslides in the MRDF region based on correlation of landslide occurrence with preconditioning and triggering predictors, such as seafloor gradient, sediment gas content, sedimentation rate, and significant wave height. This effort will serve as a parallel and complimentary approach to the process-based modelling described above. Concurrence or disparity between model results will either improve confidence in predicted outcomes or identify shortcomings in model implementation; use of both approaches in tandem will yield better results than using either alone.

A.1.3 The Team

Members are from Louisiana State University (LSU), University of New Orleans (UNO), San Diego State University (SDSU), University of Texas at Austin (UT), Monterey Bay Aquarium Research Institute (MBARI), US Geological Survey (USGS), and Naval Research Laboratory Stennis Space Center (NRL).

A.1.4 Anticipated Outcomes

- A predictive risk map of submarine landslide hazard based on modern theory and data, that will more completely address BOEM needs for the region beyond any previous study;
- A processed-based model that can be applied in the future for the same region with new data, or for other regions of interest, that provides a better understanding of seafloor hazards (the processes themselves) and risks (probability of negative impacts from hazard occurrence); this product will provide a flexible platform and tool suite for future assessment;
- The first comprehensive survey map and data for the MRDF region in over 40 years.
- A probability-based model that is trained on previous instances of submarine slope failure, and predicts future occurrence based on correlation of slope failure with known slope failure predictors described in detail elsewhere in this report. Skill of this model will also improve with future data acquisition, and inaccurate predictions can highlight areas of data deficiency (i.e., intelligently target candidate data collection areas).
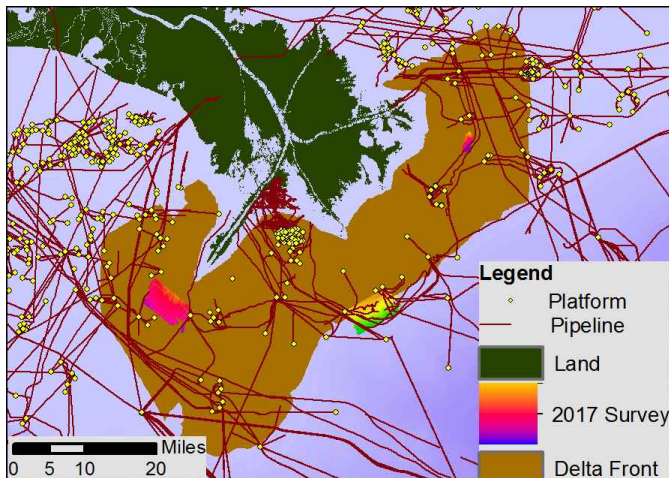
Figure 57. Mississippi River Delta Front platforms and pipelines

Location in the northern Gulf of Mexico of the MRDF (brown), surrounding and offshore from the lower Mississippi Delta (green). Petroleum pipelines, platforms, and the extent of 2017 surveys by LSU and USGS are also shown.

A.2 Background and Relevance to BOEM Issues, Information Needs, and Research Topics

For decades, evaluation of the hazards presented by submarine landslides has remained an ongoing objective of BOEM, and large knowledge gaps remain. We present a proposal for comprehensive regional observation, monitoring, and modeling of submarine mass wasting processes on the Mississippi River delta front (MRDF)(Fig. 57) to develop the next-generation geohazard assessment for the region. Results from the five years of data synthesis (Bentley et al. 2018 [this report]; Maloney et al. 2018) and pilot field study (Keller et al. 2016; Obelcz et al. 2017; Chaytor et al. 2017) (under CA M13AC00013) informed the details and scope of this plan.

A.2.1 BOEM information needs to be addressed

Subaqueous mudflows are known to be ubiquitous across the MRDF and are identified as a hazard to offshore oil and gas infrastructure (Shepard 1955; Bea et al. 1975; Coleman et al. 1980) (Fig. 57). This mudslide-prone area is highly dynamic and patterns of instability are spatially and temporally complex. Catastrophic mass failures occur with passing of each major hurricane, drastically altering the seafloor morphology and damaging or destroying offshore infrastructure. BOEM and industry previously invested considerable resources during the past decade toward better understanding the processes that drive and govern MRDF mudslides. The chief products include Hitchcock et al. (2006), Nodine et al. (2007), and affiliated products prepared by these teams. While each of these hazard assessments provided advancement and benefit, each is flawed by reliance on antiquated data sets from which predictions are made and antiquated theory to guide the predictions. In some cases, more recent research directly contradicts important findings from earlier studies (for example, the role of non-linear waves in driving submarine landslides, discussed below). More recent catastrophic failures and infrastructure loss during hurricanes Ivan (2004) and Katrina (2005) highlight the need for an updated, high-resolution regional bathymetric, geologic, geotechnical, and hazard maps of the MRDF, a modern assessment of hazard potential, and a monitoring program to better support decision making, lease valuation, oil and gas infrastructure, and environmental impacts.

A.2.2 Background

Submarine landslides represent a near-hundred-billion-dollar risk to existing seabed infrastructure offshore of the MRDF. This risk also restricts future development of existing but untapped petroleum resources. The value of risk exposure can be extrapolated from the incomplete cleanup cost of one platform toppled by Hurricane Ivan in 2004. Since Hurricane Ivan in 2004, the Taylor Energy Co. has spent about $450 million to clean up the damage to infrastructure and the environment caused by the toppling of one production platform by a submarine landslide. During Hurricane Ivan alone, at least 17 pipelines and up to 20 other platforms were significantly damaged by submarine landslides. There are many other pipelines and platforms in the landslide hazard zone of the MRDF (Figure 57) and more landslides will happen. The risk is not just to infrastructure, but to our coast and fisheries as well. For example, the Taylor Energy platform lost in 2004 during Hurricane Ivan tore the tops off of 16 oil wells that spilled into the ocean much closer to shore than the Macondo disaster. Such an event could happen again.

The MRDF is an apron of sediment wrapping around the seaward margins of the Mississippi Delta, from water depths of around 10 to 200 meters (30 to 600 feet; Figure 57). Submarine landslides occur widely on the MRDF, and have been documented by surveys since offshore oil exploration began in the 1950s. The last major regional study of submarine landslides occurred in 1977–1981. The last regional hazard assessments were completed in 2006–2007 (Hitchcock et al. 2006; Nodine et al. 2007 and associated

reports by these authors), but were based on seabed measurements from the 1970s–1980s that are now relatively primitive. Seabed data from decades ago are obsolete because even smaller landslides shift hundreds of millions of tons of sediment each year. As a result, both the MRDF seabed, and our technical ability to study it, changed substantially since these decades-old studies. In addition, the 2006–2007 assessments did not incorporate all risk factors now known to be important.

The focus of this MRDF project is to understand the stability of the delta front, which is an area that is characterized by numerous incised gullies and intervening gently sloping seafloor. The MRDF was intensely studied in the 1970s–1980s as it was the site of both geohazards and hydrocarbon development, but major new scientific research in this area is lacking since that time. However, the loss of some oil production platforms during hurricanes in the 2004–2005 seasons resulted in on-going uncontrolled release of oil, which has refocused attention on the geohazard risks of other infrastructure still operating in this area.

The first phase of this MRDF project was to synthesize data and research, much of which focused on the failure mechanisms that resulted in the loss of entire platforms. As part of this effort, repeated swath bathymetric surveys were obtained which revealed that the depth of gullies changes several meters annually as the gullies fill-up with sediment and then drain sediment to compensate (Obelcz et al. 2017). Apparently, the gullies are very active sediment transport conduits and need to be better understood. What was more surprising is that compilation of independently conducted surface ship multi-beam mapping surveys that show the entire seafloor into which the gullies are cut has shifted >500 m downslope since 2001, documented in a Science Magazine article about our work (Ahmad 2017). The extent at which this motion occurs in discrete events or as steady creep is currently unknown, but it is a cause of significant concern given that there are many more platforms and pipelines in this area. Accordingly, there is an important need for in-situ monitoring and field measurement using instrument packages deployed on and in the seabed and in the water column to measure temporal patterns in MRDF mudflows and related oceanographic processes governing mudflow activity.

The scope of this proposed project is broad because the setting is geologically and oceanographically complex. Nevertheless, the chief objective of a new process-based hazard assessment is clear and several key gaps in previous hazard assessments must be filled to reach this objective. The major gaps, but not all gaps, are listed below.

(1) Obsolete seabed data. Previous regional assessments relied upon bathymetric data sets of Coleman et al. (1980), collected in the 1970s. Our most recent publication (Maloney et al. 2018) from data synthesis identified major changes in seabed morphology caused by historical changes in sediment supply. These changes could be influencing spatial and temporal patterns in submarine landslides, but we simply do not know because of the lack of data. New bathymetric and subsurface data are needed. A corresponding gap exists in subsurface information on seabed geotechnical properties and behavior.

(2) Gas bubbles that weaken sediments (from natural methane produced by decay of organic material in sediments). Gas bubbles are abundant in MRDF sediments, and can compress and expand as hurricane waves cross the MRDF, weakening sediment, and triggering landslides (Prior and Suhayda 1978). This potential was identified in the introduction of Nodine et al. (2007), but was never incorporated in hazard assessment. Further, studies of gassy sediments in the MRDF ended in the 1980s and were conducted using methods that could not actually document where and how much gas was present in the sediments. The role of gas in preconditioning sediments for failure is postulated to be significant, *but this hypothesis has never been properly evaluated, and cannot be evaluated without field and lab studies such as those proposed herein*.

(3) How hurricane waves interact with the seabed. Since the early 1970s, storm waves were identified as important triggers of submarine landslides on the MRDF. Wave-seabed mechanics were a key part of the Nodine et al. (2007) hazard assessment, using mathematical descriptions of waves called "linear wave theory" that describe ocean waves as having sinusoidal form. Nodine et al. (2006) proposed that more complex wave theory ("nonlinear wave models") under predicted the forces applied by waves to the

seabed. Our recent research indicates that this is not the case. In particular, Obelcz et al. (2017) shows that more realistic descriptions of wave forms (which are governed by more complicated equations than linear wave theory) apply 30–40% more force to the seabed than do linear waves. This implies that the hazard assessment of Nodine et al. (2006) substantially under predicted the triggering forces of waves on landslides, whether the waves are produced by winter storms or major hurricanes.

(4) Predicting diverse styles of submarine landslides and sediment flows and their impacts. Previous hazard studies of submarine landslides built most of their assessments using highly simplified landslide theory from the 1960s and earlier (such as Henkel, 1970)(Fig. 7) that did not address the complexities, e.g., gassy sediments interacting with storm waves and strain-softening behavior of soils, for example. More advanced theory for sediment transport and submarine landslides now exists that can incorporate more diverse types of failures, happening over different spatial and temporal scales (e.g., Houssais and Jerolmack 2017). A major highlight of our recent research (Obelcz et al. 2017; Chaytor et al. 2017) is that many different styles of submarine landslides occur on the MRDF, and each type of slide moves at different rates over different regions, at times under similar hydrodynamic forcing. Although the most dramatic events are large landslides produced by major hurricanes, slower creep that is not associated with major hurricanes also occurs (Obelcz et al. 2017; Ahmad 2017; Chaytor et al. 2017), which can stress seabed infrastructure such as pipelines. Newer theory is required that can more effectively incorporate diverse forcing to predict different types of sediment slides and flows, in order to effectively predict hazards.

(5) Quantifying the importance of MRDF submarine landslide preconditioning and triggering factors. The preconditioning and triggering factors of MRDF submarine landslides are qualitatively well-constrained, as detailed elsewhere in this report. However, the relative importance of these factors in precipitating slope failure is not quantitatively known, and almost certainly varies both spatially and temporally. Machine learning algorithms (MLAs) have been recently successfully implemented to solve earth science problems, including predicting seafloor porosity based on related predictors (Martin et al. 2015) and developing probabilistic hazard maps for terrestrial landslides (Chen et al. 2017). Properly implemented MLAs can work around complications that typify earth science problems, such as spatially and/or temporally biased data, undersampled parameter spaces, and complex, multivariate systems. MLAs would serve as a complementary, data-driven predictive tool for submarine landslides to validate and augment the process-based modelling proposed in #(4), and would also quantify the importance of MRDF submarine landslide predictors.

As a result, our present understanding of hazard due to submarine landslides is based on incomplete assessment of controlling factors and outdated measurements that were gathered with now-antiquated methods. The high level of uncertainty in our present understanding of hazard is not consistent with the high value of infrastructure and resources in place, and the high cost of possible environmental damage.

We propose to develop a new comprehensive hazard assessment of submarine landslides on the MRDF, based on new seabed maps that we will create, sediment and engineering surveys that we will conduct, and cutting-edge computer models. The models will be newly developed for this project to incorporate modern measurements and understanding of the seabed dynamics, and oceanographic processes like hurricanes that can trigger submarine landslides. The models will allow us to evaluate complex scientific questions related to landslides, such as the interacting roles of soft sediments, creep, gas bubbles, and wave loading in driving landslide motion.

The core proposal-development team led by SU has been working with BOEM's New Orleans office for five years to identify the best approaches to this problem. We have collected and synthesized hundreds of historical studies, and conducted pilot studies in two known MRDF hotspots for landslides (survey areas in Figure 1)(Bentley et al., 2018 [this report]), using cutting-edge field and laboratory measurements, in preparation for this proposal. We have collaborated with the USGS to determine the best seabed mapping and sampling technologies for this complex setting. Our data synthesis has helped us identify knowledge

gaps. Our pilot studies have documented great variability of the seabed, although we have only mapped <10% of the >2,000 km^2 region (see area of 2017 surveys in Figure 57).

We propose a five-year study, funded by BOEM with cost share from the USGS. Project cost will represent a small sum compared to the risk exposure of many platforms and hundreds of kilometers of pipeline, compared to the incomplete-cleanup cost of $450M for Taylor Energy. The proposed project will be a collaboration among LSU, the USGS, SDSU, UNO, UT, Monterey Bay Aquarium Research Institute (MBARI), and NRL. The outcomes of this proposed effort will include a new regional geohazard assessment for submarine landslides based on the most advanced understanding of science and engineering; computer models and ocean monitoring networks that can be used to spur future advancements; and a team of young scientists and engineers (mentored as PhD students and postdocs by this project), trained in these new approaches, to lead this and similar work in the future.

A.3 Objectives and Hypotheses

A.3.1 Objectives

1. We will develop a next-generation geohazard assessment and map that addresses significant limitations and weaknesses of previous hazard assessments for the region. Our analysis will utilized results from the following scientific inputs.
2. We will quantify timing, extent and runout distance, and triggering of mudslide activity by monitoring the seafloor with repeat and rapid response geophysical surveys and in situ monitoring.
3. We will collect new, regional, high-resolution oceanographic, geophysical, and sediment core data to characterize oceanographic processes and geomorphic and geologic heterogeneity across the delta front to update hazard assessments and provide a baseline from which to measure future seafloor change.
4. We will develop and test predictive models using cutting-edge theory and approaches, and newly acquired geophysical and geologic data to quantify mudslide hazard susceptibility to support leasing, OCS infrastructure, resource evaluation, and environmental assessments.

A.3.2 Hypotheses

Hypothesis 1. Based on the declining sediment supply to the MRD and continued marine transport processes, we hypothesize that the delta front has entered a degradational phase, in which seabed erosion will dominate over deposition (and mudflow transport), particularly near areas with the greatest decline in sediment discharge, such as Pass a Loutre and South Pass. Further, based on new developments in our understanding of sediment transport under the combined effects of gravity, waves, and currents (such as coupled effects of storm waves and sediment-gravity flows), we suggest that important sedimentary processes and products identified by earlier studies may be better understood and thus better predicted and their effects mitigated, through our re-evaluation. This hypothesis has in part been validated by our project through publication of Maloney et al. (2018), but that research only addresses a small part of the overall study area.

Hypothesis 2. Based on Henkel (1970) evaluation of wave mechanics and Guidroz (2009) evaluation of wave temporal and spatial variations, with respect to Coleman et al. (1980) morphological characterization of seabed failures on the MRDF, ***we hypothesize that the horizontal scale of the pressure gradient under waves, which is controlled by wave length, wave height, and nonlinear wave properties/theory, is a strong control on the horizontal scale of seabed failures***. This is also supported by the occurrence of smaller failures (collapse depressions and bottleneck slides) near shore, where waves are smaller, and more extensive gullies and lobes in deeper water, where wave length and height are generally greater. The results could improve our ability to assess spatial and temporal scales and distributions of seabed hazards.

Hypothesis 3. The presence of natural gas bubbles within the seabed (produced by the ongoing decay of organic material within deltaic sediments) is an important agent of sediment weakening under cyclic loading from waves, which alters sediment properties and which lowers the threshold for wave-energy triggering of submarine landslides. This concept was first proposed decades ago and has been widely discussed, but has never been incorporated into hazard evaluation.

Hypothesis 4. We hypothesize that, on the MRDF, a semi-continuous range of seabed flow and slide phenomena exist, driven by varying forcing of waves and gravity, and preconditioned by the presence of weak, gas-charged sediments. Styles of flows and slides range from thin and frequent ones created by interaction of fluidized deposits supported by wave turbulence in the near-bed water column, to seabed creep at meters per year spanning meters into the seabed and kilometers of breadth, to rapid, deep, and catastrophic failure under large hurricane waves, mostly driven by pressure gradients under waves. This hypothesis is based on recently developed sediment-transport theory (Houssais and Jerolmack 2017) integrated with our own synthesis of MRDF research, and our recent research supported by BOEM: Keller et al. 2016; Denommee et al. 2017; Obelcz et al. 2017; Chaytor et al. 2017; and Maloney et al. 2018. Although these thinner and slower flows are not likely to be catastrophic in nature, they can nonetheless, stress, bury, or expose seabed infrastructure. This theory has not been previously applied to study or modeling of MRDF sediment dynamics, but this application will be one specific objective of our field, modeling, and data synthesis activities.

A.4 Methods and Analyses

A.4.1 Phase I

Initial data synthesis and testing of methods for this proposed effort began in 2013 with the establishment of Coastal Marine Institute Cooperative Agreement M13AC00013, and is ongoing at the time of this proposal preparation (2018). Results from this effort are described in the Draft Final Report for this project, which accompanies this proposal (Bentley et al. 2018), and are briefly summarized in the introduction to this proposal.

Data synthesis and integration are identified as specific tasks in Phases I–III, and will be essential to project success. Approaches are outlined below in Phase III.

A.4.2 Phase II (Y1–5)

Phase II of this effort will include field, laboratory, modeling research, and data-model integration described below, and lead to Phase III, which will include collection of deep pressurized cores for compositional and geotechnical measurement, continued data-model integration, and development of the hazard map.

A.4.3 Task II.A: seabed mapping

The critical starting point for this proposed work is a new comprehensive geoacoustic survey of the MRDF seabed, imaging seabed conditions and subsurface sediments and strata, to be conducted by the USGS, led by Dr. Jason Chaytor of the USGS Woods Hole campus. The last comprehensive survey was completed in the 1970s and reported by Coleman et al. (1980) and many other subsequent reports and papers. That work was conducted using then-cutting-edge technology (now more than 40 years old), and survey results led to ground-breaking discoveries and new paradigms of understanding. We anticipate that this new survey will also yield ground-breaking insights, considering the technological improvements in the last near half-century. The initial comprehensive survey will be augmented by subsequent monitoring and rapid-response surveys during annual and rapid-response cruises, led by Dr. Kevin Xu (LSU) and Dr. Jillian Maloney (SDSU), using instrumentation similar to that operated by the USGS team (Table 7). The anticipated output from initial mapping and geophysical surveying effort is a high-resolution map of the

modern seafloor and sub-surface geomorphology of the MRDF that provides a consistent framework for evaluating seafloor conditions and guiding subsequent research activities.

Comprehensive Survey, Y1–2. The proposed Comprehensive Survey (Tables 6–7, Figs. 58–59) will use SONAR tools to map the bathymetry, texture, and acoustic properties of the seabed (known as multibeam SONAR), and also the layering of sedimentary strata below the seabed (CHIRP subbottom profiler [Edgetech 512i in Figs. 59A and D]), and low-energy multichannel seismic (MCS) profiler [Fig. 59C], to subbottom depths of more than100m. Example images from data collected in the 2017 Pilot Study are shown in Chapter 4 of this report. The seafloor in Survey Areas A and B have not been systematically mapped in high-resolution and require 100% multibeam bathymetry coverage. CHIRP and MCS data will be co-acquired on each survey line during mapping of Survey Areas A and B. The bulk of the seafloor in Survey Areas C, D, E, and F have been mapped recently with modern multibeam echosounders for NOAA charting purposes, and those data have been provided to our MRDF team (and are illustrated in reduced resolution in Figure 58). The primary survey activity in Survey Areas C, D, E, and F will be high-density CHIRP and MCS data collection, with incidental multibeam bathymetry collection. Several sub-regions in Survey Area C have been the focus of repeat mapping efforts and as such those sub-regions will be re-mapped with 100% coverage as part of the Comprehensive Survey. The total area for combined multibeam bathymetric mapping and subbottom profiling during the Comprehensive Survey is approximately 2,000 km^2. This work will be conducted over two field seasons in Y1 and Y2, using an estimated 60 days of vessel operations, including transit to the field area, mobilization and demobilization, days at sea, and contingency time for weather problems. Likely vessels for this work include the R/V *Pelican* and R/V *Point Sur,* both located along the north-central Gulf Coast.

Table 7. SONAR, seismic, and other systems to be used

| Instrument Name	Application
Reson T20P dual head multibeam echosounder (USGS)	Mapping seabed bathymetry, acoustic properties, and texture
SIG mini-sparker (USGS)	Sound source for subbottom profiling 10s-100s of meters penetration
AA S-Boom (Fig. X.2C) (USGS)	Sound source for subbottom profiling 10s-100s of meters penetration
32-48 channel GeoEel Hydrophone Streamer (USGS)	Acoustic receiver for above sound sources
Edgetech 512i CHIRP (Figs. X.2A and D)(LSU and USGS)	Integrated high resolution subbottom profiling system to 100 meters penetration, m-scale resolution
Edgetech DS2000 Integrated CHIRP and sidescan Fig. X.2B)(LSU)	Very high resolution subbottom profiling system (shallower penetration than 512i but higher resolution), with seabed acoustic reflectance sidescan mapping.
Cavity Ring-down Spectroscopy Sensor (USGS)	Under-way survey of methane water (Fig. 2)
Additional instruments for positioning, motion compensation, and measurement of sound speed in water (LSU and USGS).	
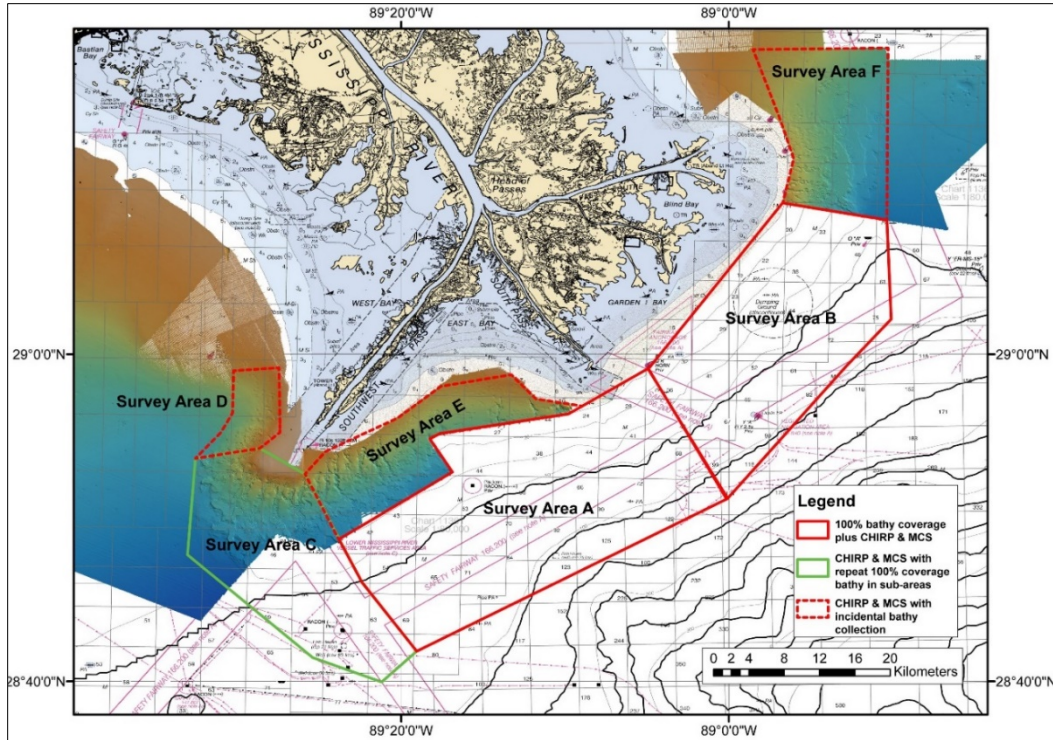
Figure 58. Comprehensive survey areas

Map of survey areas proposed for the USGS comprehensive survey, encompassing the Mississippi River Delta Front.
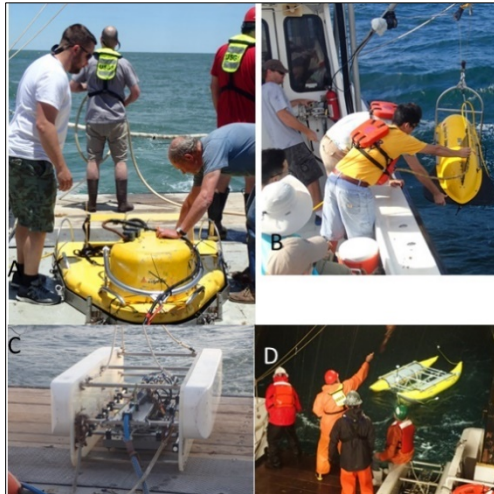
Figure 59. Geophysical instruments

(A) Edgetech 512i subbottom profiler, being serviced by USGS in 2017; (B) Edgetech DS2000 subbottom profiler and/or sidescan mapping SONAR, being deployed; (C) Applied Acoustics S-Boom sound source, prepared for deployment by USGS in 2017; USGS nighttime deployment of Edgetech 512i in 2017.

Table 8. Survey needs for Mississippi River Delta Front survey areas identified in Figure 58

Survey Area	Area (km²)	Primary Survey Needs	Secondary Survey Needs
A	690	- 100% Bathymetry Coverage (≥2 m grid resolution)	

Survey Area	Area (km²)	Primary Survey Needs	Secondary Survey Needs
		- CHIRP - Low-energy multi-channel seismic	
B	510	- 100% Bathymetry Coverage (≥ 2 m grid resolution) - CHIRP - Low-energy multi-channel seismic	
C	350	- CHIRP - Low-energy multi-channel seismic	- Repeat 100% bathymetry coverage over certain sub-areas
D	54	- CHIRP - Low-energy multi-channel seismic	- Bathymetry collection along seismic survey lines only
E	200	- CHIRP - Low-energy multi-channel seismic	- Bathymetry collection along seismic survey lines only
F	230	- CHIRP - Low-energy multi-channel seismic	- Bathymetry collection along seismic survey lines only

Methane Survey. In addition to geoacoustic instrumentation, survey sensors to detect methane in marine waters will be deployed from the survey vessel by co-PI John Pohlman, of the USGS, in conjunction with Chaytor's seabed mapping group. This technology, called "cavity ring-down spectroscopy," (CRDS; Pohlman et al. 2012) has been used to produce continuous map coverage of methane concentrations in marine waters, linked to seabed emissions (Fig. 60). This approach, along with water-column imaging of gas plumes using acoustic techniques, will provide regional coverage that will likely help determine regional distributions of in-seabed natural gas.
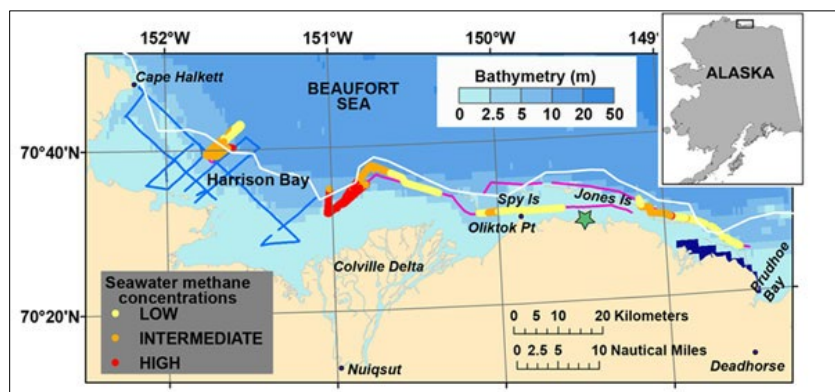

Figure 60. Alaska methane survey

Seawater methane concentrations measured via CRDS offshore of Alaska by Pohlman et al. (2012). Note continuous coverage, as opposed to discrete measurements. Image from US Geological Survey.

Rapid Response and Monitoring Surveys, Y1–5. Additional SONAR seabed mapping will be undertaken as part of annual (or more frequent) research cruises scheduled by the MRDF team, and in the event of major sediment-transport events such as hurricanes, major floods, and reports of potential submarine landslides. This mapping effort will be led by Drs. Xu and Maloney, using SONARs employed in the 2014 Pilot Study (Chapter 3), which are owned by LSU (Edgetech 4600 swath bathymetry and CHIRP subbottom systems [Figs. 59A and B], or similar). The objectives for these surveys will be to document seabed changes resulting from specific events (rapid response) or ongoing seabed motion, such as the creep-like motion documented in the 2014 and 2017 Pilot Studies, and in Obelcz et al. (2017). Small-scale surveys (i.e., 1–2 gullies) may also be collected more frequently during the 1–2 month deployments of optical and acoustic sensors on the seafloor. These frequent surveys would be used to measure seafloor changes associated with any observed signals in hydrodynamic or seafloor turbidity data recorded by the sensors. This information could help assess triggering of seafloor movement (e.g., Clare et al. 2016). On

selected cruises, methane surveys via CRDS will be conducted as well. Likely vessels for this work include the R/V *Pelican* and R/V *Point Sur* (both operated by LUMCON), as well as the R/V *Coastal Profiler*, operated by LSU.

Multibeam data will be processed to provide depth, seabed slope, relative acoustic reflectance, and other derived attributes. These are some of the properties that are used to define different sedimentary environments of the MRDF as described in Chapter 1 (including gullies, lobes, prodelta), as well as the relative potential for submarine landslide hazards. These seabed properties can be used as direct inputs for hazard assessment, such as seabed slope (see Modeling discussion below), or for semi-quantitative measures of seabed stability (sediment accumulation rate as used by Hitchcock et al. 2006). Results from the USGS 2017 Pilot Study (Chaytor et al. 2017)(Figs. 46–48) also suggest that multibeam data can be used to identify locations of gas emissions from the seabed.

Integrated multibeam, subbottom, and core data will be used to develop 3D geomorphic models of the MRDF study area, referenced both geospatially and temporally, such as the examples in Figure 61, which were developed by Xu, Bentley, and Obelcz for other BOEM-funded projects. These 3D models will allow more effective visualization and evaluation of seabed and sediment properties, and their distributions through space and time.
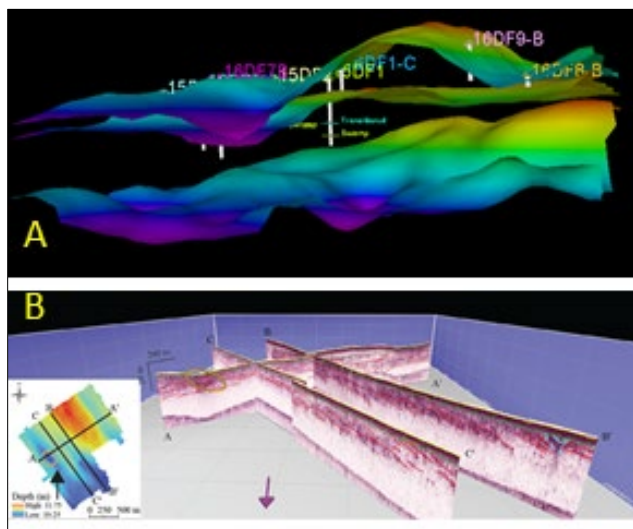

Figure 61. 3D core-geoacoustic models

Examples of data visualization using 3D surfaces and physical properties of cores and fence diagrams of interpreted seismic data collected on Alabama shelf. Both examples are from students of Bentley and Xu, supported by BOEM (Cooperative Agreement M15AC00016). (A) Using Petrel software, core data are superimposed on three surfaces derived from geophysical surveys (top: multibeam bathymetry; middle: a continuous reflector interpolated from CHIRP SONAR; bottom: regional reflector interpreted from multichannel seismic data), adapted from Gonzalez et al. 2017. (B) Fence diagram showing uninterpreted and interpreted CHIRP profiles from Obelcz et al. 2016.

A.3.4 Task II.B: model development

We will develop a comprehensive modeling system to predict seabed motions, from hydrodynamic transporttransport driven by river input, waves, and tides, to large SGFs driven by major hurricane waves, using robust physics in representation of all phenomena. From a geotechnical perspective, we are investigating sediment behavior from a continuum to viscous fluid, where the stress-strain properties control soil softening that eventually transitions to rheological properties for predicting runout lengths. This modeling system will allow us to test complex hypotheses relating diverse physical phenomena, and ultimately allow development of physics-based simulations and statistically sound representations of submarine landslide hazards. Model development will begin in Y1 of the project. Hazard-map development will be concentrated in later project years, and is discussed under Task III below. Two types of modeling will be conducted: regional modeling that encompasses the entire MRDF study area and

beyond, and local models to study wave-seabed interactions using more complex representations of wave motions and mechanics. The regional modeling system will consist of coupled models for atmosphere (especially wind forcing), ocean circulation, waves, and sediment transport, based in part on the Coupled Ocean–Atmosphere–Wave–Sediment Transport (COAWST) Modeling System (Warner et al. 2010). This system is integrated by the Model Coupling Toolkit to exchange data fields between the ocean model ROMS, the atmosphere model WRF, the wave model SWAN, and will provide inputs and boundary conditions to the local models. To model SGFs driven by ocean waves and other factors, a new sediment transport model will be developed and coupled to COAWST, based on newly developed unified theory for sediment transport, as described by Houssais et al. (2015). The local model will consist of coupled hydrodynamics from FLOW3D coupled with our new seabed model. This effort will be led by PIs David Mohrig (UT), Ioannis Georgiou (UNO), and Zuo Xue (LSU) who is affiliated with both Department of Oceanography and Coastal Sciences and the Center for Computation and Technology at LSU.

At this time, regional models like COASWT allow simulation of many complex phenomena interacting over wide regions, but simplifications have been made in ocean wave representation to reduce computational effort. As a result, COAWST cannot for now represent nonlinear wave mechanics that we know to be critical to driving SGFs on the MRDF. In contrast, models such as FLOW3D can simulate nonlinear waves using various theories, but at a very high computational effort, and thus can only be applied over smaller domains, such as a small portion of the MRDF. The smaller MRDF application footprint for FLOW3D also allows us to document transient interactions of wave-induced pressure gradients over distances that cannot be resolved by the regional COASWT model. Accordingly, we will use the regional system for regional simulations, and study local complexities in more detail using the FLOW3D system.

New Sediment Transport Model. We will develop a sediment-transport model for the system building upon recent work with granular flows (Houssais and Jerolmack 2017); this new theory demonstrates how dense granular systems exhibit regime transitions allowing a relatively single-phase rheology (i.e., mud of varying age and water content) to accurately capture sediment transport ranging from dilute suspensions to fast or slow moving mass flows to creep (Houssais and Jerolmack 2017). These models are ideal for the Mississippi River delta front because they predict a material-flow effective friction (or viscosity) that changes with the degree of shear rate and confining pressure, and encompass all of the sediment-transport phenomena that we have described here for the MRDF (thin flows, deep SGFs, creep, and others). This is illustrated in Figure 62, which shows different domains of sediment motion that can be simulated by this theory, ranging from stationary or "jammed" sediment deposits, to creeping deposits (observed by Obelcz et al. 2017 in gullies [Figs. 41 and 42], or 2017 Pilot Study measurements of mudflow lobe creep beneath the wreck of the SS *Virginia*; Figure 47), to rapidly moving mudflows, like those that toppled the MC 20 platform (Fig. 48).
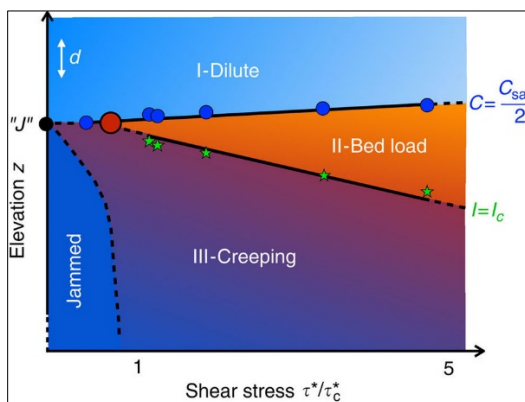

Figure 62. Rheological zones of sediment transport

Domains of sediment transport represented by depth in seabed (vertical axis) and applied shear stress (horizontal axis) from Houssais et al. 2015. The rate of sediment transport is represented as a function of the dimensionless sediment Viscous Number I, which is a ratio of sediment viscosity x shear rate divided by confining pressure. At low shear, motion ceases, or becomes "jammed" (point J), and at progressively higher shear stresses, sediment transport rate increases, and the style of motion changes from creep with little sediment mixing, to more fluidized suspensions (sediment concentration C).

This means that the rheological model will make predictions of properties that we aim to directly measure as part of the field project, providing us with the very real opportunity of using the developing model to help guide design of the field measurement plans and then feed the collected data back into the rheological model for testing and benchmarking. The proposed approach to modeling sediment transport on the delta front has a second distinct advantage in that it operates within the same framework used by physicists to study colloidal suspensions (Houssais et al. 2015). This provides an opportunity to explore floc growth and transport on the delta front by applying methods now being used in soft-matter physics to understand aggregation of colloids in water (Wu et al. 2016), and then efficiently transport this information on floc states into a constitutive relationship for the solid-fluid mixture.

Wave, tide and current measurements will still drive the flow of solids, but by developing rheological descriptions or constitutive relations for the delta front that emphasize motions of grains and grain interactions, we will produce the fullest possible descriptions of the bed state that can then be used to generate the best possible maps of submarine landslide susceptibility on the MRDF.

Prediction of MRDF submarine landslides using data-driven machine learning algorithms (MLAs). We will use various data-driven MLAs (i.e., ones that make relatively few a priori assumptions regarding prediction outcome) to predict the occurrence of existing submarine landslide hotspots, as well as zones of future submarine landslide occurrence. This work will be led by Dr. Jeff Obelcz, our collaborator at NRL. These predictions will be informed by the correlation between submarine landslide occurrence (quantified as depth change between bathymetric surveys) and various preconditioning and triggering factors, such as seafloor slope, presence of biogenic gas, and sedimentation rate. This approach has yielded positive preliminary results as part of the larger NRL seafloor prediction program (Martin et al. 2015). Preconditioning and triggering data will be acquired through a combination of data mining (public repositories, industry collaboration) and new data acquisition included in this proposal. The advantage of using this approach are numerous:

1) it is relatively computationally inexpensive,

2) it "sidesteps" the complexity of physical interactions that govern submarine slope stability,

3) it leverages existing data and benefits from future data acquisition, and

4) it test the predictive skill of (and is tested by) parallel physics-based modelling efforts described above.

A.3.5 Task II.C: seabed sampling and measurement

SONAR and seismic imaging of MRDF sediments allows mapping of sediment volumes and morphology, but not physical properties that control seabed dynamics. Geoacoustic data must be augmented with physical samples and measurements of seabed geological and geotechnical properties, and their changes in time. To this end, multiple types of spatial and temporal field measurements will be performed to study the mechanisms triggering mudflows as well as the magnitude of mudflow movement in both gullies and lobes of MRDF, including geotechnical, hydrodynamics, sediment dynamics and mudflow movements. This effort will be led by Dr. Jafari (LSU, geotechnical measurement), Dr. Xu (LSU, hydrodynamics), Dr. Paull (MBARI, seabed motion studies), and Dr. Bentley (LSU, piston core and multicore collection and analysis). These field operations will be conducted in conjunction with annual and rapid-response mapping efforts, using vessels such as the R/V *Pelican* and R/V *Point Sur* (both operated by LUMCON), as well as the R/V *Coastal Profiler*, operated by LSU.

Geotechnical Measurements and Field Monitoring The laboratory and field geotechnical measurements will be led by CoPI Jafari and will be focused on evaluating the stress-strain-strength-permeability relationships for monotonic and cyclic loadings and for saturated and partially saturated (gassy) soils.

These tests will be performed on non-pressurized core samples so the behavior of gassy soils will have to be evaluated through laboratory inoculation to generate methane gas bubbles in the soil matrix (Nageswaran 1983). The drained shear strength of saturated MRDF soils will be evaluated using the torsional ring shear apparatus (Stark and Eid 1997). This test will provide the peak and residual drained friction angle for normally consolidated soils. The compressibility and permeability of saturated soils at very low effective stresses will be obtained using settling column tests as described in the USACE engineering manual for confined dredged disposal (USACE EM 1110-2-5027). The settling column tests will be instrumented with pore pressure transducers in addition to acoustic sensors and bender elements and X-ray imaging to determine bulk density. The acoustic sensors and bender elements provide a means to determine the sediment concentration (i.e., void ratio) at zero effective stress, which defines the transition of sedimentation to soil consolidation. The time-dependent monitoring of pore pressure coupled with bulk density measurements will be used with the program Primary Consolidation, Secondary Compression, and Desiccation of Dredged Fill (PSDDF; Jafari et al. 2018a, 2018b) to back-calculate the compressibility and permeability relationships. The stress-strain properties of saturated soil will be determined using standard triaxial compression experiments consolidated at Ko and sheared under drained conditions. By determining the saturated effective stress properties, first order limit equilibrium and finite element analyses can be performed to determine the factor of safety at baseline conditions, e.g., only hydrostatic pore-water pressures. Factor of safety (F) in this case is defined as $F = c/\tau$, where c = undrained shear strength, and τ = shear stress. From this starting point, the stability model will become more complex by adding excess pore-water pressures due to self-weight consolidation, time-dependent pore pressure generation and dissipation due to wave loading, sediment softening due to creep, and gas generation and migration.

Dynamic properties of MRDF sediment are relevant to better understand the potential for pore-pressure generation with depth due to non-linear wave loadings. To achieve this objective, resonant column and cyclic triaxial tests will be performed to define the shear modulus relationship from low to large strains. These experiments will define the degradation of shear modulus as plastic strains accumulate due to cyclic forcings, which will be subsequently used in finite element models to simulate the progressive failure of the seabed. The effect of gas concentrations will be incorporated for monotonic and cyclic testing by using methods such as Nageswaran (1983). This will allow a better understanding on to what extent gas bubbles affect the stress-strain-strength properties of MRDF samples and hence impact the seabed stability. These experiments will be complimentary to the pressurized core testing to be performed by CoPI Peter Fleming at the University of Texas at Austin.

Multiple contributing factors are reported to induce submarine landslides, but waves created by energetic events are considered the root mechanism leading to MRDF submarine landslides (Coleman et al. 1998). A passing wave can cause compression and dilation of gas bubbles which generates excess pore-pressures and weakens the seabed strength, and can induce vertical and horizontal motions of the seabed which further remolds the sediments. Thus in situ fluid and/or gas pore pressure is one of the fundamental parameters required for assessing the strength and stability of sediment. Though analytical and numerical methods are available to predict pore pressures, a direct measurement is the best approach to obtain reliable pore pressures, and thus establish the effective stress state in the soil in addition to the total stress state.

Two basic approaches are available that provides sufficient accuracy of pore pressure measurements for geotechnical analysis: (1) short term dissipation tests using a cone penetrometer or piezoprobe; and (2) long term monitoring through piezometers. Piezometers installed in shallow to deep waters (e.g., 10–80 m deep) will be the focus of this project because they can reveal the temporal trends and magnitude of excess pore pressures at depths relevant to seabed mobility in the MRDF. Questions that will be answered regarding pore pressures include

(1) what is the pore pressure at specific depths, or what is the pore pressure profile;

(2) is free gas present in target layers, or are there indications of significant gas migration;

(3) are pore pressures changing over time, indicating a process like slope instability or gas migration?

For the MRDF, though not an exhaustive list, factors influencing pore pressures that will be evaluated include stable v. unstable areas, wave loading in shallow waters, presence of gas v. no gas, self-weight consolidation to define underconsolidated soils, and response in gullies v. lobes.

The piezometers developed at IFREMER Brest in cooperation with the French company nke Instrumentation are described herein as a starting point for pore pressure measurements in the MRDF. The IFREMER piezometer is a modular free-fall device composed of a 60 mm diameter rod and an upper, recoverable system of weights, power supply, and data acquisition (Sultan et al. 2007). The 60 mm diameter rod consists of sensor packages located between single rod segments (0.75 m or 1.5 m in length). As a result, individual layers of interest could be accommodated for by using this modular design. Stegmann et al. (2011) indicate the absolute length of the rod is limited to about 12 m. The sensor package includes a pore water pressure sensor (resolution of ±0.2 kPa) and temperature transducer. Pore water pressure is measured differentially, which couples the pore water pressure in the sediment of each level with the open seawater, i.e., hydrostatic reference. Stegmann et al. (2011) used two piezometer configurations during their field study. In the first configuration (PZ1), the pressure transducers for each port are installed at the top of the instrument and are connected via tubing to the corresponding pore water pressure port along the rod depth. The second configuration (PZ2) improved upon PZ1 by installing the pressure transducer with each port, i.e., the transducer was incorporated into the piezo-module. In both cases, the hydrostatic pressure (sea level and waves) line carries open flow of seawater through the inside cylinder of the rod. Saturation was accomplished with sea water and prior to each deployment by dipping the entire instrument for 20 minutes until the air was displaced. For the final stage of deployment, the instrument is lowered with a winch to the seafloor, where it penetrates the sediment under self-weight.

The piezometer array was used for short- (hours, days) and long-term (months) installations. For short-term measurements, the instrument was deployed in different locations without recovery on the deck of the vessel between penetrations. For long-term monitoring, the piezometer was connected to an underwater station to provide continuous power supply and additional data storage capacity. An acoustic communication module in the underwater station allowed the transfer of data without recovering the piezometer. Sampling rate was set up individually before each measurement, with the maximum of 1 Hz. The short-term deployment collected data for 38 hours, while the long-term study continued for approximately one year. The mid-interval duration was sited in water depth of 19 m. The piezometer was a length of 4.25 m, with sensors located at depths of 0.5, 1.25, 2.75, 3.5, and 4.25 m. Data were sampled with a frequency of 0.2 Hz. For the long-term study, the piezometer measured pore pressures at depths of 0.5, 1.5, 2.25, and 3 m. Data were sampled with a frequency of 1 Hz. In summary, the IFREMER piezometers provide a framework to obtain ample high quality data, in combination with ease of handling and maintenance, which is necessary for application in the MRDF.

Hydrodynamics and Sediment Dynamics Observation It is well known that the Mississippi River, winds, and delta and/or shelf morphology together impact the tides, waves and currents on the Mississippi shelf. In the MRDF, waves and currents play a key role in transporting water and sediment. For instance, waves play a dominant role in resuspending seabed sediment and generating large pressure differences in water depths of 10–30 m (Obelcz et al. 2017), and westward longshore currents drive the long-term net sediment transport in the Mississippi shelf. The purpose of observation of hydrodynamics and sediment dynamics is to study the hydrodynamic processes triggering submarine landslides.

Multiple optical and acoustic sensors will be mounted to the tripods to measure time series data (hourly or higher frequency, for a duration of 1–2 months) of temperature, salinity, waves, tides, currents, sediment concentration and gas concentrations (e.g., methane). Sensors may include wave gauge, acoustic Doppler current profiler (ADCP), acoustic backscatter sensor (ABS), optical backscatter sensor (OBS), acoustic Doppler velocimeter (ADV), pulse-coherent acoustic Doppler profiler (PC-ADP) and gas sensor. At least two tripods will be deployed on the undisturbed delta front in varying depths (e.g., 20 and 50 m) in Year 1–2, mostly likely between the axis of two adjacent gullies. A downward-looking Sontek 5-MHz ADV

Ocean will be deployed to capture time-series sea bed elevation change as well as pressure, wave and current conditions at 10s cm above bed. A downward-looking 1200 kHz RDI PC-ADP will measure high-resolution current velocities in the lower 1 m of the water column. An upward-looking ADCP will measure current velocities in the middle and upper water column. An Aquatec ABS will measure the profile of suspended sediment concentration throughout the bottom boundary layer using four frequencies at 0.5, 1, 2, and 4 MHz. An OBS-3A will be used to measure turbidity, temperature, pressure and conductivity at 10s cm above bed. An OBS5+ sensor will be mounted about 0.2 m above sea bed to capture high turbidity event close to sea bed. Acoustic releases will be used to retrieve the tripods and, when available, the tripods can be tethered to the legs of nearby oil platforms. After testing of equipment in shallow waters on undisturbed delta front, we plan to deploy tripods to observe hydrodynamics and sediment dynamics in deeper waters (50–150 m) in Year 3–5.

Submarine Landslide Movement Measurements Because of MBARI's experiences with developing and using seafloor motion sensors, Dr. Charles Paull (MBARI) is joining this phase of the MRDF research consortium. The goal will be to determine whether sections of the delta front are continuously creeping or move in discreet failure events. To do this an array of motion sensors consisting of Benthic Event Detectors (BEDs) will be deployed for 1–3 years (Fig. 63).

Figure 63. BED deployment

MBARI engineers lower a benthic event detector into Monterey Bay. Image: Denis Klimov © 2015 MBARI.

Arrays of BEDs, or "smart boulders," will be deployed which are capable of detecting the changes associated with creep, recording the actual movements in discreet energetic failure events, and transmitting data back to surface receivers (Fig. 63). These instruments were developed by MBARI to record seabed motion during turbidity currents. BEDs contain three-axis accelerometers, a clock, pressure sensor, and acoustic beacons and/or modems, all housed in a pressure case. Acceleration of ≥0.1 G trigger a 50 Hz recording rate until the BED stops moving (Gwiazda et al. 2017). Previously BEDs have been housed in beach-ball-like housing designed to be carried down-slope within sediment flows, and left buried in the resulting deposits. BEDs are intentionally placed in channels or gullies where they are most like to move. BEDs can also be attached to other seafloor instrument packages that might move. Acoustic beacons and/or modems built into the BEDs allow them to located, tracked, and allow autonomous data transmission to surface receivers. Previous experience show that BEDs commonly survive being swept several km down slope; data are recorded, preserved and transmitted that document discrete energetic movements of the seabed, even when BEDs are buried to depths of >1 m of sediment (Gwiazda et al. 2017).

WaveGliders (self-propelled robotic surface vehicles) are used as mobile-hotspots to communicate with BEDs on and/or /or within the seafloor. WaveGliders can be programed to search for BEDs, determine if they have moved, establish how far they moved once relocated, extract the motion data associated with their trip downslope and send it back to shore. Data transmitted back to shore provides early detection that failure events have happened and allow appropriate rapid response survey to be designed.

The motion data from individual BEDs provide novel insights critical to understanding the dynamics of seafloor failures (i.e., when they moved, how fast, how long they were moving, how far they went, and

whether the sense of motion was sliding or rolling). Data from multiple BEDs also provides an opportunity to constrain the geometry and propagation of the entire event.

The acoustic beacon and/or modem on each BED also provides a seafloor bench mark. Recent developments using survey grade navigation systems on WaveGliders now allow the absolute positions of the acoustic beacons and/or modems on individual BED to be determined to better than 10 cm accuracy after a 24-hour long survey (Chadwell, 2017). By resurveying the position of each instrument frequently (monthly), small movements associated with creep can be detected. Relative movements between multiple instruments in arrays covering particular features will allow the dimensions of the creeping area to be determined. These methods were developed for the study of submarine sediment flows on the California coast, neither these nor similar methods have ever been attempted to study MRDF seabed motions.

SAA Tiltmeter. The ShapeAccelArray (SAA) developed by Measurand, Inc. was used to measure time-lapse displacement of the Nice Slope (Stegmann et al. 2012). The SAA is a flexible rod consisting of 0.3 m rigid segments, with MEMS (micro-electro-mechanical systems) gravity sensors located in each segment to quantify the tilt along three axes. A special driving rod was developed by IFREMER to deploy the SAA in soft marine sediments. In particular, an 8 m segment of SAA was inserted into a rod, which was connected to an anchor at the base. The driving rod was used to ensure the penetration of the SAA is by free fall weight. Before deployment, the space between the inner of the rod and SAA was filled with sand to ensure a perfect contact between the SAA and marine sediments. After penetrating via free fall, the removal of the driving rod breaks the connection to the anchor, leaving behind a vertical SAA in the sediment. As a result, the driving rod and deployment unit, including weight ballast which is the same for the piezometer deployment, can be recovered. A marine cable connects the SAA to a buoy, which contained solar panels to permanently provide power to the transducers and the data storage unit. A cellular modem data uplink system allows quais-real time data transfer from the buoy to a mobile phone. Stegmann et al. (2012) report the SAA tiltmeter was deployed in spring 2012 to monitor in situ displacements at a sampling rate of 5 minutes. To date, data obtained by the SAA tiltmeter have not been published. To the author's knowledge, no other measurements of sediment displacements with depth currently exists. However, Wang et al. (2017) performed in-situ observation of storm-wave-induced seabed deformation in the subaqueous delta of Yellow River with the SAA tiltmeter. They showed that SAA can be implemented in offshore environment and they linked subsurface deformations with storm events through wave measurements.

Seabed Coring Direct seabed sampling using sediment cores provides information on seabed conditions and motions that is complementary to hydrodynamic and geotechnical studies and direct measurement of seabed motions described above. Two types of coring activities are proposed herein: shallow seabed coring spanning below-seabed depths of 0.5–10 m (during Phase II, years 1–5, using piston corers and multicorers with no pressure containment, deployed from research vessels), and deep coring from stationary jackup rigs, using pressure vessels to keep cores at seabed pressure (described in Project Phase II, below).

The primary objectives of sediment core collection in Phase II will be to document distribution, geological and geotechnical properties, and age of deposition for sediment deposits recently created or remobilized by hydrodynamic and seabed phenomena. This work will use coring tools and analytical methods applied during Phase I pilot studies (Keller et al. 2016; Obelcz et al. 2017; Courtois et al. 2017; Smith et al. 2017) that have allowed us to identify and date deposits created over seasonal to decadal timescales. Because patterns of rapid sediment deposition and accumulation are known to be strong preconditions for submarine landslide development (Hitchcock et al. 2006), documenting these phenomena remain important (Fig. 64).
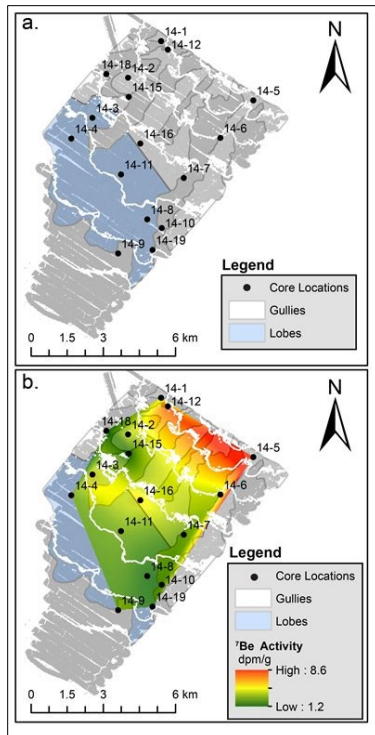
Figure 64. Example map of 7Be data

Sediment deposits near Southwest Pass, including a map of (a) core locations and seabed morphology and (b) seasonal flood deposit distribution revealed by mapping ^{7}Be distribution in sediments. From Keller et al. 2016. Warm colors in (b) indicate thickest seasonal flood deposits.

Piston and multicores will be collected during annual and rapid-response cruises, and analyzed for physical and geotechnical properties, and sediment age and/or accumulation rate, using the radiochemical methods of Keller et al. (2016). These results will provide seabed confirmation of hydrodynamical sediment transport and seabed motion phenomena described above.

A.3.5 Task II.D: deep coring and pressurized core collection (Y3)

Through our data synthesis and pilot studies (both geological and geophysical), we have determined that biogenic gas in MRDF sediments is likely a major factor in preconditioning sediments for failure at a range of scales, and that free bubble-phase gas appears to be widely distributed in sediments (evident in historical studies, from partings in cores and sediment expulsion from cores in 2017 [Figs. 56 and 65], and bubble plumes in 2017 geophysical data: Fig. 46). We have also determined that no reliable data for in situ gas concentrations exist for any portion of the MRDF seabed, which presents a huge knowledge gap in our ability to assess submarine landslide hazard. Gas expands at least ten-fold in volume from seabed depths to the surface, causing uncontrolled sediment expulsion and gas release as cores are collected, brought to the surface, and processed on board (Figs. 56 and 65). Piezometers described above provide important in situ information on pressure states within the seabed, but only indirect estimates of gas distribution. The only way to collect data that can reliably fill this gap is to collect cores in pressurized housings that retain seabed pressures. Geotechnical coring technology has improved greatly since the last major studies to characterize MRDF gas and geotechnical properties (Whelan et al. 1976), and limited early efforts to collect pressurized cores for gas study (Denk et al. 1981).

We propose to partner with DOSECC Exploration Services, LLC (for drilling operations) and Geotek Ltd, (for core analysis) to collect and analyze pressurized cores from the MRDF study area. Geotek Ltd. scientists and engineers are world leaders in pressurized core collection and analysis. DOSECC LLC is a team that evolved to provide specialized coring services for the International Ocean Discovery Program

(formerly the International Ocean Drilling Program). DOSECC will be responsible for vessel and drilling derrick operations. Geotek will be responsible for pressurized core recovery using the Geotek PCATS - Pressure Core Analysis and Transfer System. Cores will be imaged on the drillship using 3D X-ray tomography; Fig. 66), and transferred to the laboratory of CoPI Peter Flemings at the University of Texas (UT) at Austin, where measurements of gas concentration, and geological and geotechnical properties will be conducted using instruments built and installed by Geotek. The PCATS sampling preserves in situ pressures during core recovery for analysis of undisturbed physical and chemical properties in the laboratory. The system includes a 3D x-ray tomographic core scanner (Fig. 66), a multi-sensor logger for physical properties (data for unpressurized core shown in Fig. 56), and methods for sectioning the core under pressure.

Figure 65. Gas expansion in core.

Photograph of piston core collected in 2017, showing separation and remolding of sediment in core, produced by expansion of gas after core collection. Such partings occur throughout most piston cores collected, along with expulsion of sediment from ends of sampling tubes, due to gas expansion.
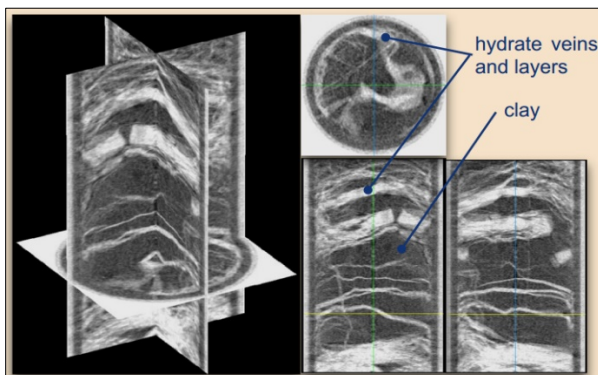

Figure 66. 3D x-ray in pressurized core

Example of 3-D x-ray tomographic image from core collected with GEOTEK PCATS (Schultheiss et al. 2014). These pressurized cores preserve original sediment structures, which are important for interpreting slide history and geotechnical properties.

Because of the technical challenges and costs associated with this coring program, and, because it is a discrete component of our proposed research, this activity is proposed to occur during Y3 of this project. Timing will allow use of the first three years of Phase II data collection and analysis, model development, and model-data integration, to inform the exact site selections and technical approaches to be used.

During Y3 of this project, DOSECC will charter a jackup vessel from Falcon Global LLC of Houma, Louisiana, to be used as a drilling platform. Falcon Global has previously partnered with DOSECC for drilling programs on the New Jersey Margin, and the Chicxulub Impact Crater on the Yucatan Peninsula, Mexico. DOSECC will mobilize drilling equipment using tools compatible with Geotek pressure-core

assemblies. The initial plan is to core three locations in water 20–75 m deep, targeting gully, lobe, and undisturbed seabed (Cite block diagram).

At each of the three locations, three major sampling operations will occur. First, a cone penetrometer (CPT) developed by CoPI Peter Flemings at UT will be mounted on the drill string and pushed to a nominal depth of 100 m below seabed. CoPI Flemings has used this approach previously to delineate anomalous pressure readings in the vicinity of known submarine landslide deposits (Flemings et al., 2008). Second, an initial continuous core will be collected to 100 m subbottom depth using conventional hydraulic piston coring tools with no pressure cores (Fig. 67A). Third, once gassy horizons have been identified, a second borehole will be completed using direct push tools and pressure-core housings for some to all core sections. Onboard analyses will include 3D computed tomographic imaging, gamma density, compressional wave speed, and other physical properties (Fig. 67B). Core sections will then be transferred to UT (Fig. 67C) using special DOT-approved containers (built by Geotek) that are required for transport of gas-containing cores at seabed pressure. PCATS analyses under pressure at UT Austin will include gas content, fluid permeability, compressibility, elastic moduli, and large strain triaxial measurements. These ensemble measurements have never been conducted before on MRDF core sediments (or any sediment cores outside of deep-sea hydrate zones), and are all important for determining the susceptibility of MRDF sediments to failure.

A.3.6 Task II.E: data and model integration

This project began as a data synthesis and integration study in 2013, and that approach remains essential to project success. Through regular meetings and workshops that we have undertaken for this and other BOEM-funded projects, we will continue to use 3D visualization to bring together disparate data sets such as geoacoustic surveys, core data, geotechnical data, and modeling results, to better understand process interactions and geological products. Examples of this integrative approach include the MRDF publications of Obelcz et al. (2017) and Maloney et al. (2018) which incorporate both old and new data and approaches to develop new insights.

Beginning in Y1, early model versions (and later more advanced ones) will be used test hypotheses, evaluate data and compare to models, and also refine the models themselves. Because model development will occur at the same time as field measurements, and after the initial five years of data synthesis in Phase I, both our understanding of observations and model results, and also model robustness, will co-evolve. This task will continue through all years of the project.

A.5 Phase III (Y4-5) Hazard Assessment

A.5.1 Task III.A: production runs using regional model

We anticipate having a relatively refined and fully operational regional landslide model by the start of Y4. At this time, we will begin define a suite of regional simulations we wish to complete, to evaluate regional seabed response to storm forcings of a range of intensities and trajectories. End-member examples will include: annual-return-period simulations of winter-storm waves (such as those simulated by CoPI Georgiou, for publication of Obelcz et al. 2017); and major hurricanes that cross the MRDF region slowly, such as Hurricanes Camille, Ivan, and Katrina that exceeded the strength and trajectory criteria defined by Guidroz (2009) required to generate major submarine landslides.

To complete the spectrum of seabed responses between these two end members for storm intensity, we will emulate the Joint Probability Method (JPM) that is used by FEMA for tropical cyclone storm-surge frequency analysis (FEMA, 2012) and maps of predicted coastal flood depth. When used for surge analysis, the JPM considers surge impacts from "all possible storms consistent with the local climatology, each weighted by its appropriate rate of occurrence" (FEMA 2012, p.1). This approach is undertaken in conjunction with the Optimal Sampling Method, to reduce the total number of simulations required to an

achievable number, and still capture the entire storm parameter space (size, intensity, track, speed, etc.) (FEMA 2012). In our case, rather than evaluating coastal flood risk, we will be evaluating the seabed impacts (for producing seabed motion) of waves produced by storms of different track, speed, and intensity, ranging from annual winter storms, to Category 5 hurricanes.

A.5.2 Task III.B: hazard map development

Simply put, our regional model for submarine landslide development will be able to predict sediment-transport rates (in the form of submarine landslides and other phenomena) for particular points in space and time, given seabed conditions and the seabed forces produced by waves of a particular storm. To create a hazard map, the regional impacts of many storms must be brought together. The approach used for coastal storm surge mapping is to combine the maximum flood depths from all JPM simulations, to produce map layers showing maximum inundation depth expected for all storms of a particular return period, or probability of occurrence. A simple way to imagine this is to produce repeated simulations of one storm with a particular return period (usually 100 or 500 years) with the trajectory shifted for each simulation, so that the entire coastal region is impacted by maximum flooding conditions for this rank of storm. Similar to the flood mapping approach, our approach to producing regional hazard maps for submarine landslides will be to combine all regional JPM simulation results for a particular storm intensity, so as to create a map of maximum sediment transport rate for each map grid point predicted from any simulation of that intensity, regardless of track. Multiple map layers will be produced, representing difference types and intensities of storms. In this way, we will be able to represent the probability of submarine landslide occurrence based on accurate representations of ocean and seabed physics and storm climatologies, rather than proxy measurements that have been the focus of previous hazard assessments.

A.6 Project Deliverables and Planned Products

The following documents and materials will be deliverables for this proposed effort:

1. Hazard map
2. Models
3. Data sets from project
4. Reports: quarterly, annual, draft and final reports will be prepared in accordance with BOEM requirements.
5. We will conduct regularly scheduled monthly meetings and/or conference calls for the MRDF research team throughout the performance period.
6. LSU will host a shared network drive that provides BOEM remote access for upload and/or download so that literature, data, reports, and other materials. Data on the drive will be backed up so it will be secure from loss or damage.
7. We will prepare and archive an organized catalog of all relevant existing studies, reports, data products with spatial data (e.g., a spatial database where applicable) in a format agreed upon between BOEM and LSU.
8. We will present our findings at one annual science conference, and one BOEM Information Transfer Meeting per year.

The Department of the Interior Mission

As the Nation's principal conservation agency, the Department of the Interior has responsibility for most of our nationally owned public lands and natural resources. This includes fostering sound use of our land and water resources; protecting our fish, wildlife, and biological diversity; preserving the environmental and cultural values of our national parks and historical places; and providing for the enjoyment of life through outdoor recreation. The Department assesses our energy and mineral resources and works to ensure that their development is in the best interests of all our people by encouraging stewardship and citizen participation in their care. The Department also has a major responsibility for American Indian reservation communities and for people who live in island territories under US administration.

The Bureau of Ocean Energy Management Mission

The Bureau of Ocean Energy Management (BOEM) promotes energy independence, environmental protection and economic development through responsible, science-based management of offshore conventional and renewable energy resources.

The BOEM Environmental Studies Program Mission

The mission of the Environmental Studies Program (ESP) is to provide the information needed to predict, assess, and manage impacts from offshore energy and marine mineral exploration, development, and production activities on human, marine, and coastal environments.